

THE DEVELOPMENT OF SIMPLIFIED MICROREACTORS FOR USE IN  
MULTI-STEP REACTION SEQUENCES

A Dissertation

Presented to the Faculty of the Graduate School

of Cornell University

In Partial Fulfillment of the Requirements for the Degree of

Doctor of Philosophy

by

Andrew R. Bogdan

August 2009

© 2009 Andrew R. Bogdan

# THE DEVELOPMENT OF SIMPLIFIED MICROREACTORS FOR USE IN MULTI-STEP REACTION SEQUENCES

Andrew R. Bogdan, Ph. D.

Cornell University 2009

This dissertation describes the development of simplified microreactors to be used in multi-step reaction sequences. Microreactors are a developing technology with numerous benefits and whose modular design permits multi-step reaction sequences to be performed in a continuous flow process. The first chapter discusses the physical properties of microreactors and describes how performing reactions in these miniaturized reactors leads to safer, more efficient and more selective chemical transformations. A brief discussion of multi-step reaction sequences already performed in flow will also be presented. These multi-step reaction sequences, however, rarely rely on catalysis to facilitate chemical transformations. This area therefore has room for great improvement. The next two chapters discuss the development and application of solid-supported catalysts to be used in flow. In the first of these two chapters, two catalysts are immobilized on a solid-support and used in a simplified flow reactor. These reactions proved to be more efficient than similar batch reaction and the catalysts were highly recyclable. The next chapter presents a supported TEMPO catalyst used to oxidize alcohols to carbonyl species. These three catalysts set the foundation for multi-step flow reaction to be potentially performed in the group. The ensuing chapter uses a flow reactor to facilitate a two-step click reaction starting from an alkyl halide, sodium azide and a terminal acetylene. This process proved to be high throughput and rapidly synthesized vast libraries of

compounds to be submitted for biological testing. The next two chapters discuss the synthesis of the ibuprofen and atropine in flow. Initial studies were carried out to synthesize both of these drugs in flow as part of a project geared toward synthesizing drugs on-demand. Later, a continuous flow synthesis of ibuprofen was realized using a series of reactions in which excess reagents and byproducts were compatible with downstream reactions. Finally, on-going work to develop asymmetric, multi-step reaction sequences in flow will be discussed in which the majority of reaction steps utilize solid-supported catalysts.

## BIOGRAPHICAL SKETCH

Andrew Robert Bogdan (known as Drew to everybody who knows him) was born in State College, PA in 1982. He spent the next 18 years growing up in the shadows of Penn State University, but despite his love for Nittany Lion football, he pledged that he would never be a student there. During his senior year in high school, Drew applied to only one college, Franklin & Marshall, and thankfully they let him in.

Knowing from the start that he was going to be a chemistry major, Drew immersed himself in the chemistry department and became close to various faculty members. After his sophomore year, Drew was granted the opportunity to perform undergraduate research at Syracuse University under the supervision of Dr. John E. Baldwin. Upon returning to Franklin and Marshall in August of 2002, Drew continued to collaborate with Dr. Baldwin while working in Dr. Phyllis A. Leber's laboratory, ultimately continuing this research until graduation. Drew graduated *cum laude* from Franklin and Marshall in May of 2004, having achieved various departmental chemistry awards during his time in school.

Drew decided to head to New York state for graduate school, where he joined the group of Dr. D. Tyler McQuade at Cornell University in late 2004. Soon thereafter he started working with microcapsules and microreactors, in efforts to develop multi-step reaction sequences. In September of 2007, Drew joined the group during its move to Florida State University, where he would complete his doctorate. Friends back in Ithaca were jealous of Drew for living in the Sunshine State. Unfortunately for Drew, he remained as pasty as ever during his time in Tallahassee, rarely venturing outside during the daylight hours. Drew focused on completing his degree and instead of getting a tan.

To my family.

## ACKNOWLEDGMENTS

Graduate school was anything but typical for me. At one point, I was a Florida resident living in California who was enrolled at a school in New York State. That being said, I cannot imagine going through graduate school without the constant support of numerous people. My family and friends were always there, serving as perpetual sources of advice and laughter, helping me through complicated times.

Thanks to my advisor D. Tyler McQuade, who provided me with the guidance and knowledge necessary to help me complete this degree. Furthermore, his confidence in me helped me develop as an independent scientist and made me realize that no matter what challenges I am confronted with, I have the ability to overcome them. I would also like to thank Phyllis Leber, who provided constant support and advice throughout both my undergraduate and graduate careers.

I am deeply grateful for my parents. Throughout my life, they have always been supportive of the decisions I have made, and made it possible to be in places that I never thought I would be. Thanks to my big brother, Matt, who finally stopped abusing me as a child, having finally realized that sending me to the hospital repeatedly was not in anybody's best interest.

Steve Broadwater showed me the ropes in graduate school and helped set the foundation for my graduate career. He has always been the source of valuable insight and I cannot thank him enough. I would also like to thank Sarah Poe who was with me since the first day in the group. She has always been there when I needed advice, a laugh, cookies, or somebody to annoy (despite the fact she graduated months before I did). I cannot imagine graduate school without these two, and thankfully the memories go beyond lab, ranging from tire fires to the more traditional barbeques.

To everybody else who has helped me along the way, in both Ithaca and Tallahassee, thank you.

## TABLE OF CONTENTS

Biographical Sketch.....	iii
Dedication.....	iv
Acknowledgements.....	v
Table of Contents.....	vi
List of Figures.....	vii
List of Schemes.....	x
List of Tables.....	xii
List of Equations.....	xiii
Chapter 1: The Application of Microreactors to Organic Synthesis.....	1
Chapter 2: Improving Solid-Supported Catalyst Productivity by Using a Simplified Packed-Bed Microreactor.....	17
Chapter 3: A Biphasic Oxidation of Alcohols to Aldehydes and Ketones Using a Simplified Packed-Bed Microreactor.....	42
Chapter 4: The Use of Copper Flow Reactor Technology for the Continuous Synthesis of 1,4-Disubstituted 1,2,3-Triazoles.....	61
Chapter 5: The Flow Syntheses of Active Pharmaceutical Ingredients.....	87
Chapter 6: The Continuous Flow Synthesis of Ibuprofen.....	113
Chapter 7: Progress Toward Multi-Step Reaction Sequences Using Solid-Supported Catalysis.....	137
Appendix 1: Supporting Information for Chapter 2.....	165
Appendix 2: Supporting Information for Chapter 3.....	168
Appendix 3: Supporting Information for Chapter 4.....	171
Appendix 4: Supporting Information for Chapter 6.....	173

## LIST OF FIGURES

1.1	Surface area-to-volume ratios of two 1 mL reactors.....	2
1.2	Temperature profiles for batch and flow reactors.....	3
1.3	Mixing profiles for batch and flow reactors.....	5
1.4	Retrosynthetic analysis of the drug naproxinod.....	6
1.5	Ley's continuous flow synthesis of oxomaritidine.....	8
1.6	Ley's continuous flow synthesis of 1,4-disubstituted 1,2,3-triazoles.....	9
1.7	Experimental setup for Jensen's carbamate synthesis in flow.....	10
1.8	Cosford's three-step continuous flow synthesis of 1,2,4-oxadiazoles.....	12
2.1	Flow reactions with a packed-bed microreactor.....	18
2.2	The simplified microreactor setup.....	22
2.3	Conversion of Knoevenagel condensation vs. residence time.....	23
2.4	Conversion of acylation vs. residence time.....	26
2.5	Yield from a single-channel AO-TBD packed-bed microreactor.....	27
2.6	Long-term activity of single-channel AO-TBD microreactor.....	28
2.7	Yield from an eight-channel AO-TBD packed-bed microreactor.....	28
2.8	Long-term activity of eight-channel AO-TBD microreactor.....	29
2.9	Heat exchanger.....	30
2.10	Packed-bed microreactor regeneration.....	31
3.1	Catalytic cycle of the TEMPO-catalyzed oxidation of alcohols.....	44
3.2	Redox reactions for the generation of the oxoammonium cation.....	44
3.3	The simplified microreactor setup.....	47
3.4	Plug flow and coalescence.....	47
3.5	The long-term activity of AO-TEMPO packed-bed microreactors.....	52
4.1	Drug derivative synthesis using click chemistry.....	62

4.2	Catalytic cycle of the click reaction.....	64
4.3	Conjure Flow Reactor schematic.....	65
4.4	Copper reactor diskette.....	66
4.5	Contour plot for the click reaction at 100 °C.....	68
4.6	Contour plot for the click reaction at a 5-minute residence time.....	69
4.7	Contour plot for the click reaction with 2.0 eq alkyl azide.....	70
4.8	Starting materials for triazole library.....	71
4.9	Triazole library.....	72
5.1	The structures of ibuprofen and atropine.....	89
5.2	The flow reaction setup.....	96
5.3	The flow Friedel-Crafts acylation setup.....	90
5.4	The flow 1,2-aryl migration setup.....	99
6.1	Simplified microreactor setup.....	115
6.2	The flow Friedel-Crafts acylation reaction setup.....	116
6.3	The mixed anhydride.....	116
6.4	Reagent flow for the Friedel-Crafts acylation.....	119
6.5	The two-step reaction sequence.....	122
6.6	The three-step, continuous flow synthesis of ibuprofen.....	122
7.1	Multi-step catalytic reaction sequence in flow.....	138
7.2	Seeberger's aldol condensation in flow.....	140
7.3	The structure of AO-proline.....	140
7.4	Bifunctional urea structure.....	142
7.5	AO-proline-catalyzed $\alpha$ -aminoxylation with and without urea.....	143
7.6	Results of the flow $\alpha$ -aminoxylation of hexanal.....	144
7.7	The structure of AO-PTPE.....	144
7.8	Proposed two-step, catalytic reaction sequences in flow.....	147

7.9	Proposed three-step, catalytic reaction sequence in flow.....	148
7.10	The continuous flow synthesis of ibuprofen.....	149
7.11	The structure of pregabalin.....	149
7.12	The continuous flow synthesis of pregabalin.....	151
A1.1	<sup>1</sup> H NMR spectrum of acetylene-modified DMAP.....	165
A2.1	AT-IR spectrum of AO-TEMPO.....	168
A2.2	<sup>13</sup> C NMR spectrum of acetylene-modified TEMPO.....	169
A2.3	<sup>1</sup> H NMR spectrum of 4-chlorobenzaldehyde from flow oxidation.....	170
A4.1	The three-step flow reaction setup.....	173
A4.2	<sup>1</sup> H NMR spectrum of PhI(OAc) <sub>2</sub> .....	174
A4.3	<sup>1</sup> H NMR spectrum of methyl 2-phenylpropanoate.....	175
A4.4	<sup>13</sup> C NMR spectrum of methyl 2-phenylpropanoate.....	176
A4.5	<sup>1</sup> H NMR spectrum of 4-isobutylpropiophenone.....	177
A4.6	<sup>13</sup> C NMR spectrum of 4-isobutylpropiophenone.....	178
A4.7	<sup>1</sup> H NMR spectrum of methyl 2-(4-isobutylphenyl)propanoate.....	179
A4.8	<sup>13</sup> C NMR spectrum of methyl 2-(4-isobutylphenyl)propanoate.....	180
A4.9	<sup>1</sup> H NMR spectrum of ibuprofen.....	181
A4.10	<sup>13</sup> C NMR spectrum of ibuprofen.....	182
A4.11	GC/MS trace of recrystallized ibuprofen.....	183
A4.12	The structure of naproxen.....	184
A4.13	Catalytic cycle of the stereoselective 1,2-aryl migration.....	185

## LIST OF SCHEMES

1.1	Model reaction for the carbamate synthesis.....	11
2.1	Preparation of AO-TBD resin.....	21
2.2	The Knoevenagel condensation.....	21
2.3	Preparation of AO-N <sub>3</sub> resin.....	25
2.4	Preparation of AO-DMAP resin.....	25
2.5	The acylation of <i>sec</i> -phenethyl alcohol.....	25
3.1	Preparation of AO-N <sub>3</sub> resin.....	45
3.2	Preparation of AO-TEMPO resin.....	46
3.3	The AO-TEMPO-catalyzed oxidation of benzyl alcohol.....	48
4.1	The one-pot click reaction.....	64
4.2	The optimized one-pot click reaction.....	67
5.1	The BHC Company's synthesis of ibuprofen.....	89
5.2	The synthesis of atropine.....	90
5.3	The syntheses of ibuprofen and atropine via 2-phenylprop-2-enoic acids.....	90
5.4	The syntheses of ibuprofen and atropine via 2-arylpropanoates.....	91
5.5	The batch synthesis of ibuprofen.....	92
5.6	Retrosynthetic analysis of atropine.....	92
5.7	The synthesis of 3-methoxypropiophenone.....	93
5.8	The PhI(OAc) <sub>2</sub> -mediated 1,2-aryl migration of 3-methoxypropiophenone.....	93
5.9	Alternative methods of atropine esterification.....	94
5.10	The complete synthesis of atropine.....	95
5.11	The synthesis of atropine using Mackenzie and Ward's tropic acid.....	95
5.12	Friedel-Crafts acylation of isobutylbenzene.....	96
5.13	The PhI(OAc) <sub>2</sub> -mediated 1,2-aryl migration of 4-isobutylpropiophenone.....	99

5.14	Methyl ester saponification in the synthesis of ibuprofen.....	100
5.15	The synthesis of 3-methoxypropiophenone.....	102
5.16	The 1,2-aryl migration of 3-methoxypropiophenone.....	102
5.17	The coupling of tropine with the activated carboxylic acid.....	104
6.1	Proposed synthetic route to ibuprofen.....	115
6.2	The $\text{PhI}(\text{OAc})_2$ -mediated 1,2-aryl migration of 4-isobutylpropiophenone...	120
7.1	The preparation of $\text{AO-N}_3$ .....	141
7.2	The synthesis of AO-proline.....	141
7.3	The AO-proline-catalyzed $\alpha$ -aminooxylation of hexanal.....	143
7.4	The asymmetric addition of diethyl zinc to benzaldehyde.....	145
7.5	The synthesis of AO-PTPE.....	145
7.6	The one-pot reaction for the pregabalin intermediate.....	150
A3.1	Model reaction for DOE.....	171
A4.1	The stereoselective $\text{PhI}(\text{OAc})_2$ -mediated 1,2-aryl migration.....	184

## LIST OF TABLES

2.1	Packing materials tested as supports for packed-bed microreactors.....	20
2.2	Flow reaction productivities.....	24
3.1	Oxidation of alcohols using AO-TEMPO packed-bed microreactor.....	50
4.1	Boundary conditions for DOE optimization.....	68
4.2	Triazole library scale-up.....	73
5.1	Results of the flow Friedel-Crafts acylation.....	98
5.2	Results of the flow $\text{PhI}(\text{OAc})_2$ -mediated aryl migration.....	100
5.3	Results of the ibuprofen methyl ester saponification in flow.....	101
5.4	Results of the 3-methoxypropiophenone synthesis in flow.....	102
5.5	Results of the 1,2-aryl migration of 3-methoxypropiophenone on flow.....	103
5.6	Results of the atropine methyl ester saponification in flow.....	104
6.1	Reactions screened for the Friedel-Crafts acylation.....	117
6.2	The optimization of the flow Friedel-Crafts acylation.....	118
6.3	The optimization of the flow 1,2-aryl migration.....	121
6.4	Microreactor components.....	125
7.1	Results of the $\alpha$ -aminoxylation of aldehydes.....	142
A1.1	Residence time as a function of column length.....	165
A1.2	Residence time as a function of flow rate.....	166
A3.1	Conditions screened in DOE.....	171
A3.2	Results of DOE.....	172
A4.1	Results of the stereoselective 1,2-aryl migration.....	186

## LIST OF EQUATIONS

1.1	Calculation of heat transfer.....	4
2.1	Calculation of productivity.....	19
3.1	Reaction of NaOCl, H <sub>2</sub> SO <sub>4</sub> , and KI.....	57
3.2	Reaction of I <sub>2</sub> with Na <sub>2</sub> S <sub>2</sub> O <sub>3</sub> .....	57
3.3	Calculation of NaOCl molarity.....	57
A1.1	Calculation of residence time.....	166

## CHAPTER 1

### The Application of Microreactors to Organic Synthesis

#### *Abstract*

This dissertation describes the application of microreactors to organic synthesis with the ultimate goal of performing multi-step reaction sequences in a continuous flow framework. In this introduction to microreactors, the benefits of performing reactions in these devices will be highlighted, followed by a discussion of multi-step reaction sequences already presented in the literature. It will then conclude by discussing how McQuade group technology is being applied to new multi-step continuous reactions.

#### *Introduction*

Microreactor technology has gained a substantial amount of attention in both industrial and academic laboratories.<sup>1-12</sup> While a majority of the seminal publications focused on engineering aspects of microreactors,<sup>2, 3, 13</sup> an increasing body of literature has begun to apply these devices to organic synthesis.

Organic synthesis is a powerful enterprise that continues to develop more selective and efficient chemical methods and synthetic routes. For the most part, however, the technology used to perform chemical reactions has remained unchanged for the past 140 years: that is, syntheses continue to be performed in batch reactors (round bottom flasks or tank reactors).<sup>14</sup> While these methods have proven to be successful, they are also wasteful and are potentially unsustainable.<sup>15</sup> Applying new technologies, such as microreactors, to organic synthesis can be used to improve synthetic efficiency as microreactors produce less waste than traditional methods due to precise reaction control, resulting in cleaner, more efficient syntheses. The modular

nature of microreactors also permits multi-step reaction sequences to be performed in a continuous flow process, thereby removing wasteful purification and isolation steps.

Petrochemical plants often perform reactions in flow using reactors with diameters as large as 4 m.<sup>16</sup> Microreactors, on the other hand, are devices that facilitate reactions by passing starting materials through a series of channels on order of 10-1000  $\mu\text{m}$  in diameter.<sup>1</sup> This chapter discusses the benefits of performing reactions in microreactors, in both academic and industrial settings, and presents three different methods to perform multi-step reaction sequences in flow. The chapter concludes with a discussion of how McQuade group technology is being applied to these systems to increase their already highly efficient nature.

### ***Increased Surface Area-to-Volume Ratios in Flow***

Microreactors offer far superior surface area-to-volume ratios than batch reactors (Figure 1.1). As a result, heat transfer and mixing are greatly improved, which leads to safer, more efficient chemical reactions.<sup>17</sup>

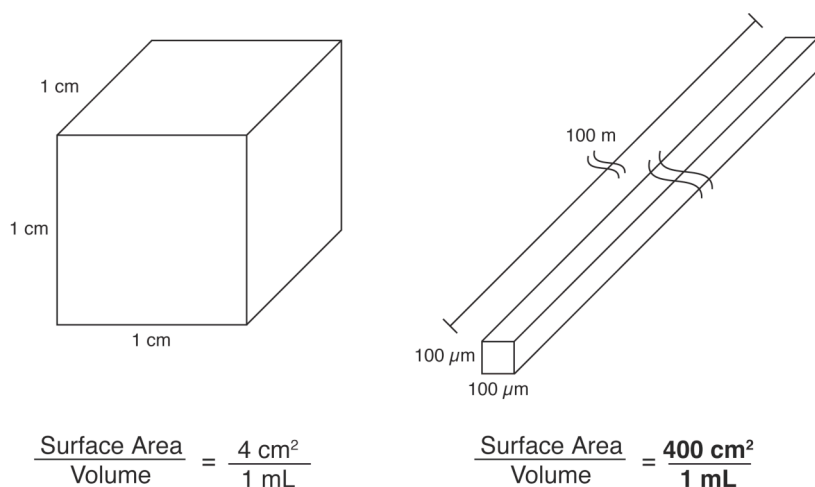


**Figure 1.1.** Surface area-to-volume ratios of two 1 mL reactors.

Figure 1.1 shows two reactors with an internal volume of one milliliter. Placing a 1 mL reaction into a 1 cm cubic tube provides a surface area-to-volume ratio of  $4 \text{ cm}^2 \text{ mL}^{-1}$ . Alternatively, stretching this cubic reactor into a channel 100 m long and  $100 \mu\text{m}$  wide increases the surface area-to-volume ratio to  $400 \text{ cm}^2 \text{ mL}^{-1}$ .<sup>17</sup> Heat transfer and mixing are dictated by surface area-to-volume ratios for the reasons outlined below.

Heat transfer is one of the most important variables to be considered when performing a chemical reaction. Heat is either supplied in order to facilitate slow reactions or removed from exothermic reactions to prevent runaway reactions/undesired pathways. Temperature profiles of a batch reactor can be very broad (Figure 1.2).<sup>18</sup> For an exothermic reaction being cooled in a large batch reactor,

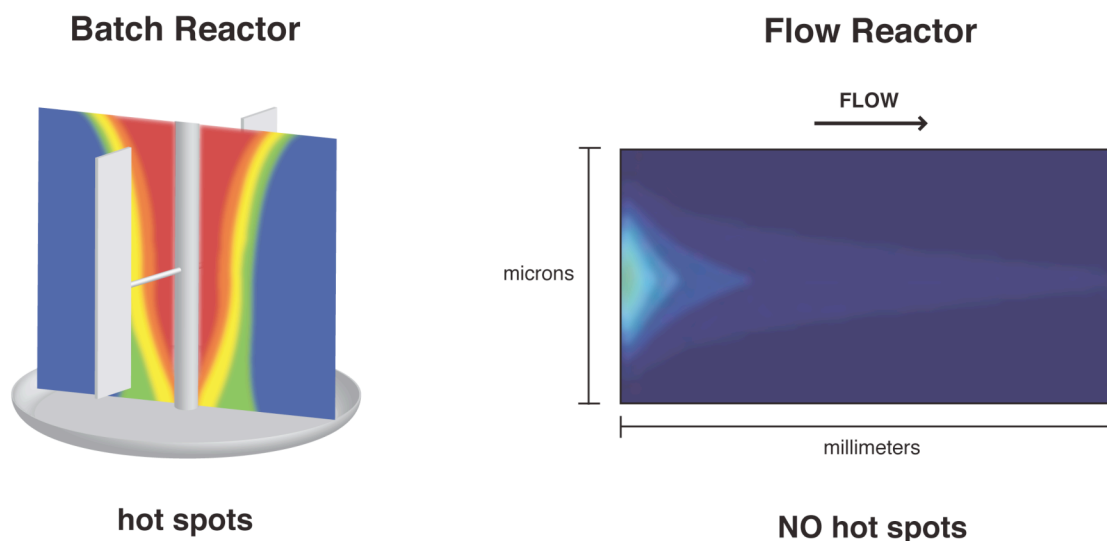


**Figure 1.2.** Temperature profiles for a batch reactor (left) and a flow reactor (right). The blue area represents areas where the reaction is cooled effectively. The red area represents areas with poor heat transfer (i.e. hot spots).<sup>18</sup>

for instance, the temperature around the periphery of the reactor is cooler than the temperature toward the center.<sup>18</sup> This heterogeneity of the temperature leads to areas

known as hot spots. Hot spots are localized temperature gradients that allow access to undesired pathways.<sup>1, 19</sup> The presence of hot spots leads to greater byproduct formation, and ultimately diminishes the efficiency of a given process. Conversely, when cooling a microreactor, no temperature gradients exist (Figure 1.2). Heat transfer is proportional to the diameter of the reactor (Equation 1.1).<sup>20, 21</sup> In this equation,  $k$  represents the overall heat transfer coefficient,  $Q$  is heat flow (expressed in W),  $\Delta T$  is the mean logarithmic temperature difference in degrees K, and  $A$  is the cross-sectional area (expressed in m<sup>2</sup>). Heat transfer therefore increases with a decrease in reactor diameter, and is therefore higher for microreactors. This improved heat transfer in microreactors subsequently enables reactions to proceed much more cleanly and efficiently.

$$k = \frac{Q}{A \Delta T} \quad (\text{Equation 1.1})$$

Mixing is also greatly improved when using microreactors.<sup>2</sup> Common batch reactors, such as round bottom flasks or tank reactors, suffer from inhomogeneities in mixing that are caused by their stirring mechanisms.<sup>1, 22, 23</sup> These mechanisms lead to chaotic mixing and convection, which causes weak to no mixing in parts of the reactor (Figure 1.3).<sup>18</sup> Poor mixing may lead to local concentration gradients, causing more byproduct formation. It has been shown that rapid mixing results in faster and cleaner chemical transformations, but this can be difficult to accomplish in batch for the reasons outlined above.

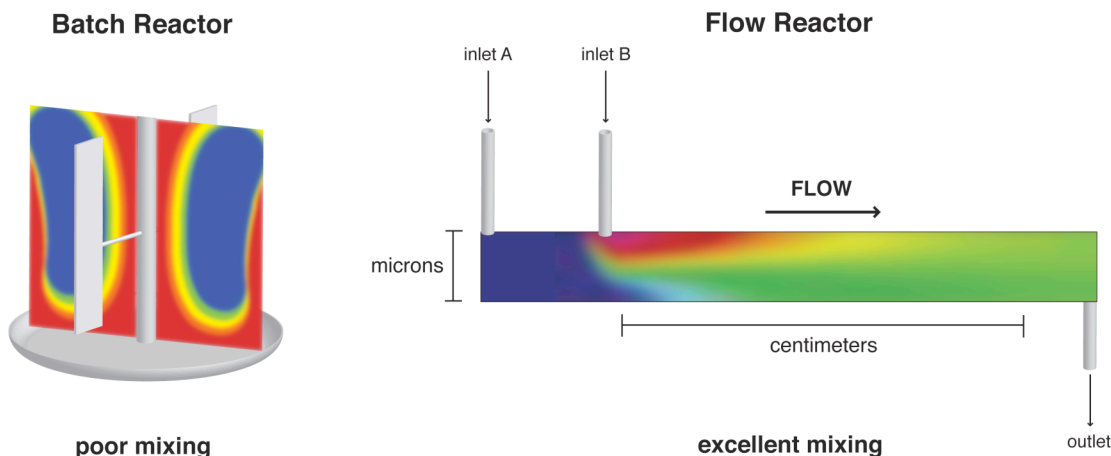


**Figure 1.3.** Mixing profiles in a batch reactor (left) and a flow reactor (right). Two components are being mixed, red and blue, to give green color after effective mixing. In the batch reactor, better mixing occurs close to the impellers and poor mixing occurs toward the middle and periphery. In the flow reactor, the two phases rapidly diffuse due to the narrow dimensions of the reactor.<sup>18</sup>

It has been shown that complete mixing in batch occurs within seconds, whereas complete mixing in microreactors takes a matter of microseconds.<sup>19</sup> The narrow dimensions of microreactors allow for rapid mixing to take place (Figure 1.3). For example, two reagent streams can be flowed together in lamellae on the order of 50-200  $\mu\text{m}$  thick. These small dimensions permit rapid mixing to take place by diffusion in as little as 100  $\mu\text{s}$ . Microreactors can achieve this rapid mixing because the lamellae are capable of achieving surface area-to-volume ratios of 30,000  $\text{m}^2 \text{m}^{-3}$ . In comparison, in a typical laboratory batch reactor, the lamellae have surface area-to-volume ratios ranging from 4-100  $\text{m}^2 \text{m}^{-3}$ .<sup>24, 25</sup>

This increased heat transfer and mixing is highly beneficial from a waste perspective as well. Solvents are used for a number of reasons in organic synthesis, one of which is their ability to help dissipate heat. Batch reactions frequently require more dilute conditions in order to assist with heat transfer. Microreactors permit reactions to be run at higher concentrations (or even neat) because heat transfer is so

rapid, thereby generating fewer by-products, and ergo less waste.<sup>1, 8, 22</sup> Products typically elute from the microreactors having higher purity profiles, meaning intermediate purification steps can be eliminated. A growing number of chemical manufacturers are beginning to capitalize on the benefits of microreactors not only because this unprecedented reaction control, but also because of safety and marketing concerns.<sup>16</sup>

### ***Improved Safety and Scale-Up***

As stated earlier, microreactors permit the careful control of exothermic reactions. Microreactors also enable hazardous reactions to be safely used due to limited active chemistry volumes and rapid reaction times. This is perhaps best highlighted by the microreactor-enabled production of an intermediate for the drug naproxenolone (Figure 1.4).

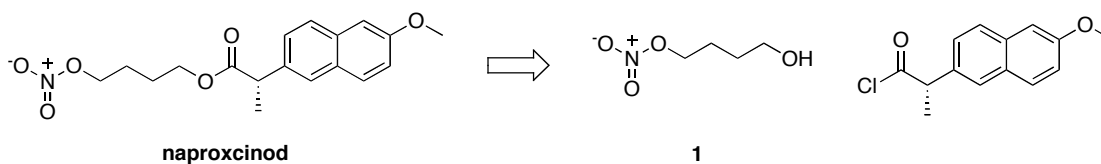


**Figure 1.4.** A retrosynthetic analysis of the drug naproxenolone.

NiCox, a France-based chemical manufacturer, in collaboration with manufacturers DSM and Corning, has designed a microreactor-based synthesis to safely generate a nitrated intermediate **1** (Figure 1.4). The use of microreactors in this process permits large quantities of **1** to be synthesized in a safe, and cost-effective manner.<sup>26</sup> Nitrations are notoriously dangerous processes on industrial scale as they can be uncontrollably exothermic and generate explosive products and byproducts.<sup>27</sup> In order to achieve high yields in batch, very strict control of reaction conditions must be maintained, and dilute reaction conditions are used to prevent exotherms. In a

microreactor, small dimensions allow heat transfer to be efficiently controlled and the residence time of unstable materials to be limited. Also, because the product stream is immediately quenched at the reactor outlet, a high concentration of dangerous material is never reached, as would occur in a batch reactor. Excellent reaction control in the microreactor thus permits the reaction to proceed with higher yield and purity, in a much safer overall process.<sup>26</sup>

Reaction scale-up of the flow reactions can be performed using one of three simplified methods.<sup>13,28,29</sup> The first process is known as ‘numbering up,’ which entails the addition of identical reactors in parallel, changing only the flow rate of the reagent stream. Alternatively, the microchannels could also be made longer or the flow reactions simply could be run for a longer period of time.<sup>30</sup> These processes are highly advantageous since reactions do not need to be reengineered to work on a larger scale. As a result, the development of a large-scale synthesis of compounds such as intermediate **1** is much faster, and the expenses associated with this scale-up are greatly diminished.<sup>16</sup>

### ***Multi-step Reaction Sequences in Flow***

While the majority of microreactor work in organic synthesis has focused on single reaction steps,<sup>1-12</sup> recent examples have demonstrated multi-step reaction sequences in flow. Microreactors have a modular nature that allows the outlet stream of one reaction to be mixed with a new set of reagents, thereby permitting multiple reactions to be run in sequence and limiting the number of isolation and purification steps. Three different methods for running continuous flow syntheses will be highlighted in the sections to come.

**Continuous Flow Synthesis Using Solid-Supported Reagents and Scavengers.** The Ley group at Cambridge is a pioneer in the field of flow chemistry.

The work done by Ley and co-workers relies on a catch-and-release strategy coupled with supported-reagents and scavengers that permits pure product to elute from the microreactor.<sup>9</sup> In their most elaborate continuous flow synthesis, Ley and co-workers synthesized the natural product oxomaritidine in a continuous flow process, requiring no intermediate purification steps (Figure 1.5).<sup>31</sup> Five of the seven steps in this synthesis involve passing starting materials through cartridges containing solid-supported reagents, permitting a pure stream of product to elute from the cartridge before being relayed directly into the next reaction step. In all, a 40% yield was obtained after seven steps with a purity of 90% by NMR.

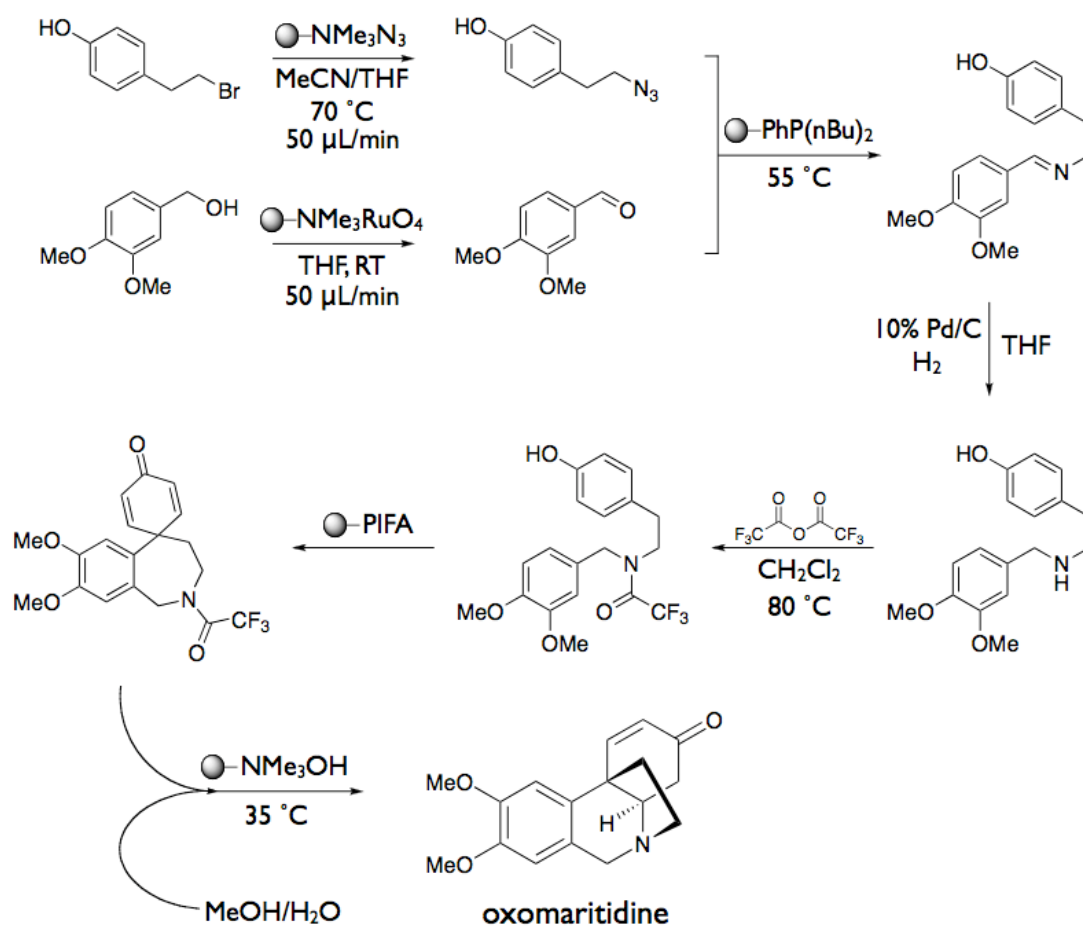


**Figure 1.5.** Ley's continuous flow synthesis of the natural product oxomaritidine using solid-supported reagent cartridges.

More recently, Ley and co-workers developed a three-step synthesis of 1,4-disubstituted 1,2,3-triazoles using a combination of solid-supported reagent and scavenger cartridges in series (Figure 1.6).<sup>32</sup> The reaction sequence starts with two inlet streams, one containing the Bestmann-Ohira reagent **2**,<sup>33-35</sup> an alcohol **3**, and an organic azide **4**, and another stream containing a solution of KO*t*Bu in methanol. This stream is passed through a cartridge packed with an immobilized TEMPO reagent, used to oxidize the alcohol to the aldehyde. This stream is subsequently mixed with a solution of KO*t*Bu in methanol and heated to 100 °C for 48 minutes. The Bestmann-Ohira reagent converts the aldehyde into a terminal acetylene, which

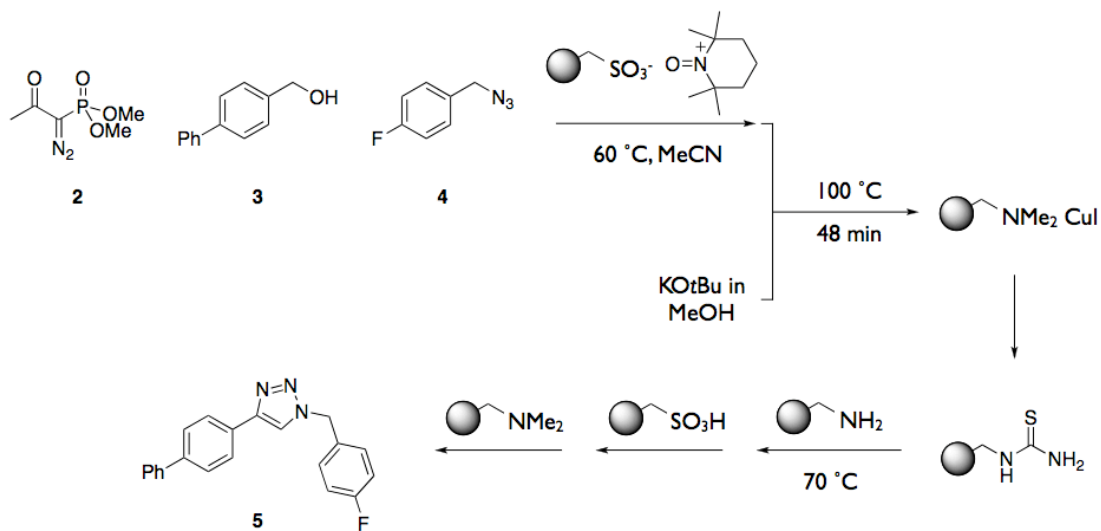


**Figure 1.6.** Ley's continuous flow synthesis of 1,4-disubstituted 1,2,3-triazoles.

elutes from the channel and enters a cartridge packed with immobilized copper. This immobilized copper cartridge facilitates the click reaction between the terminal acetylene and the organic azide. Residual copper is removed from the reaction stream using a cartridge packed with an immobilized-thiourea scavenging resin. Three successive scavenger cartridges are then used to remove residual starting materials, and basic and acidic residues from the reaction stream. A stream of pure triazole **5**

elutes from the reactor in a 55% yield with greater than 95% purity after recrystallization.

While these methods are effective, they rely on solid-supported reagent and scavenger cartridges that over time become depleted and need to be regenerated or discarded. Intermediate purification steps have been eliminated, but having to dispose of reagent/scavenger cartridges becomes a downfall of this process.

**Continuous Flow Synthesis Using In-Line Microextractors.** Another method developed by the Jensen group at MIT uses solution-phase reactions coupled with in-line microextractors to purify products before being passed into the next reaction (Figure 1.7).<sup>36</sup> Jensen and co-workers synthesized various carbamates in a three-step process, starting from acid chlorides with two in-line purification steps (Scheme 1.1).

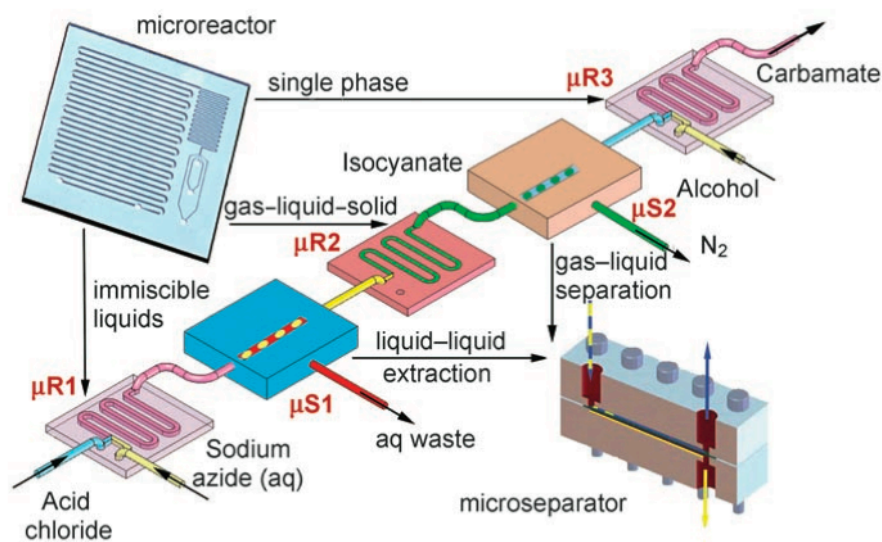
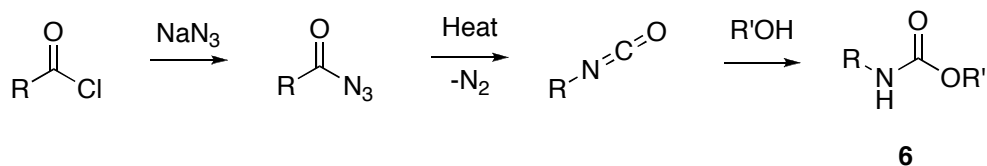


**Figure 1.7.** The experimental setup for the carbamate synthesis in flow. Reproduced with permission from: Sahoo, H. R.; Kralj, J. G.; Jensen, K. F. Multistep Continuous-Flow Microchemical Synthesis Involving Multiple Reactions and Separations. *Angew. Chem. Int. Ed.* **2007**, *46*, 5704-5708. Copyright 2007 Wiley-VCH Verlag GmbH & Co. KGaA.



**Scheme 1.1.** Model reaction for carbamate synthesis.

The first step of the reaction sequence converts an acid chloride to the acyl azide intermediate (Scheme 1.1). An in-line microextractor removes the water from the system before heating the organic stream to generate the isocyanate (the Curtius rearrangement). The isocyanate is subsequently mixed with an alcohol stream, affording various carbamates (**6**) in nearly quantitative yield with no breaks in the synthesis. This continuous flow synthesis benefits from generating and consuming intermediates such as acyl azides and isocyanates *in situ*, eliminating the need to store these dangerous compounds.

The microextractors used in this work use a fluoropolymer membrane that is selectively wetted by organic solvents.<sup>37-40</sup> This wetting enables the organic phase to pass through the membrane, separating it from the aqueous and gaseous phases. While these proof-of-concept cases are very promising, excess waste is generated due to the intermediate purification steps. Having the ability to run multiple reactions in sequence without purification or isolation brings about a significant advantage in terms of not only increased waste, but also in terms of maximizing the speed and efficiency of the process.

#### **Continuous Flow Syntheses Requiring No Intermediate Purification Steps.**

Recently Cosford and co-workers have developed a multi-step synthesis for 1,2,4-oxadiazoles in a continuous flow framework, requiring no intermediate purification steps.<sup>41</sup> The goal of this work was to develop a three-step, continuous flow process

that could generate sufficient amounts of product to be supplied for biological testing in a short amount of time (~30 minutes) (Figure 1.8).

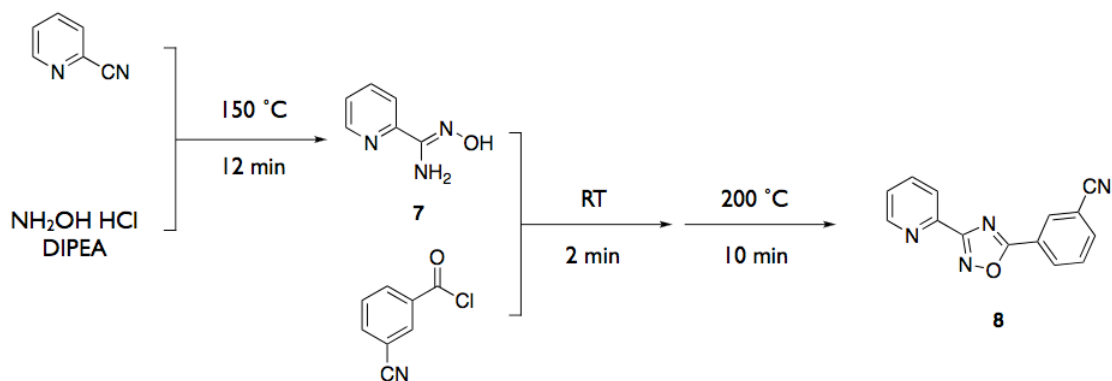


**Figure 1.8.** Cosford's three-step continuous flow synthesis of 1,2,4-oxadiazoles.

Mixing a stream of aryl nitrile with hydroxylamine hydrochloride and Hunig's base at  $150\text{ }^\circ\text{C}$  showed complete conversion to the corresponding amidoxime **7** after 12 minutes in the flow reactor. This outlet stream was cooled to  $0\text{ }^\circ\text{C}$  before adding a solution of acid chloride. The amidoxime and acid chloride reacted at room temperature to give the *O*-acyl amidoxime, which was immediately relayed into a reactor heated to  $200\text{ }^\circ\text{C}$ , yielding 1,2,4-oxadiazoles **8**.

These syntheses were very efficient, and purification by preparative HPLC was performed after the entire sequence had been completed. This methodology permits the facile development of chemical libraries of 1,2,4-oxadiazoles in 40-60% yield solely by changing the aryl nitrile and acid chloride inputs. Furthermore, this work by Cosford and co-workers is a prime example of how reaction kinetics can be increased using flow. An identical reaction sequence in batch takes in upwards of four days to complete. The flow sequence is much faster as reactions are superheated to temperatures well above reagent boiling points using backpressure regulators.

## ***Conclusion***

The multi-step reaction sequences outlined above are very elegant techniques, but could potentially be improved using other technology. Perhaps one of the most significant innovations in organic chemistry is the development of highly efficient catalytic reactions. While the continuous flow syntheses discussed in this chapter are groundbreaking, they are essentially void of any catalytic steps! The use of catalysis oftentimes increases reaction efficiency and selectivity.<sup>42</sup> Additional benefits include reduced use and cost of raw materials such as solvents and reagents, as well as the ability to introduce chemical complexity.<sup>43</sup> Few reports discuss the use of catalytic microreactors *in series* to realize multi-step reactions, although recent advances using catalysts in flow for single-step reactions suggest that coupling catalysts in series is soon to be achieved.

Perhaps even more promising is the use of heterogeneous catalysis in these microflow systems. Catalysts are typically the most expensive component of a reaction mixture and can be difficult to separate. Immobilizing a catalyst for use in flow is advantageous since it permits facile recycling and does not need to be separated from reaction streams. Furthermore, no agitation or stress is exerted on these supported catalysts, which oftentimes shortens the lifetime of these materials. As a result, these catalytic systems can be used continuously, enabling a high throughput of material.<sup>44, 45</sup> In this dissertation, the development of innovative strategies to make small molecules continuously in microreactors will be discussed, with the ultimate goal being entirely catalytic routes to important small molecules in flow. These continuous routes will ensure that these molecules are produced more efficiently, selectively and with a higher degree of safety, thus leading to reduced waste and cost.

## REFERENCES

1. Mason, B. P.; Price, K. E.; Steinbacher, J. L.; Bogdan, A. R.; McQuade, D. T. *Chem. Rev.* **2007**, *107*, 2300.
2. Hessel, V.; Lob, P.; Lowe, H. *Curr. Org. Chem.* **2005**, *9*, 765.
3. Hessel, V.; Lowe, H. *Chem. Eng. Technol.* **2005**, *28*, 267.
4. Hodge, P. *Curr. Opin. Chem. Biol.* **2003**, *7*, 362.
5. Jas, G.; Kirschning, A. *Chem. Eur. J.* **2003**, *9*, 5708.
6. Kirschning, A.; Monenschein, H.; Wittenberg, R. *Angew. Chem. Int. Ed.* **2001**, *40*, 650.
7. Pennemann, H.; Watts, P.; Haswell, S. J.; Hessel, V.; Lowe, H. *Org. Process Res. Dev.* **2004**, *8*, 422.
8. Haswell, S. J.; Watts, P. *Green Chem.* **2003**, *5*, 240.
9. *Microreactors in Organic Synthesis and Catalysis*: Wirth, T., Ed. Wiley-VCH: Weinheim, 2008.
10. Yoshida, J.; Nagaki, A.; Yamada, T. *Chem. Eur. J.* **2008**, *14*, 7450.
11. Watts, P.; Wiles, C. *Org. Biomol. Chem.* **2007**, *5*, 727.
12. Ahmed-Omer, B.; Brandt, J. C.; Wirth, T. *Org. Biomol. Chem.* **2007**, *5*, 733.
13. Ehrfeld, W.; Hessel, V.; Lowe, H. *Microreactors*; Wiley-VCH: Weinheim, 2000.
14. Roberge, D. M.; Ducry, L.; Bieler, N.; Cretton, P.; Zimmermann, B. *Chem. Eng. Technol.* **2005**, *28*, 318.
15. Dunn, P. J.; Galvin, S.; Hettenbach, K. *Green Chem.* **2004**, *6*, 43.
16. Boswell, C. More Than Meets the Eye. *ICIS Chemical Business*, April 29, 2009, pp 18-24.
17. Fukuyama, T.; Rahman, M. T.; Sato, M.; Ryu, I. *Synlett* **2008**, *2*, 151.

18. Sach, N. W. Automated Synthesis through Lab Automation. Presented at the 2008 Lab Automation Conference, Palm Springs, CA, 2008.
19. Steinbacher, J. L.; McQuade, D. T. *J. Polym. Sci. A: Polym. Chem.* **2006**, *44*, 6505.
20. Jahnisch, K.; Baerns, M.; Hessel, V.; Lowe, H. *Angew. Chem. Int. Ed.* **2004**, *43*, 406.
21. Schubert, K.; Brandner, J.; Fichtner, M.; Linder, G.; Schygulla, U.; Wenka, A. *Microscale Thermophys. Eng.* **2001**, *5*, 17.
22. Taghavi-Moghadam, S.; Kleemann, A.; Golbig, K. G. *Org. Process Res. Dev.* **2001**, *5*, 652.
23. Baldyga, J.; Pohorecki, R. *Chem. Eng. J.* **1995**, *58*, 183.
24. Bayer, T.; Himmler, K. *Chem. Eng. Technol.* **2005**, *28*, 285.
25. Hessel, V.; Lowe, H.; Stange, T. *Lab Chip* **2002**, *2*, 14N.
26. Thayer, A. M. Handle With Care. *C&E News*, March 16, 2009, pp 17-19.
27. Ducry, L.; Roberge, D. M. *Angew. Chem., Int. Ed.* **2005**, *44*, 7972.
28. Hornung, C. H.; Mackley, M. R.; Baxendale, I. R.; Ley, S. V. *Org. Process Res. Dev.* **2007**, *11*, 399.
29. Acke, D. R. J.; Stevens, C. V. *Org. Process Res. Dev.* **2006**, *10*, 417.
30. Bogdan, A. R.; Sach, N. W. *Adv. Synth. Catal.* **2009**, *351*, 849.
31. Baxendale, I. R.; Deeley, J.; Griffiths-Jones, C. M.; Ley, S. V.; Saaby, S.; Tranmer, G. K. *Chem. Commun.* **2006**, 2566.
32. Baxendale, I. R.; Ley, S. V.; Mansfield, A. C.; Smith, C. D. *Angew. Chem. Int. Ed.* **2009**, *48*, 4017.
33. Ohira, S. *Synth. Commun.* **1989**, *19*, 561.
34. Roth, G. J.; Liepold, B.; Muller, S. G.; Bestmann, H. J. *Synthesis* **2004**, 59-62.
35. Pietruszka, J.; Witt, A. *Synthesis* **2006**, 4266.
36. Sahoo, H. G.; Kralj, J. G.; Jensen, K. F. *Angew. Chem. Int. Ed.* **2007**, *46*, 5704.

37. Hartman, R. L.; Jensen, K. F. *Lab Chip* **2009**, DOI: 10.1039/b906343a.
38. Gunther, A.; Jensen, K. F. *Lab Chip* **2006**, *6*, 1487.
39. Aota, A.; Nonaka, M.; Hibara, A.; Kitamori, T. *Angew. Chem. Int. Ed.* **2007**, *46*, 878.
40. Kralj, J. G.; Sahoo, H. R.; Jensen, K. F. *Lab Chip* **2007**, *7*, 256.
41. Grant, D.; Dahl, R.; Cosford, N. D. P. *J. Org. Chem.* **2008**, *73*, 7219.
42. Denmark, S. E.; Jacobsen, E. N. *Acc. Chem. Res.* **2000**, *33*, 324.
43. Federsel, H. J. *Drug Discovery Today* **2006**, *11*, 966.
44. Bogdan, A. R. ; Mason, B. P.; Sylvester, K. T.; McQuade, D. T. *Angew. Chem. Int. Ed.* **2007**, *46*, 1698.
45. Bogdan, A. R.; McQuade, D. T. *Beilstein Journal of Organic Chemistry*, **2009**, *5*, 17.

## CHAPTER 2

### Improving Solid-Supported Catalyst Productivity by Using Simplified Packed-Bed Microreactors

#### *Preface*

Upon my arrival in the McQuade group, former McQuade group members Jeremy Steinbacher and Elizabeth Quevedo were developing a simplified microfluidic device using syringe pumps, syringes, needles and tubing. While this platform was initially used to synthesize polymeric materials, we saw the potential to run organic reactions within these channels as well. We therefore started to development of a novel microreactor to be used in organic synthesis that relied on solid-supported catalysts. The work described in this chapter set the foundation for future flow chemistry work performed in the group.

#### *Abstract\**

Packed-bed microreactors are formed from polymeric tubing and a resin-supported catalyst. By using supported catalysts in flow systems, productivity and recycling are greatly improved. This approach can be used to couple multiple catalysts together for generating complex molecules in one flow-through process.

#### *Introduction*

Catalysts supported on polymeric resins are readily synthesized and offer the promise of recycling and easy removal from reaction mixtures through filtration.<sup>1-4</sup>

---

\* Reproduced in part with permission from: Bogdan, A. R.; Mason, B. P.; Sylvester, K. T.; McQuade, D. T. Improving Solid-Supported Catalyst Productivity Using Packed-Bed Microreactors. *Angew. Chem. Int. Ed.* **2007**, *46*, 1698-1701. Copyright 2007 Wiley-VCH Verlag GmbH & Co. KGaA.

Often, however, such a support significantly diminishes a catalyst's activity.<sup>5</sup> Although homogeneous catalyst loadings in a batch reactor are simply increased by the addition of more catalyst, additional supported catalyst can hinder reagent mixing within a reaction vessel. These issues are circumvented by using continuous-flow systems. The use of flow is advantageous as the support does not need to be removed from the reaction mixture and continuous processing is also possible.<sup>6,7</sup> Our interest in microreactors prompted us to ask if supported catalysts would work when packed into small channels.

Microreactors are a relatively new technology for performing safer, more-efficient, and more-selective reactions.<sup>1,8-13</sup> The improved performance is attributed to faster heat transfer and mixing as a result of the increased surface area-to-volume ratio.<sup>8</sup> Despite the increasing body of literature on microreactors, few reports discuss the use of packed-bed microreactors applied to synthetic chemistry (Figure 2.1). What literature does exist concerning synthesis within these channels describes reactions performed by using solid-supported reagents that require regeneration.<sup>14-25</sup>

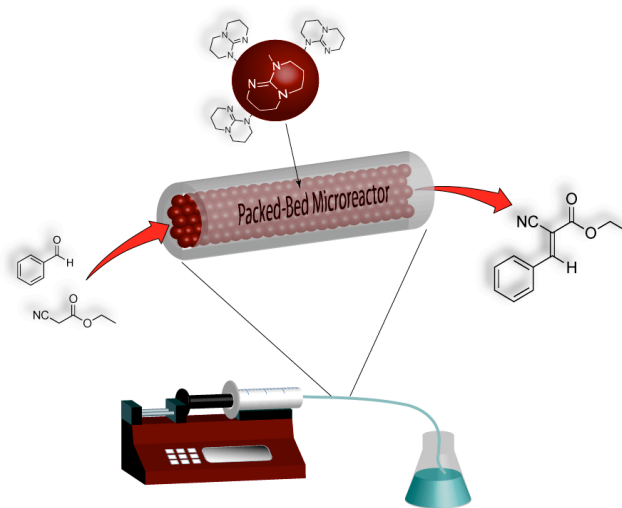


**Figure 2.1.** Flow reactions with a packed-bed microreactor.

A major issue encountered in packing microchannels with supported-catalysts is the pressure drop across the channel caused by either the swelling or size of the packing material.<sup>26-28</sup> Common Merrifield-type and gel-like resins are not appropriate for microchannel packing as they clog the channels when swollen with solvent, leading to irreproducible flow.<sup>26,27</sup> Other than monolithic materials,<sup>29-35</sup> no material investigated so far permits facile flow through packed-bed microreactors in a wide range of solvents. Herein, we demonstrate that a commercially available resin works well as a catalyst support in a high throughput, packed-bed microreactor and that supported catalysts in flow systems yield greater productivity (Equation 2.1). We limit this discussion to commercially available polymeric resins.

$$\text{productivity} = \frac{\text{moles product}}{\text{reactor volume} \times \text{time} \times \text{moles catalyst}} \quad (\text{Equation 2.1})$$

### ***Results and Discussion***

Although the use of electroosmotic flow permits flow through a wider range of packing materials,<sup>36</sup> these systems are far more complex than pressure-driven systems and only work with polar solvents. We subsequently examined a wide range of resins to be used in a pressure-driven system by passing different solvents through a 10-cm packed bed and qualitatively assessing whether flow was free or constricted (Table 2.1). Typically, lightly cross-linked resins swell in certain solvents, which prohibits flow through the microchannels. Highly cross-linked or macroreticular resins and silicas, on the other hand, allow flow under nearly all solvent conditions as they do not swell. Numerous solid-supported catalysts have been reported in the literature, including analogues of the supported catalysts discussed herein.<sup>1</sup> Nonetheless, our flow experiments showed that many polymeric resins do not permit flow in a wide array of solvents. A packing material that does not restrict flow is desired as higher

flow rates and output can be attained.

**Table. 2.1** Packing materials tested as supports for packed-bed microreactors.

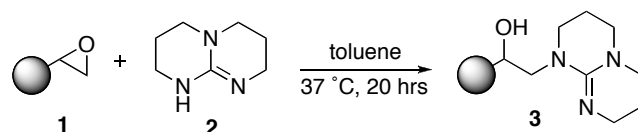
Packing Material	Composition	H <sub>2</sub> O	EtOH	Acetone	CHCl <sub>3</sub>	THF
Silica Gel (225-420 mesh)	SiO <sub>2</sub>	+ <sup>a</sup>	+	+	+	+
Amberlite XAD2	PS	+	+	+		
Amberlite CG50	methacrylate, carboxylic functionalization	–	–	–		
Amberlite IRA-900	PS, quaternary ammonium		–			
PS Beads (1% DVB)	PS	–	+/-	+/-	–	–
PS Beads (2% DVB)	PS	–	–	+	–	–
Amberlyst 15(dry)	acrylic, macroreticular		+		+	
Dowex 1X2-200 (2% crosslink)	PS, quaternary ammonium	–	–			
Dowex 50WX8-200 (8% crosslink)	PS, sulfonic acid	+	+		+	
PS-DMAP	PS, 2% DVB		–		–	+
Amberzyme Oxirane	methacrylic, macroreticular	+	+	+	+	+

<sup>a</sup> (+) – unencumbered flow, (–) – restricted flow

Of the two supports that passed our flow tests (flow with no pressure drop), we favored the methacrylate-based Amberzyme Oxirane resin (AO, **1**), a macroreticular resin with a large, fixed pore volume and pendant epoxide groups designed for enzyme immobilization. Catalysts were attached to the resin by direct nucleophilic

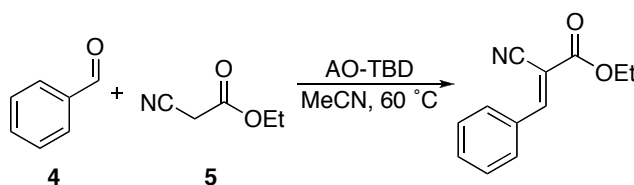
attack or by a Huisgen cycloaddition to an azide-modified AO. These catalysts showed excellent batch activity, but when they were used in packed-bed microreactors, their productivity increased significantly (Equation 2.1).

We tethered organocatalysts containing nucleophilic groups to AO. As an example, we reacted 1,5,7-triazabicyclo-[4.4.0]undec-3-ene (TBD, **2**) with the epoxide



**Scheme 2.1.** Preparation of AO-TBD resin.

(Scheme 2.1). Solid-supported TBD has been demonstrated to catalyze a number of reactions<sup>1,37</sup> but has not yet been used in a pressure-driven flow system.<sup>36,38</sup> TBD on AO (AO-TBD, **3**, Scheme 2.1) is a highly active, Knoevenagel catalyst in batch systems but works significantly better in flow systems. We selected a Knoevenagel



**Scheme 2.2.** The Knoevenagel condensation between benzaldehyde and ethyl cyanoacetate.

condensation between benzaldehyde (**4**) and ethyl cyanoacetate (**5**) as a demonstration (Scheme 2.2). All flow experiments were performed by using a simplified packed-bed microreactor based on a platform developed within our group and also by others (Figure 2.2).<sup>39-42</sup> The present device consisted of fluoroelastomeric tubing (1.6-mm inner diameter) packed with functionalized AO resins (Figure 2.2b).

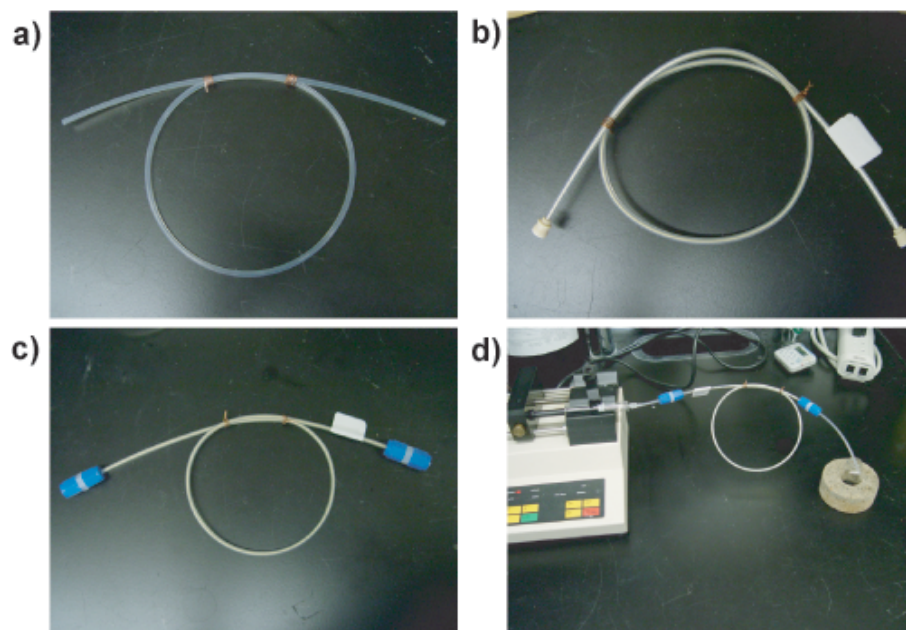


**Figure 2.2.** The simplified microreactor: empty tubing (a) filled with AO resin (b) with filter caps (c) and attached to syringe pumps (d).

For the flow Knoevenagel condensation experiments, a 30-cm segment of tubing was packed with AO-TBD and placed in an HPLC column oven set to 60 °C. A solution of benzaldehyde in acetonitrile was prepared, to which ethyl cyanoacetate was added prior to the flow experiment. At a flow rate of 50  $\mu\text{L min}^{-1}$  (approximately 280 s residence time), a conversion of 93% was obtained (Figure 2.3). This flow rate gives over 200 mg of product per hour from a single channel. The device presented provides roughly forty times the output of previously reported flow devices.<sup>29</sup> The increased performance of a packed-bed microreactor is due to the small dimensions of the channel, allowing rapid and uniform heating. In addition, all packed-bed reactors benefit from flowing reagents over the catalyst-bound resin. This feature allows the catalyst loading to be maximized and for transfer of reagents and starting materials into and out of the beads.

As anticipated, increasing the flow rate (decreasing the residence time) gave lower conversions (Figure 2.3). The process of numbering up could be applied to acquire higher outputs since reactor conditions need not be changed upon reaction scaling.<sup>43</sup> The AO–TBD packed channel was used 30 times without apparent catalyst degradation. After each trial, the column was simply regenerated with aqueous ammonia and washed with acetonitrile to maintain activity.

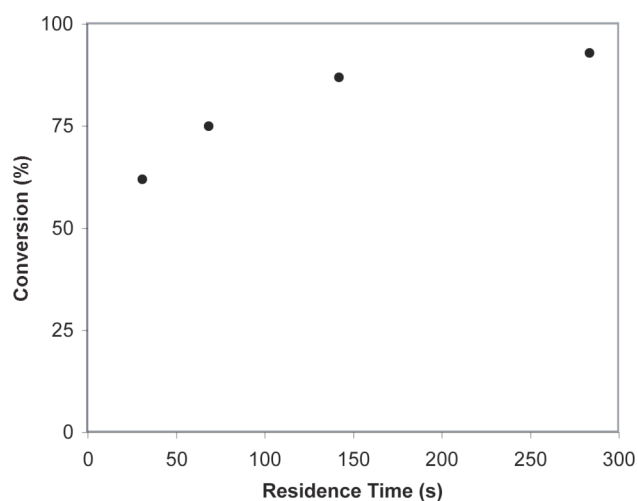


**Figure 2.3.** Conversion of flow Knoevenagel condensations as a function of residence time.

Knoevenagel condensations were run on an identical scale and concentration in both the batch and flow experiments. In both cases, the resulting reaction-mixture volume and amount of AO–TBD catalyst were the same. A conversion of 90% was achieved in the flow system (at  $50 \mu\text{L min}^{-1}$ , resulting in 3 mL total volume in one hour), and the reaction mixture could be concentrated under high vacuum to yield the product. Batch reactions, however, yielded only 69% conversion after one hour (reaction volume of 3 mL). The microreactor productivity for the flow reactions was

3.4 times greater than the batch reaction owing to the decreased dimensions of the reactor and better mixing (Table 2.2).

**Table 2.2.** Flow reaction productivities.

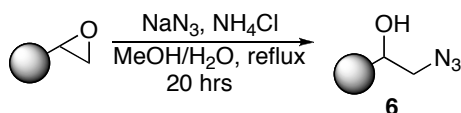
<b>Reaction</b>	<b>Flow Productivity<sup>a</sup></b>	<b>Batch Productivity</b>	<b>Flow/Batch Productivity</b>
TBD Knoevenagel	1.12	0.33	3.4
TBD Knoevenagel (double scale)	0.75	0.13	5.8
DMAP acylation <sup>b</sup>	3.2	1.0	3.2

<sup>a</sup> Productivities are measured in mmol product mL<sup>-1</sup> min<sup>-1</sup> mmol catalyst<sup>-1</sup>.

<sup>b</sup> Batch reaction for the acylation run by using 10 mg of catalyst compared with 215 mg for the flow reaction.

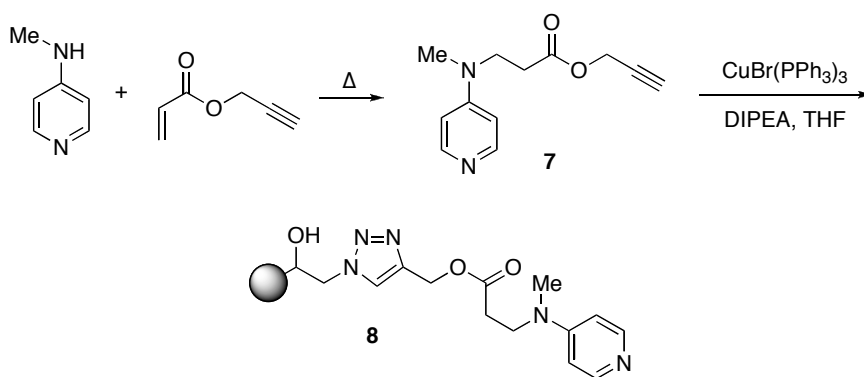
Increasing the scale of the reaction emphasizes the benefits of using the packed-bed reactor. By doubling the reaction size and maintaining a constant mass of AO-TBD, the productivity for batch reactions decreased by 2.5, whereas the productivity of the flow reactions changed very little. We propose that the microreactor performs better because the molar ratio of the starting material for AO-TBD remains constant in the microreactor as new reaction mixture is continuously introduced. The productivity at this larger scale is 5.8, which should increase as the scale of the reaction increases (Table 2.2).

We then prepared a packed-bed reactor by using immobilized 4-dimethylaminopyridine (DMAP), a catalyst that has been studied extensively on solid supports.<sup>5, 44-46</sup> Azide-functionalized AO resin (AO-N<sub>3</sub>, **6**) was prepared by treatment

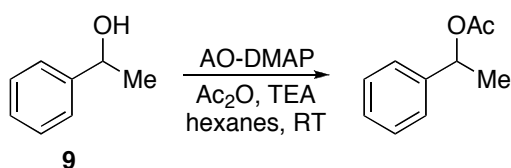


**Scheme 2.3.** Preparation of AO-N<sub>3</sub> resin.

of AO with sodium azide (Scheme 2.3).<sup>47</sup> An acetylene-functionalized DMAP (7), synthesized by using a Michael addition,<sup>48</sup> was conjugated to AO-N<sub>3</sub>, affording the DMAP-functionalized resin (AO-DMAP, 8, Scheme 2.4). The acylation of sec-phenethyl alcohol (9) was used as a test reaction (Scheme 2.5).



**Scheme 2.4.** Preparation of AO-DMAP resin.



**Scheme 2.5.** The acylation of sec-phenethyl alcohol.

Acetic anhydride was added to a stock solution of sec-phenethyl alcohol and triethylamine in hexanes and used immediately in the flow experiment. Full conversion was achieved at a flow rate of 0.5 mL min<sup>-1</sup> (approximately 48 s

residence time; Figure 2.4). At  $0.5 \text{ mL min}^{-1}$ , extrapolation of this output suggests that 1.6 g of product per hour could be obtained from a single 60-cm channel. Use of the highest flow rate of the syringe pump ( $3.9 \text{ mL min}^{-1}$ ) gave the highest throughput of the acylated product ( $50.5 \text{ mmol h}^{-1}$ ), albeit the lowest conversion (68.5%).

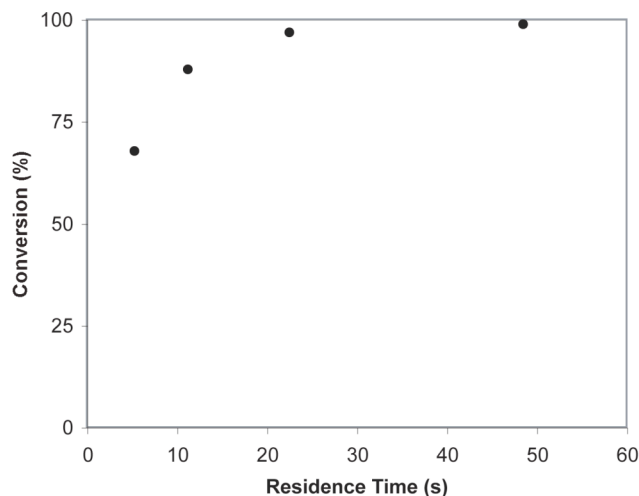


**Figure 2.4.** AO-DMAP-catalyzed flow acylation of sec-phenethyl alcohol.

As with the Knoevenagel condensation, the flow acylation was run in direct comparison with the batch reaction by using identical amounts of catalyst, reagent concentrations, and final reaction volumes (3 mL). In this case, the flow acylation was marginally superior to the batch reaction, generating 95% conversion in flow experiments (at  $50 \text{ mL min}^{-1}$ , resulting in 3-mL total volume in one hour) versus 92% conversion in one hour in batch experiments.

However, AO-DMAP catalyzed acylations were more productive in flow experiments compared with batch experiments (Table 2.2). Furthermore, the AO-DMAP packed columns were reusable, and each column could be used in 35 trials without showing any apparent loss in catalytic activity (no regeneration was required).

For this reason the AO-DMAP packed-bed microreactor is again superior to the batch system, because in flow systems, the catalyst is left in place and does not have to be recovered from the reaction.

Reaction scale-up of flow reactions comprises of a process known as numbering up.<sup>43, 49, 50</sup> Numbering up a reaction entails the addition of identical reactors in parallel and requires only changing the flow rate of the reagent stream. This process is highly advantageous as small scale reactions do not need to be reengineered to work on a larger scale. As a result, the development of large-scale synthesis is much faster, and the expenses associated with this scale-up are greatly diminished.

We chose to demonstrate this simplified reaction scale-up using the AO-TBD-catalyzed Knoevenagel condensation between benzaldehyde and ethyl cyanoacetate (Scheme 2.2). Using a single AO-TBD packed bed at a flow rate of 50  $\mu\text{L}/\text{min}$ , approximately a 93% conversion was obtained. This corresponded to an output of 210 mg/hr product (90% yield) (Figure 2.5). Simple concentration of the output stream afforded an off-white crystalline material.

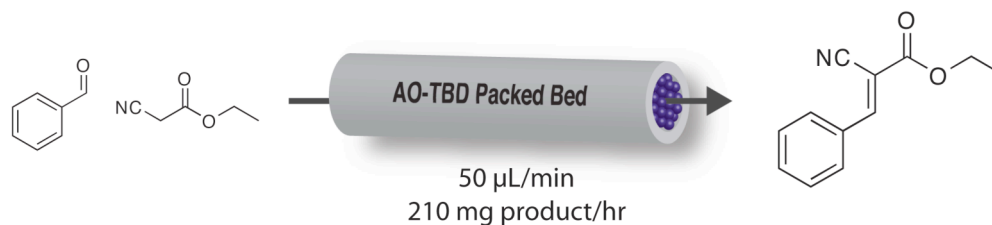


**Figure 2.5.** Yield from a single-channel AO-TBD packed-bed microreactor.

The activity of this single-channel system was monitored over the course of one hour (Figure 2.6). After about 60 minutes of continuous use, the conversion starts to diminish, indicating that the AO-TBD packed bed needs to be regenerated. After

flushing the column with 1 M aqueous ammonia, the system once again reached its high activity.

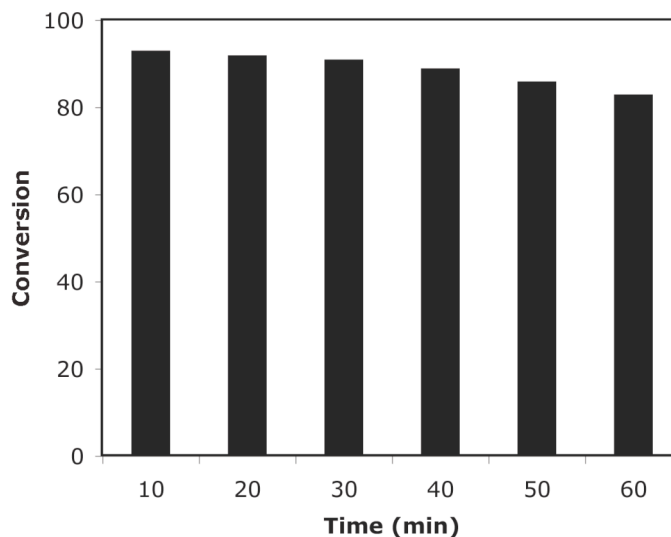


**Figure 2.6.** Long-term activity of single channel AO-TBD microreactor.

The Knoevenagel condensation was subsequently scaled-up to an eight-channel system. The only variable that needed to be changed in this case was the flow rate; having increased the flow rate eightfold, from 50  $\mu\text{L}/\text{min}$  to 400  $\mu\text{L}/\text{min}$ . In this scaled-up reaction, the hourly output increased from 210 mg/hr to 1.85 g/hr (98% yield) (Figure 2.7).

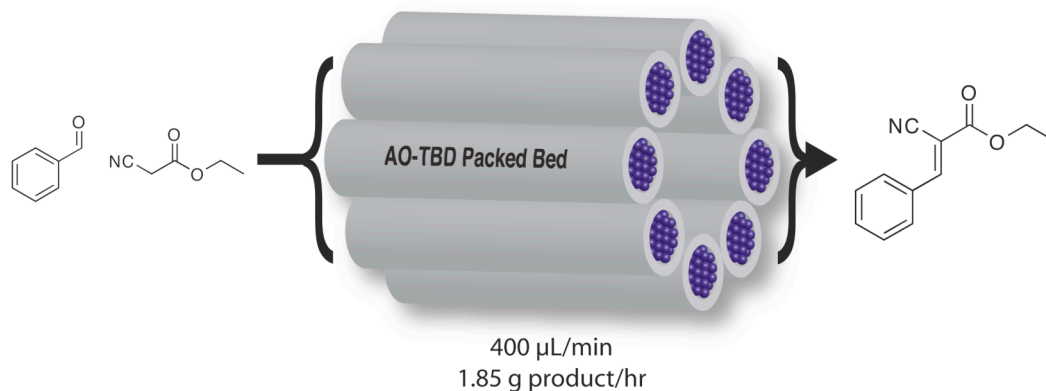


**Figure 2.7.** Yield from an eight-channel AO-TBD packed-bed microreactor.

The activity of this 8-channel system also remained high, however, after an hour of continuous use, the activity started to drop sharply (Figure 2.8). As with the one-channel system, the AO-TBD resin needed to be regenerated in order to maintain its high activity.

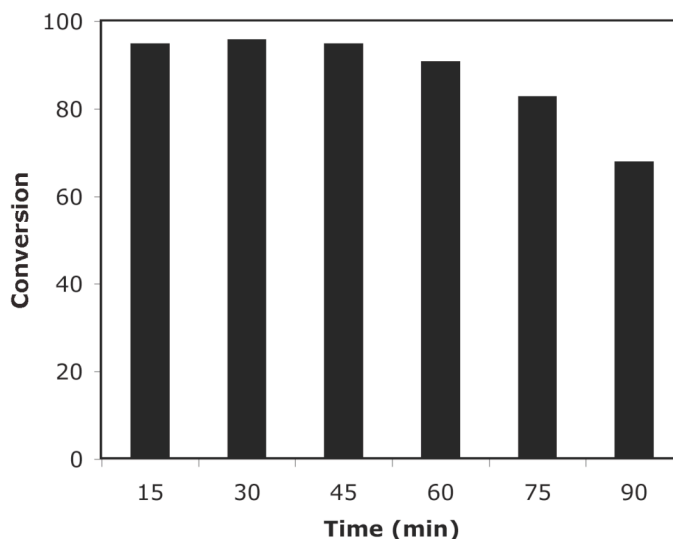


**Figure 2.8.** Long-term activity of eight-channel AO-TBD microreactor.

A higher yield was obtained during the 8-channel system, a result that may be attributed to the different heating sources that were employed. For the single-channel example, an HPLC column heater over was utilized which may not have provided intimate contact with the microchannels. For the 8-channel system, however, a new heat exchanger was developed (Figure 2.9). The eight channels were connected using a series of Y-junctions to split the flow of the reagent stream. The 8-channel AO-TBD packed bed was subsequently placed within a piece of PVC tubing, having been equipped with a water inlet and outlet (similar to that which is present on a condenser). Using a temperature controller and a pumping mechanism, a stream of

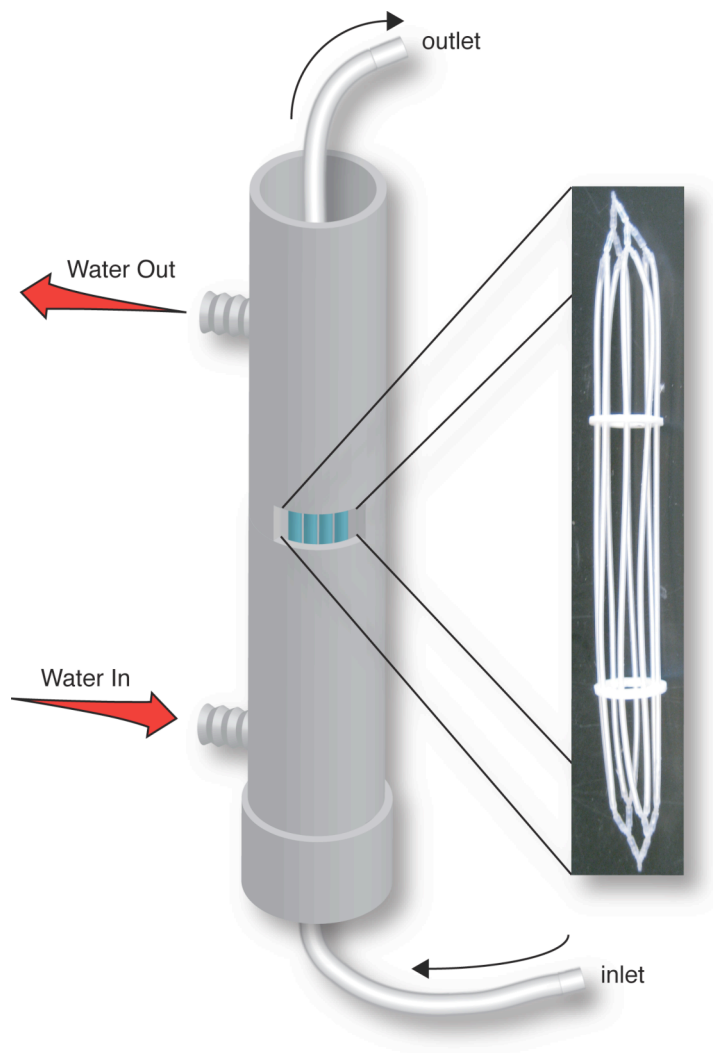


**Figure 2.9.** Heat exchanger for large-scale flow reactions.

60 °C water was passed through the heat exchanger. This method of heating ensured that the tubing was in intimate contact with the heat source, whereas in the column heater, this was not necessarily guaranteed.

To permit continuous processing in this packed-bed system, the issue of regeneration must be addressed. To do this, one could envision a dual reactor set-up, in which one reactor is being regenerated and one reactor is functioning (Figure 2.10).

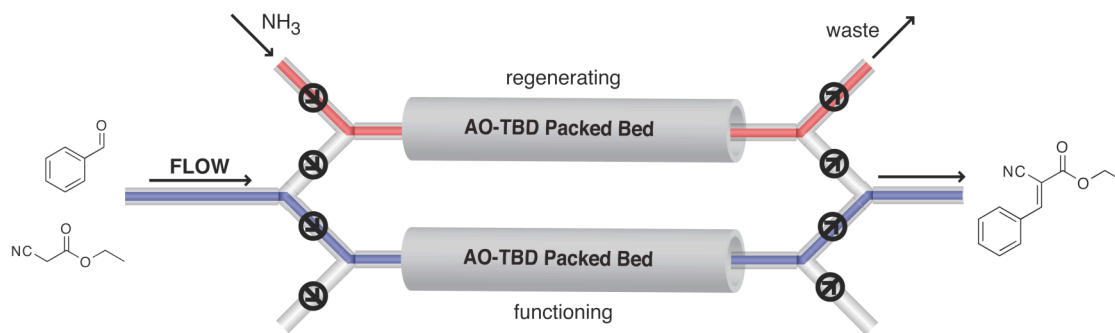


**Figure 2.10.** Two channel packed-bed microreactor with one functioning and one regenerating AO-TBD channel.

Using a series of valves, the flow could be diverted through one AO-TBD channel while the aqueous ammonia stream is regenerating the other channel. Once the activity of the functioning packed-bed starts to diminish and the other packed-bed has been regenerated, the valves can be switched to maintain the high output of product. This process would enable continuous processing as the system would not need to be stopped at any time to regenerate the catalyst.

### ***Conclusion***

Aside from increased productivity and ease of use, packed-bed microreactors containing AO-modified resins are superior to batch reactions for other reasons. The resin within the reactor remains intact throughout the course of the flow reaction, whereas in batch systems, most resins, including AO, showed signs of structural damage.<sup>33</sup> Flow reactions also increase mixing without destroying the packing material by splitting the substrate stream into smaller segments of flow, leading to turbulent mixing.<sup>51</sup>

Though monolithic packed beds may provide more efficient contact between reagents and starting materials, we feel that the use of resins has advantages; namely the resin's ease of modification and characterization prior to channel packing.

These materials showed remarkable activity when used in batch reactors, yet were even more productive in the continuous-flow system. The device also enables a facile method to run high-throughput processes compared with previous literature that used microreactors. Compared with batch reactors, both AO-TBD and AO-DMAP show increased productivity owing to the improved mixing and decreased dimensions of the channel. This simplified approach to continuous catalytic chemistry can be used to couple multiple catalysts together for generating complex molecules in one flow-through process. The use of purely catalytic-flow reactors will provide higher throughput and efficiency relative to the groundbreaking continuous-flow systems that use both resin-bound catalysts and reagents.<sup>14-20</sup> Finally, the use of packed-bed microreactors instead of larger bore-flow reactors will allow much faster heating and heat removal. Consistent temperature across the channel will combine the advantages of microreactors with packed-bed reactors.

### ***Experimental Section***

**General Considerations.** Solvents were purified by standard procedures. Triethylamine was purified by sequential treatment with benzoyl chloride, drying over CaH<sub>2</sub>, and distillation. All other reagents were used as received, unless otherwise noted. <sup>1</sup>H NMR spectra were recorded in CDCl<sub>3</sub> on Varian Mercury 300MHz and Inova 400 MHz spectrometers operating at 299.763 MHz and 399.780 MHz, respectively, using residual solvent as the reference. ATR-IR was performed on a Nicolet Avatar DTGS 370 infrared spectrometer with Avatar OMNI sampler and OMNIC software. Elemental analysis was performed by Robertson Microlit Laboratories, Inc., in Madison, New Jersey. Gas chromatographic (GC) analyses were carried out on a Varian Model 3800 using a CP-Sil regular phase column (30.0 m x 0.25 mm i.d.).

**Channel Packing.** A 60 cm section of tubing (Swagelok PFA Tubing, 1/8" outer diameter) was attached to a Swagelok PFA union packed with glass wool. A separate union (not packed with glass wool) was attached to the inlet side of the 60 cm column. Two 10 cm sections of tubing were attached to the channel, serving as the outlet. A 1/16" female Luer was attached to the inlet. Functionalized (**3** or **4**) resin was suspended in CH<sub>2</sub>Cl<sub>2</sub> and the column slurry packed using a syringe.

**AO-TBD (1).** Amberzyme<sup>TM</sup> Oxirane (302.9 mg, 1.0 mmol epoxide/g resin, 0.30 mmol epoxide) was suspended in a solution of TBD (193.7 mg, 1.4 mmol, 4.6 eq.) in dry toluene (10 mL). The suspension was shaken for 24 hrs at 37 °C. The resin was filtered and washed with CH<sub>2</sub>Cl<sub>2</sub> (2x 10 mL), MeOH (2x 10 mL), and Et<sub>2</sub>O (1x 10 mL) and dried under vacuum to give 322.7 mg of resin (0.44 mmol TBD/g resin). The loading was calculated by mass difference.

**Representative Flow Knoevenagel Condensation Procedure.** A 2.5 mL aliquot of a stock solution containing benzaldehyde (0.39 M, 0.98 mmol, 1.0 eq) in acetonitrile was placed in a 4 mL screw cap vial. Ethyl cyanoacetate (120 μL, 1.13 mmol, 1.1 eq) was added to the aliquot and transferred to a 5.0 mL syringe. A 30 cm channel was packed with 102.4 mg AO-TBD, flushed with acetonitrile and placed in an HPLC column oven set to 60 °C. The syringe was placed on the syringe pump, attached to the microchannel and flow initiated. Reaction mixtures were collected in a 4 mL screw cap vial until the entire solution had been flushed from the syringe. After each trial, the column was regenerated with 5 mL 1 M NH<sub>3</sub>, followed by 5 mL acetonitrile. Conversions were calculated as the area of product divided by the sum of product and starting material area.

**Batch Knoevenagel Condensations.** A 2.5 mL aliquot of a stock solution containing benzaldehyde (0.39 M, 0.98 mmol, 1.0 eq) in acetonitrile was placed in a 4 mL screw cap vial. Ethyl cyanoacetate (120  $\mu$ L, 1.13 mmol, 1.1 eq.) and **3** (103.3 mg, 0.0424 mmol, 0.043 eq.) were added to the stock solution and heated to 60 °C with gentle stirring. 20  $\mu$ L samples were quenched using CH<sub>2</sub>Cl<sub>2</sub> and conversions were calculated as the area of product divided by the sum of product and starting material area.

**AO-N<sub>3</sub> (6).** Sodium azide (5.26 g, 81 mmol, 8.1 eq.) and ammonium chloride (2.27 g, 42.4 mmol, 4.2 eq.) were dissolved in 500 mL 90:10 v/v water in methanol. Amberzyme<sup>TM</sup> Oxirane (10.0 g, 1.0 mmol epoxide/g resin, 10.0 mmol, 1.0 eq.) was suspended in the azide solution and the reaction mixture refluxed overnight with gentle stirring. The resin was filtered using a Buchner funnel, washed with DI H<sub>2</sub>O (2x 50 mL), MeOH (2x 50 mL), Et<sub>2</sub>O (1x 25 mL), and dried under vacuum. Elemental analysis afforded a loading of 1.0 mmol N<sub>3</sub>/g resin.

**Acetylene-Modified DMAP (7).** *N*-methylamino pyridine (500 mg, 4.6 mmol) and propargyl acrylate (2.0 mL, 18.1 mmol) were heated to 90°C for 2 hours. The residual acrylate was removed by vacuum distillation. The product was purified by column chromatography (silica gel, 10:1 CH<sub>2</sub>Cl<sub>2</sub>/MeOH) to afford a tan solid (653 mg, 65%). <sup>1</sup>H NMR (400 MHz, CDCl<sub>3</sub>)  $\delta$  8.19 (d, *J* = 5.55 Hz, 2H), 7.14-7.36 (m, 5H), 6.65 (d, *J* = 6.43 Hz, 2H), 4.59 (s, 2H), 3.08 (s, 3H). <sup>13</sup>C NMR (400 MHz, CDCl<sub>3</sub>)  $\delta$  171.05, 153.22, 149.91, 110.00, 106.93, 75.49, 52.54, 47.29, 37.88, 31.82.

**AO-DMAP (8).** **3** (72.6 mg, 0.33 mmol, 1.0 eq), CuBr(PPh<sub>3</sub>)<sub>3</sub> (35.0 mg, 0.037 mmol, 0.11 eq) and DIPEA (280  $\mu$ L, 1.7 mmol, 5.1 eq) were dissolved in anhydrous THF (20 mL). **2** (305 mg, 1.0 mmol N<sub>3</sub>/g resin, 0.31 mmol, 0.9 eq) was added to the solution

and placed under a N<sub>2</sub> atmosphere. The suspension was heated to 50 °C for 3 days. The resulting resin was green, most likely due to Cu chelation. The resin was washed with THF (2x 10 mL), MeOH (1x 10 mL), 1 M HCl (2x 10 mL), DI H<sub>2</sub>O (1x 10 mL), sat. NaHCO<sub>3</sub> (2x 10 mL), DI H<sub>2</sub>O (1x 10 mL), MeOH (1x 10 mL) and Et<sub>2</sub>O (1x 10 mL), and dried under vacuum to yield the beige AO-DMAP resin (342 mg, 0.50 mmol DMAP/g resin). The loading was calculated by mass difference. ICP showed a negligible Cu loading (0.01 mmol/g resin) and this was concluded to be too small to be catalyzing the acylation reaction.

**Representative Flow Acylation Procedure.** A 2.5 mL aliquot of a stock solution containing *sec*-phenethyl alcohol (0.33 M, 0.825 mmol, 1.0 eq) and TEA (0.50 M, 1.25 mmol, 1.5 eq) in hexanes was placed in a 4 mL screw cap vial. Acetic anhydride (120 μL, 1.25 mmol, 1.5 eq) was added to the aliquot and transferred to a 5.0 mL syringe. Prior to syringe attachment, the channel was flushed with hexanes. The syringe was placed on the syringe pump and flow was initiated. The reaction mixture was collected in a 4 mL screw cap vial until the sample had eluted through the channel. After each trial, the channel was washed with 5 mL CH<sub>2</sub>Cl<sub>2</sub> followed by 5 mL hexanes. Conversions were calculated as the area of product divided by the sum of product and starting material area.

**Representative Batch Acylation Procedure.** A 2.5 mL aliquot of a stock solution containing *sec*-phenethyl alcohol (0.33 M, 0.825 mmol, 1.0 eq) and TEA (0.50 M, 1.25 mmol, 1.5 eq) in hexanes was added to a vial containing **2** (10.9 mg, 0.005 mmol, 0.007 eq). Acetic anhydride (120 μL, 1.25 mmol, 1.5 eq.) was added to the sample and rocked gently. Conversions were calculated as the area of product divided by the sum of product and starting material area.

**Representative Batch Acylation Procedure.** A 2.5 mL aliquot of a stock solution containing *sec*-phenethyl alcohol (0.33 M, 0.825 mmol, 1.0 eq) and TEA (0.50 M, 1.25 mmol, 1.5 eq) in hexanes was added to a vial containing **2** (10.9 mg, 0.005 mmol, 0.007 eq). Acetic anhydride (120  $\mu$ L, 1.25 mmol, 1.5 eq.) was added to the sample and rocked gently. Conversions were calculated as the area of product divided by the sum of product and starting material area.

**Equivalent Acylation Reactions in Batch and Flow.** *Batch* - Three 4 mL screw vials were each charged with **2** (30.0 mg, 0.015 mmol, 0.015 eq). A 3.0 mL aliquot of a stock solution containing *sec*-phenethyl alcohol (0.33 M, 0.990 mmol, 1.0 eq) and TEA (0.50 M, 1.50 mmol, 1.5 eq) in hexanes was added to each vial. Acetic anhydride (150  $\mu$ L, 150 mmol, 1.5 eq) was added to the reaction vessels. Each batch reaction was gently rocked and sampled at 20, 40, and 60 minutes. Conversions were determined by calculating the area of product divided by the sum of product and starting material areas.

*Flow* - Flow reactions were run using a 6 cm column packed with **2** (30.5 mg, 0.0015 mmol, 0.011 eq). The column was rinsed with methylene chloride and hexanes prior to each flow experiment. A 4 mL aliquot of stock solution containing *sec*-phenethyl alcohol (0.33 M, 1.32 mmol, 1.0 eq) and TEA (0.50 M, 2.00 mmol, 1.5 eq) was added to a 20 mL screw cap vial along with acetic anhydride (195  $\mu$ L, 2.04 mmol, 1.5 eq). The mixture was collected in a syringe and flowed through the column containing **2** and then stirred vigorously. Product was collected for one hour at a flow rate of 50  $\mu$ L/min and sampled directly from the channel at 10, 20, 23, 36, 40, 50, and 60 minutes. At the end of the hour, roughly 3.0 mL had been flowed through the column making the flow reaction identical to the batch reaction. Also, the entire 3.0 mL

volume collected was sampled. Product conversion was measured by comparing the GC area of the product to the sum of the areas of the product and starting material.

## REFERENCES

1. Kirschning, A.; Monenschein, H.; Wittenberg, R. *Angew. Chem. Int. Ed.* **2001**, *40*, 650.
2. Ley, S. V.; Baxendale, I. R.; Bream, R. N.; Jackson, P. S.; Leach, A. G.; Longbottom, D. A.; Nesi, M.; Scott, J. S.; Storer, R. I.; Taylor, S. J. *J. Chem. Soc. Perkin Trans. 1* **2000**, 3815.
3. Broadwater, S. J.; Roth, S. L.; Price, K. E.; Kobašlija, M.; McQuade, D. T. *Org. Biomol. Chem.* **2005**, *3*, 2899.
4. Frenzel, T.; Solodenko, W.; Kirschning, A. in *Polymeric Materials in Organic Synthesis and Catalysis* (Ed.: M. R. Buchmeiser), Wiley-VCH, Weinheim, 2006, pp. 201.
5. Price, K. E.; Mason, B. P.; Bogdan, A. R.; Broadwater, S. J.; Steinbacher, J. L.; McQuade, D. T. *J. Am. Chem. Soc.* **2006**, *128*, 10376.
6. Kirschning, A.; Solodenko, W.; Mennecke, K. *Chem. Eur. J.* **2006**, *12*, 5972.
7. Cozzi, F. *Adv. Synth. Catal.* **2006**, *348*, 1367.
8. Hessel, V.; Lowe, H. *Chem. Eng. Technol.* **2005**, *28*, 267.
9. Hessel, V.; Lob, P.; Lowe, H. *Curr. Org. Chem.* **2005**, *9*, 765.
10. Pennemann, H.; Watts, P.; Haswell, S. J.; Hessel, V.; Lowe, H. *Org. Process Res. Dev.* **2004**, *8*, 422.
11. Jas, G.; Kirschning, A. *Chem. Eur. J.* **2003**, *9*, 5708.
12. Hodge, P. *Curr. Opin. Chem. Biol.* **2003**, *7*, 362.
13. Haswell, S. J.; Watts, P. *Green Chem.* **2003**, *5*, 240.
14. Baxendale, I. R.; Deeley, J.; Griffiths-Jones, C. M.; Ley, S. V.; Saaby, S.; Tranmer, G. K. *Chem. Commun.* **2006**, 2566.
15. Baxendale, I. R.; Griffiths-Jones, C. M.; Ley, S. V.; Tranmer, G. K. *Synlett* **2006**, 427.
16. France, S.; Bernstein, D.; Weatherwax, A.; Lectka, T. *Org. Lett.* **2005**, *7*, 3009.

17. Hafez, A. M.; Dudding, T.; Wagerle, T. R.; Shah, M. H.; Taggi, A. E.; Lectka, T. *J. Org. Chem.* **2003**, *68*, 5819.
18. Hafez, A. M.; Taggi, A. E.; Dudding, T.; Lectka, T. *J. Am. Chem. Soc.* **2001**, *123*, 10853.
19. Hafez, A. M.; Taggi, A. E.; Lectka, T. *Chem. Eur. J.* **2002**, *8*, 4114.
20. Hafez, A. M.; Taggi, A. E.; Wack, H.; Drury, W. J.; Lectka, T. *Org. Lett.* **2000**, *2*, 3963.
21. Papers exist that use activated carbon and functionalized walls as a support for palladium. Nonetheless, these supports are not discussed as the focus is polymeric resins and silicas.
22. Saaby, S.; Knudsen, K. R.; Ladlow, M.; Ley, S. V. *Chem. Commun.* **2005**, 2909.
23. Kobayashi, J.; Mori, Y.; Kobayashi, S. *Adv. Synth. Catal.* **2005**, *347*, 1889.
24. Kobayashi, J.; Mori, Y.; Kobayashi, S. *Chem. Commun.* **2005**, 2567.
25. Kobayashi, J.; Mori, Y.; Okamoto, K.; Akiyama, R.; Ueno, M.; Kitamori, T.; Kobayashi, S. *Science* **2004**, *304*, 1305.
26. Nikbin, N.; Watts, P. *Org. Process Res. Dev.* **2004**, *8*, 942.
27. Phan, N. T. S.; Brown, D. H.; Styring, P. *Green Chem.* **2004**, *6*, 526.
28. Svec, F.; Frechet, J. M. J. *Science* **1996**, *273*, 205.
29. Svec, F.; Frechet, J. M. J. *Anal. Chem.* **1992**, *64*, 820.
30. Svec, F.; Frechet, J. M. J. *Chem. Mater.* **1995**, *7*, 707.
31. Viklund, C.; Svec, F.; Frechet, J. M. J.; Irgum, K. *Chem. Mater.* **1996**, *8*, 744.
32. Kunz, U.; Kirschning, A.; Wen, H. L.; Solodenko, W.; Cecilia, R.; Kappe, C. O.; Turek, T. *Catal. Today* **2005**, *105*, 318.
33. Solodenko, W.; Wen, H. L.; Leue, S.; Stuhlmann, F.; Sourkouni-Argirusi, G.; Jas, G.; Schonfeld, H.; Kunz, U.; Kirschning, A. *Eur. J. Org. Chem.* **2004**, 3601.

34. Altava, B.; Burguete, M. I.; Garcia-Verdugo, E.; Luis, S. V.; Vicent, M. J. *Green Chem.* **2006**, *8*, 717.
35. Burguete, M. I.; Garcia-Verdugo, E.; Vicent, M. J.; Luis, S. V.; Pennemann, H.; von Keyserling, N. G.; Martens, J. *Org. Lett.* **2002**, *4*, 3947.
36. Wiles, C.; Watts, P.; Haswell, S. J. *Tetrahedron* **2004**, *60*, 8421.
37. Fringuelli, F.; Pizzo, F.; Vittoriani, C.; Vaccaro, L. *Chem. Commun.* **2004**, 2756.
38. Rao, Y. V. S.; De Vos, D. E.; Jacobs, P. A. *Angew. Chem. Int. Ed.* **1997**, *36*, 2661.
39. Steinbacher, J. L.; Moy, R. W. Y.; Price, K. E.; Cummings, M. A.; Roychowdhury, C.; Buffy, J. J.; Olbricht, W. L.; Haaf, M.; McQuade, D. T. *J. Am. Chem. Soc.* **2006**, *128*, 9442.
40. Poe, S. L.; Cummings, M. A.; Haaf, M. R.; McQuade, D. T. *Angew. Chem. Int. Ed.* **2006**, *45*, 1544.
41. Quevedo, E.; Steinbacher, J.; McQuade, D. T. *J. Am. Chem. Soc.* **2005**, *127*, 10498.
42. Hatakeyama, T.; Chen, D. L. L.; Ismagilov, R. F. *J. Am. Chem. Soc.* **2006**, *128*, 2518.
43. Ehrfeld, W.; Hessel, V.; Lowe, H. *Microreactors: New Technology for Modern Chemistry*, Wiley-VCH, Weinheim, 2000.
44. Deratani, A.; Darling, G. D.; Frechet, J. M. J. *Polymer* **1987**, *28*, 825.
45. Menger, F. M.; McCann, D. J. *J. Org. Chem.* **1985**, *50*, 3928.
46. Tomoi, M.; Goto, M.; Kakiuchi, H. *J. Polym. Sci. Part A* **1987**, *25*, 77.
47. Chini, M.; Crotti, P.; Macchia, F. *Tetrahedron Lett.* **1990**, *31*, 5641.
48. Delaney, E. J.; Wood, L. E.; Klotz, I. M. *J. Am. Chem. Soc.* **1982**, *104*, 799.
49. Hornung, C. H.; Mackley, M. R.; Baxendale, I. R.; Ley, S. V. *Org. Process Res. Dev.* **2007**, *11*, 399.
50. Acke, D. R. J.; Stevens, C. V. *Org. Process Res. Dev.* **2006**, *10*, 417.

51. Seong, G. H.; Crooks, R. M. *J. Am. Chem. Soc.* **2002**, *124*, 1336.

## CHAPTER 3

### A Biphasic Oxidation of Alcohols to Aldehydes and Ketones Using a Simplified Packed-Bed Microreactor

#### *Preface*

Aldehydes and ketones are common building blocks in organic synthesis, but have the disadvantage of readily decomposing. Having the ability to generate aldehydes *in situ* from more stable alcohols in a reaction sequence is, therefore, highly advantageous. We chose to develop a packed-bed microreactor that could oxidize alcohols to their corresponding carbonyl species, with the ultimate goal of developing multi-step reaction sequences that required a carbonyl (i.e. the Knoevenagel condensation or the proline-catalyzed  $\alpha$ -aminooxylation).

#### *Abstract*\*

We demonstrate the preparation and characterization of a simplified packed-bed microreactor using an immobilized TEMPO catalyst shown to oxidize primary and secondary alcohols via the biphasic Anelli-Montanari protocol. Oxidations occurred in high yields with great stability over time. We observed that the aqueous oxidant and organic alcohol entered the reactor as plugs but merged into an emulsion on the packed-bed. The emulsion coalesced into larger plugs upon exiting the reactor, leaving the organic product separate from the aqueous by-products. Furthermore, the microreactor oxidized a wide range of alcohols and remained active in excess of 100 trials without showing any loss of catalytic activity.

---

\* Reproduced with permission from: Bogdan, A. R.; McQuade, D. T. A Biphasic Oxidation of Alcohols to Aldehydes and Ketones Using a Simplified Packed-Bed Microreactor. *Beilstein Journal of Organic Chemistry* **2009**, *5*, 17.

## ***Introduction***

Microreactors have gained attention because they can help run chemical transformations more efficiently, more selectively, and with greater safety.<sup>1-12</sup> Alcohol oxidations are well suited for microreactors due to high by-product formation, catalyst contamination and safety concerns often associated with scale-up in batch reactors.<sup>13</sup> Recent developments in microreactor technology and solid-supported catalysis have aimed to solve these issues. Numerous flow oxidations have been presented in the literature,<sup>13-16</sup> however many rely on stoichiometric reagents,<sup>17, 18</sup> suffer from catalyst deactivation,<sup>19, 20</sup> or rely on soluble catalysts,<sup>21</sup> all of which limit their potential as continuous flow processes. Realizing this, we developed a catalytic packed-bed microreactor that could be used for the continuous flow oxidation of alcohols to aldehydes or ketones.

Oxidations that do not require transition metal catalysts are particularly appealing since there is neither leaching nor the need for catalyst regeneration.<sup>22</sup> Nitroxyl radicals, such as 2,2,6,6-tetramethylpiperidine-1-oxyl (TEMPO), immobilized on silicates,<sup>23-32</sup> fluoros supports,<sup>33</sup> soluble and insoluble polymers,<sup>22, 34-36</sup> magnetic nanoparticles,<sup>37</sup> and ionic liquids<sup>38</sup> have been extensively studied and are useful because the oxidation conditions are mild, selective, and the catalysts do not require regeneration (Figure 3.1 and Figure 3.2). TEMPO, however, is expensive and difficult to remove from reaction mixtures. For these reasons, TEMPO immobilization is an important goal because it enables facile removal and recycling.

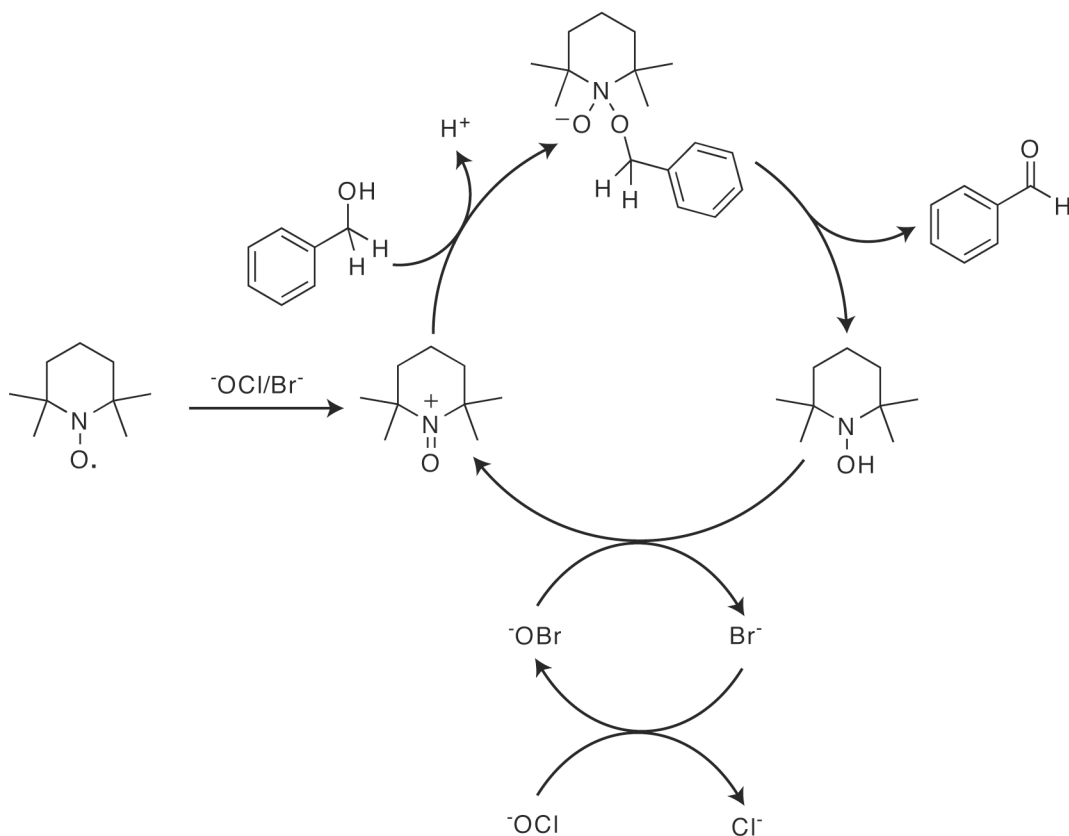


**Figure 3.1.** The catalytic cycle of the TEMPO-catalyzed oxidation of alcohols

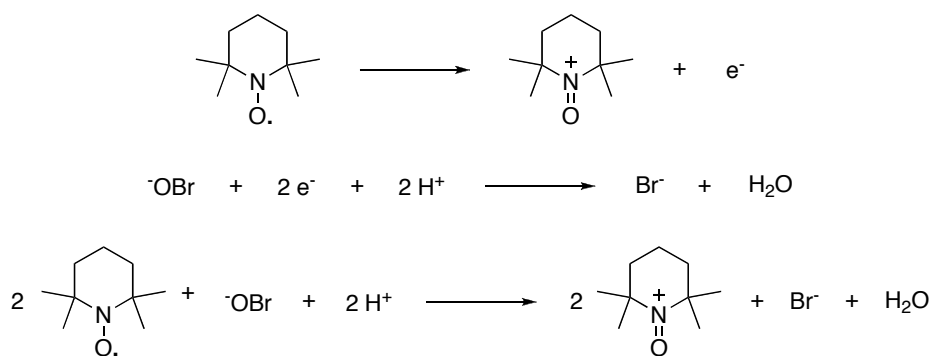


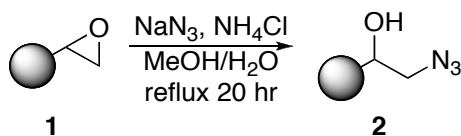
**Figure 3.2.** Redox reactions for the generation of the oxoammonium cation.

We recently reported the development of an effective solid-support for use in packed-bed microreactors,<sup>39</sup> AMBERZYME® Oxirane (AO, **1**), a commercially available resin with pendant epoxide functionalities designed for enzyme

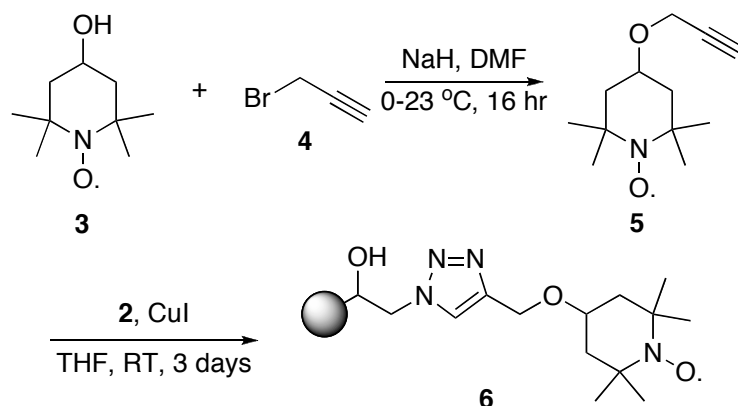
immobilization. AO is readily functionalized with a range of catalysts and works well as packing material for flow chemistry.<sup>39</sup> In this report, we demonstrate the immobilization of TEMPO and its use in a flow system using the Anelli-Montanari protocol for the oxidation of primary and secondary alcohols.<sup>30, 40</sup> Our simplified reactor is advantageous because the reactions not only run continuously, but since the microreactor is made of cheap, disposable fluoroelastomeric tubing, wall oxidation that is commonplace with metal microchannels is not observed.<sup>21</sup> The narrow dimensions of the microreactor also allows excellent heat transfer, increasing the safety of large-scale oxidations. Furthermore, it was determined that the use of a packed-bed microreactor facilitates efficient mixing of a biphasic system without destroying the solid-support, a common problem with stirred systems.<sup>4</sup>

### ***Results and Discussion***

Previously we reported that catalysts functionalized with an acetylene moiety can be tethered to AO using a Huisgen cycloaddition.<sup>39</sup> Azide-functionalized AO resin (AO-N<sub>3</sub>, **2**) was prepared by treating AO with sodium azide (Scheme 3.1).<sup>41</sup> The coupling of 4-hydroxy-TEMPO **3** with propargyl bromide **4** using sodium hydride yielded the acetylene-modified TEMPO species **5**.<sup>33, 34, 37</sup> TEMPO derivative **5** was then covalently bound to AO-N<sub>3</sub> using copper(I) iodide,<sup>42-45</sup> yielding the TEMPO-functionalized resin (AO-TEMPO, **6**, Scheme 3.2, 0.46 mmol TEMPO/g resin).



**Scheme 3.1.** Preparation of AO-N<sub>3</sub> resin.



**Scheme 3.2.** Preparation of AO-TEMPO resin.

Using a simplified procedure developed within our group and others,<sup>39, 46-49</sup> flow reactions were performed by packing fluoroelastomeric tubing (60 cm, 1.6 mm i.d.) with the AO-TEMPO resin. The tubing was subsequently woven between metal bars, to improve mixing and to enable facile microreactor cooling (Figure 3.3). A Y-junction placed at the inlet of the microreactor allowed the immiscible bleach (adjusted to pH 9.1 using  $\text{NaHCO}_3$ ) and organic alcohol solutions to form plugs before reaching the packed bed (Figure 3.4A). When passing through the AO-TEMPO catalyst bed, the plugs emulsified, as indicated by visual inspection and by the plug coalescence at the microchannel outlet (Figure 3.4B). The effective mixing was later supported by the high yields and conversions that were achieved for this biphasic reaction.

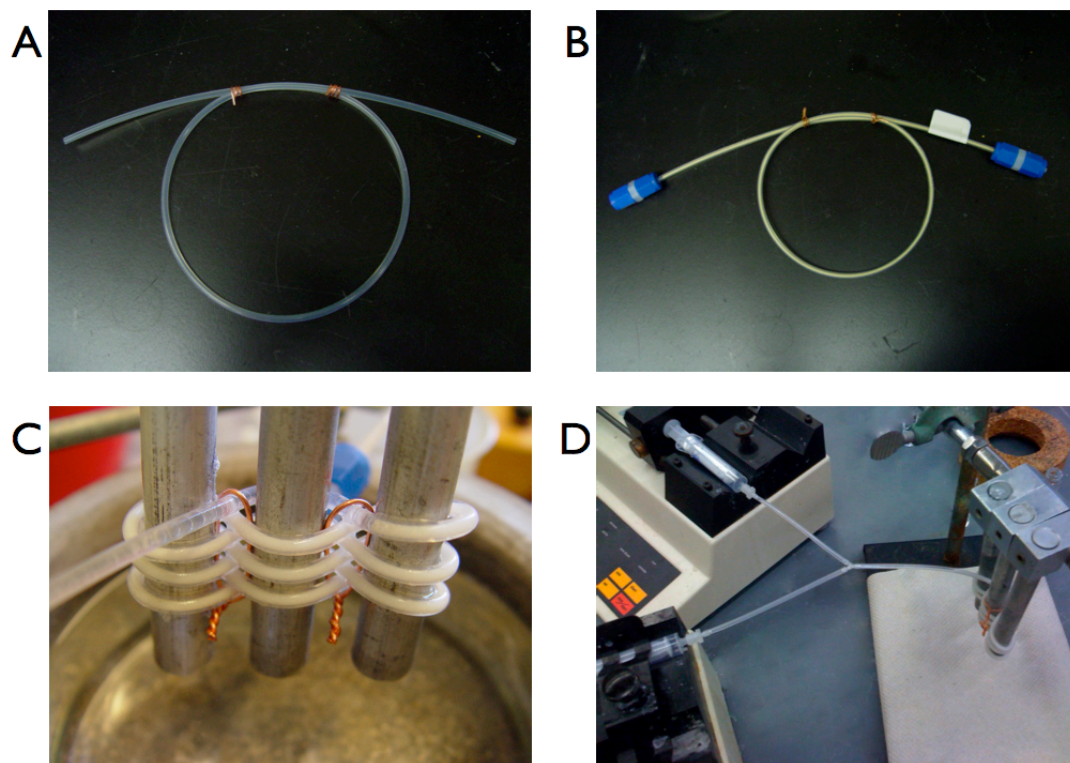


**Figure 3.3.** The simplified microreactor setup. Empty tubing (A) is packed with functionalized AO resin and attached to caps (B). The packed bed is woven between metal bars (C) and connected to syringe pumps (D).

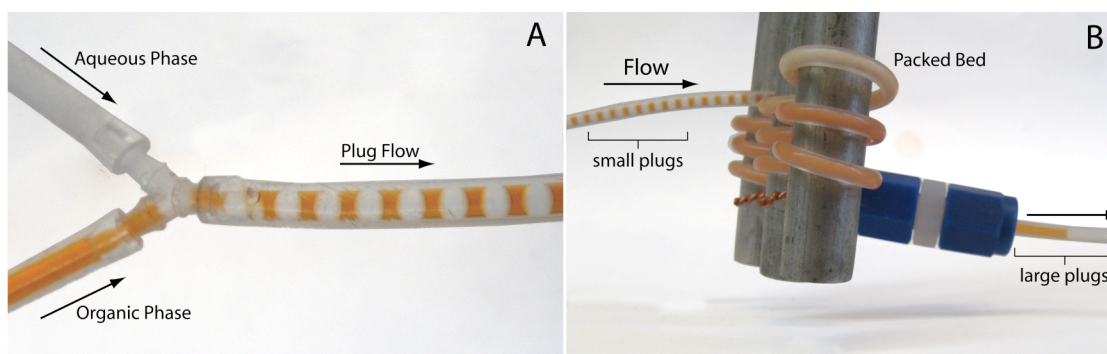
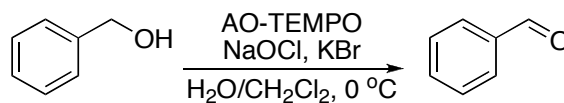


**Figure 3.4.** The organic (colored solution) and aqueous phases (colorless solution) forming plugs at the Y-junction (A). The phases mix upon reaching the packed bed, leading to a coalescence of drops at the outlet of the microchannel (B).

Preliminary reactions were performed using benzyl alcohol as the test substrate in order to establish the optimal flow conditions (Scheme 3.3). A solution of benzyl alcohol in  $\text{CH}_2\text{Cl}_2$  (0.2 M), an aqueous NaOCl solution (0.25 M, adjusted to pH 9.1 using  $\text{NaHCO}_3$ ), and an aqueous KBr solution (0.5 M) were prepared. The organic phase was loaded into one syringe and a mixture of NaOCl and KBr (30  $\mu\text{L}$  KBr solution per mL NaOCl solution) was added to another. The syringes were placed on separate syringe pumps and the flow rates were regulated such that 1.0 eq alcohol  $\text{min}^{-1}$ , 1.5 eq NaOCl  $\text{min}^{-1}$ , and 0.10 eq KBr  $\text{min}^{-1}$  were delivered to the packed bed. Various flow rates were examined to determine the optimal flow conditions for the oxidation. For data relating flow rate to residence time, see Appendix 1. During our optimization studies, it was shown that a total flow rate of 100  $\mu\text{L min}^{-1}$  (aqueous flow rate 56  $\mu\text{L min}^{-1}$  and organic flow rate 44  $\mu\text{L min}^{-1}$ , approximately 4.8 minute residence time) afforded quantitative conversion of benzyl alcohol to benzaldehyde, indicating that efficient mixing was occurring in the column at this flow rate. Faster flow rates (200 or 400  $\mu\text{L min}^{-1}$ ) could also be used to obtain higher outputs of benzaldehyde, however these reaction conditions did not provide complete conversion of starting material.



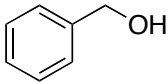
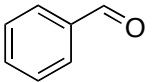
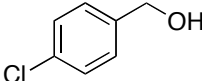
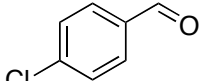
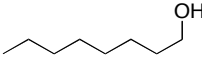
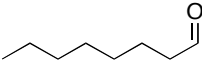
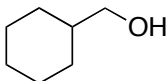
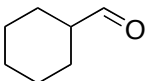
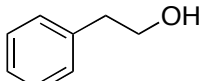
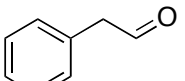
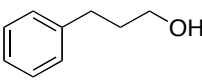
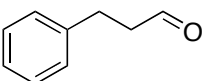
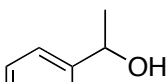
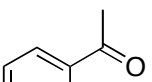
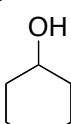
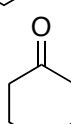
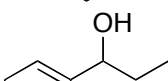
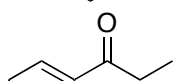
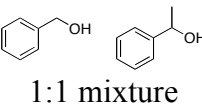
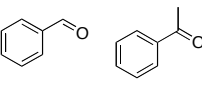
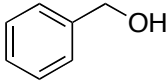
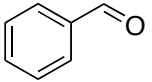
**Scheme 3.3.** The AO-TEMPO-catalyzed oxidation of benzyl alcohol.

Using these optimized flow conditions for the benzyl alcohol oxidation, a number of different substrates were examined to test the generality of the AO-TEMPO packed-bed microreactor. High conversions were achieved when using both aromatic and aliphatic alcohols (Table 3.1, Entries 1-6). Secondary alcohols, which are known

to be oxidized at a slower rate than primary alcohols, could effectively be oxidized to ketones by increasing the equivalents of NaOCl with respect to the alcohol concentration (Table 3.1, Entries 7-9). Primary alcohols were shown to be oxidized selectively over secondary alcohols (Table 3.1, Entry 10). Interestingly, it was also demonstrated that ethyl acetate was almost as effective a solvent as methylene chloride, opening the possibility of making this process “green” (Table 3.1, Entry 11). While reactions range from modest to high yields, systems that do not perform as efficiently could readily be optimized to afford higher conversions and yields. In this paper however, we were solely testing the generality of the method and, therefore, did not optimize every substrate. Similar to our previous packed-bed systems, these AO-TEMPO microchannels showed a high degree of recyclability, in some cases being used in excess of 100 trials without any apparent loss of catalytic activity. Channels also maintained a high activity after three months of not being used.

**Table 3.1.** Oxidation of alcohols using AO-TEMPO packed-bed microreactor.

$$\text{R}-\text{CH}(\text{OH})-\text{R}' \xrightarrow[\text{Method A, B or C}]{\text{AO-TEMPO Packed-Bed}} \text{R}-\text{C}(=\text{O})-\text{R}'$$

Entry	Alcohol	Method	Product	Conversion <sup>e</sup>	Yield <sup>e</sup>
1		A <sup>a</sup>		>99%	95%
2		A		>99%	93% (86%) <sup>f</sup>
3		A		88%	85%
4		A		89%	86%
5		A		88%	71%
6		A		80%	74%
7		B <sup>b</sup>		>99%	95%
8		B		95%	84%
9		B		89%	85%
10		C <sup>c</sup>		79%/16%	71%/11%
11		A <sup>d</sup>		84%	81%

<sup>a</sup> **Method A:** Organic Phase - Alcohol (0.2 M) in CH<sub>2</sub>Cl<sub>2</sub> or EtOAc set to 44 μL min<sup>-1</sup> (8.8 μmol alcohol min<sup>-1</sup>, 1.0 eq min<sup>-1</sup>). Aqueous Phase - Aqueous NaOCl (0.25 M), adjusted to pH 9.1 with NaHCO<sub>3</sub>, mixed with aqueous KBr (0.5 M, 30 μL per mL NaOCl) set to 56 μL min<sup>-1</sup> (1.5 eq NaOCl min<sup>-1</sup>, 0.10 eq KBr min<sup>-1</sup>). The phases combined at a Y-junction and passed through a 60 cm channel packed with AO-TEMPO (300 mg, 0.138 mmol TEMPO) submerged in an ice bath.

**Table 3.1 (continued).**

- <sup>b</sup> **Method B:** Organic Phase - Alcohol (0.1 M) in CH<sub>2</sub>Cl<sub>2</sub> set to 44 μL min<sup>-1</sup> (4.4 μmol alcohol min<sup>-1</sup>, 1.0 eq min<sup>-1</sup>). Aqueous Phase - Aqueous NaOCl (0.25 M), adjusted to pH 9.1 with NaHCO<sub>3</sub>, mixed with aqueous KBr (0.5 M, 30 μL per mL NaOCl) set to 56 μL min<sup>-1</sup> (3.0 eq NaOCl min<sup>-1</sup>, 0.20 eq KBr min<sup>-1</sup>). The phases combined at a Y-junction and passed through a 60 cm channel packed with AO-TEMPO (300 mg, 0.138 mmol TEMPO) submerged in an ice bath.
- <sup>c</sup> **Method C:** Organic Phase – Benzyl alcohol (0.2 M) and 1-phenylethanol (0.2 M) in CH<sub>2</sub>Cl<sub>2</sub> set to 44 μL min<sup>-1</sup> (8.8 μmol alcohol min<sup>-1</sup>, 1.0 eq min<sup>-1</sup>). Aqueous Phase - Aqueous NaOCl (0.20 M), adjusted to pH 9.1 with NaHCO<sub>3</sub>, mixed with aqueous KBr (0.5 M, 30 μL per mL NaOCl) set to 56 μL min<sup>-1</sup> (1.25 eq NaOCl min<sup>-1</sup>, 0.10 eq KBr min<sup>-1</sup>). The phases combined at a Y-junction and passed through a 60 cm channel packed with AO-TEMPO (300 mg, 0.138 mmol TEMPO) submerged in an ice bath.
- <sup>d</sup> EtOAc solvent.
- <sup>e</sup> Conversions and yields determined by GC using cyclooctane as an internal standard.
- <sup>f</sup> Number in parentheses corresponds to isolated yield.

To test the long-term activity of the AO-TEMPO packed beds, the oxidation of 4-chlorobenzyl alcohol to 4-chlorobenzaldehyde was run continuously and sampled periodically to monitor its activity. As seen in Figure 3.5, the activity of the catalyst bed remained high even after hours of use. Furthermore, the work-up of this simplified oxidation scale-up comprised only of phase separation followed by concentration, yielding a white crystalline solid with greater than 95% purity by <sup>1</sup>H NMR.

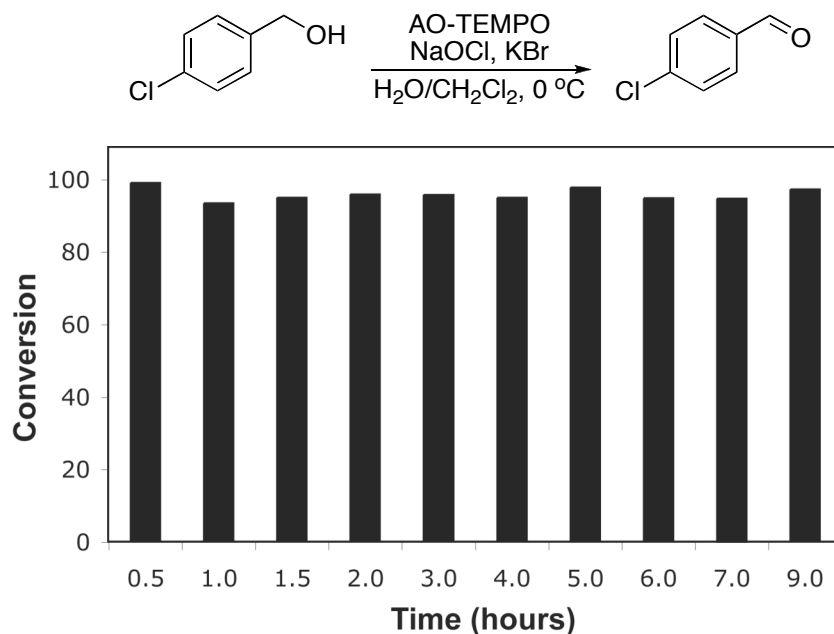


**Figure 3.5.** The long-term activity of AO-TEMPO packed beds in the oxidation of 4-chlorobenzyl alcohol. A solution of 4-chlorobenzyl alcohol (0.2 M in CH<sub>2</sub>Cl<sub>2</sub>) set to 44  $\mu\text{L min}^{-1}$  (8.8  $\mu\text{mol min}^{-1}$ , 1.0 eq  $\text{min}^{-1}$ ) and an aqueous solution consisting of NaOCl (0.25 M), adjusted to pH 9.1 with NaHCO<sub>3</sub>, and KBr (0.5 M, 30  $\mu\text{L per mL NaOCl}$ ) set to 56  $\mu\text{L min}^{-1}$  (1.5 eq NaOCl  $\text{min}^{-1}$ , 0.10 eq KBr  $\text{min}^{-1}$ ) were passed through the AO-TEMPO packed bed for nine hours. Fractions were collected and analyzed by GC using an internal standard.

### ***Conclusion***

We demonstrated that using supported TEMPO is an efficient method to oxidize alcohols using a simplified packed-bed microreactor. A biphasic mixture was thoroughly mixed by passing the immiscible liquids through the catalytic packed-bed, leading to no disruptions or degradation of the packing material. Thus, the AO-TEMPO resins are recyclable, showing no loss of catalytic activity and a substrate scope that encompasses many primary and secondary alcohols. The devices presented are predicted to be readily scaled-up to achieve the desired output of a reaction and is of higher throughput than other reported packed-bed microreactors.

## ***Experimental Section***

**General Considerations.** Solvents were purified by standard procedures. All other reagents were used as received, unless otherwise noted. Sodium hypochlorite solution (reagent grade, available chlorine 10-15%) was purchased from Aldrich and titrated before use.  $^1\text{H}$  NMR and  $^{13}\text{C}$  NMR spectra were recorded in  $\text{CDCl}_3$  on Varian Mercury 300 MHz operating at 300.070 MHz and 75.452 MHz, respectively, using the residual solvent peak as reference. ATR-IR was performed on a Nicolet Avatar DTGS 370 infrared spectrometer with Avatar OMNI sampler and OMNIC software. Elemental analysis was performed by Robertson Microlit Laboratories, Inc., in Madison, New Jersey. Gas chromatographic (GC) analyses were performed using an Agilent 7890A GC equipped with an Agilent 7683B autosampler, a flame ionization detector (FID), and a J&W Scientific 19091J-413 column (length = 30 m, inner diameter = 320  $\mu\text{m}$ , and film thickness = 250  $\mu\text{m}$ ). The temperature program for GC analysis held the temperature constant at 80  $^\circ\text{C}$  for 1 minute, heated samples from 80 to 200  $^\circ\text{C}$  at 20  $^\circ\text{C}/\text{min}$  and held at 200  $^\circ\text{C}$  for 1 minute. Inlet and detector temperatures were set constant at 220 and 250  $^\circ\text{C}$ , respectively. Cyclooctane was used as an internal standard to calculate reaction conversion and yield. Gas chromatography-mass spectrometry (GC/MS) analyses were performed using a Hewlett Packard HP 6890 Series Gas Chromatograph, a Hewlett Packard HP 5973 Mass Spectrometer Detector (MSD), and a J&W Scientific DB\*-5 Column (length = 30 m, inner diameter = 0.325 mm, film thickness = 1.0  $\mu\text{m}$ , catalog number 123-5033). The temperature program for the analyses held the temperature constant at 50  $^\circ\text{C}$  for 3 minutes, heated samples from 50 to 80  $^\circ\text{C}$  at 30  $^\circ\text{C}/\text{min}$ , holding at 80  $^\circ\text{C}$  for 2 minutes, then heating samples from 80 to 200  $^\circ\text{C}$  at 17  $^\circ\text{C}/\text{min}$ , and holding at 200  $^\circ\text{C}$  for 1.94 minutes. The MSD temperature was held at 300  $^\circ\text{C}$  for 15 minutes.

**Channel Packing.** A 60 cm section of tubing (Swagelok PFA Tubing, 1/8" outer diameter) was attached to a Swagelok PFA union packed with glass wool. A separate union (not packed with glass wool) was attached to the inlet side of the 60 cm column. Two 10 cm sections of tubing were attached to the channel, serving as the outlet. A 1/16" female Luer was attached to the inlet. Functionalized resin was suspended in CH<sub>2</sub>Cl<sub>2</sub> and the column slurry packed using a syringe.

**Azide Modified AMBERZYME® Oxirane (AO-N<sub>3</sub>, 2).** Sodium azide (5.26 g, 81 mmol, 8.1 eq.) and ammonium chloride (2.27 g, 42.4 mmol, 4.2 eq.) were dissolved in 500 mL 90:10 v/v water in methanol. AMBERZYME® Oxirane (10.0 g, 1.0 mmol epoxide/g resin, 10.0 mmol, 1.0 eq.) was suspended in the azide solution and the reaction mixture refluxed overnight with gentle stirring. The resin was filtered using a Buchner funnel, washed with deionized H<sub>2</sub>O (2x 50 mL), MeOH (2x 50 mL), Et<sub>2</sub>O (1x 25 mL), and dried under vacuum. Elemental analysis afforded a loading of 1.0 mmol N<sub>3</sub>/g resin.

**Propargyl Ether TEMPO (5).** Sodium hydride (150 mg, 6.3 mmol, 1.1 eq) was added to DMF (10 mL) and stirred at RT. 4-hydroxy-TEMPO (1.02 g, 5.9 mmol, 1.0 eq) in DMF (10 mL) was added drop wise to the sodium hydride suspension at 0 °C and stirred until gas evolution ceased. Propargyl bromide (80% in toluene, 800 µL, 7.4 mmol, 1.3 eq) in DMF (10 mL) was added at 0 °C and the reaction was allowed to warm up to RT and stirred overnight. The reaction was quenched with water and the aqueous phase was extracted with ethyl acetate (3x 50 mL) and the combined organic extracts dried over MgSO<sub>4</sub>, concentrated and dried under vacuum. The product was purified using column chromatography (silica gel, 1:1 → 1:2 hexanes/ethyl acetate, R<sub>f</sub> = 0.40) to yield a dark orange solid (841 mg, 68%). <sup>13</sup>C NMR (75 MHz, CDCl<sub>3</sub>): δ

20.619, 32.199, 44.530, 55.298, 59.198, 69.905, 74.238; EM  $m/z$  210 ( $M^+$ ). To obtain NMR spectra, a few drops of phenylhydrazine were added to the NMR tube to reduce the product to the corresponding hydroxyl amine.

**AO-TEMPO (6).** **5** (450 mg, 2.14 mmol, 1.3 eq) and CuI (40 mg, 0.2 mmol, 0.13 eq) were dissolved in anhydrous THF (20 mL). **2** (1.64 g, 1.0 mmol  $N_3/g$  resin, 1.64 mmol, 1.0 eq) was added to the solution and placed under a  $N_2$  atmosphere. The suspension was shaken for 3 days. The resin was washed with THF (2x 10 mL), MeOH (1x 10 mL), 1 M HCl (2x 10 mL), deionized  $H_2O$  (1x 10 mL), sat.  $NaHCO_3$  (2x 10 mL), deionized  $H_2O$  (1x 10 mL), MeOH (1x 10 mL) and  $CH_2Cl_2$  (1x 10 mL), and dried under vacuum to yield the white AO-TEMPO resin (1.81 g, 0.46 mmol TEMPO/g resin). The loading was calculated by mass difference.

**Representative Primary Alcohol Flow Oxidation Procedure.** Benzyl alcohol (0.2 M) and cyclooctane (0.02 M) in  $CH_2Cl_2$  or EtOAc was placed in a syringe and placed on a syringe pump set to  $44 \mu L \text{ min}^{-1}$  ( $8.8 \mu \text{mol alcohol min}^{-1}$ ,  $1.0 \text{ eq min}^{-1}$ ). Aqueous NaOCl (purchased from Sigma Aldrich and diluted to 0.25 M), adjusted to pH 9.1 with  $NaHCO_3$ , mixed with aqueous KBr (0.5 M,  $30 \mu L$  per mL NaOCl) were placed in a separate syringe and placed on another syringe pump set to  $56 \mu L \text{ min}^{-1}$  ( $1.5 \text{ eq NaOCl min}^{-1}$ ,  $0.10 \text{ eq KBr min}^{-1}$ ). The phases combined at a Y-junction and passed through a 60 cm channel packed with AO-TEMPO (300 mg) submerged in an ice bath. The reaction mixture was collected in a 4 mL screw cap vial until the sample had eluted through the channel. Upon completion of each experiment, the organic phase was separated from the aqueous phase using a pipette and transferred to a separate 4 mL screw cap vial. After each trial, the channel was washed with 5 mL deionized  $H_2O$ , 5 mL MeOH, and 5 mL  $CH_2Cl_2$ . The column was flushed with air

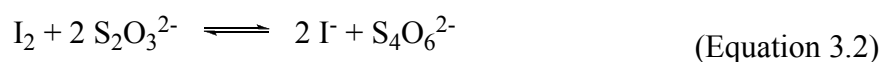
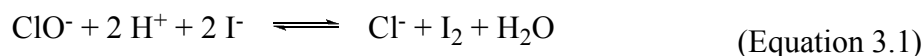
prior to each run. Samples were analyzed by GC and conversions and yields obtained by comparing starting material and product to an internal standard.

**Representative Secondary Alcohol Flow Oxidation Procedure.** 1-phenylethanol (0.1 M) and cyclooctane (0.01 M) in  $\text{CH}_2\text{Cl}_2$  was placed in a syringe and placed on a syringe pump set to  $44 \mu\text{L min}^{-1}$  ( $4.4 \mu\text{mol alcohol min}^{-1}$ ,  $1.0 \text{ eq min}^{-1}$ ). Aqueous NaOCl (purchased from Sigma Aldrich and diluted to 0.25 M), adjusted to pH 9.1 with  $\text{NaHCO}_3$ , mixed with aqueous KBr (0.5 M,  $30 \mu\text{L per mL NaOCl}$ ) were placed in a separate syringe and placed on another syringe pump set to  $56 \mu\text{L min}^{-1}$  ( $3.0 \text{ eq NaOCl min}^{-1}$ ,  $0.20 \text{ eq KBr min}^{-1}$ ). The phases combined at a Y-junction and passed through a 60 cm channel packed with AO-TEMPO (300 mg) submerged in an ice bath. The reaction mixture was collected in a 4 mL screw cap vial until the sample had eluted through the channel. Upon completion of each experiment, the organic phase was separated from the aqueous phase using a pipette and transferred to a separate 4 mL screw cap vial. After each trial, the channel was washed with 5 mL deionized  $\text{H}_2\text{O}$ , 5 mL MeOH, and 5 mL  $\text{CH}_2\text{Cl}_2$ . The column was flushed with air prior to each run. Samples were analyzed by GC and conversions and yields obtained by comparing starting material and product to an internal standard.

**4-Chlorobenzyl Alcohol Flow Oxidation Isolated Yield.** 4-Chlorobenzyl alcohol (0.2 M) and cyclooctane (0.02 M) in  $\text{CH}_2\text{Cl}_2$  was placed in a syringe and placed on a syringe pump set to  $44 \mu\text{L min}^{-1}$  ( $8.8 \mu\text{mol alcohol min}^{-1}$ ,  $1.0 \text{ eq min}^{-1}$ ). Aqueous NaOCl (purchased from Sigma Aldrich and diluted to 0.25 M), adjusted to pH 9.1 with  $\text{NaHCO}_3$ , mixed with aqueous KBr (0.5 M,  $30 \mu\text{L per mL NaOCl}$ ) were placed in a separate syringe and placed on another syringe pump set to  $56 \mu\text{L min}^{-1}$  ( $1.5 \text{ eq NaOCl min}^{-1}$ ,  $0.10 \text{ eq KBr min}^{-1}$ ). The phases combined at a Y-junction and passed

through a 60 cm channel packed with AO-TEMPO (300 mg) submerged in an ice bath. The reaction was collected in a vial and 60 minutes, whereupon the reaction was transferred to a separatory funnel and phase separated. The organic layer was concentrated and dried under vacuum to yield a white, crystalline material (64 mg, 86% yield).

**Bleach Titration.** Sodium hypochlorite solution (Sigma Aldrich, reagent grade, 500  $\mu\text{L}$ ) was diluted to 100 mL with deionized  $\text{H}_2\text{O}$  in an Erlenmeyer flask equipped with a stir bar. Excess KI and excess  $\text{H}_2\text{SO}_4$  (conc.) were added to the flask, yielding a dark burgundy solution. Sodium thiosulfate pentahydrate (1.0 M in deionized  $\text{H}_2\text{O}$ ) was added drop wise to the flask until the color of the solution dissipated (the equivalence point). The concentration of NaOCl in the solution was calculated using Equation 3.1, Equation 3.2, and Equation 3.3.



$$\text{M NaOCl} = \frac{0.5 \times \text{mmol Na}_2\text{S}_2\text{O}_3}{0.5 \text{ mL NaOCl solution}} \quad (\text{Equation 3.3})$$

## REFERENCES

1. Mason, B. P.; Price, K. E.; Steinbacher, J. L.; Bogdan, A. R.; McQuade, D. T. *Chem. Rev.* **2007**, *107*, 2300-2318.
2. Hessel, V.; Lob, P.; Lowe, H. *Curr. Org. Chem.* **2005**, *9*, 765-787.
3. Hessel, V.; Lowe, H. *Chem. Eng. Technol.* **2005**, *28*, 267-284.
4. Hodge, P. *Curr. Opin. Chem. Biol.* **2003**, *7*, 362-373.
5. Jas, G.; Kirschning, A. *Chem. Eur. J.* **2003**, *9*, 5708-5723.
6. Kirschning, A.; Monenschein, H.; Wittenberg, R. *Angew. Chem. Int. Ed.* **2001**, *40*, 650-679.
7. Pennemann, H.; Watts, P.; Haswell, S. J.; Hessel, V.; Lowe, H. *Org. Process Res. Dev.* **2004**, *8*, 422-439.
8. Haswell, S. J.; Watts, P. *Green Chem.* **2003**, *5*, 240-249.
9. *Microreactors in Organic Synthesis and Catalysis*, Wirth, T., Ed. Wiley-VCH: Weinheim, 2008.
10. Yoshida, J.; Nagaki, A.; Yamada, T. *Chem. Eur. J.* **2008**, *14*, 7450-7459.
11. Watts, P.; Wiles, C. *Org. Biomol. Chem.* **2007**, *5*, 727-732.
12. Ahmed-Omer, B.; Brandt, J. C.; Wirth, T. *Org. Biomol. Chem.* **2007**, *5*, 733-740.
13. Kawaguchi, T.; Miyata, H.; Ataka, K.; Mae, K.; Yoshida, J. *Angew. Chem. Int. Ed.* **2005**, *44*, 2413-2416.
14. Kobayashi, S.; Miyamura, H.; Akiyama, R.; Ishida, T. *J. Am. Chem. Soc.* **2005**, *127*, 9251-9254.
15. Tanaka, H.; Chou, J. Y.; Mine, M.; Kuroboshi, M. *Bull. Chem. Soc. Jpn.* **2004**, *77*, 1745-1755.
16. Kirschning, A.; Altwicker, C.; Dräger, G.; Harders, J.; Hoffmann, N.; Hoffman, U.; Schönfeld, H.; Solodenko, W.; Kunz, U. *Angew. Chem. Int. Ed.* **2001**, *41*, 3995-3998.

17. Baxendale, I. R.; Deeley, J.; Griffiths-Jones, C. M.; Ley, S. V.; Saaby, S.; Tranmer, G. K. *Chem. Commun.* **2006**, 2566-2568.
18. Wiles, C.; Watts, P.; Haswell, S. J. *Tetrahedron Lett.* **2006**, *47*, 5261-5264.
19. Cao, E. H.; Motherwell, W. B.; Gavriilidis, A. *Chem. Eng. Technol.* **2006**, *29*, 1372-1375.
20. Kuno, H.; Shibagaki, M.; Takahashi, K.; Matsushita, H. *Bull. Chem. Soc. Jpn.* **1991**, *64*, 312-314.
21. Fritz-Langhals, E. *Org. Process Res. Dev.* **2005**, *9*, 577-582.
22. Pozzi, G.; Cavazzini, M.; Quici, S.; Benaglia, M.; Dell'Anna, G. *Org. Lett.* **2004**, *6*, 441-443.
23. Ciriminna, R.; Bolm, C.; Fey, T.; Pagliaro, M. *Adv. Synth. Catal.* **2002**, *344*, 159-163.
24. Ciriminna, R.; Pagliaro, M. *Adv. Synth. Catal.* **2003**, *345*, 383-388.
25. Ciriminna, R.; Pagliaro, M. *Org. Process Res. Dev.* **2006**, *10*, 320-326.
26. Gancitano, P.; Ciriminna, R.; Testa, M. L.; Fidalgo, A.; Ilharco, L. M.; Pagliaro, M. *Org. Biomol. Chem.* **2005**, *3*, 2389-2392.
27. Pagliaro, M.; Ciriminna, R.; Man, M. W. C.; Campestrini, S. *J. Phys. Chem. B* **2006**, *110*, 1976-1988.
28. Fidalgo, A.; Ciriminna, R.; Ilharco, L. M.; M. Pagliaro, *Chem. Mater.* **2005**, *17*, 6686-6694.
29. Testa, M. L.; Ciriminna, R.; Hajji, C.; Garcia, E. Z.; Ciclosi, M.; Arques, J. S.; Pagliaro, M. *Adv. Synth. Catal.* **2004**, *346*, 655-660.
30. Bolm, C.; Fey, T. *Chem. Commun.* **1999**, 1795-1796.
31. Brunel, D.; Fajula, F.; Nagy, J. B.; Deroide, B.; Verhoef, M. J.; Veum, L.; Peters, J. A.; van Bekkum, H. *App. Cat. A* **2001**, *213*, 73-82.
32. Fey, T.; Fischer, H.; Bachmann, S.; Albert, K.; Bolm, C. *J. Org. Chem.* **2001**, *66*, 8154-8159.
33. Gheorghe, A.; Cuevas-Yanez, E.; Horn, J.; Bannwarth, W.; Narsaiah, B.; Reiser, O. *Synlett* **2006**, 2767-2770.

34. Gheorghe, A.; Matsuno, A.; Reiser, O. *Adv. Synth. Catal.* **2006**, *348*, 1016-1020.
35. Gilhespy, M.; Lok, M.; Baucherel, X. *Chem. Commun.* **2005**, 1085-1086.
36. Gilhespy, M.; Lok, M.; Baucherel, X. *Catal. Today* **2006**, *117*, 114-119.
37. Schätz, A.; Grass, R. N.; Stark, W. J.; Reiser, O. *Chem. Eur. J.* **2008**, *14*, 8262.
38. Wu, X.; Ma, L.; Ding, M.; Gao, L. *Synlett* **2005**, *4*, 0607.
39. Bogdan, A. R.; Mason, B. P.; Sylvester, K. T.; McQuade, D. T. *Angew. Chem. Int. Ed.* **2007**, *46*, 1698-1701.
40. Anelli, P. L.; Biffi, C.; Montanari, F.; Quici, S. *J. Org. Chem.* **1987**, *52*, 2559-2562.
41. Chini, M.; Crotti, P.; Macchia, F. *Tetrahedron Lett.* **1990**, *31*, 5641.
42. Kolb, H. C.; Finn, M. G.; Sharpless, K. B. *Angew. Chem. Int. Ed.* **2001**, *40*, 2004.
43. Rostovtsev, V. V.; Green, L. G.; Fokin, V. V.; Sharpless, K. B. *Angew. Chem. Int. Ed.* **2002**, *41*, 2596.
44. Wu, P.; Feldman, A. K.; Nugent, A. K.; Hawker, C. J.; Scheel, A.; Voit, B.; Pyun, J.; Fréchet, J. M. J.; Sharpless, K. B.; Fokin, V. V. *Angew. Chem. Int. Ed.* **2004**, *43*, 3928.
45. Tornøe, C. W.; Christensen, C.; Meldal, M. *J. Org. Chem.* **2002**, *67*, 3057.
46. Poe, S. L.; Cummings, M. A.; Haaf, M. R.; McQuade, D. T. *Angew. Chem. Int. Ed.* **2006**, *45*, 1544-1548.
47. Quevedo, E.; Steinbacher, J.; McQuade, D. T. *J. Am. Chem. Soc.* **2005**, *127*, 10498-10499.
48. Steinbacher, J. L.; Moy, R. W. Y.; Price, K. E.; Cummings, M. A.; Roychowdhury, C.; Buffy, J. J.; Olbricht, W. L.; Haaf, M.; McQuade, D. T. *J. Am. Chem. Soc.* **2006**, *128*, 9442-9447.
49. Hatakeyama, T.; Chen, D. L. L.; Ismagilov, R. F. *J. Am. Chem. Soc.* **2006**, *128*, 2518-2519.

## CHAPTER 4

### The Use of Copper Flow Reactor Technology for the Continuous Synthesis of 1,4-Disubstituted 1,2,3-Triazoles

#### *Preface*

In the summer of 2008, I was granted the opportunity to explore the use of click chemistry in medicinal chemistry, using a prototype flow reactor at Pfizer La Jolla. A one-pot click reaction was utilized that permitted a large number of organic azides to be generated *in situ* and tethered to acetylene-modified drug head pieces. A proof of concept triazole library was also developed in order to publish the new methodology towards flow discovery.

#### *Abstract\**

A library of 1,4-disubstituted 1,2,3-triazoles was synthesized using a copper flow reactor. Organic azides, generated *in situ* from alkyl halides and sodium azide, were reacted with acetylenes using the copper-catalyzed Huisgen 1,3-dipolar cycloaddition. This process eliminates both the handling of organic azides and the need for additional copper catalyst and permits the facile preparation of numerous triazoles in a continuous flow process.

---

\* Reproduced in part with permission from: Bogdan, A. R.; Sach, N. W. The Use of Copper Flow Reactor Technology for the Continuous Synthesis of 1,4-Disubstituted 1,2,3-Triazoles. *Adv. Synth. Catal.* **2009**, 351, 849-854. Copyright 2009 Wiley-VCH Verlag GmbH & Co. KGaA.

## Introduction

The click reaction between organic azides and acetylenes has gained a considerable amount of attention since its discovery in 2001.<sup>1-7</sup> The resulting 1,2,3-triazoles are an interesting class of heterocycles, as they have found use in many biological applications, antifungal agents, as well as dyes.<sup>8-12</sup> Chemists are attracted to click chemistry in drug discovery due to its high dependability, its use in combinatorial chemistry, and its compatibility with biological systems.<sup>13-15</sup>

A high percentage of pharmaceutical agents contain either a triazole or tetrazole heterocycle (see Diovan, Atacand, Virazole, and Maraviroc, for examples). Similar to the heterocycles within these drugs, 1,2,3-triazoles are also of great interest due to the biological activity they possess.<sup>13</sup> It is therefore conceivable that derivatives of these drugs could be synthesized using click chemistry (Figure 4.1). By modifying drug headpieces with an acetylene, derivatives of these drugs could subsequently be synthesized by varying the organic azide that is used in the reaction.

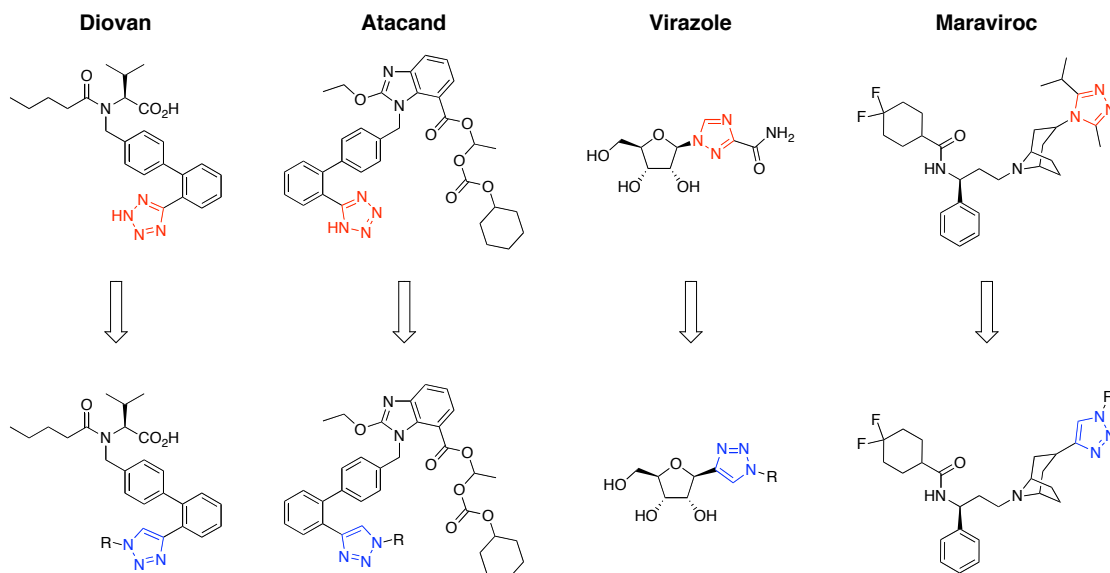


**Figure 4.1.** Drug derivative synthesis using click chemistry.

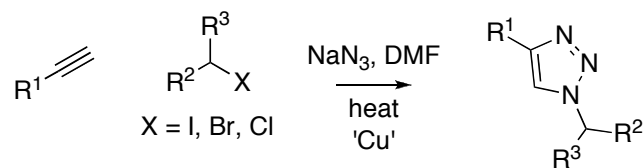
Whilst acetylenes can be readily prepared using high-yielding methodologies such as the Sonogashira coupling, azide preparation is more problematic. Azides are a class of compounds known to readily decompose<sup>16</sup> and as such their preparation and isolation must be handled with care, particularly on scale.

Eliminating the need to isolate azides would be a significant advantage and while reports have shown that alkyl azides can be generated *in situ* prior to the copper-catalyzed cycloaddition, these methodologies have either been slow or relied on microwave technology.<sup>17-20</sup>

Flow chemistry is an important, emerging field that pushes the boundaries of organic synthesis by accessing so-called ‘forbidden chemistries’ through unparalleled reaction control.<sup>21-29</sup> The numerous advantages of running reactions in flow are often attributed to the large surface area-to-volume ratios.<sup>23</sup> Small dimensions lead to good mixing<sup>30-34</sup> and the superb heat transfer within these systems enables excellent control of exotherms, limiting the impact of runaway reactions.<sup>22</sup> Back-pressure regulation technology enables solvent boiling suppression and reaction kinetics can be substantially increased.<sup>35</sup> In addition, scale-up becomes a facile process compared with batch systems and output is measured as a function of time rather than batch size.<sup>36-38</sup>

## ***Results and Discussion***

Realizing the benefits of flow chemistry we sought to explore a one-pot click methodology (Scheme 1 and Figure 4.2). Organic azides could be generated in small volumes from their corresponding alkyl halides at high temperatures and immediately reacted with acetylenes. By adopting this approach we hoped to overcome the safety and supply issues of azides and dramatically increase the monomers available to us, enabling a greater number of triazoles to be synthesized.



**Scheme 4.1.** The one-pot click reaction.

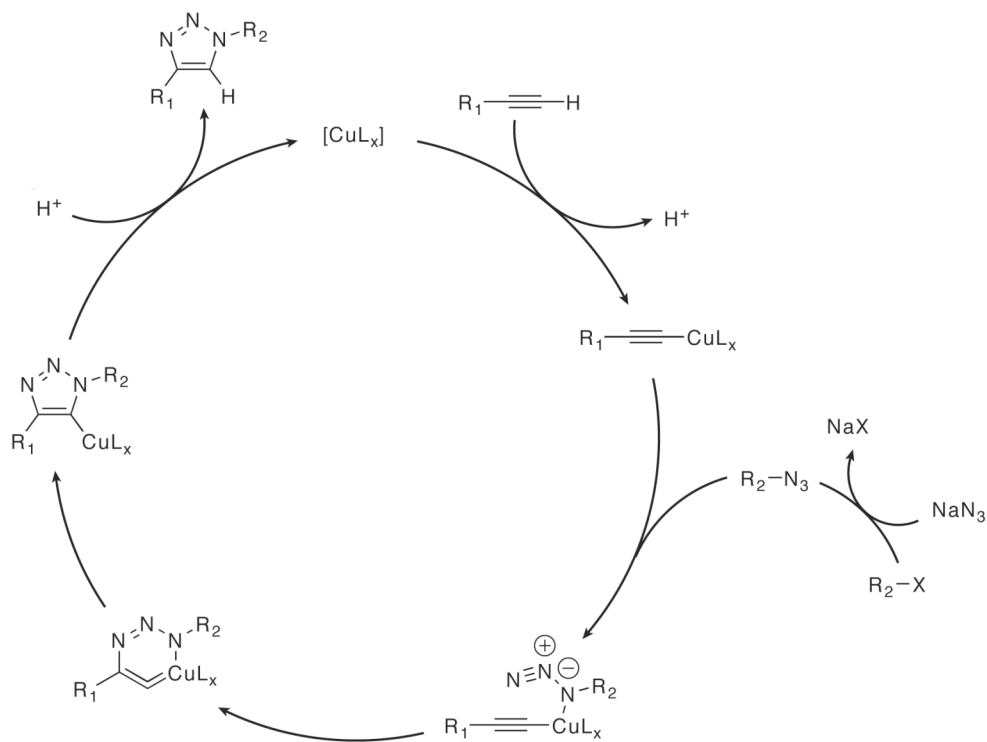


**Figure 4.2.** The catalytic cycle of the click reaction.

We report herein the rapid synthesis of a 1,4-disubstituted 1,2,3-triazole library in a flow reactor using this one-pot click methodology. A copper flow reactor has been developed to catalyze the reaction, enabling triazoles to be synthesized from simple starting materials without the need for additional catalyst. The facile scale-up of one triazole is also demonstrated, and the application of this technology to drug discovery is discussed.

The Conjure Flow Reactor (Figure 4.3) was designed to operate on a scale suitable for both medicinal chemistry and process research. The instrument adopts a segmented flow approach versus a continuous stream approach in order to minimize material consumption and limit reaction size. Reaction segments are separated by an immiscible fluoruous spacer, perfluoromethyldecalin, that prevents segment diffusion and reaction trailing.<sup>39-46</sup> Using this approach, multiple segments can flow through the reactor at any one time, maximizing the system's efficiency and permitting rapid library development (medicinal chemistry) or reaction optimization (process research).

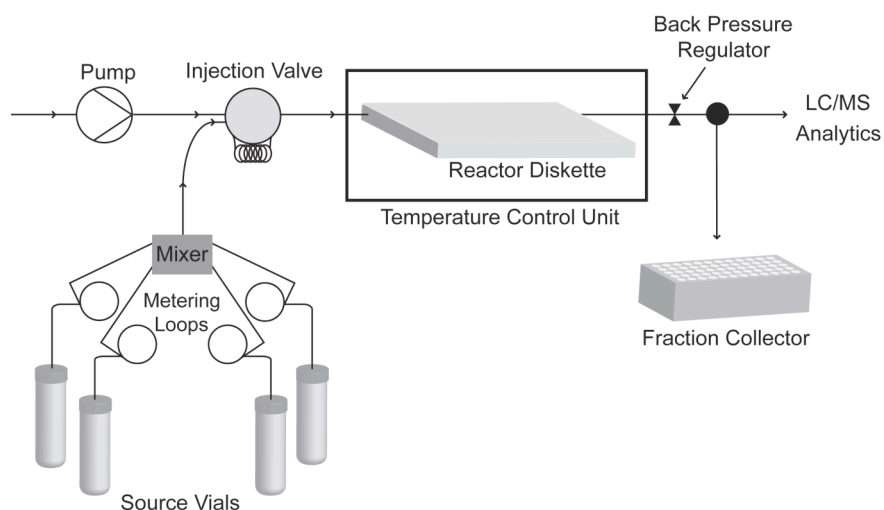


**Figure 4.3.** Conjure Flow Reactor schematic.

The reactor diskette consists of a reaction coil made of copper, Hastelloy or PTFE tubing placed between two copper plates (Figure 4.4). Multiple segments can be passed through the system sequentially since the internal volume of the reactor diskette ranges from 2-10 mL and reaction segments are on the order of 400  $\mu$ L.

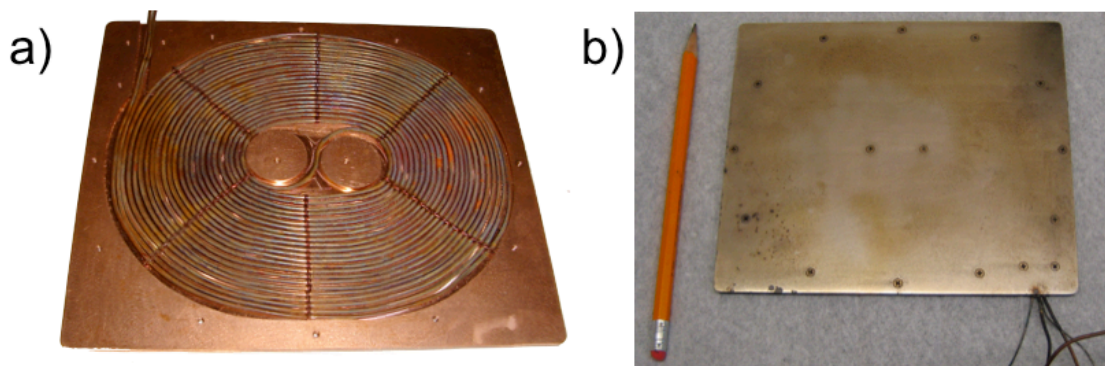
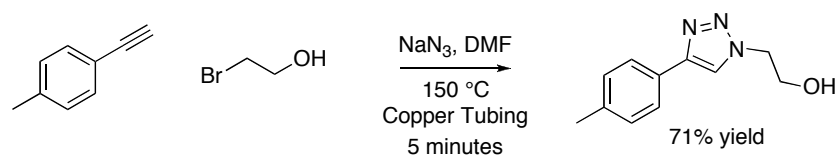


**Figure 4.4.** a) A reactor diskette with the top copper plate removed, exposing the copper tubing within (0.75 mm i.d.). b) An assembled reactor diskette for the flow reactor (145 mm x 165 mm x 5 mm).

Heterogeneous catalysis has been used extensively in flow systems and is highly recyclable and selective.<sup>47-51</sup> Because even Cu(0) sources such as copper wire<sup>2</sup> and copper metal turnings<sup>17</sup> are effective catalysts for the click reaction, we used a reactor diskette prepared from copper. We envisioned that no additional copper catalyst would be necessary, removing a level of complexity from the system. Indeed, when reaction segments containing sodium azide, an alkyl halide, and acetylene in DMF were passed through the copper flow reactor, high conversions were obtained within 5 minutes.

Depending on the solvent used for this reaction, the rate of copper leaching from the reactor diskette greatly varied. When EtOH was used as the reaction solvent at 150 °C, elemental analysis showed a copper concentration of 78 ppm. However, as EtOH proved to be a poor solvent for the triazole products, precipitation ultimately blocked the channels. When DMF was chosen as the reaction solvent, elemental analysis showed a copper concentration of ~300 ppm. The addition of QuadraPure TU scavenging resin reduced the copper concentration to <5 ppm, effectively removing all copper from the system.

Replacing the copper reactor with a Hastelloy reactor diskette prohibited the reaction, supporting the necessity of the copper and proving the triazole formation was not occurring under thermal conditions.<sup>52</sup> The copper reactor was used to catalyze hundreds of reactions, never showing a loss of catalytic activity<sup>53</sup> and was also shown to effectively catalyze other copper-mediated reactions such as the Sonogashira and Ullman couplings.



**Scheme 4.2.** The optimized one-pot click reaction using 4-ethynyltoluene and 2-bromoethanol.

We optimized the one-pot click methodology using 4-ethynyltoluene, 2-bromoethanol and sodium azide in DMF (Scheme 4.2).<sup>54</sup> By varying the residence time, reactor temperature, and equivalents of alkyl azide, we were able to rapidly obtain optimal reaction conditions using minimal amounts of material.<sup>55</sup> By linking the instrument's analytical output to DOE software such as Design Expert®, reports are generated after the optimization, dictating the optimal reaction conditions for this transformation.

DOE is a common method used to optimize reaction conditions using a planned variation of parameters. Experiments were designed by choosing three variables (residence time, reactor temperature, and equivalents of alkyl azide), and setting high and low values for each (Table 4.1). In all, sixteen total experiments were performed while running the DOE. It should also be noted, that each of these reactions had a total reaction volume of  $400\text{ }\mu\text{L}$  and required no chemical handling.

**Table 4.1.** Boundary conditions for DOE optimization.

Variable	Low	High
Residence Time	5 min	15 min
Reactor Temperature	100 °C	175 °C
Alkyl Azide Eq.	1.0	2.0

Figure 4.5 depicts the correlation between alkyl azide equivalents and residence time when the reactor temperature is held constant at 100 °C. It can be determined from these data that low temperatures are unfavorable conditions for the one-pot click reaction as conversion of greater than 20% are not obtained. The azide displacement of the alkyl halide is most likely not occurring at lower temperatures, thereby inhibiting the formation of the 1,4-disubstituted triazoles.

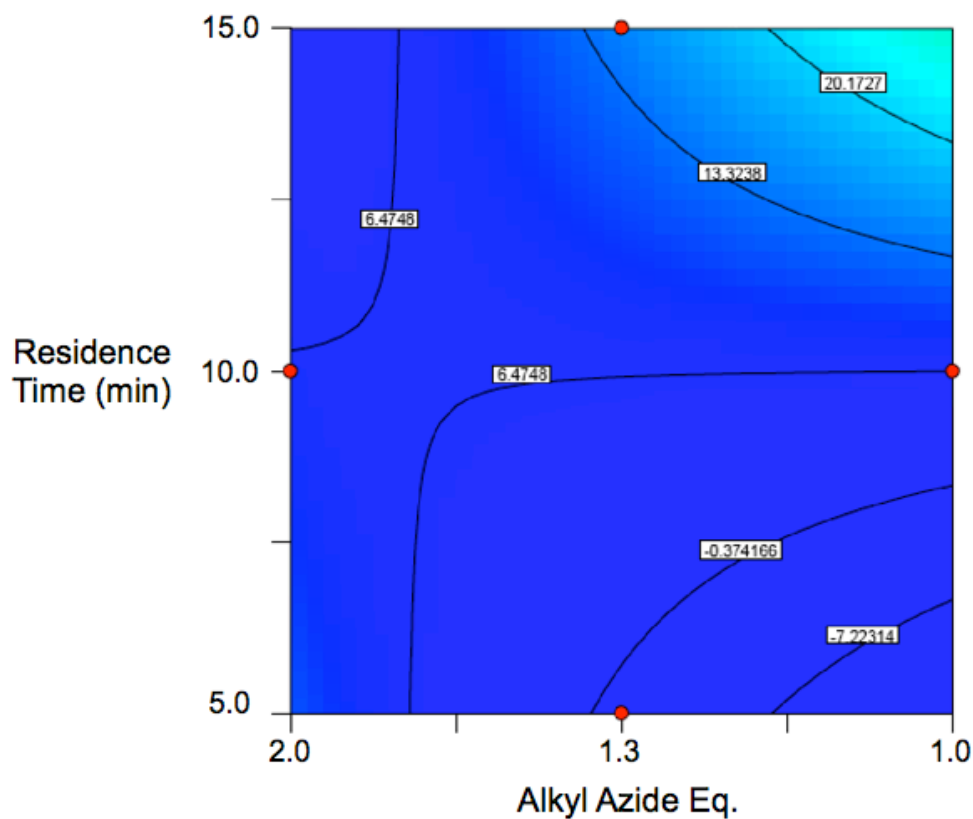


**Figure 4.5.** Contour plot for the one-pot click reaction at 100 °C.

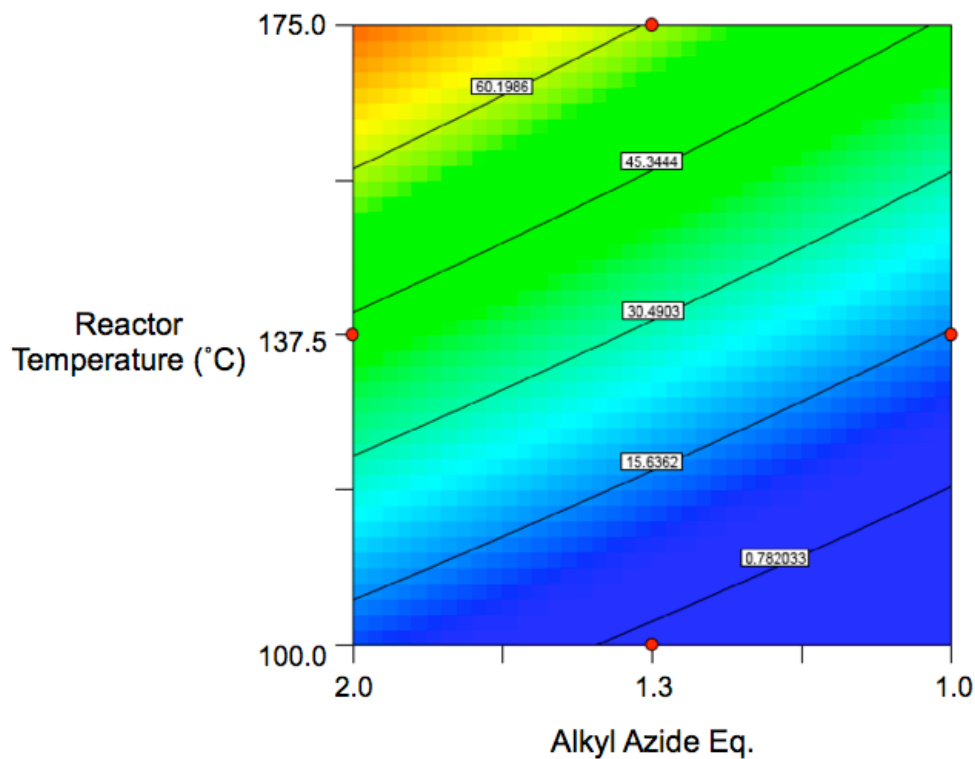


**Figure 4.6.** Contour plot for the one-pot click reaction with a 5-minute residence time.

The relationship between alkyl azide equivalents and reactor temperature, with the residence time being held constant at 5 minutes, is illustrated in Figure 4.6. At low temperature and 1 equivalent alkyl azide, it can be seen that there is essentially no reaction. As the temperature increases, however, conversions between 45-60% are obtained, with higher conversions at higher alkyl azide equivalents.

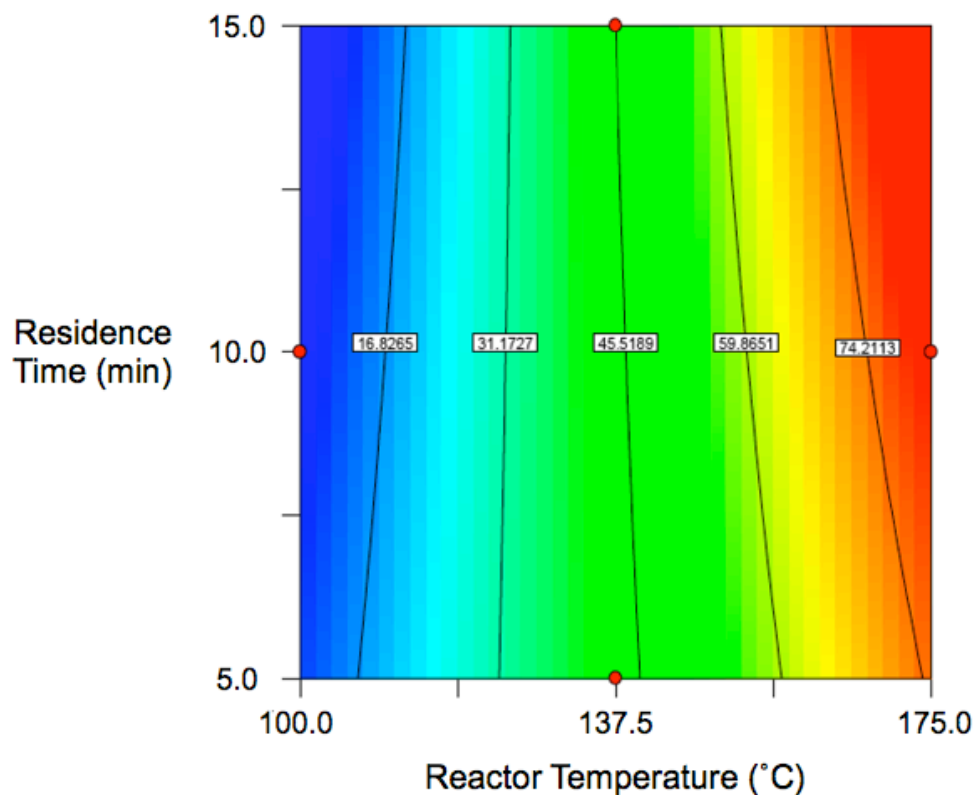
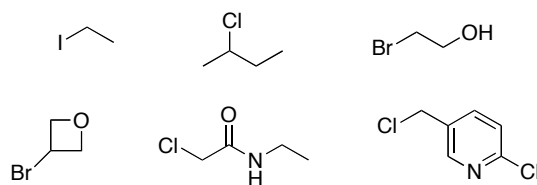


**Figure 4.7.** Contour plot for the one-pot click reaction using 2.0 eq alkyl azide.

Understanding that excess alkyl azide (2 equivalents) was favorable in this one-pot click reaction, the relationship between residence time and reactor temperature was explored to determine the optimal reaction conditions. As can be seen in Figure 4.7, there is a dramatic increase in conversion with increases in temperature. However, there is a very subtle dependence of conversion and residence time. While a 15 minute residence time did provide slightly higher conversion, we chose optimal reaction conditions in terms of product output, as opposed to yield, and settled on a 5 minute residence time. Furthermore, after running a few test substrates, a reactor temperature of 150 °C was chosen as there appeared to be no significant changes in yield. This lower temperature also made reagents less susceptible to thermal degradation.

### Alkyl Halides



### Terminal Acetylenes

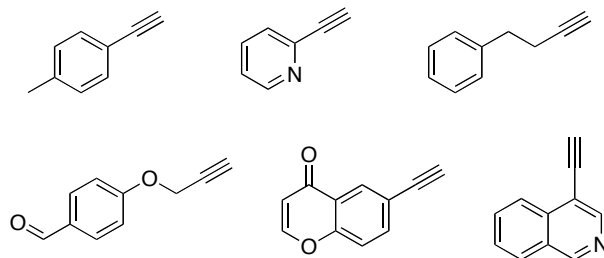


**Figure 4.8.** Alkyl halides and terminal acetylenes used for the triazole library.

Using these conditions, a library was prepared combining six different acetylenes, six different alkyl halides, and sodium azide (Figure 4.8). It should be noted that the preparation of six acetylene source vials (0.25 M in DMF), six alkyl halide source vials (0.5 M in DMF) and a sodium azide source vial (0.5 M in DMF/H<sub>2</sub>O 4:1 v/v) was the only chemical handling necessary to run the library synthesis. Using the optimized conditions for the flow click methodology, thirty triazoles were synthesized in a matter of hours in modest to excellent yield (Figure 4.9). LC traces of reaction segments were very clean, showing the presence of products, unreacted acetylene starting materials, as well as trace amounts of the free triazole (formed from the reaction of the terminal acetylene with sodium azide). For reactions resulting in low yields, an optimization could be carried out in order to increase the yield. In this proof of concept work, the optimization conditions from the DOE between 4-ethynyltoluene and 2-bromoethanol were the only conditions used. The click methodology worked for aliphatic and aromatic acetylenes, as well as

primary and secondary alkyl halides. Low molecular weight azides such as azidoethane and 3-azidooxetane were also used safely in the Conjure Flow Reactor.

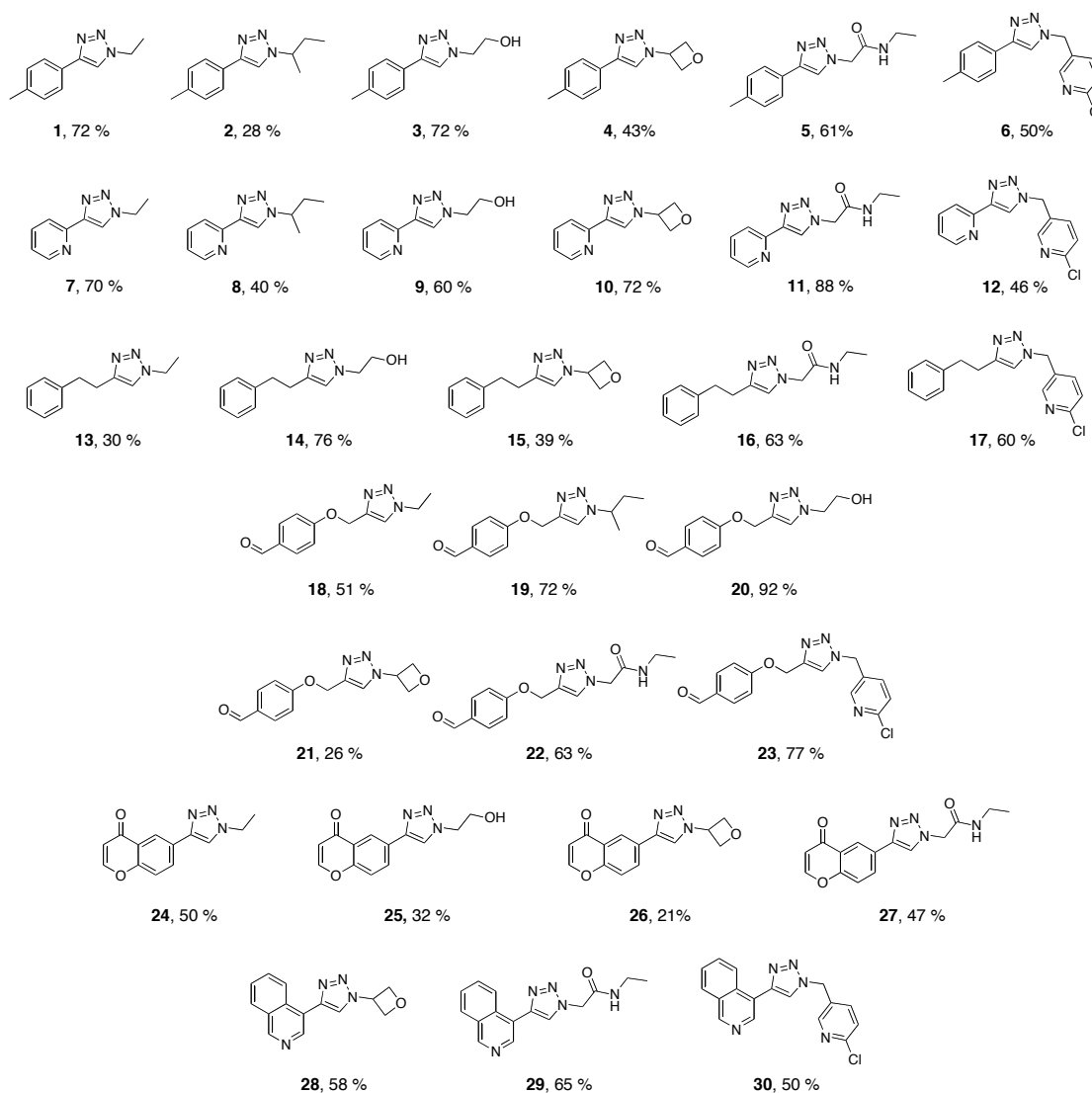


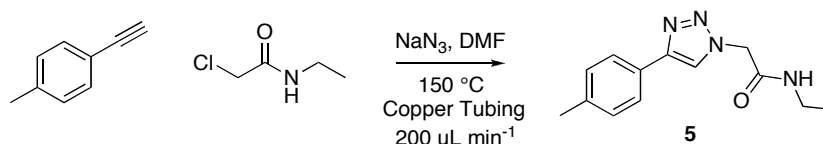
**Figure 4.9.** The 1,4-disubstituted 1,2,3-triazole synthesized using the Conjure Flow Reactor. Yields determined by  $^1\text{H}$  NMR using an internal standard.

The batch scale up of processes involving energetic intermediates such as organic azides can be dangerous as high concentrations can accumulate, thus creating an explosion hazard. Such reactions can require extensive process safety investigation

and costly custom engineered facilities. In flow this danger is significantly reduced as scale-up is a function of time and flow rate and the volume of active chemistry remains small. Through this principle, processes developed using flow technology on a small scale can subsequently be used to prepare larger scale batches as compounds move through development, minimizing process development and capital equipment costs.

To demonstrate the preparative capability of the Conjure Flow Reactor, the click reaction between 4-ethynyltoluene and N-ethyl chloroacetamide was scaled-up (Table 4.2). The stoichiometry was adjusted such that only 1 equivalent of alkyl azide was generated, thus limiting excess azide (either organic or inorganic) in the output stream. After 12 minutes, 115 mg (60%) of triazole 5 was isolated after the simple work-up of aqueous precipitation and filtration. If run continuously, this output extrapolates to generating 575 mg of product per hour, or 13.8 g of product per day (Table 4.2).

**Table 4.2.** Triazole synthesis scale-up.



Time	Triazole Output
12 minutes	115 mg <sup>a</sup>
1 hour	575 mg
1 day	13.8 g

<sup>a</sup> isolated yield

## ***Conclusion***

In summary, we have developed a one-pot click reaction using a copper flow reactor that permits *in situ* generation of organic azides and facile preparation of triazole libraries. The use of a custom engineered copper reactor serves as the catalyst to facilitate the cycloaddition. Reactions are readily scaled up with fewer safety concerns than the corresponding batch processes. The high-throughput, automated nature of the instrument greatly adds to the appeal of this process and this technology is currently being employed in the drug discovery process to rapidly synthesize vast numbers of compounds towards flow discovery.<sup>39</sup>

## ***Experimental Section***

**General Considerations.** All reagents and solvents were used as received. <sup>1</sup>H NMR analysis was carried out using a Capillary NMR probe (Protasis MRM Division, Savoy, IL) on a Varian Inova spectrometer with a Larmor frequency of 499.667 MHz. The Capillary NMR probe consisted of a 5  $\mu$ L flow cell (active volume 2.5  $\mu$ L) double-tuned to <sup>1</sup>H and <sup>13</sup>C with a deuterium lock channel and z-gradient (Protasis MRM Division, Savoy, IL). The spectrometer was equipped with a CTC HTC-PAL autosampler (Leap Technologies, Carrboro, NC). Samples were prepared using d<sub>6</sub>-DMSO spiked with the internal standard 2,5-dimethylfuran. Peaks were referenced to 2,5-dimethylfuran (5.8 ppm for <sup>1</sup>H). LC/MS analyses were carried out using an Agilent Technologies HPLC (Agilent Technologies 1200 Series diode array detector, Agilent Technologies 1200 Series column heater, Agilent 1100 Series fraction collector, Agilent 1100 Series pump, and Agilent 1100 Series degasser) interfaced with an Agilent Technologies 6120 Quadrupole LC/MS. Elemental analysis was carried out by QTI Analytical.

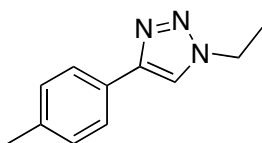
**LC/MS Analysis.** HPLC analyses was performed using a water (formic acid 0.1% w/v / ammonium formate 0.05% w/v) and MeCN (water 5% v/v, formic acid 0.1% v/v, ammonium formate 0.05% w/v) based gradient from 0-100% MeCN over 4 minutes. An Agilent ZORBAX SB-C18 1.8  $\mu\text{m}$  (4.6 x 50 mm) column was used at 80 °C with a flow rate of 3 mL min<sup>-1</sup>. Injections (0.5  $\mu\text{L}$ ) were made directly from diluted reaction mixtures and ionization monitored in positive mode.

**Typical Experimental Procedure for Triazole Library Synthesis.** 4-ethynyltoluene (133.3  $\mu\text{L}$ , 0.25 M in DMF, 0.033 mmol, 1.0 eq), ethyl iodide (133.3  $\mu\text{L}$ , 0.5 M in DMF, 0.066 mmol, 2.0 eq), and NaN<sub>3</sub> (133.3  $\mu\text{L}$ , 0.5 M in DMF/H<sub>2</sub>O 4:1 v/v, 0.066 mmol, 2.0 eq) were aspirated from their respective source vials, mixed through a PFA mixing tube (0.2 mm i. d.), loaded into an injection loop and injected into the flow reactor set at 150 °C at a rate of 400  $\mu\text{L}$  min<sup>-1</sup> (5 minute residence time). Reaction segments were collected in a 96-well plate containing QuadraPure TU copper-scavenging resin. Segments were filtered, concentrated, and analyzed using <sup>1</sup>H NMR.

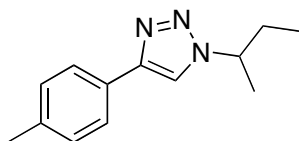
**Experimental Procedure for Scaled-Up Triazole Synthesis.** 4-ethynyltoluene (133.3  $\mu\text{L}$ , 1.0 M in DMF, 0.1333 mmol, 1.0 eq), N-ethyl chloroacetamide (133.3  $\mu\text{L}$ , 1.0 M in DMF, 0.1333 mmol, 1.0 eq), and NaN<sub>3</sub> (133.3  $\mu\text{L}$ , 1.0 M in DMF/H<sub>2</sub>O 4:1 v/v, 0.1333 mmol, 1.0 eq) were aspirated from their respective source vials, mixed through a PFA mixing tube (0.2 mm i. d.), and loaded into an injection loop. Six reaction segments were injected into the flow reactor set at 150 °C, passed through the reactor at 200  $\mu\text{L}$  min<sup>-1</sup> (10 minute residence time) and collected in a reaction vial containing heptane and water. The yellow precipitate was collected by filtration,

washed with water (2x), heptane (2x) and dried under vacuum to yield triazole 5 (115 mg, 60% yield).

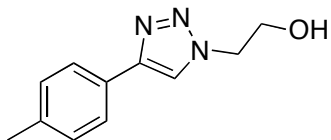
### Triazole Library Characterization Data.



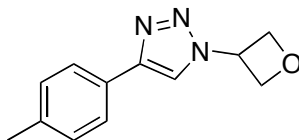
**1:**  $m/z = 188.20$   $[M+H]^+$ .  $^1\text{H NMR}$  (500 MHz,  $d_6$ -DMSO)  $\delta$  8.40 (s, 1H), 7.62 (d, 2H), 7.17 (d, 2H), 4.31 (q, 2H), 2.23 (s, 3H), 1.39 (t, 3H).



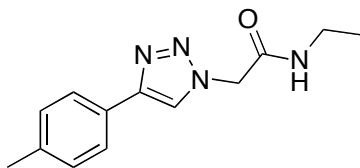
**2:**  $m/z = 216.20$   $[M+H]^+$ .  $^1\text{H NMR}$  (500 MHz,  $d_6$ -DMSO)  $\delta$  8.46 (s, 1H), 7.65 (d, 2H), 7.16 (d, 2H), 4.53 (m, 1H), 2.24 (s, 1H), 1.42 (d, 3H), 0.69 (t, 3H).



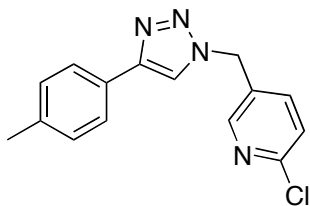
**3:**  $m/z = 204.10$   $[M+H]^+$ .  $^1\text{H NMR}$  (500 MHz,  $d_6$ -DMSO)  $\delta$  8.35 (s, 1H), 7.63 (d, 2H), 7.17 (d, 2H), 4.34 (t, 2H), 3.74 (m, 2H), 3.48 (m, 1H), 2.24 (s, 3H).



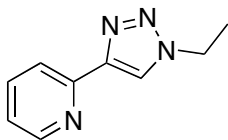
**4:**  $m/z = 216.15$   $[M+H]^+$ .  $^1\text{H NMR}$  (500 MHz,  $d_6$ -DMSO)  $\delta$  8.69 (s, 1H), 7.66 (d, 2H), 7.17 (d, 2H), 5.77 (m, 1H), 4.96 (t, 2H), 4.86 (t, 2H), 2.24 (s, 3H).



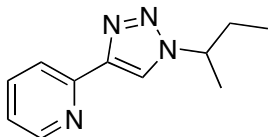
**5:**  $m/z = 245.20$   $[M+H]^+$ .  $^1\text{H NMR}$  (500 MHz,  $d_6$ -DMSO)  $\delta$  8.24 (s, 1H), 8.22 (bs, 1H), 7.64 (d, 2H), 7.16 (d, 2H), 4.99 (s, 2H), 2.24 (s, 3H), 0.94 (t, 3H). A solvent suppression pulse sequence also suppressed the  $-\text{NCH}_2\text{CH}_3$  protons (predicted 3.11 ppm).



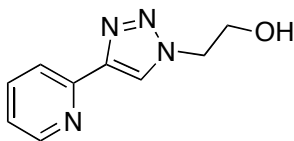
**6:**  $m/z = 285.10$   $[M+H]^+$ .  $^1\text{H NMR}$  (500 MHz,  $d_6$ -DMSO)  $\delta$  8.49 (s, 1H), 8.34 (s, 1H), 7.78 (d, 1H), 7.62 (d, 2H), 7.48 (d, 1H), 7.16 (d, 2H), 5.61 (s, 2H), 2.23 (s, 3H).



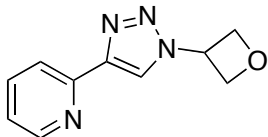
**7:**  $m/z = 175.20$   $[M+H]^+$ .  $^1\text{H NMR}$  (500 MHz,  $d_6$ -DMSO)  $\delta$  8.51 (m, 2H), 7.86 (m, 1H), 7.79 (m, 1H), 7.22 (m, 1H), 4.36 (q, 2H), 1.40 (t, 3H).



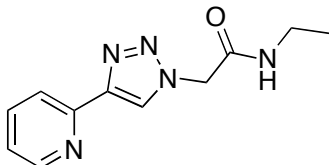
**8:**  $m/z = 203.15$   $[M+H]^+$ .  $^1\text{H NMR}$  (500 MHz,  $d_6$ -DMSO)  $\delta$  8.56 (s, 1H), 8.50 (m, 1H), 7.93 (d, 1H), 7.79 (t, 1H), 7.24 (m, 1H), 4.62 (m, 1H), 1.80 (m, 2H), 1.44 (d, 3H), 0.68 (t, 3H).



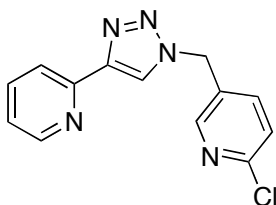
**9:**  $m/z = 191.15$   $[M+H]^+$ .  $^1\text{H NMR}$  (500 MHz,  $d_6$ -DMSO)  $\delta$  8.50 (m, 1H), 8.44 (s, 1H), 7.93 (d, 1H), 7.79 (t, 1H), 7.24 (t, 1H), 4.39 (t, 2H), 3.75 (m, 2H), 3.52 (bs, 1H).



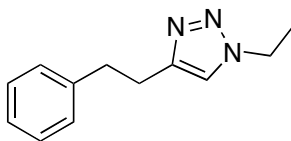
**10:**  $m/z = 203.10$   $[M+H]^+$ .  $^1\text{H NMR}$  (500 MHz,  $d_6$ -DMSO)  $\delta$  8.72 (s, 1H), 8.52 (m, 1H), 7.96 (d, 1H), 7.81 (t, 1H), 7.27 (m, 1H), 5.82 (m, 1H), 4.95 (m, 2H), 4.90 (m, 2H).



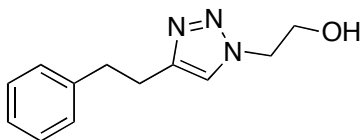
**11:**  $m/z = 232.15$   $[M+H]^+$ .  $^1\text{H NMR}$  (500 MHz,  $d_6$ -DMSO)  $\delta$  8.52 (m, 1H), 8.42 (s, 1H), 8.23 (bs, 1H), 7.93 (d, 1H), 7.80 (t, 1H), 7.25 (m, 1H), 5.05 (s, 2H), 0.976 (t, 3H). A solvent suppression pulse sequence also suppressed the  $-\text{NCH}_2\text{CH}_3$  protons (predicted 3.11 ppm).



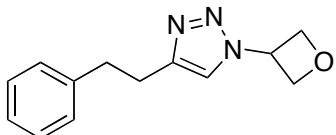
**12:**  $m/z = 272.10$   $[M+H]^+$ .  $^1\text{H NMR}$  (500 MHz,  $d_6$ -DMSO)  $\delta$  8.64 (s, 1H), 8.43 (s, 1H), 8.34 (s, 1H), 7.82 (s, 1H), 7.78 (t, 2H), 7.46 (t, 1H), 7.26 (bs, 1H), 5.66 (s, 2H).



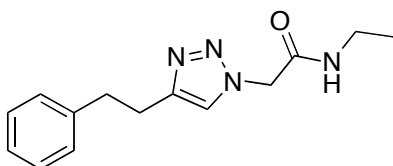
**13:**  $m/z = 202.20$   $[M+H]^+$ .  $^1\text{H NMR}$  (500 MHz,  $d_6$ -DMSO)  $\delta$  7.70 (s, 1H), 7.16 (m, 5H), 4.21 (q, 2H), 1.30 (t, 3H). A solvent suppression pulse sequence also suppressed the  $\text{Ar-CH}_2\text{CH}_2$ - protons (predicted 2.9 and 3.1 ppm).



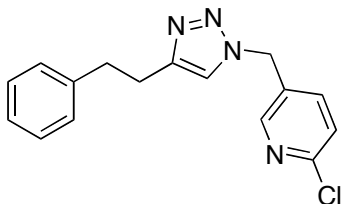
**14:**  $m/z = 218.20$   $[M+H]^+$ .  $^1\text{H NMR}$  (500 MHz,  $d_6$ -DMSO)  $\delta$  7.67 (s, 1H), 7.15 (m, 5H), 4.87 (t, 2H), 3.49 (m, 2H). A solvent suppression pulse sequence also suppressed the Ar- $\text{CH}_2\text{CH}_2$ - protons (predicted 2.9 and 3.1 ppm).



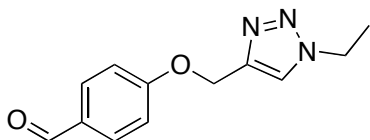
**15:**  $m/z = 230.20$   $[M+H]^+$ .  $^1\text{H NMR}$  (500 MHz,  $d_6$ -DMSO)  $\delta$  7.86 (s, 1H), 7.15 (m, 5H), 5.68 (m, 1H), 4.90 (t, 2H), 4.76 (t, 2H). A solvent suppression pulse sequence also suppressed the Ar- $\text{CH}_2\text{CH}_2$ - protons (predicted 2.9 and 3.1 ppm).



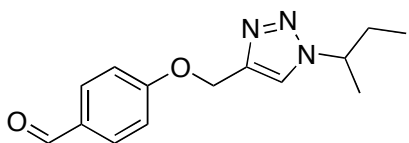
**16:**  $m/z = 259.20$   $[M+H]^+$ .  $^1\text{H NMR}$  (500 MHz,  $d_6$ -DMSO)  $\delta$  8.14 (bs, 1H), 7.66 (s, 1H), 7.16 (m, 5H), 4.89 (s, 2H), 0.96 (t, 3H). A solvent suppression pulse sequence also suppressed the Ar- $\text{CH}_2\text{CH}_2$ - protons (predicted 2.9 and 3.1 ppm) and the  $-\text{NCH}_2\text{CH}_3$  protons (predicted 3.11 ppm).



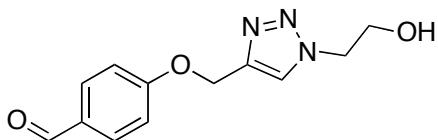
**17:**  $m/z = 299.10$   $[M+H]^+$ .  $^1\text{H NMR}$  (500 MHz,  $d_6$ -DMSO)  $\delta$  8.34 (s, 1H), 7.82 (m, 1H), 7.67 (s, 1H), 7.09 (m, 5H), 5.59 (s, 2H). A solvent suppression pulse sequence also suppressed the Ar- $\text{CH}_2\text{CH}_2$ - protons (predicted 2.9 and 3.1 ppm).



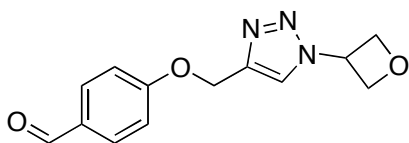
**18:**  $m/z = 232.10$   $[M+H]^+$ .  $^1H$  NMR (500 MHz,  $d_6$ -DMSO)  $\delta$  9.79 (s, 1H), 8.17 (s, 1H), 7.78 (d, 2H), 7.14 (d, 2H), 5.18 (s, 2H), 4.30 (q, 2H), 1.35 (t, 3H).



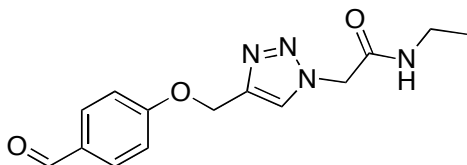
**19:**  $m/z = 260.20$   $[M+H]^+$ .  $^1H$  NMR (500 MHz,  $d_6$ -DMSO)  $\delta$  9.80 (s, 1H), 8.22 (s, 1H), 7.79 (d, 2H), 7.14 (d, 2H), 5.18 (s, 2H), 3.23 (m, 1H), 1.72 (m, 2H), 1.40 (d, 3H), 0.68 (t, 3H).



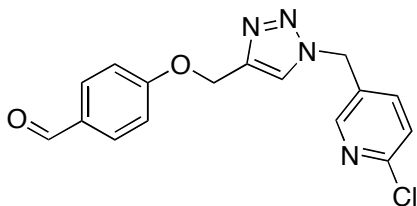
**20:**  $m/z = 248.10$   $[M+H]^+$ .  $^1H$  NMR (500 MHz,  $d_6$ -DMSO)  $\delta$  9.79 (s, 1H), 8.12 (s, 1H), 7.80 (d, 2H), 7.15 (d, 2H), 5.19 (s, 2H), 4.33 (t, 2H), 3.69 (q, 2H).



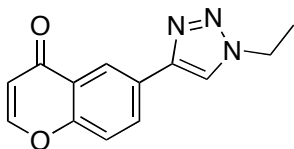
**21:**  $m/z = 260.15$   $[M+H]^+$ .  $^1H$  NMR (500 MHz,  $d_6$ -DMSO)  $\delta$  9.79 (s, 1H), 9.41 (s, 1H), 7.78 (d, 2H), 7.15 (d, 2H), 5.76 (m, 1H), 4.93 (t, 2H), 4.82 (t, 2H).



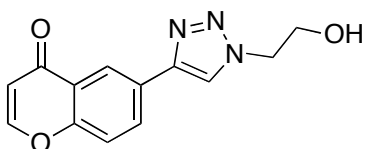
**22:**  $m/z = 289.15$   $[M+H]^+$ .  $^1H$  NMR (500 MHz,  $d_6$ -DMSO)  $\delta$  9.79 (s, 1H), 8.22 (bs, 1H), 8.12 (s, 1H), 7.78 (d, 2H), 7.15 (d, 2H), 5.20 (s, 2H), 4.97 (s, 2H), 0.94 (t, 3H). A solvent suppression pulse sequence also suppressed the  $-NCH_2CH_3$  protons (predicted 3.11 ppm).



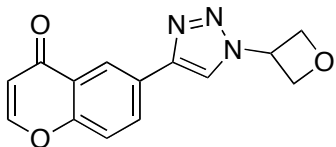
**23:**  $m/z = 329.10$   $[M+H]^+$ .  $^1H$  NMR (500 MHz,  $d_6$ -DMSO)  $\delta$  9.79 (s, 1H), 8.36 (s, 1H), 8.28 (s, 1H), 7.79 (d, 2H), 7.46 (t, 2H), 7.14 (d, 2H), 5.60 (s, 2H), 5.19 (s, 2H).



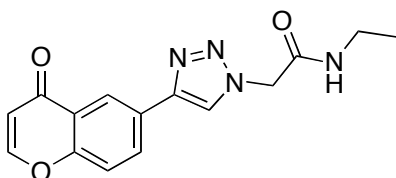
**24:**  $m/z = 242.10$   $[M+H]^+$ .  $^1H$  NMR (500 MHz,  $d_6$ -DMSO)  $\delta$  8.77 (s, 1H), 8.37 (s, 1H), 8.23 (d, 1H), 8.17 (d, 1H), 7.65 (d, 1H), 6.64 (d, 1H), 4.35 (q, 2H), 1.42 (t, 3H).



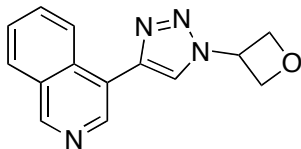
**25:**  $m/z = 258.10$   $[M+H]^+$ .  $^1H$  NMR (500 MHz,  $d_6$ -DMSO)  $\delta$  8.62 (s, 1H), 8.38 (s, 1H), 8.21 (d, 1H), 8.19 (d, 1H), 7.66 (d, 1H), 6.31 (d, 1H), 4.37 (t, 2H), 3.77 (q, 2H).



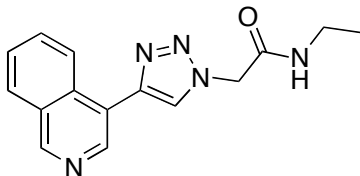
**26:**  $m/z = 270.10$   $[M+H]^+$ .  $^1H$  NMR (500 MHz,  $d_6$ -DMSO)  $\delta$  8.98 (s, 1H), 8.42 (s, 1H), 8.22 (m, 2H), 7.67 (d, 2H), 6.29 (d, 2H), 5.79 (m, 1H), 4.98 (t, 2H), 4.88 (t, 2H).



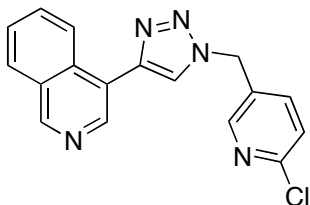
**27:**  $m/z = 299.10$   $[M+H]^+$ .  $^1H$  NMR (500 MHz,  $d_6$ -DMSO)  $\delta$  8.60 (s, 1H), 8.39 (s, 1H), 8.20 (m, 2H), 7.96 (d, 2H), 6.28 (d, 1H), 5.03 (s, 2H), 0.95 (t, 3H). A solvent suppression pulse sequence also suppressed the  $-NCH_2CH_3$  protons (predicted 3.11 ppm).



**28:**  $m/z = 253.10 [M+H]^+$ .  $^1\text{H NMR}$  (500 MHz,  $d_6$ -DMSO)  $\delta$  9.26 (s, 1H), 8.89 (s, 1H), 8.72 (s, 1H), 8.13 (d, 1H), 7.79 (t, 1H), 7.68 (t, 1H), 5.89 (m, 1H), 5.01 (t, 2H), 4.97 (t, 2H).



**29:**  $m/z = 282.10 [M+H]^+$ .  $^1\text{H NMR}$  (500 MHz,  $d_6$ -DMSO)  $\delta$  9.25 (s, 1H), 8.68 (s, 1H), 8.58 (s, 1H), 8.29 (bs, 1H), 8.12 (d, 1H), 7.78 (t, 1H), 7.68 (t, 1H), 5.12 (s, 2H), 0.96 (t, 3H). A solvent suppression pulse sequence also suppressed the  $-\text{NCH}_2\text{CH}_3$  protons (predicted 3.11 ppm).



**30:**  $m/z = 322.10 [M+H]^+$ .  $^1\text{H NMR}$  (500 MHz,  $d_6$ -DMSO)  $\delta$  9.24 (s, 1H), 8.75 (s, 1H), 8.68 (s, 1H), 8.48 (s, 1H), 8.34 (s, 1H), 8.12 (d, 1H), 7.85 (m, 1H), 7.78 (t, 1H), 7.47 (t, 2H), 5.73 (s, 2H).

## REFERENCES

1. Kolb, H. C.; Finn, M. G.; Sharpless, K. B. *Angew. Chem. Int. Ed.* **2001**, *40*, 2004.
2. Rostovtsev, V. V.; Green, L. G.; Fokin, V. V.; Sharpless, K. B. *Angew. Chem. Int. Ed.* **2002**, *41*, 2596.
3. Wu, P.; Feldman, A. K.; Nugent, A. K.; Hawker, C. J.; Scheel, A.; Voit, B.; Pyun, J.; Fréchet, J. M. J.; Sharpless, K. B.; Fokin, V. V. *Angew. Chem. Int. Ed.* **2004**, *43*, 3928.
4. Rodionov, V. O.; Fokin, V. V.; Finn, M. G. *Angew. Chem. Int. Ed.* **2005**, *44*, 2210.
5. Punna, S.; Kuzelka, J.; Wang, Q.; Finn, M. G. *Angew. Chem. Int. Ed.* **2005**, *117*, 2255.
6. Himo, F.; Lovell, T.; Hilgraf, R.; Rostovtsev, V. V.; Noodleman, L.; Sharpless, K. B.; Fokin, V. V. *J. Am. Chem. Soc.* **2005**, *127*, 210.
7. Wu, P.; Fokin, V. V. *Aldrichim. Acta* **2007**, *40*, 7.
8. Buckle, D. R.; Outred, D. J.; Rockell, C. J. M.; Smith, H.; Spicer, B. A. *J. Med. Chem.* **1983**, *26*, 251.
9. Buckle, D. R.; Rockell, C. J. M.; Smith, H.; Spicer, B. A. *J. Med. Chem.* **1986**, *29*, 2269.
10. Genin, M. J.; Allwine, D. A.; Anderson, D. J.; Barbachyn, M. R.; Emmert, D. E.; Garmon, S. A.; Graber, D. R.; Grega, K. C.; Hester, J. B.; Hutchinson, D. K.; Morris, J.; Reischer, R. J.; Ford, C. W.; Zurenko, G. E.; Hamel, J. C.; Schaadt, R. D.; Stapert, D.; Yagi, B. H. *J. Med. Chem.* **2000**, *43*, 953.
11. Alvarez, R.; Velazquez, S.; San-Felix, A.; Aquaro, S.; De Clercq, E.; Perno, C. F.; Karlsson, A.; Balzarini, J.; Camarasa, M. J. *J. Med. Chem.* **1994**, *37*, 4185.
12. H. Wamhoff, in *Comprehensive Heterocyclic Chemistry*, Vol. 5 (Eds; A. R. Katrizky, C. W. Rees) Pergamon, Oxford, **1984**, pp 669.
13. Bock, V. D.; Hiemstra, H.; van Maarseveen, J. H. *Eur. J. Org. Chem.* **2006**, 51.
14. Kolb, H. C.; Sharpless, K. B. *Drug Discovery Today*, **2004**, *8*, 1128.

15. Krasinski, A.; Radic, Z.; Manetsch, R.; Raushel, J.; Taylor, P.; Sharpless, K. B.; Kolb, H. C. *J. Am. Chem. Soc.* **2005**, *127*, 6686.
16. For a review on organic azides, see: Bräse, S.; Gil, C.; Knepper, K.; Zimmermann, V. *Angew. Chem. Int. Ed.* **2005**, *44*, 5188.
17. Appukkuttan, P.; Dehaen, W.; Fokin, V. V.; Van der Eycken, E. *Org. Lett.* **2004**, *6*, 4223.
18. Feldman, A. K.; Colasson, B.; Fokin, V. V. *Org. Lett.* **2004**, *6*, 3897.
19. Kacprzak, K. *Synlett* **2005**, *6*, 943.
20. Chittaboina, S.; Xie, F.; Wang, Q. *Tet. Lett.* **2005**, *46*, 2331.
21. Mason, B. P.; Price, K. E.; Steinbacher, J. L.; Bogdan, A. R.; McQuade, D. T. *Chem. Rev.* **2007**, *107*, 2300.
22. Hessel, V.; Lob, P.; Lowe, H. *Curr. Org. Chem.* **2005**, *9*, 765A.
23. Hessel, V.; Lowe, H. *Chem. Eng. Technol.* **2005**, *28*, 267.
24. Hessel, V.; Lob, P.; Lowe, H. *Curr. Org. Chem.* **2005**, *9*, 765.
25. Penneman, H.; Watts, P.; Haswell, S. J.; Hessel, V.; Lowe, H. *Org. Process Res. Dev.* **2004**, *8*, 422.
26. Jas, G.; Kirschning, A. *Chem. Eur. J.* **2003**, *9*, 5708.
27. Hodge, P. *Curr. Opin. Chem. Biol.* **2003**, *7*, 362.
28. Haswell, S. J.; Watts, P. *Green Chem.* **2003**, *5*, 240.
29. Kirschning, A.; Solodenko, W.; Mennecke, K. *Chem. Eur. J.* **2006**, *12*, 5972.
30. Yoshida, J.; Nagaki, A.; Yamada, T. *Chem. Eur. J.* **2008**, *14*, 7450 and references within.
31. Nagaki, A.; Takabayashi, N.; Tomida, Y.; Yoshida, J. *Org. Lett.* **2008**, *10*, 3937.
32. Nagaki, A.; Kim, H.; Yoshida, J. *Angew. Chemie. Int. Ed.* **2008**, *47*, 7833.

33. van der Linden, J. M. J.; Hilberink, P. W.; Kronenburg, C. M. P.; Kemperman, G. J. *Org. Process Res. Dev.* **2008**, *12*, 911.
34. Grant, D.; Dahl, R.; Cosford, N. D. P. *J. Org. Chem.* **2008**, *73*, 7219.
35. Hamper, B. C.; Tesfu, E. *Synlett*, **2007**, 2257.
36. The process of numbering-up may also be used to scale-up flow reactions. Numbering-up is simply the process of adding more reactors to the flow setup, without needing to change any variables other than flow rates. Ehrfeld, W.; Hessel, V.; Lowe, H. *Microreactors: New Technology for Modern Chemistry*, Wiley-VCH, Weinheim, **2000**.
37. Hornung, C. H.; Mackley, M. R.; Baxendale I. R.; Ley, S. V. *Org. Process Res. Dev.* **2007**, *11*, 399.
38. Acke, D. R. J.; Stevens, C. V. *Org. Process Res. Dev.* **2006**, *10*, 417.
39. Wheeler, R. C.; Benali, O.; Deal, M.; Farrant, E.; MacDonald, S. J. F.; Warrington, B. H. *Org. Process Res. Dev.* **2007**, *11*, 704.
40. Benali, O.; Deal, M.; Farrant, E.; Tapolczay, D.; Wheeler, R. *Org. Process Res. Dev.* **2008**, *12*, 1007.
41. Rahman, T.; Fukuyama, T.; Kamata, N.; Sato, M.; Ryu, I. *Chem. Commun.* **2006**, *21*, 2236.
42. Song, H.; Tice, J. D.; Ismagilov, R. F. *Angew. Chem. Int. Ed.* **2003**, *42*, 767.
43. Zheng, B.; Roach, L. S.; Ismagilov, R. F. *J. Am. Chem. Soc.* **2003**, *125*, 11170.
44. Song, H.; Ismagilov, R. F. *J. Am. Chem. Soc.* **2003**, *125*, 14613.
45. Shestopalov, I.; Tice, J. D.; Ismagilov, R. F. *Lab Chip*, **2004**, *4*, 316.
46. Zheng, B.; Ismagilov, R. F. *Angew. Chem. Int. Ed.* **2004**, *44*, 2520.
47. Bogdan, A. R.; Mason, B. P.; Sylvester, K. T.; McQuade, D. T. *Angew. Chem. Int. Ed.* **2007**, *46*, 1098.
48. Saaby, S.; Knudsen, K. R.; Ladlow, M.; Ley, S. V. *Chem. Commun.* **2005**, 2909.
49. Kobayashi, J.; Mori, Y.; Kobayashi, S. *Adv. Synth. Catal.* **2005**, *347*, 1889.

50. Kobayashi, J.; Mori, Y.; Kobayashi, S. *Chem. Commun.* **2005**, 2567.
51. Kobayashi, J.; Mori, Y.; Okamoto, K.; Akiyama, R.; Ueno, M.; Kitamori, T.; Kobayashi, S. *Science* **2004**, *304*, 1305.
52. The Husigen [3+2] thermal addition of organic azides to acetylenes is a slow process that requires extensive heating. This thermal cycloaddition also yields a mixture of isomers, whereas the copper-catalyzed cycloaddition preferentially generates the 1,4-triazole. There were no traces of the 1,5-disubstituted isomers by LC/MS and NMR.
53. The reactor was frequently washed with 1M NH<sub>3</sub> (aq), 1 M HCl, and again with 1 M NH<sub>3</sub> (aq) to ensure there was not a build-up of dangerous copper azide within the reactor.
54. The reaction was optimized in terms of reactor output to demonstrate the high-throughput synthetic capabilities of the flow reactor.
55. Equivalents of alkyl azide is defined as the equivalents of alkyl halide, coupled with equivalents of sodium azide. For instance, 1 eq alkyl halide and 1 eq sodium azide is assumed to be 1 eq alkyl azide.

## CHAPTER 5

### The Flow Syntheses of Active Pharmaceutical Ingredients

#### *Preface*\*

In 2007, the startup company Systanix, started by my advisor and former McQuade group member Dr. Steven Broadwater, began a nine-month collaboration with the engineering firm Foster Miller, Inc. The goal was to develop common synthetic pathways for various active pharmaceutical ingredients (APIs), demonstrate these syntheses using traditional batch chemistry, and subsequently transition these syntheses into flow reactors. Sarah Poe, Daniel Kubis and I were hired by Systanix as consultants to develop these syntheses and carry them out in flow. By the time the project ended in August of 2007, great progress was made with regards to performing these reactions in flow, however due to time constraints, some work remained unfinished. This chapter highlights the batch syntheses of ibuprofen and atropine and demonstrates the efforts put forth to develop flow syntheses for these two APIs.

#### *Abstract*

Syntheses for the APIs ibuprofen and atropine were developed containing common reaction pathways. The syntheses were initially demonstrated in batch and were transitioned into flow using a simplified microreactor. The step-wise synthesis of ibuprofen was successfully completed in flow, as was the synthesis of methyl ether-protected atropine. While some work in this project remained unfinished, it set a foundation for future flow syntheses performed in the group.

---

\* The author thanks Dr. Steven Broadwater, Dr. Sarah Poe, and Daniel Kubis for their contributions to this unpublished work.

## ***Introduction***

Although traditional organic synthesis is a wildly successful enterprise, the pharmaceutical industry produces 25-100 kg of waste on average for every kilogram of product synthesized.<sup>1</sup> With increasing oil prices and diminishing natural resources, more sustainable methods and technologies are needed to synthesize molecules of importance. The issue of sustainable chemistry has recently been gaining a significant amount of attention, as indicated by the new green chemistry-oriented journals and conferences present in the chemistry community. Furthermore, the Obama Administration recently allocated \$200 million for development of chemical methodologies and tools to promote green chemistry. Special interest is specifically being paid to invoke innovation in the discovery, development, and production of APIs.

Despite these initiatives aimed to develop new, cleaner syntheses, other issues that contribute to the waste associated with pharmaceutical synthesis such as the packaging, transport and storage of reagents and products, are typically neglected.<sup>2</sup> Funded by the Defense Advanced Research Projects Agency (DARPA), the goal of this project was to develop common syntheses for two APIs in flow, with the ultimate goal being on-demand drug production in a portable flow reactor. By developing syntheses that relied on common reagents and reaction conditions, the number and types of materials required for synthesis and purification would be minimized. Furthermore, the ability for the flow reactor to synthesize APIs on-demand would eliminate the need for product packaging and storage. The molecules studied in this project are the APIs ibuprofen (**1**) and atropine (**2**) (Figure 5.1).

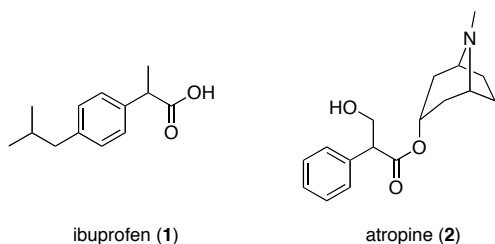
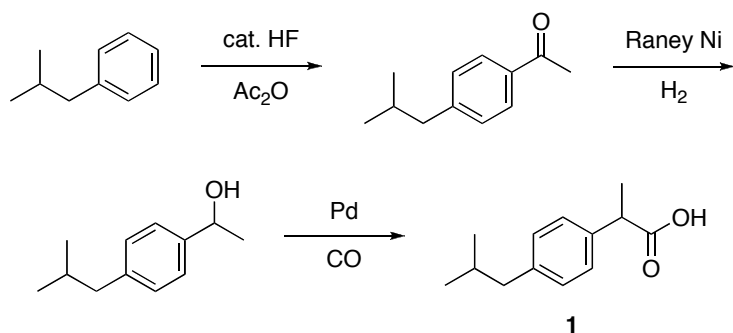


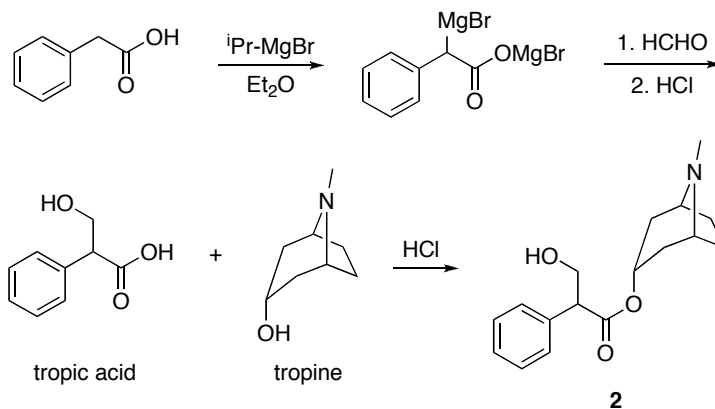
**Figure 5.1.** The structures of ibuprofen and atropine.

Ibuprofen is a non-steroidal anti-inflammatory drug (NSAID) used to alleviate various types of pain, fevers and mild inflammations. As of 2007, ibuprofen was one of the top-selling 100 generic drugs globally and was added to a list of essential medicines by the World Health Organization that dictates which medicines are necessary for providing basic health care. The BHC Company (now BASF) won the 1997 Presidential Green Chemistry Challenge for its synthesis of ibuprofen shown below in Scheme 5.1.<sup>3,4</sup>



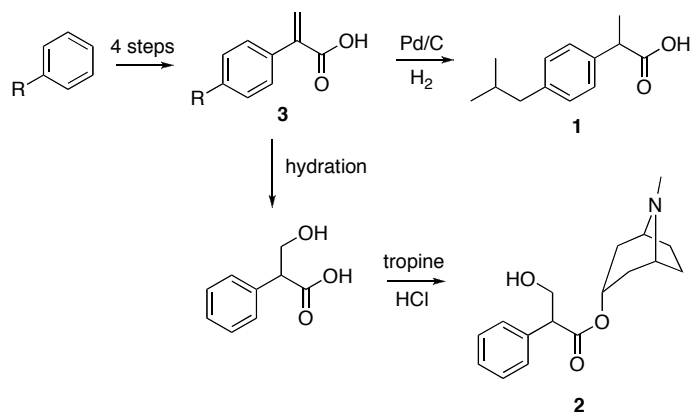
**Scheme 5.1.** The BHC Company's synthesis of ibuprofen.

Atropine is an anticholinergic agent and is also considered an essential medicine by the World Health Organization. While atropine is commonly extracted from natural sources, there are many examples of its synthesis. One synthesis for atropine is shown below in Scheme 5.2 and Scheme 5.3.<sup>5-7</sup>



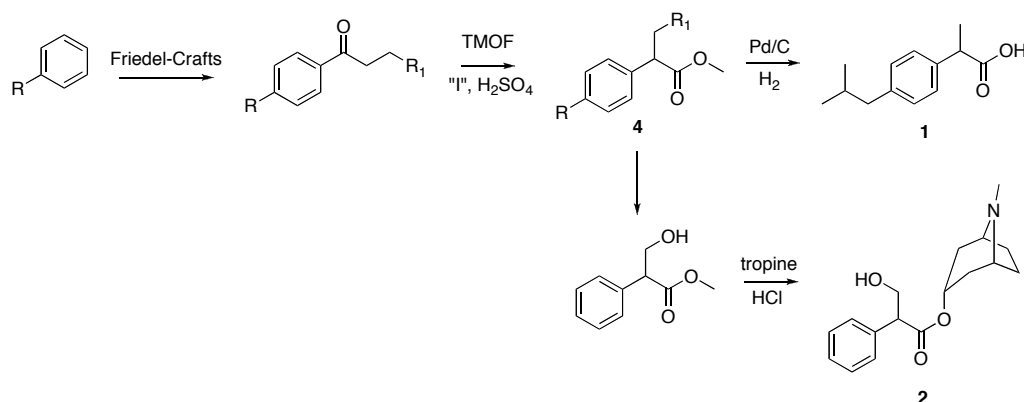
**Scheme 5.2.** The synthesis of atropine.

The first goal of this project was to develop syntheses for ibuprofen and atropine that utilized a common set of reactions. The initial reaction design shown below in Scheme 5.3 relied on synthesizing a 2-phenylprop-2-enoic acid derivative (**3**) that could be converted to the final products.



**Scheme 5.3.** The syntheses of ibuprofen and atropine utilizing 2-phenylprop-2-enoic acid intermediates.

After many unsuccessful attempts at the chemistry in Scheme 5.3, a new set of reactions was developed that greatly reduced the number of steps and relied on 2-arylpropanoates (**4**) as the common intermediate (Scheme 5.4).



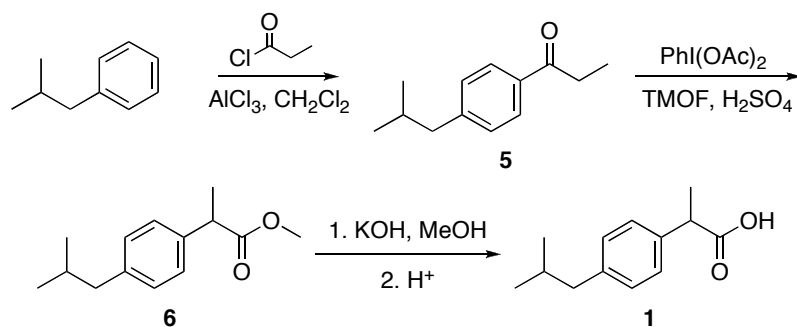
**Scheme 5.4.** The syntheses of ibuprofen and atropine utilizing 2-arylpropanoate intermediates.

This chapter begins by discussing our efforts to synthesize ibuprofen and atropine in batch using the reaction design shown in Scheme X. The remainder of the chapter discusses translating these reactions into flow using a simplified microreactor platform.

### ***Results and Discussion***

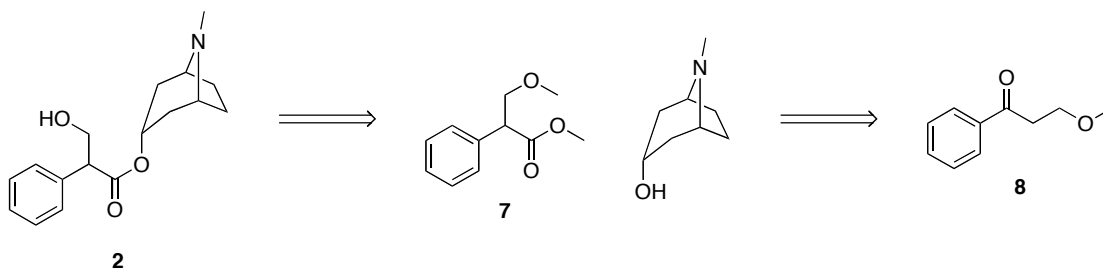
**Batch Syntheses of Ibuprofen and Atropine.** A majority of the batch synthesis of ibuprofen was carried out by Sarah Poe and will not be discussed in great detail here. The reactions performed will be highlighted, however, as this chemistry was ultimately translated into our flow reactor.

The first step of our synthesis involved the Friedel-Crafts acylation of isobutylbenzene using propionyl chloride and  $\text{AlCl}_3$  to afford 4-isobutylpropiophenone (**5**). The second step relied on the  $\text{PhI}(\text{OAc})_2$ -mediated 1,2-aryl migration<sup>8-10</sup> to give methyl ester (**6**), which was subsequently saponified using KOH. Ibuprofen was obtained after an acidic workup with high purity and yield (Scheme 5.5).



**Scheme 5.5.** The batch synthesis of ibuprofen.

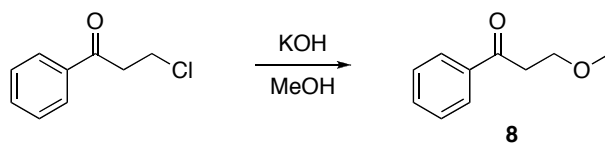
Having demonstrated this successful synthesis of ibuprofen in batch, a synthesis of atropine was explored that relied on a somewhat similar set of reaction conditions. A retrosynthetic analysis of atropine reveals a 2-phenylpropanoic ester (**7**) similar to methyl ester (**6**) in the ibuprofen synthesis (Scheme 5.6). It was anticipated that a similar 1,2-aryl migration could be used to produce (**7**), starting from a substituted propiophenone (**8**).



**Scheme 5.6.** The retrosynthetic analysis of atropine revealing a 2-phenylpropanoic ester.

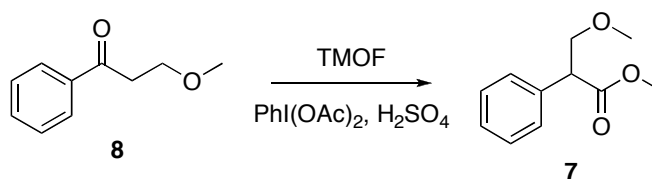
The first step of the atropine synthesis utilized a substitution reaction to yield 3-methoxypropiophenone (**8**, Scheme 5.7). While the individual steps to synthesize ibuprofen and atropine are not identical, they do utilize common reagents in the chemical transformations. This displacement, for instance, relies on the use of a

methanolic KOH, which was used in the saponification of methyl ester **6** in the ibuprofen synthesis.



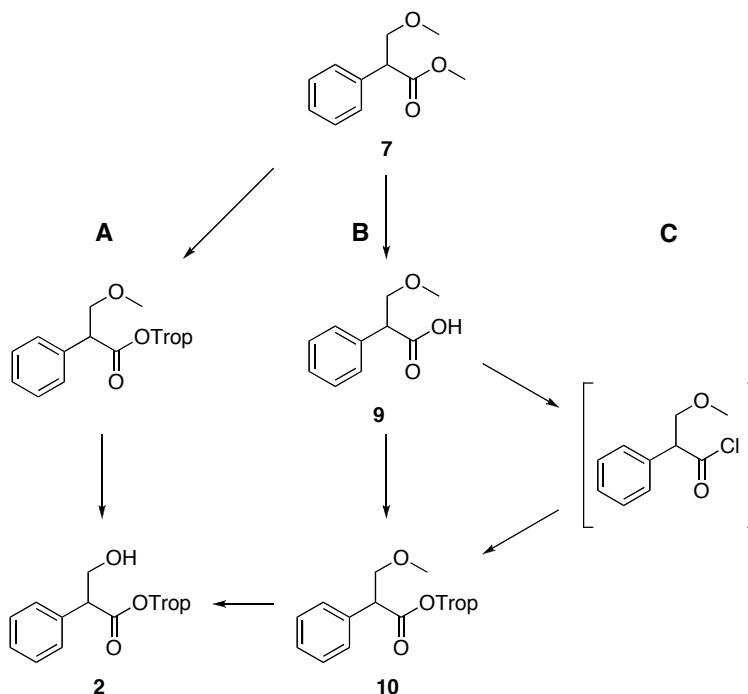
**Scheme 5.7.** The synthesis of 3-methoxypropiofenone.

The second step of the atropine synthesis used a  $\text{PhI}(\text{OAc})_2$ -mediated 1,2-aryl migration to yield methyl ester **7** (Scheme 5.8).



**Scheme 5.8.** The  $\text{PhI}(\text{OAc})_2$ -mediated 1,2-aryl migration of 3-methoxypropiofenone.

Methyl ester **7** permitted three different plausible routes to complete the synthesis of atropine (Scheme 5.9). The first (Scheme 5.9A) would use a transesterification using tropine, followed by a deprotection of the methyl ether. In an alternative route, the saponification of methyl ester **7** would be followed by an esterification (Scheme 5.9B). The final possible route relied on the saponification of methyl ester **7**, followed by treatment with thionyl chloride to activate the carboxylic acid to facilitate the tropine esterification (Scheme 5.9C).

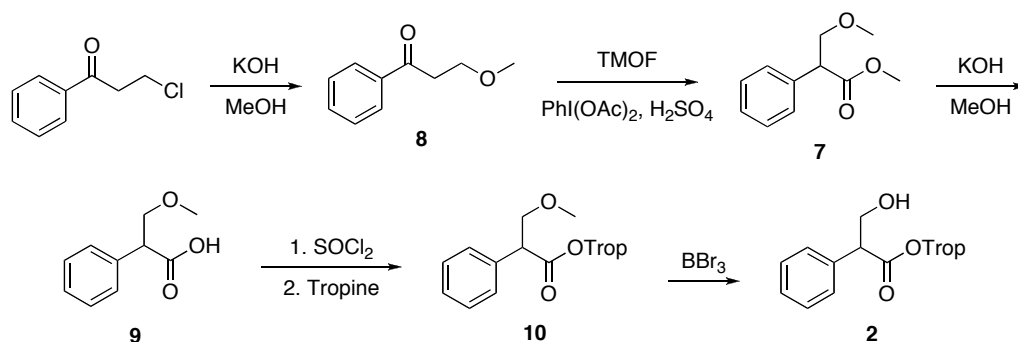


**Scheme 5.9.** Alternative methods for the synthesis of atropine starting from methyl ester **7**. A) transesterification; B) esterification; C) esterification using an activated carboxylic acid.

After screening a variety of reaction conditions, the transesterification shown in Scheme 5.9A proved to be an unproductive route. For the direct esterification route shown in Scheme 5.9B, a methanolic solution of KOH afforded carboxylic acid **9** in an 88% yield, but the subsequent esterification with tropine to give ester **10** was unsuccessful. The most effective route to couple tropine with carboxylic acid **9** was using thionyl chloride to make the activated carboxylic acid (Scheme X C). After removing excess thionyl chloride under vacuum, the acid chloride was coupled with tropine to form ester **10** in 52% isolated yield.

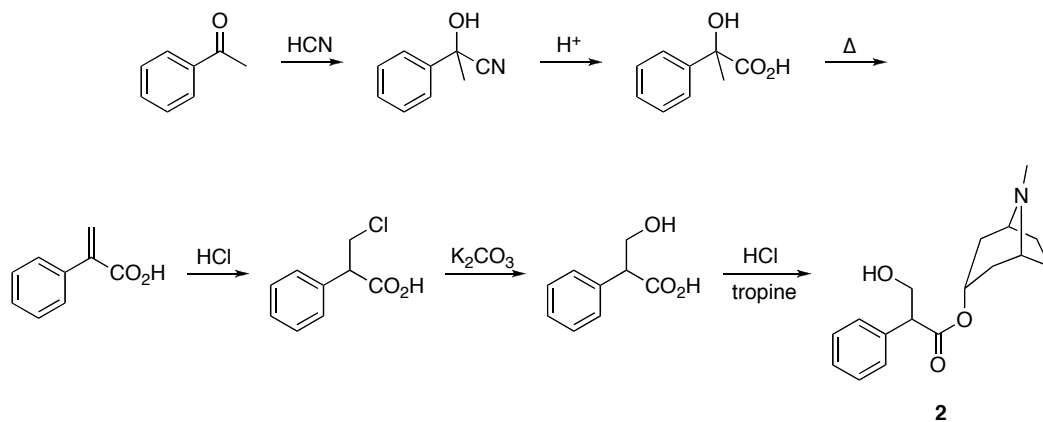
The final step of the atropine synthesis relied on a boron tribromide-mediated demethylation (Scheme 5.10). Analysis of this reaction using thin layer chromatography indicated that atropine was being formed under these conditions, however no isolated yield was obtained. It is possible that the tertiary amine in the

tropine moiety was slowly being methylated by the methyl bromide byproduct that is formed during the course of the reaction. This method is very promising and could be optimized if more time was available. The complete synthesis of atropine is shown below in Scheme 5.10.



**Scheme 5.10.** The complete synthesis of atropine.

This synthesis of atropine is comparable to other atropine preparations in terms of the number of steps. In the early 1900s, Mackenzie and Ward synthesized tropic acid using a five-step process starting from acetophenone (Scheme 5.11).<sup>11</sup> The coupling of tropic acid with tropine is achieved using anhydrous HCl, generating atropine.



**Scheme 5.11.** The synthesis of atropine using Mackenzie and Ward's tropic acid synthesis.

**Ibuprofen Synthesis in Flow.** Having successfully synthesized both ibuprofen and atropine in batch, the next goal of this project was to run the reactions in a simplified flow reactor setup developed in our group. We have published a series of papers highlighting the use of simplified microreactors to organic synthesis.<sup>12-16</sup> The microreactors consist of perfluoroelastomeric tubing (1.6 mm i.d.), Y-junctions and syringe pumps to provide reagent flow (Figure 5.2).

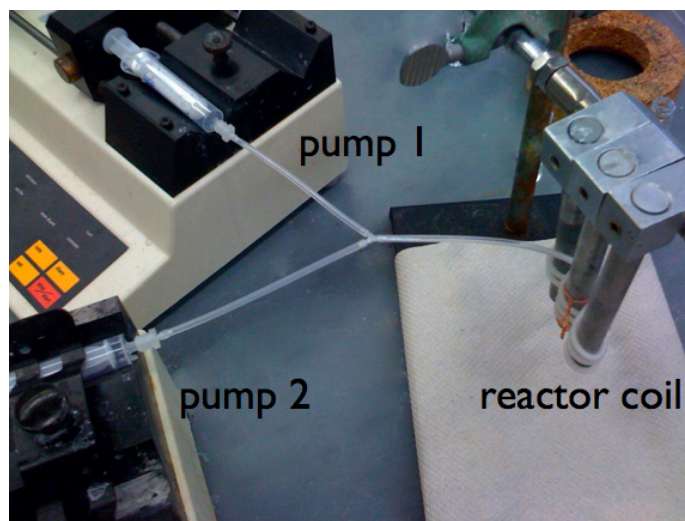
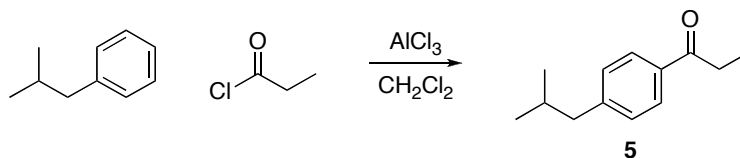


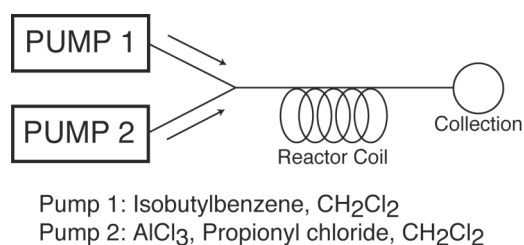
**Figure 5.2.** The flow reaction setup. Two syringe pumps provide reagent flow to the reactor coil.

The first step of our ibuprofen synthesis in flow was completed using the Friedel-Crafts acylation previously optimized in batch (Scheme 5.12).



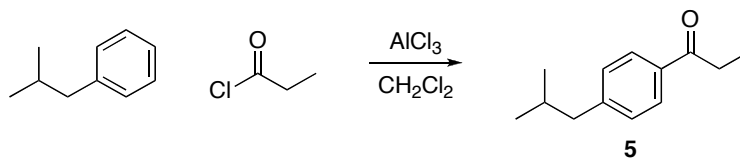
**Scheme 5.12.** Friedel-Crafts acylation of isobutylbenzene.

To optimize this reaction in flow, we used the setup shown in Figure 5.3. These two fluid streams were combined at a Y-junction where they would mix before passing through the microchannel. At the outlet of the reactor, the stream was collected in water to quench the reactions. Reaction times were subsequently varied by changing the flow rates. The optimization of the flow Friedel-Crafts acylation is shown in Table 5.1.



**Figure 5.3.** The flow Friedel-Crafts acylation setup.

From Table 5.1, it can be determined that an excess of the acylating agent is required to achieve high conversions. Slower flow rates, and thus longer residence times, are also preferred. Initially the most success was achieved using 2 equivalents of both AlCl<sub>3</sub> and propionyl chloride (Table 5.1, entries 8-10). In particular, using a 0.5 M stock solution of isobutylbenzene was particularly appealing as it provided approximately 140 mg hr<sup>-1</sup> of 4-isobutylpropiophenone (**5**). The reaction was optimized further by reducing the equivalents of AlCl<sub>3</sub> and propionyl chloride by 25% (Table 5.1, entries 12-15). Having determined these optimal conditions for the flow Friedel-Crafts acylation, the second step of the ibuprofen synthesis was optimized in flow.

**Table 5.1.** Results of the flow Friedel-Crafts acylation.<sup>a</sup>

Entry	Eq. AlCl <sub>3</sub>	Eq. Prop. Cl	Flow Rate (μL min <sup>-1</sup> )	Residence Time (min)	Conversion <sup>b</sup> (%)
1	1.5	1.0	30	42.8	76
2	1.5	1.0	40	32.1	42
3	2.0	1.0	40	32.1	82
4	2.0	1.5	40	32.1	86
5	2.0	1.5	50	25.7	80
6	2.0	1.5	80	16.0	83
7	2.0	2.0	40	32.1	78
8	2.0	2.0	50	25.7	94
9	2.0	2.0	50	25.7	>99 <sup>c</sup>
10	2.0	2.0	50	25.7	>99 <sup>d</sup>
11	2.0	2.0	80	16.0	70
12	1.5	1.5	50	25.7	98 <sup>c</sup>
13	1.5	1.5	40	32.1	97 <sup>c</sup>
14	1.5	1.5	60	21.4	98 <sup>c</sup>
15	1.5	1.5	65	19.7	97 <sup>c</sup>

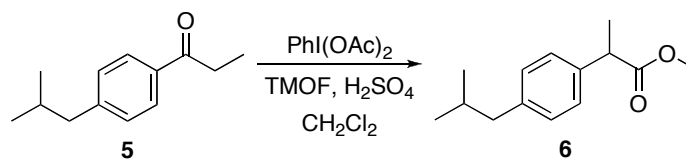
<sup>a</sup> Reactions carried out using a 0.1 M stock solution of isobutylbenzene at room temperature unless otherwise noted.

<sup>b</sup> Conversion based on GC.

<sup>c</sup> Using a 0.25 M stock solution of isobutylbenzene.

<sup>d</sup> Using a 0.5 M stock solution of isobutylbenzene.

The second step of the ibuprofen synthesis was successfully completed using the PhI(OAc)<sub>2</sub>-mediated 1,2-aryl migration in our flow reactor (Scheme 5.13).



**Scheme 5.13.** The  $\text{PhI}(\text{OAc})_2$ -mediated 1,2-aryl migration of 4-isobutylpropiophenone.

The setup of the flow reaction is shown in Figure 5.4. A stream of concentrated sulfuric acid was added to a stream of 4-isobutylpropiophenone, trimethylorthoformate (TMOF), and  $\text{PhI}(\text{OAc})_2$  in dichloromethane at room temperature.

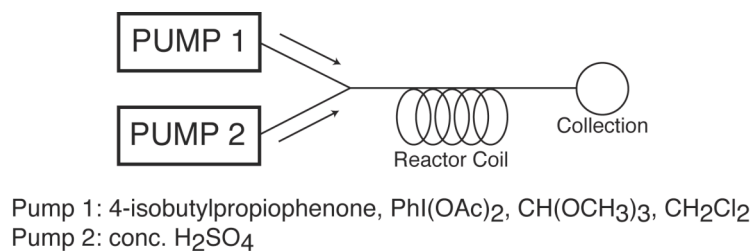
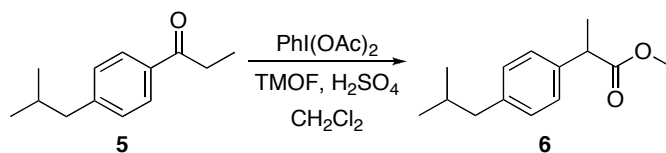


**Figure 5.4.** The flow 1,2-aryl migration setup.

Data for the optimization of the  $\text{PhI}(\text{OAc})_2$ -mediated 1,2-aryl migration in flow are shown in Table 5.2.

As can be from Table 5.2, using excess TMOF permits shorter residence times (Table 5.2, entries 1-4). However, one goal of this synthesis was to reduce the amount of waste generated during the synthesis. The number of equivalents of TMOF was therefore reduced from 17 equivalents to 2 equivalents while maintaining a high yield of 96%, albeit at a lower flow rate (Table 5.2, entry 11).

**Table 5.2.** Results of the flow  $\text{PhI}(\text{OAc})_2$ -mediated aryl migration.<sup>a</sup>

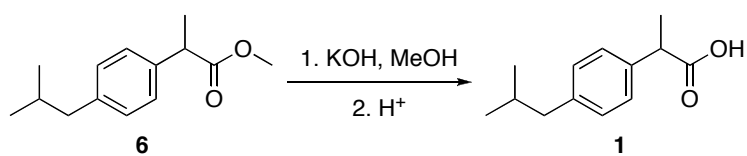


Entry	Eq. TMOF	Eq. $\text{PhI}(\text{OAc})_2$	Eq. $\text{H}_2\text{SO}_4$	Flow Rate ( $\mu\text{L min}^{-1}$ )	Residence Time (min)	Conversion <sup>b</sup> (%)
1	33	1.2	2.0	141.8	9.0	91
2	33	1.2	2.0	121.5	10.6	>99
3	17	1.2	2.0	121.5	10.6	94
4	13.5	1.2	2.0	112.1	10.8	>99
5	9.8	1.2	2.0	112.1	10.8	97
6	5.1	1.2	2.0	61.1	19.7	>99
7	3.0	1.2	2.0	45.9	26.3	93
8	3.1	1.2	2.0	35.7	33.8	87
9	3.1	1.2	2.0	56.0	21.5	>99
10	2.1	1.2	2.0	56.0	21.5	94
11	2.1	1.2	2.0	45.1	26.8	96

<sup>a</sup> Reactions carried out using a 0.12 M stock solution of 4-isobutylpropiophenone at room temperature unless otherwise noted.

<sup>b</sup> Conversion based on GC.

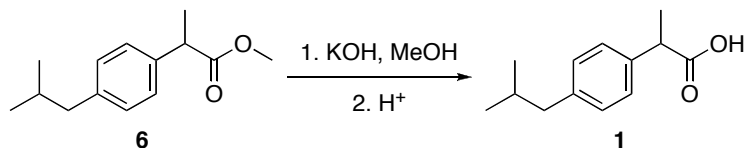
The final step of the ibuprofen synthesis in flow was successfully completed using a methanolic solution of KOH to saponify methyl ester 6 (Scheme 5.14).



**Scheme 5.14.** The saponification of methyl ester 6 to yield ibuprofen.

Results of the saponification are shown in Table 5.3. Using a flow rate of 50  $\mu\text{L min}^{-1}$  provided an isolated yield of 88%. It should be noted that this reaction was not optimized, and therefore a higher isolated yield could potentially be obtained.

**Table 5.3.** Results of the methyl ester saponification in flow.<sup>a</sup>



Entry	Eq. KOH	Flow Rate ( $\mu\text{L min}^{-1}$ )	Residence Time (min)	Yield <sup>b</sup> (%)
1	5	50	25.7	88

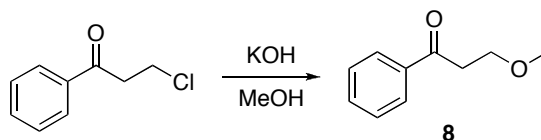
<sup>a</sup> Reactions carried out using a 0.20 M stock solution of methyl ester **7** at room temperature.

<sup>b</sup> Isolated yield.

Having identified appropriate flow conditions homogeneous synthesis of ibuprofen, efforts were made to develop a similar set of flow reaction conditions for the synthesis of atropine.

**Atropine Synthesis in Flow.** Attempts to put our atropine synthesis into flow were also met with success. The atropine synthesis in the microreactors encountered similar problems to the batch synthesis, namely the tropine esterification. For these reasons the route using the activated carboxylic acid shown in Scheme 5.9C was explored in flow.

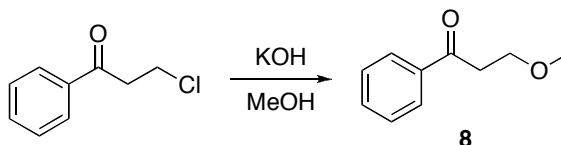
The synthesis of 3-methoxypropiophenone **8** was carried out in our microreactor using a 0.3 M solution of methanolic KOH (Scheme 5.15). The transformation was carried out at room temperature, eliminating the need to run the reaction at low temperatures (as was necessary in batch). Batch reactions had the major byproduct phenyl vinyl ketone, which was not detected.



**Scheme 5.15.** The synthesis of 3-methoxypropiphenone.

Results of the ether synthesis are shown in Table 5.4. It can be seen that the reaction was very efficient using a 12.1 minute residence time (Table 5.4, entry 1) and almost equally effective using a residence time of 9.3 minutes (Table 5.4, entry 3).

**Table 5.4.** Results of the 3-methoxypropiphenone synthesis in flow.<sup>a</sup>



Entry	Eq. KOH	Flow Rate ( $\mu\text{L min}^{-1}$ )	Residence Time (min)	Conversion <sup>b</sup> (%)
1	1.5	100	12.1	>99
2	1.5	120	10.1	98
3	1.5	130	9.3	98
4	1.5	150	8.0	94

<sup>a</sup> Reactions carried out using a 0.20 M stock solution of 3-chloropropiphenone and 0.30 M KOH in methanol at room temperature

<sup>b</sup> Conversion based on GC.

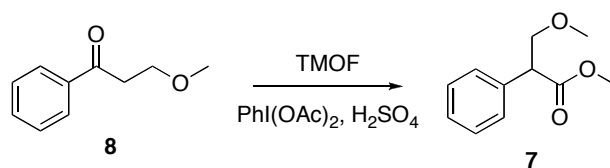
The rearrangement of 3-methoxypropiphenone (**8**) was also performed successfully in our flow reactor (Scheme 5.16).



**Scheme 5.16.** The 1,2-aryl migration of 3-methoxypropiphenone.

A high conversion was achieved in this reaction using 13.5 equivalents of TMOF (Table 5.5). This reaction was not optimized, however, to determine the minimum amount of TMOF that could be used to perform the transformation. Given our prior success with the  $\text{PhI}(\text{OAc})_2$ -mediated 1,2-aryl migration in the synthesis of ibuprofen, we are confident that this reaction could be optimized further to reduce the amount of waste generated from this process.

**Table 5.5.** Results for the 1,2-aryl migration of 3-methoxypropiophenone in flow.<sup>a</sup>



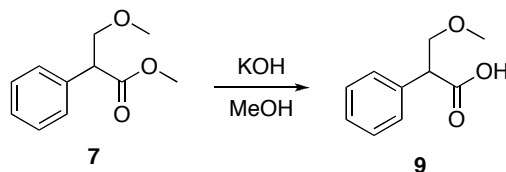
Entry	Eq. TMOF	Eq. $\text{PhI}(\text{OAc})_2$	Eq. $\text{H}_2\text{SO}_4$	Flow Rate ( $\mu\text{L min}^{-1}$ )	Residence Time (min)	Conversion <sup>b</sup> (%)
1	13.5	1.2	2.0	132.5	9.1	97

<sup>a</sup> Reactions carried out using a 0.12 M stock solution of 3-methoxypropiophenone **9** at room temperature.

<sup>b</sup> Conversion based on GC.

Treatment of methyl ester **7** with methanolic KOH successfully produced carboxylic acid **9** in high yield (Table 5.6). Table 5.6 shows that a 25.7 minute residence time was necessary to reach a 74% isolated yield. It should be noted however that these reaction conditions are not optimized.

**Table 5.6.** Results for the saponification of methyl ester **7** in flow.<sup>a</sup>

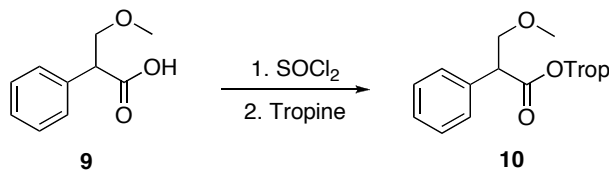


Entry	Eq. KOH	Flow Rate ( $\mu\text{L min}^{-1}$ )	Residence Time (min)	Yield <sup>b</sup> (%)
1	5	50	25.7	74

<sup>a</sup> Reactions carried out using a 0.20 M stock solution of methyl ester **8** at room temperature.

<sup>b</sup> Isolated yield.

In order to couple tropine with carboxylic acid **9**, the acid was mixed with one equivalent of thionyl chloride before being quenched into a solution of tropine in toluene at 80 °C (Scheme 5.17). As the protected atropine **10** generated during the course of this reaction precipitates, performing the coupling in flow was problematic due to channel blockages. Following column chromatography, an isolated yield of 30% was obtained. As only one equivalent of thionyl chloride was used, no intermediate distillation step was required to remove excess thionyl chloride in this reaction (which would potentially react with tropine). Further optimization of this reaction would undoubtedly increase the yield.



**Scheme 5.17.** The coupling of tropine with carboxylic acid **9**.

Due to time constraints, the final step of the atropine synthesis, the methyl ether deprotection, was not attempted. Preliminary results for this transformation in

batch were promising, however, demonstrating how there is great potential for this final reaction to be carried out effectively in flow.

### ***Conclusion***

We have successfully designed syntheses for two APIs, ibuprofen and atropine, which rely on similar reaction pathways using a common set of reagents. While elements of our synthesis of ibuprofen have been previously reported,<sup>8</sup> we developed a new synthesis of atropine that relies on a similar set of reaction conditions. These syntheses were validated in batch and significant headway was made toward performing all reactions in flow. Given more time, these reactions could be optimized further and potentially strung together, using in-line microextractors to purify the reactions in flow. Knowledge gained from this project was applied to future flow reactions, helping to make a unique continuous flow synthesis of ibuprofen.

### ***Experimental Methods***

**General Considerations.** Solvents were purified by standard procedures. All other reagents were used as received, unless otherwise noted. <sup>1</sup>H NMR spectra were recorded in CDCl<sub>3</sub> on Varian Mercury 300MHz and Inova 400 MHz spectrometers operating at 299.763 MHz and 399.780 MHz, respectively, using residual solvent as the reference. Gas chromatographic (GC) analyses were carried out on a Varian Model 3800 using a CP-Sil regular phase column (30.0 m x 0.25 mm i.d.). The temperature program for GC analysis held the temperature constant at 80 °C, heated samples from 80 to 200 °C at 17 °C/min, and held at 200 °C for 2 min. Inlet and detector temperatures were set constant to 220 and 250 °C, respectively. Microreactor components included Harvard Apparatus Standard Pump 22 syringe pumps and PFA tubing (1.6 mm i. d.).

**4-isobutylpropiophenone (5) in batch.** Propionyl chloride (1.3 mL, 15.0 mmol, 1.5 eq) was added dropwise to a solution of isobutylbenzene (1.6 mL, 10.2 mmol, 1.0 eq) and AlCl<sub>3</sub> (2.0 g, 15.0 mmol, 1.5 eq) in CH<sub>2</sub>Cl<sub>2</sub> (20 mL) at room temperature for 5 hours. When the reaction was deemed complete by GC, it was cooled over ice and quenched with sat. NaHCO<sub>3</sub> (20 mL). The mixture was extracted with CH<sub>2</sub>Cl<sub>2</sub> (2x 50 mL), dried over MgSO<sub>4</sub>, concentrated and dried under vacuum to give 4-isobutylpropiophenone as a colorless oil (1.81 g, 93% yield): <sup>1</sup>H NMR (300 MHz, CDCl<sub>3</sub>): δ 7.89 (d, 2H), 7.23 (d, 2H), 2.99 (q, 2H), 2.53 (d, 2H), 1.89 (m, 1H), 1.22 (t, 3H), 0.91 (d, 6H); <sup>13</sup>C NMR (75 MHz, CDCl<sub>3</sub>): δ 200.3, 147.2, 134.7, 129.2, 127.9, 45.3, 31.6, 30.1, 22.3, 8.3.

**Methyl 3-methoxy-2-phenylpropanoate (7) in batch.** 3-methoxypropiophenone (693 mg, 4.22 mmol, 1.0 eq), PhI(OAc)<sub>2</sub> (1.63 g, 5.1 mmol, 1.2 eq), and trimethylorthoformate (17 mL, 155.4 mmol, 37.0 eq) were stirred at room temperature. Concentrated H<sub>2</sub>SO<sub>4</sub> (450 μL, 8.44 mmol, 2.0 eq) was added drop-wise and the reaction was stirred overnight. The reaction was quenched with H<sub>2</sub>O, and reaction was concentrated in vacuo to remove any organic solvents. The aqueous phase was extracted with Et<sub>2</sub>O (3x 50 mL), dried over MgSO<sub>4</sub>, concentrated and dried under vacuum. The product was purified using column chromatography (silica gel, 80:20 hexanes/EtOAc) to give methyl 3-methoxy-2-phenylpropanoate as a colorless oil (497 mg, 61% yield): <sup>1</sup>H NMR (300 MHz, CDCl<sub>3</sub>): δ 7.38 (m, 5H), 3.96 (m, 2H), 3.70 (s, 3H), 3.60 (dd, 1H), 3.37 (s, 3H).

**3-methoxy-2-phenylpropanoic acid (9) in batch.** 3-methoxy-2-phenylpropanoate (290.8 mg, 1.5 mmol, 1.0 eq) was added to a 3 mL of a 20% w/w solution of KOH in MeOH and stirred overnight at room temperature. The reaction was concentrated,

dissolved in EtOAc and H<sub>2</sub>O. The aqueous phase was removed and acidified with 1 M HCl, extracted with EtOAc (3x 15 mL), dried over MgSO<sub>4</sub>, concentrated and dried under vacuum to yield 3-methoxy-2-phenylpropanoic acid as a white solid (200 mg, 88% yield): <sup>1</sup>H NMR (300 MHz, CDCl<sub>3</sub>): δ 7.34 (m, 5H), 3.96 (m, 2H), 3.62 (dd, 1H), 3.39 (s, 3H).

**Atropine methyl ether (10) in batch.** 3-methoxy-2-phenylpropanoic acid (200 mg, 1.03 mmol, 1.0 eq) was stirred with SOCl<sub>2</sub> (650 μL, 8.9 mmol, 8.9 eq) at 60 °C until gas evolution ceased (~2-3 hr). Residual SOCl<sub>2</sub> was removed under vacuum. The resulting oil was washed with toluene (5 mL), concentrated and dried under vacuum overnight. The acid chloride was dissolved in toluene (5 mL) and heated to 80 °C. Tropine (149 mg, 1.1 mmol, 1.1 eq) in toluene (5 mL) was added to the acid chloride solution and stirred until gas evolution ceased (~3-4 hrs). During the course of the reaction, a white precipitate formed. The reaction was concentrated and dried under vacuum. The product was purified using column chromatography (silica gel, 75:10:15:2 CHCl<sub>3</sub>/acetone/MeOH/NH<sub>4</sub>OH) to give atropine methyl ether (90 mg, 29% yield): <sup>1</sup>H NMR (300 MHz, CDCl<sub>3</sub>): δ 7.32 (m, 5H), 5.10 (m, 1H), 3.99 (t, 1H), 3.80 (dd, 1H), 3.63 (m, 5H), 3.36 (s, 3H), 3.01 (m, 1H), 2.66 (m, 3H), 1.95 (m, 6H). <sup>13</sup>C NMR (75 MHz, CDCl<sub>3</sub>): δ 171.6, 136.0, 129.0, 128.2, 127.9, 74.0, 68.0, 60.0, 59.9, 59.2, 52.6, 40.4, 36.4, 36.3, 25.5, 25.2.

**BBr<sub>3</sub>-Mediated Methyl Ether Deprotection.** Atropine methyl ether (90 mg, 0.3 mmol, 1.0 eq) was dissolved in dry CH<sub>2</sub>Cl<sub>2</sub> (5 mL) under nitrogen and cooled to -78 °C. BBr<sub>3</sub> (1.0 M in CH<sub>2</sub>Cl<sub>2</sub>, 900 μL, 0.9 mmol, 3.0 eq) was added dropwise at -78 °C and allowed to stir for an hour before being warmed to 0 °C. The reaction was monitored by TLC (75:10:15:2 CHCl<sub>3</sub>/acetone/MeOH/NH<sub>4</sub>OH eluent).

**Setup of Flow Reactions.** For all flow reactions, a 60 cm segment of PFA tubing (1.6 mm i.d., 1.21 mL total volume) was wrapped into a 'Figure 8' pattern around metal bars. A polypropylene Y-junction was connected to the inlet of the tubing and syringes were connected to the union using a 10 cm segment of PFA tubing and polypropylene female Leur adapter. Two syringe pumps were used in each system and reactions were sampled at the outlet and analyzed by GC to determine reaction conversion.

**Representative Flow Friedel-Crafts Acylation.** In one syringe was placed a solution of isobutylbenzene (0.25 M) in  $\text{CH}_2\text{Cl}_2$  and in another syringe was placed a solution of propionyl chloride (0.375 M) and  $\text{AlCl}_3$  (0.375 M) in  $\text{CH}_2\text{Cl}_2$ . The two syringes were placed on separate syringe pumps set to  $25 \mu\text{L min}^{-1}$ . Flow was initiated and the reaction stream was allowed to pass through the tubing. The reaction was collected in a 4 mL screw cap vial containing 1.5 mL saturated  $\text{NaHCO}_3$  and 1.5 mL  $\text{Et}_2\text{O}$ . The organic layer was sampled and analyzed using GC. Flow rates and stock solution concentrations were varied during the optimization.

**Representative Flow  $\text{PhI}(\text{OAc})_2$ -Mediated 1,2-Aryl Migration for the Ibuprofen Synthesis.** In one syringe was placed a solution of 4-isobutylpropiophenone (0.18 M),  $\text{PhI}(\text{OAc})_2$  (0.22 M) and trimethylorthoformate (0.36 M) in  $\text{CH}_2\text{Cl}_2$  and in another syringe was placed concentrated  $\text{H}_2\text{SO}_4$ . The two syringes were placed on separate syringe pumps and the 4-isobutylpropiophenone syringe was set to  $55 \mu\text{L min}^{-1}$  and the  $\text{H}_2\text{SO}_4$  syringe was set to  $1.04 \mu\text{L min}^{-1}$ . Flow was initiated and the reaction stream was allowed to pass through the tubing. The reaction was collected in a 4 mL screw cap vial containing 1.5 mL saturated  $\text{NaHCO}_3$  and 1.5 mL  $\text{Et}_2\text{O}$ . The organic

layer was sampled and analyzed using GC. Flow rates and stock solution concentrations were varied during the optimization.

**Flow Synthesis of Ibuprofen.** In one syringe was placed a solution of methyl 2-(4-isobutylphenyl)propanoate (0.2 M) in MeOH and in another syringe was placed a solution of KOH (1.0 M) in MeOH. The two syringes were placed on separate syringe pumps set to 25  $\mu\text{L min}^{-1}$ . Flow was initiated and the reaction stream was allowed to pass through the tubing for 2 hours. Samples were taken directly from the outlet stream and analyzed by GC, proving the reaction was complete upon exiting the reactor. The reaction was concentrated, dissolved in EtOAc and H<sub>2</sub>O. The aqueous phase was removed and acidified with 5 M HCl, extracted with EtOAc (3x 15 mL), dried over MgSO<sub>4</sub>, concentrated and dried under vacuum to yield ibuprofen as a viscous oil (88% yield): <sup>1</sup>H NMR (300 MHz, CDCl<sub>3</sub>):  $\delta$  7.23 (d, 2H), 7.13 (d, 2H), 3.71 (m, 4H), 2.48 (d, 2H), 1.86 (m, 1H), 1.52 (d, 3H), 0.93 (d, 6H).

**Representative Flow 3-Methoxypropiophenone Synthesis.** In one syringe was placed a solution of 3-chloropropiophenone (0.2 M) in MeOH and in another syringe was placed a solution of KOH (0.3 M) in MeOH. The two syringes were placed on separate syringe pumps set to 50  $\mu\text{L min}^{-1}$ . Flow was initiated and the reaction stream was allowed to pass through the tubing. Samples were taken directly from the outlet stream and analyzed by GC, to determine the reaction conversion. Flow rates and stock solution concentrations were varied during the optimization.

**Representative Flow PhI(OAc)<sub>2</sub>-Mediated 1,2-Aryl Migration for the Atropine Synthesis.** In one syringe was placed a solution of 3-methoxypropiophenone (0.18 M), PhI(OAc)<sub>2</sub> (0.22 M) and trimethylorthoformate (2.5 M) in CH<sub>2</sub>Cl<sub>2</sub> and in another

syringe was placed concentrated H<sub>2</sub>SO<sub>4</sub>. The two syringes were placed on separate syringe pumps and the 4-isobutylpropiophenone syringe was set to 110 μL min<sup>-1</sup> and the H<sub>2</sub>SO<sub>4</sub> syringe was set to 2.07 μL min<sup>-1</sup>. Flow was initiated and the reaction stream was allowed to pass through the tubing. The reaction was collected in a 4 mL screw cap vial containing 1.5 mL saturated NaHCO<sub>3</sub> and 1.5 mL Et<sub>2</sub>O. The organic layer was sampled and analyzed using GC. Flow rates and stock solution concentrations were varied during the optimization.

**Flow Synthesis of 3-Methoxy-2-Phenylpropanoic Acid.** In one syringe was placed a solution of methyl 3-methoxy-2-phenylpropanoate (0.2 M) in MeOH and in another syringe was placed a solution of KOH (1.0 M) in MeOH. The two syringes were placed on separate syringe pumps set to 25 μL min<sup>-1</sup>. Flow was initiated and the reaction stream was allowed to pass through the tubing for 1.7 hours. Samples were taken directly from the outlet stream and analyzed by GC, proving the reaction was complete upon exiting the reactor. The reaction was concentrated, dissolved in Et<sub>2</sub>O and H<sub>2</sub>O. The aqueous phase was removed and acidified with 5 M HCl, extracted with Et<sub>2</sub>O (3x 15 mL), dried over MgSO<sub>4</sub>, concentrated and dried under vacuum to yield 3-methoxy-2-phenylpropanoic acid (74% yield).

**Flow Synthesis of Atropine Methyl Ether.** In one syringe was placed a solution of 3-methoxy-2-phenylpropanoic acid (1.0 M) in toluene and in another syringe was placed neat SOCl<sub>2</sub>. The two syringes were placed on separate syringe pumps and the 3-methoxy-2-phenylpropanoic acid syringe was set to 30 μL min<sup>-1</sup> and the SOCl<sub>2</sub> syringe was set to 2.19 μL min<sup>-1</sup>. Flow was initiated and the reaction stream was allowed to pass through the tubing for 88 minutes. At the outlet of the reactor was placed a solution of tropine (1.0 M) in toluene at 80 °C in which the acid chloride was

quenched. The reaction was concentrated, and the residue was dissolved in  $\text{CHCl}_3$  and added to a solution of saturated  $\text{Na}_2\text{CO}_3$ . The aqueous phase was extracted with  $\text{CHCl}_3$  (3x 25 mL), dried over  $\text{MgSO}_4$ , concentrated and dried under vacuum. The product was purified using column chromatography (silica gel, 75:10:15:2  $\text{CHCl}_3$ /acetone/MeOH/ $\text{NH}_4\text{OH}$ ) to give atropine methyl ether (240 mg, 30% yield).

## REFERENCES

1. Sheldon, R. A. *J. Chem. Tech. Biotechnol.* **1997**, *68*, 381.
2. Personal communication with Berkeley W. Cue, Jr., Green Chemistry Institute.
3. Elango, V.; Murphy, M. A.; Smith, B. L.; Davenport, K. G.; Mott, G. N.; Zey, E. G.; Moss, G. L. U.S. Patent No. 4,981,995, **1991**.
4. Lindley, D. D.; Curtis, T. A.; Ryan, T. R.; de la Garze, E. M.; Hilton, C. B.; Kenesson, T. M. U.S. Patent No. 5,068,448, **1991**.
5. Blicke, F. F.; Raffelson, H.; Barna, B. *J. Am. Chem. Soc.* **1952**, *74*, 253.
6. Robinson, R. *J. Chem. Soc.* **1917**, *111*, 762.
7. Finar, I. L. *Organic Chemistry Vol. 24th. Edn.* Longman 1965, p. 636.
8. Tamura, Y.; Yakura, T.; Shirouchi, Y.; Haruta, J. *Chem. Pharm. Bull.* **33**, *3*, 1097.
9. Singh, O. V.; Prakash, O.; Garg, C. P.; Kapoor, R. P. *Ind. J. Org. Chem.* **1989**, *28B*, 814.
10. Prakash, O.; Goyal, S.; Moriarty, R. M.; Khosrowshahi, J. S. *Ind. J. Org. Chem.* **1990**, *289B*, 304.
11. Finar, I. L. *Organic Chemistry Volume 2, 4<sup>th</sup> Edition*, Longman 1965, pp. 636.
12. Steinbacher, J. L.; Moy, R. W. Y.; Price, K. E.; Cummings, M. A.; Roychowdhury, C.; Buffy, J. J.; Olbricht, W. L.; Haaf, M.; McQuade, D. T. *J. Am. Chem. Soc.* **2006**, *128*, 9442.
13. Quevedo, E.; Steinbacher, J.; McQuade, D. T. *J. Am. Chem. Soc.* **2005**, *127*, 10498.
14. Poe, S. L.; Cummings, M. A.; Haaf, M. R.; McQuade, D. T. *Angew. Chem. Int. Ed.* **2006**, *45*, 1544.
15. Bogdan, A. R.; Mason, B. P.; Sylvester, K. T.; McQuade, D. T. *Angew. Chem., Int. Ed.* **2007**, *46*, 1698–1701.
16. Bogdan, A. R.; McQuade, D. T. *Beilstein Journal of Organic Chemistry.* **2009**, *5*, 17.

## CHAPTER 6

### The Continuous Flow Synthesis of Ibuprofen

#### *Preface*

After the joint venture between Systanix and Foster Miller, Inc. had come to a close, we chose to continue investigating the flow synthesis of one of the two APIs, ibuprofen. Having expanded upon my knowledge of flow chemistry after my time at Pfizer, the project was tackled with a fresh perspective and the group's first continuous flow synthesis of an active pharmaceutical ingredient.

#### *Abstract*

A three-step, continuous flow synthesis of ibuprofen was accomplished using a simplified microreactor. By designing a synthesis in which excess reagents and byproducts are compatible with downstream reactions, no intermediate purification or isolation steps are required.

#### *Introduction*

Organic synthesis is a powerful enterprise that continues to develop more selective and efficient chemical methods and synthetic routes. To synthesize complex molecules, whether in academic laboratories or industrial manufacturing, reactions are often performed iteratively in batch reactors. While these stepwise methods are powerful, they are also highly wasteful. The pharmaceutical industry, for example, produces 25-100 kg of waste for every kilogram of product synthesized.<sup>1</sup> Though chemists are constantly striving to create more efficient syntheses, recent reminders of a resource-limited world underscore the need for more sustainable methods and technologies to synthesize molecules of importance.<sup>2</sup> The application of new

technologies, such as microreactors, to organic synthesis can be used to achieve this goal.<sup>3-13</sup>

Microreactors are a developing technology used to perform safer, more efficient and more selective chemical transformations in microchannels or narrow-bore tubing.<sup>3-13</sup> The many advantages associated with running reactions in flow are attributed to large surface area-to-volume ratios.<sup>5</sup> Small dimensions allow for precise reaction control through rapid heat transfer and mixing that cannot be obtained in batch reactors.<sup>14-17</sup> Scale-up of syntheses is also readily achieved by running a single reactor for extended periods of time<sup>18</sup> or by the addition of more identical flow reactors in parallel, a process known as numbering up.<sup>19-21</sup>

While the majority of microreactor work in organic synthesis has focused on single-step reactions,<sup>3-13</sup> recent examples have demonstrated multi-step reaction sequences in flow.<sup>14, 22-25</sup> Our group has a long-standing interest in the development of new methodologies that enable the rapid and efficient synthesis of important small molecules.<sup>26-29</sup> Specifically, we have aimed to run multi-step reaction sequences in one pot (i.e. batch)<sup>28, 29</sup> or in series (i.e. microreactors).<sup>26, 27</sup> We report herein a three-step, continuous flow synthesis of ibuprofen using a simplified microreactor<sup>29</sup> that eliminates the need for purification and isolation steps.

We previously reported the development of simplified microreactors using a combination of polymeric tubing, unions, and syringe pumps.<sup>26, 27</sup> In all flow reactions described herein, PFA tubing (0.75 mm i.d.) was wrapped around metal bars in a serpentine-like manner to assist in mixing and to enable facile reactor heating/cooling (Figure 6.1).<sup>27</sup>

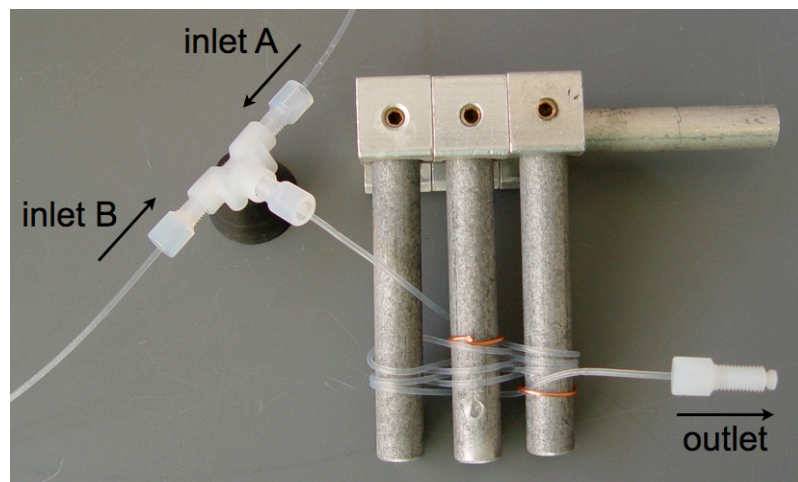
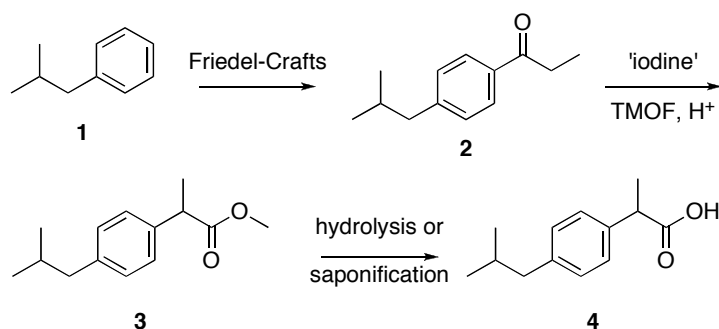


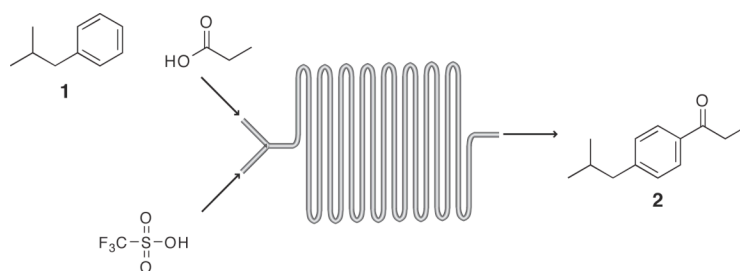
**Figure 6.1.** The simplified microreactor setup using PFA tubing wrapped around metal bars. Reagent streams are mixed using a PFA tee junction.

To achieve this continuous flow synthesis, a retrosynthetic analysis of ibuprofen was performed, paying careful attention to reaction compatibility. To be successful, the entire synthesis had to be considered as an entity, as opposed to a series of independent reactions steps. In other words, reactions had to be designed such that byproducts and excess starting materials from one reaction were compatible with downstream reactions. By doing so, reactions could be performed in sequence without any breaks in the synthesis. The general three-step synthesis of ibuprofen we investigated is outlined in Scheme 6.1.<sup>30</sup>

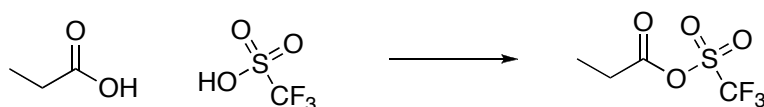


**Scheme 6.1.** Proposed synthetic route to ibuprofen. 'iodine' =  $I_2$ , or  $PhI(OAc)_2$ , TMOF = trimethylorthoformate.

We surveyed multiple conditions for the Friedel-Crafts acylations (Table 6.1). Of these, the use of  $\text{AlCl}_3$  provided the highest yield, but byproducts from this reaction proved to be incompatible with downstream steps. Mixing isobutylbenzene (IBB, **1**) and propionic acid with triflic acid ( $\text{TfOH}$ ) proved to also be an effective method to synthesize **2** (Figure 6.2).<sup>31, 32</sup> It is proposed that the reaction of triflic acid with propionic acid leads to the generation of a mixed anhydride, a very active acylating agent (Figure 6.3). This  $\text{TfOH}$ /propionic acid system was not only effective with the first step but was also synergistic with the second step.

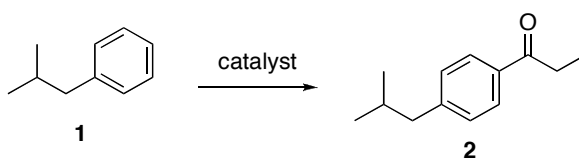


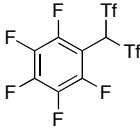
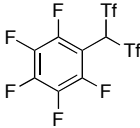
**Figure 6.2.** The flow Friedel-Crafts acylation reaction setup.



**Figure 6.3.** The mixed anhydride formed by the reaction of propionic acid with triflic acid.

**Table 6.1.** Reaction conditions screened for the Friedel-Crafts acylation of isobutylbenzene.



Entry	Catalyst	Acyating Agent	Conversion <sup>a</sup>
1	AlCl <sub>3</sub>	propionyl chloride	>99%
2	SiO <sub>2</sub> -supported AlCl <sub>3</sub>	propionyl chloride	N.R.
3		propionyl chloride	N.R.
4		propionic anhydride	N.R.
5	TfOH (10%)	propionyl chloride	N.R.
6	TfOH (10%)	propionyl anhydride	N.R.
7	ZnO (50%)	propionyl chloride	N.R.
8	ZnO (100%)	propionyl chloride	N.R.
9	Sc(OTf) <sub>3</sub>	propionyl chloride	N.R.
10	Sc(OTf) <sub>3</sub> (10%)	propionic chloride	N.R.
11	Sc(OTf) <sub>3</sub> (10%)	propionic anhydride	N.R.
12	Sc(OTf) <sub>3</sub> (10%), LiClO <sub>4</sub>	propionic chloride	N.R.
13	Sc(OTf) <sub>3</sub> (10%), LiClO <sub>4</sub>	propionic anhydride	N.R.
14	Zeolite H-β	propionic anhydride	N.R.
15	Zeolite H-β	propionic acid	N.R.
16	NaFeCl <sub>4</sub> (50%)	propionic chloride	16%
17	NaFeCl <sub>4</sub> (100%)	propionic chloride	70%
18	TfOH (20 eq)	propionic acid	>99%
19	TfOH (5 eq)	propionic acid	92%

<sup>a</sup> Conversion based upon consumption of starting material by GC.

To run flow acylation experiments, a solution of IBB and propionic acid was mixed with a stream of TfOH, adjusting flow rates such that 5 equivalents of TfOH were being delivered relative to IBB (Figure 6.2).<sup>33</sup> The reagent streams were combined at a tee junction, resulting in plug flow due to the immiscibility of these reagents at low temperature (Figure 6.4a). When heated to 50 °C with a 5-minute residence time, only a 15% conversion was obtained (Table 6.2, entry 1). Plug flow continued throughout the reactor, suggesting that poor mixing and low temperatures lead to low conversion (Figure 6.4b).<sup>34</sup> Increasing the reaction temperature produced better results, with 150 °C giving the highest conversion and yield (Table 6.2, entry 3).<sup>35</sup> By visual inspection, the plugs coalesced at 150 °C, resulting in a homogeneous outlet stream (Figure 6.4d), indicating efficient mixing.

**Table 6.2.** The optimization of the flow Friedel-Crafts acylation.

Entry	Flow Rate ( $\mu\text{L}/\text{min}$ )	Residence Time (min)	TfOH (equiv)	Propionic Acid (equiv)	T (°C)	Conversion <sup>a</sup>
1	87.5	5	5	1.0	50	15%
2	87.5	5	5	1.0	100	52%
3	87.5	5	5	1.0	150	91% (70%) <sup>b</sup>
4	43.8	10	5	1.0	150	92% <sup>c</sup>
5	22	20	5	1.0	150	93% <sup>c</sup>
6	87.5	5	5	1.1	150	89%
7	87.5	5	5	1.5	150	85%
8	87.5	5	4	1.0	150	80%

<sup>a</sup> Conversion determined using GC with dodecane as an internal standard.

<sup>b</sup> Number in parentheses corresponds to isolated yield after column chromatography.

<sup>c</sup> Longer residence times led to inconsistent flow rates.

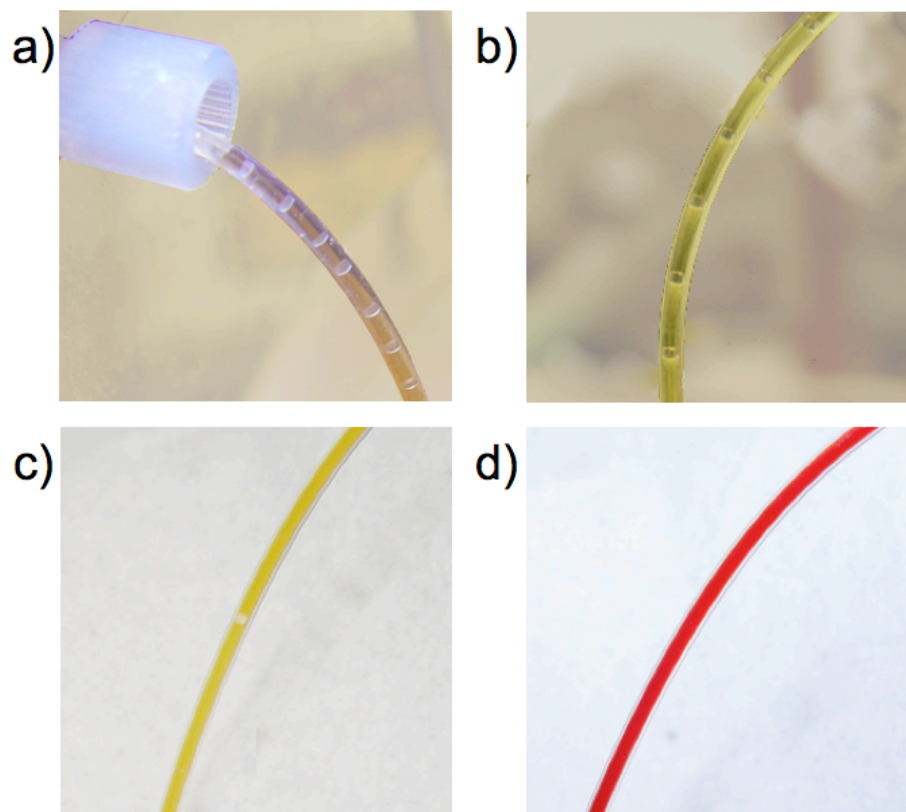
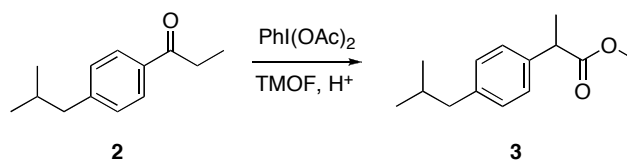


**Figure 6.4.** Reagent flow for the Friedel-Crafts acylation. Plug flow (a) at the inlet of the reactor. Plugs are colorless, but are photographed in front of dark background to assist with visualization. At a reactor temperature of 50 °C, plug flow continues at the outlet of the reactor (b). Increasing the temperature to 100 °C decreases the frequency of the plugs (c) and provides an increase in conversion. Increasing the temperature to 150 °C leads to a homogeneous stream at the outlet of the reactor (d). The reaction becomes a dark red color as it proceeds.

As stipulated earlier, in a continuous synthesis requiring no intermediate purification steps, all byproducts and excess reagents from prior steps must be compatible with downstream reactions. Therefore, it was essential that the excess reagents (TfOH and unreacted IBB) used in the Friedel-Crafts acylation were compatible with the second step of our reaction sequence, the 1,2-aryl migration. Literature precedence indicates the addition of acid to a mixture of aryl ketones, trimethyl orthoformate (TMOF), and  $\text{PhI}(\text{OAc})_2$  affords 2-arylpropanoates in high

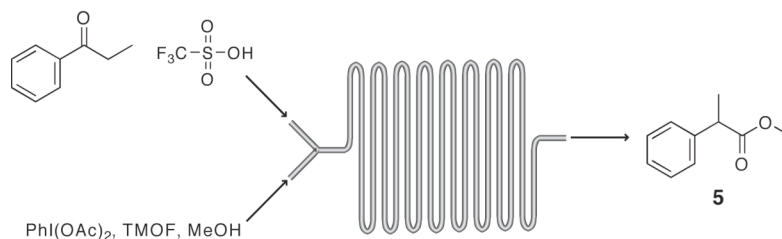
yield (Scheme 6.2).<sup>30, 36, 37</sup> We selected this reaction as it requires no transition metals, and the iodobenzene byproduct has the potential to be recycled.<sup>38</sup>



**Scheme 6.2.** The  $\text{PhI}(\text{OAc})_2$ -mediated 1,2-aryl migration of 4-isobutylpropiophenone.

Using propiophenone as a test substrate, we discovered that TfOH is compatible with the 1,2-aryl migration (Scheme 6.2), providing high yields of methyl ester **5** with short residence times (Table 6.3). Using 9 equivalents of TMOF provided near quantitative conversion with 5 equivalents TfOH at 35 °C (Table 6.3, entry 1). Decreasing the amount of TMOF to 4 equivalents also gave high yields at 35 °C (Table 6.3, entry 2). Increasing the temperature to 50 °C had the added benefit of increasing reaction rates, and thereby permitting faster flow rates to be used (higher output) (Table 6.3, entries 3 and 4). Reducing the amount of TMOF to 2 equivalents was detrimental to both the conversion and yield (Table 6.3, entry 5), leading to the generation of a major byproduct, presumably 2-methoxypropiophenone. From these data, it was determined that a residence time of 2 minutes was optimal for the second step of our multi-step reaction sequence to convert 4-isobutylpropiophenone **2** to methyl ester **3**.

Additional work has also been carried out to perform this reaction enantioselectively. For a discussion on this topic, see Appendix 4.

**Table 6.3.** The optimization of the flow  $\text{PhI}(\text{OAc})_2$ -mediated 1,2-aryl migration.<sup>a</sup>

Entry	Flow Rate ( $\mu\text{L min}^{-1}$ )	Residence Time (min)	TMOF (equiv)	T ( $^{\circ}\text{C}$ )	Conversion <sup>b</sup>	Yield <sup>b</sup>
1	110	2.0	9.0	35	>98%	78%
2	110	2.0	4.0	35	>98%	92%
3	110	2.0	4.0	50	98%	96%
4	220	1.0	4.0	50	94%	81%
5	110	2.0	2.0	50	81%	60%

<sup>a</sup> Standard reactions conditions used 1.0 eq propiophenone and 1.0 eq  $\text{PhI}(\text{OAc})_2$ , and 5.0 eq TfOH.

<sup>b</sup> Calculated by GC using cyclooctane as an internal standard

With the first two separately optimized, we assembled the system so that the product stream from the Friedel-Crafts acylation was immediately relayed into the 1,2-aryl migration using the conditions outlined above (Figure 6.5). This system requires no additional acid because the TfOH from the Friedel-Crafts acylation also facilitates the 1,2-aryl migration. To achieve efficient mixing of the outlet stream from the first step with the  $\text{PhI}(\text{OAc})_2$ /TMOF reagent stream for the second step, a tee junction was modified such that the inner diameter was 0.75 mm and packed with glass beads (250-300  $\mu\text{m}$ ). This mixer was cooled to 0  $^{\circ}\text{C}$  and proved to mix the two streams effectively,<sup>39</sup> resulting in a 70% two-step yield after column chromatography, with quantitative conversion of 4-isobutylpropiophenone **2** to methyl ester **3**.

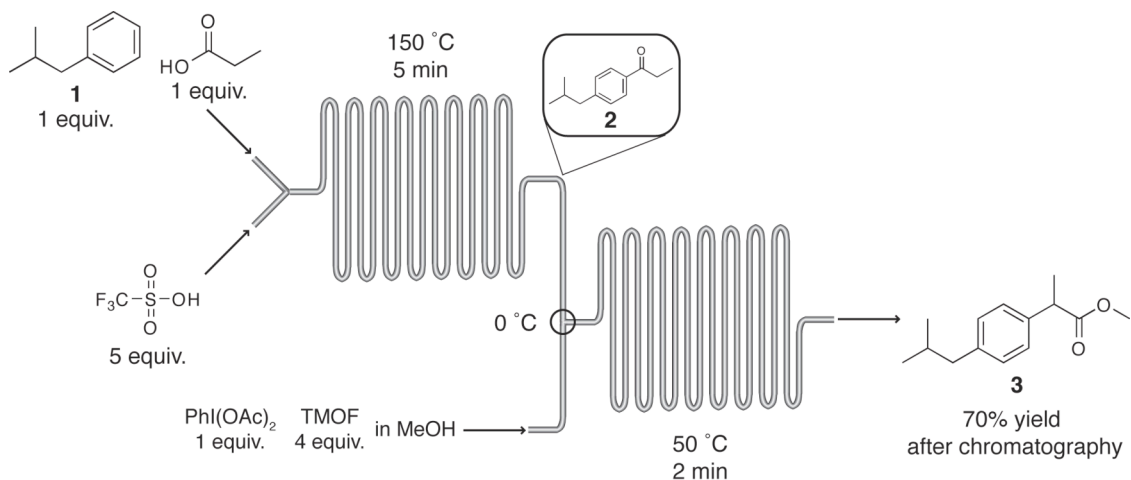


**Figure 6.5.** The two-step reaction sequence.

The final step in the continuous flow ibuprofen synthesis was achieved by saponifying methyl ester **3** with KOH (Figure 6.6). The outlet from the second step was combined with a stream of 5 M KOH and heated to 65 °C for 3 minutes. The excellent heat transfer of the microreactor allows the acidic stream to be mixed with the basic stream without a dangerous exotherm. Sampling the outlet stream showed only the presence of residual IBB, iodobenzene, and trace amounts of methyl ester **3**. After an acidic work-up, ibuprofen **4** was obtained in 68% crude yield and 51% yield (99% purity by GC and NMR) after recrystallization.<sup>40</sup>

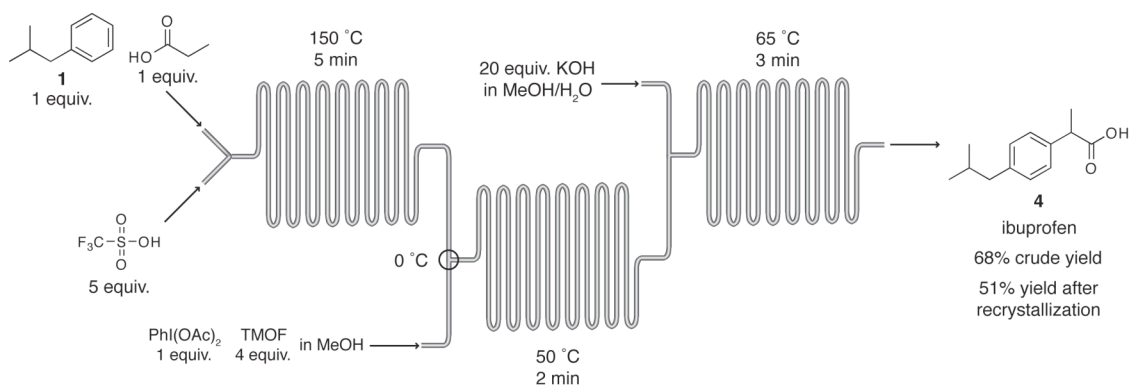


**Figure 6.6.** The three-step, continuous flow synthesis of ibuprofen.

## ***Conclusion***

In summary, we have developed a continuous flow synthesis of an active pharmaceutical ingredient, ibuprofen, using an efficient three-step process that requires no intermediate purifications steps. Using less than 500 cm of tubing and five syringe pumps, the flow synthesis reported herein generates approximately 9 mg/min crude ibuprofen. Addition of parallel reactors or lengthening the channels would permit a high throughput synthesis of ibuprofen. Potential scale-up of this method would also benefit from the precise temperature control (from 150 °C to 50 °C in sequential steps) and the excellent control of exotherms (caused by transitioning from pH 1 to 14). Performing this series of reactions on large scale in batch would be unfavorable due to the energy requirements needed to safely control these temperature changes and exotherms. Investigations are currently being carried out to apply this methodology to other 2-arylpropionic acid derivatives, such as naproxen, and to develop recyclable, supported catalysts for the Friedel-Crafts acylation and 1,2-aryl migration.

## ***Experimental Methods***

**General Considerations.** Solvents were purified by standard procedures. All other reagents were used as received, unless otherwise noted. <sup>1</sup>H NMR and <sup>13</sup>C NMR spectra were recorded in CDCl<sub>3</sub> on Varian Mercury 300 MHz operating at 300.070 MHz and 75.452 MHz, respectively, using the residual solvent peak as reference. Data are reported as s = singlet, d = doublet, t = triplet, q = quadruplet, m = multiplet. Gas chromatographic (GC) analyses were performed using an Agilent 7890A GC equipped with an Agilent 7683B autosampler, a flame ionization detector (FID), and a J&W Scientific 19091J-413 column (length = 30 m, inner diameter = 320 μm, and film thickness = 250 μm). The temperature program for GC analysis held the

temperature constant at 80 °C for 1 minute, heated samples from 80 to 200 °C at 20 °C/min and held at 200 °C for 1 minute. Inlet and detector temperatures were set constant at 220 and 250 °C, respectively. Cyclooctane and dodecane used as internal standards to calculate reaction conversion and yield. Gas chromatography-mass spectrometry (GC/MS) analyses were performed using a Hewlett Packard HP 6890 Series Gas Chromatograph, a Hewlett Packard HP 5973 Mass Spectrometer Detector (MSD), and a J&W Scientific DB\*-5 Column (length = 30 m, inner diameter = 0.325 mm, film thickness = 1.0 µm, catalog number 123-5033). The temperature program for the analyses held the temperature constant at 50 °C for 3 min, heated samples from 50 to 80 °C at 30 °C/min, holding at 80 °C for 2 min, then heating samples from 80 to 200 °C at 17 °C/min, and holding at 200 °C for 1.94 min. The MSD temperature was held at 300 °C for 15 min.

**Microreactor Components.** The selection of the proper materials for this systems proved to be very important. The caustic nature of triflic acid rendered many materials, such as polypropylene and polyoxymethylene (Delrin), unusable and led to hazardous leaks. PFA and ETFE materials proved to be highly stable.

**Table 6.4.** Microreactor components.

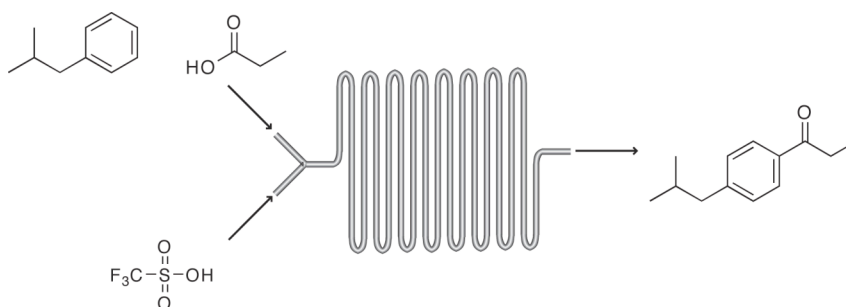
<b>Equipment</b>	<b>Materials</b>
Pumping Mechanism	Harvard Apparatus Standard Pump 22 syringe pumps
Tubing	Teflon PFA (perfluoroelastomeric), 0.030" (0.75 mm) i.d., 1/16" (1.6 mm) o.d.
Mixers	Upchurch Scientific ETFE Tees, 0.020" (0.50 mm) thru-hole, 2.9 $\mu$ L swept volume
Nuts	Upchurch Scientific Flangeless Nuts, PFA 1/4-28 thread for 1/16" o.d. tubing
Ferrules	Upchurch Scientific ETFE Flangeless Ferrules
Unions	Upchurch Scientific ETFE Standard Union, 1/4-28 threads
Luer Adapter	Upchurch Scientific ETFE Female Leur to 1/4-28 Female thread, 0.05" (1.3 mm) thru-hole

**Iodobenzene diacetate (PhI(OAc)<sub>2</sub>).** Hydrogen peroxide (30% w/w in water, 10.0 mL, 0.1 mol, 1 eq) and acetic anhydride (45.0 mL, 0.48 mol, 4.8 eq) were charged into a 100 mL round bottom flask equipped with a bubbler and stirred at 40 °C for 4 hours. Iodobenzene (3.9 mL, 36 mmol, 0.36 eq) was added dropwise at 40 °C and allowed to stir overnight. The reaction was cooled to room temperature and *partially* concentrated under vacuum until a white precipitate formed. The precipitate was filtered, washed with Et<sub>2</sub>O and dried under vacuum to give iodobenzene diacetate as a white solid (8.04 g, 71% yield): <sup>1</sup>H NMR (300 MHz, d<sub>6</sub>-DMSO):  $\delta$  8.25 (d, *J*=8.4 Hz, 2H), 7.67 (t, *J*=6.6 Hz, 1H), 7.57 (t, *J*=7.5 Hz, 2H), 1.91 (s, 6H).

**Methyl 2-phenylpropanoate.** Propiophenone (1.0 mL, 7.5 mmol, 1.0 eq), PhI(OAc)<sub>2</sub> (2.5 g, 7.7 mmol, 1.03 eq) and trimethyl orthoformate (4 mL, 36.6 mmol, 4.9 eq) were charged into a 100 mL round bottom flask equipped with a bubbler at room

temperature. Concentrated  $\text{H}_2\text{SO}_4$  (900  $\mu\text{L}$ , 16.2 mmol, 2.2 eq) was added drop wise over 5 minutes. The reaction was stirred at room temperature until TLC indicated the reaction was complete (about 15 minutes). The reaction was quenched with water, and the aqueous phase extracted with  $\text{CH}_2\text{Cl}_2$  (3x 50 mL), dried over  $\text{Na}_2\text{SO}_4$ , filtered and concentrated in vacuo. The product was purified by column chromatography (silica gel, 95:5 hexanes/EtOAc,  $R_f=0.26$ ) to give methyl 2-phenylpropanoate as a colorless oil:  $^1\text{H}$  NMR (300 MHz,  $\text{CDCl}_3$ ):  $\delta$  7.30 (m, 5H), 3.775 (q,  $J=7.2$  Hz, 1H), 3.67 (s, 3H), 1.55 (d,  $J=7.2$  Hz, 3H);  $^{13}\text{C}$  NMR (75 MHz,  $\text{CDCl}_3$ ):  $\delta$  175.0, 140.6, 128.7, 127.5, 127.2, 52.0, 45.5, 18.7.

#### Representative Flow Friedel-Crafts Acylation Optimization Experiment.

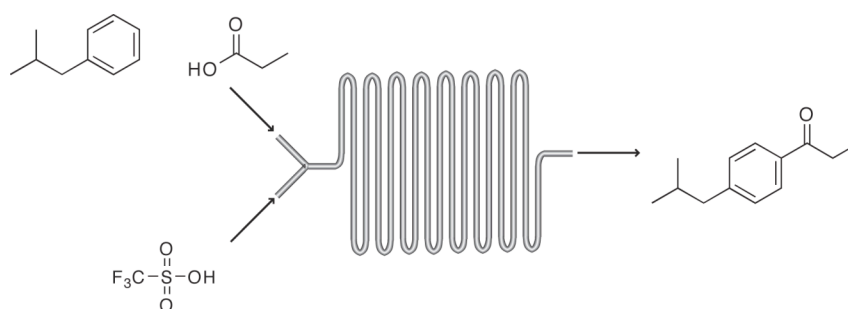


For the flow Friedel Crafts acylation, a 100 cm segment of PFA tubing (0.75 mm i.d., 441.79  $\mu\text{L}$  total volume) was wrapped into a ‘Figure 8’ pattern and submerged into an oil bath set to the desired temperature (50, 100, or 150  $^\circ\text{C}$ ). An ETFE tee was connected to the inlet of the tubing using a PFA flangeless nut. Syringes were connected to the tee using a 10 cm segment of PFA tubing and an ETFE female Leur adapter.

In one syringe was placed a solution of isobutylbenzene, propionic acid and dodecane and in another syringe was placed neat triflic acid (11.3 M). The two syringes were placed on separate syringe pumps and flow rates were attenuated to

provide the desired stoichiometry. Flow was initiated and the reaction stream was allowed to pass through the tubing. The reaction was collected in a 4 mL screw cap vial containing 1.5 mL saturated  $\text{NaHCO}_3$  and 1.5 mL  $\text{Et}_2\text{O}$ . The organic layer was sampled and analyzed using GC. Conversion was calculated using dodecane as the internal standard.

### Flow Friedel-Crafts Acylation Isolated Yield Experiment.

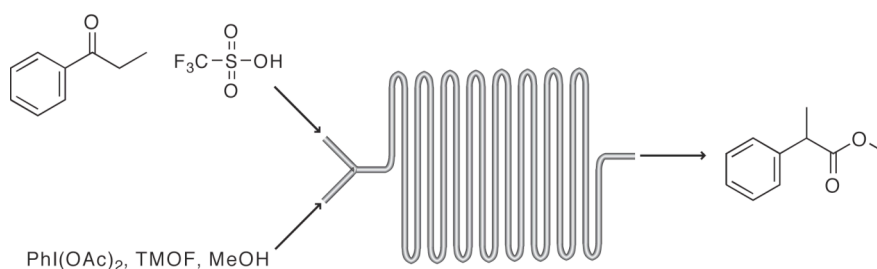


A 50 cm segment of PFA tubing (0.75 mm i.d., 220.89  $\mu\text{L}$  total volume) was wrapped into a ‘Figure 8’ pattern and submerged into an oil bath set to 150  $^{\circ}\text{C}$ . An ETFE tee was connected to the inlet of the tubing using a PFA flangeless nut. Syringes were connected to the tee using a 10 cm segment of PFA tubing and an ETFE female Leur adapter.

In one syringe was placed a solution of isobutylbenzene (4.3 M) and propionic acid (4.3 M) and in another syringe was placed neat triflic acid (11.3 M). The two syringes were placed on separate syringe pumps and flow rates were attenuated to provide the desired stoichiometry. The isobutylbenzene/propionic acid syringe was set to 15.1  $\mu\text{L min}^{-1}$  (64.9  $\mu\text{mol min}^{-1}$ , 1.0 eq  $\text{min}^{-1}$  each) and the triflic acid syringe was set to 28.7  $\mu\text{L min}^{-1}$  (324.6  $\mu\text{mol min}^{-1}$ , 5.0 eq  $\text{min}^{-1}$ ). Flow was initiated and the reaction stream was allowed to pass through the tubing. The reaction was collected in a 60 mL separatory funnel containing 20 mL saturated  $\text{NaHCO}_3$ . The aqueous layer

was extracted with Et<sub>2</sub>O (3x 25 mL), dried over Na<sub>2</sub>SO<sub>4</sub> and filtered. To the organic extracts was added a small amount of silica gel, used to pre-adsorb the product prior to column chromatography. The product was purified using column chromatography (silica gel, hexanes → 95:5 hexanes/EtOAc, R<sub>f</sub> = 0.34) to give 4-isobutylpropiofenone as light-yellow oil (70% yield, average of two trials): <sup>1</sup>H NMR (300 MHz, CDCl<sub>3</sub>): δ 7.89 (d, *J*=7.8, 2H), 7.23 (d, *J*=7.8 Hz, 2H), 2.99 (q, *J*=7.2 Hz, 2H), 2.53 (d, *J*=7.2 Hz, 2H), 1.89 (m, *J*= 6.6 Hz, 1H), 1.22 (t, *J*= 7.2 Hz, 3H), 0.91 (d, *J*= 6.6 Hz, 6H); <sup>13</sup>C NMR (75 MHz, CDCl<sub>3</sub>): δ 200.3, 147.2, 134.7, 129.2, 127.9, 45.3, 31.6, 30.1, 22.3, 8.3. MS *m/z* 190 (M<sup>+</sup>).

#### Representative Flow PhI(OAc)<sub>2</sub> Rearrangement Optimization Experiment.

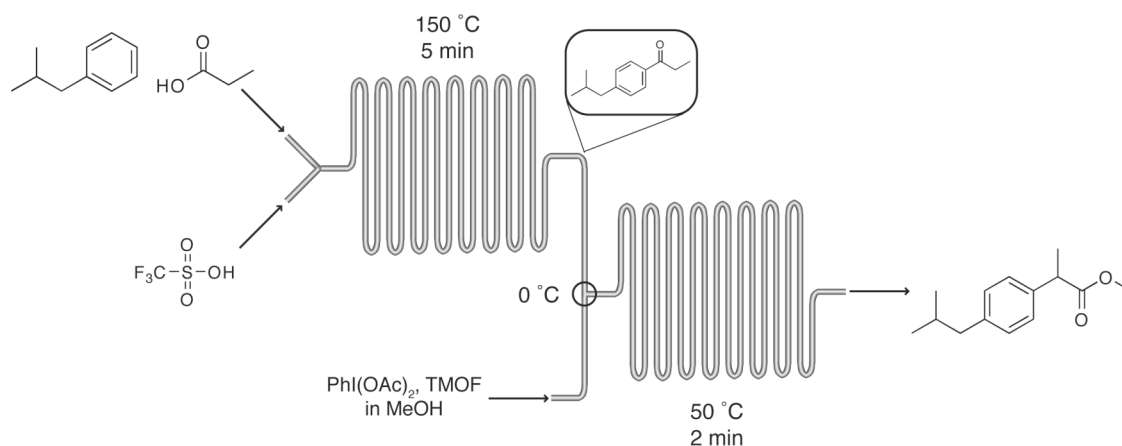


For the flow Friedel-Crafts acylation, a 50 cm segment of PFA tubing (0.75 mm i.d., 220.89 μL total volume) was wrapped into a ‘Figure 8’ pattern and submerged into an oil bath set to the desired temperature (35, 50 or 60 °C). An ETFE tee was connected to the inlet of the tubing using a PFA flangeless nut. Syringes were connected to the tee using a 10 cm segment of PFA tubing and an ETFE female Leur adapter.

In one syringe was placed a solution of propiophenone, triflic acid and cyclooctane and in another syringe was placed a solution of trimethylorthoformate (TMOF) and PhI(OAc)<sub>2</sub> in MeOH. The two syringes were placed on separate syringe pumps and flow rates were attenuated to provide the desired stoichiometry. Flow was

initiated and the reaction stream was allowed to pass through the tubing. The reaction was collected in a 4 mL screw cap vial containing 1.5 mL saturated  $\text{NaHCO}_3$  and 1.5 mL  $\text{Et}_2\text{O}$ . The organic layer was sampled and analyzed using GC. Conversion and yield were calculated using cyclooctane as the internal standard.

### Two-Step Flow Isolated Yield Experiment.



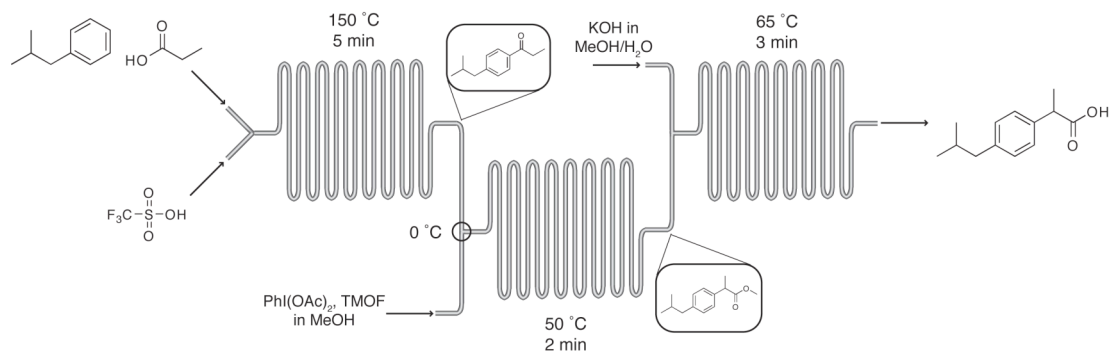
A 50 cm segment of PFA tubing (0.75 mm i.d., 220.89  $\mu\text{L}$  total volume) was wrapped into a ‘Figure 8’ pattern and submerged into an oil bath set to 150 °C. An ETFE tee was connected to the inlet of the tubing using a PFA flangeless nut. Syringes were connected to the tee using a 10 cm segment of PFA tubing and an ETFE female Leur adapter.

In one syringe was placed a solution of isobutylbenzene (4.3 M) and propionic acid (4.3 M) and in another syringe was placed neat triflic acid (11.3 M). The two syringes were placed on separate syringe pumps and flow rates were attenuated to provide the desired stoichiometry. The isobutylbenzene/propionic acid syringe was set to 15.1  $\mu\text{L min}^{-1}$  (64.9  $\mu\text{mol min}^{-1}$ , 1.0 eq  $\text{min}^{-1}$  each) and the triflic acid syringe was set to 28.7  $\mu\text{L min}^{-1}$  (324.6  $\mu\text{mol min}^{-1}$ , 5.0 eq  $\text{min}^{-1}$ ). Flow was initiated and the reaction stream was allowed to pass through the tubing.

To the outlet of the first reactor was attached an ETFE tee using a flangeless nut. An additional syringe was connected to the tee using a 10 cm segment of PFA tubing and an ETFE female Leur adapter. This tee was modified such that the inner diameter of the junction was 0.75 mm and packed with glass beads (250-300  $\mu\text{m}$ ). The outlet of the tee was connected to an 80 cm segment of PFA tubing (0.75 mm i.d., 353.43  $\mu\text{L}$  total volume), wrapped into a 'Figure 8' pattern and submerged into an oil bath set to 50  $^{\circ}\text{C}$ . A solution of  $\text{PhI}(\text{OAc})_2$  (0.5 M) and TMOF (2.0 M) in MeOH was placed in this syringe and set to 131.5  $\mu\text{L min}^{-1}$  (65.8  $\mu\text{mol IBD min}^{-1}$ , 1.01 eq IBD  $\text{min}^{-1}$  and 259.6  $\mu\text{mol TMOF min}^{-1}$ , 4.0 eq TMOF  $\text{min}^{-1}$ ). The tee was submerged in an ice bath to prevent off-gassing from mixing the two phases.

The reaction was collected in a 60 mL separatory funnel containing 20 mL saturated  $\text{NaHCO}_3$ . The aqueous layer was extracted with  $\text{Et}_2\text{O}$  (3x 25 mL), dried over  $\text{Na}_2\text{SO}_4$  and filtered. To the organic extracts was added a small amount of silica gel, used to pre-adsorb the product prior to column chromatography. The product was purified using column chromatography (silica gel, hexanes  $\rightarrow$  95:5 hexanes/ $\text{EtOAc}$ ,  $R_f = 0.37$ ) to give methyl 2-(4-isobutylphenyl)propanoate as light-yellow oil (70% yield, average of two trials):  $^1\text{H NMR}$  (300 MHz,  $\text{CDCl}_3$ ):  $\delta$  7.23 (d,  $J=8.4$ , 2H), 7.13 (d,  $J=7.8$  Hz, 2H), 3.71 (m, 4H), 2.48 (d,  $J=7.2$  Hz, 2H), 1.86 (m,  $J= 6.6$  Hz, 1H), 1.52 (d,  $J= 7.2$  Hz, 3H), 0.93 (d,  $J= 6.6$  Hz, 6H);  $^{13}\text{C NMR}$  (75 MHz,  $\text{CDCl}_3$ ):  $\delta$  175.4, 140.7, 137.9, 129.5, 127.3, 52.1, 45.21, 45.18, 30.3, 22.6, 18.8. MS  $m/z$  220 ( $\text{M}^+$ ).

## Continuous Flow Ibuprofen Isolated Yield Experiment.



A 50 cm segment of PFA tubing (0.75 mm i.d., 220.89  $\mu\text{L}$  total volume) was wrapped into a ‘Figure 8’ pattern and submerged into an oil bath set to 150 °C. An ETFE tee was connected to the inlet of the tubing using a PFA flangeless nut. Syringes were connected to the tee using a 10 cm segment of PFA tubing and an ETFE female Leur adapter.

In one syringe was placed a solution of isobutylbenzene (4.3 M) and propionic acid (4.3 M) and in another syringe was placed neat triflic acid (11.3 M). The two syringes were placed on separate syringe pumps and flow rates were attenuated to provide the desired stoichiometry. The isobutylbenzene/propionic acid syringe was set to 15.1  $\mu\text{L min}^{-1}$  (64.9  $\mu\text{mol min}^{-1}$ , 1.0 eq  $\text{min}^{-1}$  each) and the triflic acid syringe was set to 28.7  $\mu\text{L min}^{-1}$  (324.6  $\mu\text{mol min}^{-1}$ , 5.0 eq  $\text{min}^{-1}$ ). Flow was initiated and the reaction stream was allowed to pass through the tubing.

To the outlet of the first reactor was attached an ETFE tee using a flangeless nut. An additional syringe was connected to the tee using a 10 cm segment of PFA tubing and an ETFE female Leur adapter. This tee was modified such that the inner diameter of the junction was 0.75 mm and packed with glass beads (250-300  $\mu\text{m}$ ). The outlet of the tee was connected to an 80 cm segment of PFA tubing (0.75 mm i.d., 353.43  $\mu\text{L}$  total volume), wrapped into a ‘Figure 8’ pattern and submerged into an oil bath set to 50 °C. A solution of PhI(OAc)<sub>2</sub> (0.5 M) and TMOF (2.0 M) in MeOH was

placed in this syringe and set to  $131.5 \mu\text{L min}^{-1}$  ( $65.8 \mu\text{mol PhI(OAc)}_2 \text{ min}^{-1}$ ,  $1.01 \text{ eq PhI(OAc)}_2 \text{ min}^{-1}$  and  $259.6 \mu\text{mol TMOF min}^{-1}$ ,  $4.0 \text{ eq TMOF min}^{-1}$ ). The tee was submerged in an ice bath to prevent off-gassing from mixing the two phases.

To the outlet of the second reactor was attached an ETFE tee using a flangeless nut. An additional syringe was connected to the tee using a 20 cm segment of PFA tubing and an ETFE female Leur adapter. The outlet of the tee was connected to a 300 cm segment of PFA tubing (0.75 mm i.d.,  $1325.36 \mu\text{L}$  total volume), wrapped into a 'Figure 8' pattern and submerged into a water bath set to  $65 \text{ }^\circ\text{C}$ . A solution of KOH (5.0 M) in MeOH/H<sub>2</sub>O (4:1 v/v) was placed in this syringe and set to  $260.0 \mu\text{L min}^{-1}$  ( $1300.0 \mu\text{mol min}^{-1}$ ,  $20.0 \text{ eq min}^{-1}$ ).

The reaction was collected in a 100 mL round bottom flask. The outlet stream was periodically sampled, quenched into EtOAc, and analyzed by GC to determine the composition of the reaction stream. Once the collection was complete, DI H<sub>2</sub>O (25 mL) was added to the round bottom flask and the methanol was evaporated using rotary evaporation. The aqueous phase was washed with Et<sub>2</sub>O (3x 30 mL) and the organic washes analyzed by GC. The aqueous phase was acidified with concentrated HCl, and the aqueous phase was extracted with Et<sub>2</sub>O (3x 30 mL). The organic extracts were repeatedly washed with DI H<sub>2</sub>O (5x 20 mL) until the pH of the aqueous phase was neutral. The organic extracts were subsequently washed with brine (1x 20 mL), dried over Na<sub>2</sub>SO<sub>4</sub>, filtered, concentrated and dried *in vacuo* to yield a light orange solid (68% crude yield, average of three trials). Seed crystals were added to initiate crystallization. The solid was dissolved in Et<sub>2</sub>O and treated with activated carbon. The activated carbon was removed by filtering the suspension through a plug of anhydrous MgSO<sub>4</sub>. The Et<sub>2</sub>O was concentrated to yield an off-white solid, which was recrystallized with warm heptane. Ibuprofen has a solubility of  $\sim 100 \text{ mg ibuprofen}/250 \mu\text{L heptane}$  at  $50 \text{ }^\circ\text{C}$  and  $5 \text{ mg ibuprofen}/250 \mu\text{L heptane}$  at  $0 \text{ }^\circ\text{C}$ .<sup>41</sup> The

filtrate was removed and the crystals were dried under vacuum to afford ibuprofen as an off-white solid (51% yield, average of three trials). Additional charcoal treatments could be performed to remove residual color after recrystallization without impacting yield:  $^1\text{H}$  NMR (300 MHz,  $\text{CDCl}_3$ ):  $\delta$  7.23 (d,  $J=8.4$ , 2H), 7.13 (d,  $J=7.8$  Hz, 2H), 3.71 (m, 4H), 2.48 (d,  $J=7.2$  Hz, 2H), 1.86 (m,  $J=6.6$  Hz, 1H), 1.52 (d,  $J=7.2$  Hz, 3H), 0.93 (d,  $J=6.6$  Hz, 6H);  $^{13}\text{C}$  NMR (75 MHz,  $\text{CDCl}_3$ ):  $\delta$  175.4, 140.7, 137.9, 129.5, 127.3, 52.1, 45.21, 45.18, 30.3, 22.6, 18.8. MS  $m/z$  220 ( $\text{M}^+$ ).

## REFERENCES

1. Sheldon, R. A. *J. Chem. Tech. Biotechnol.* **1997**, *68*, 381.
2. Anastas, P.T.; Kirchhoff, M. M. *Acc. Chem. Res.* **2002**, *35*, 686.
3. Mason, B. P.; Price, K. E.; Steinbacher, J. L.; Bogdan, A. R.; McQuade, D. T. *Chem. Rev.* **2007**, *107*, 2300.
4. Hessel, V.; Löb, P.; Löwe, H. *Curr. Org. Chem.* **2005**, *9*, 765.
5. Hessel, V.; Löwe, H. *Chem. Eng. Technol.* **2005**, *28*, 267.
6. Hodge, P. *Curr. Opin. Chem. Biol.* **2003**, *7*, 362.
7. Jas, G.; Kirschning, A. *Chem.–Eur. J.* **2003**, *9*, 5708.
8. Kirschning, A.; Monenschein, H.; Wittenberg, R. *Angew. Chem., Int. Ed.* **2001**, *40*, 650.
9. Pennemann, H.; Watts, P.; Haswell, S. J.; Hessel, V.; Löwe, H. *Org. Process Res. Dev.* **2004**, *8*, 422.
10. Wirth, T., Ed. *Microreactors in Organic Synthesis and Catalysis*; Wiley-VCH: Weinheim, 2008.
11. Watts, P.; Wiles, C. *Org. Biomol. Chem.* **2007**, *5*, 727.
12. Fukuyama, C.; Rahman, M. T.; Sato, M.; Ryu, I. *Synlett* **2008**, *2*, 151.
13. Ahmed-Omer, B.; Brandt, J. C.; Wirth, T. *Org. Biomol. Chem.* **2007**, *5*, 733.
14. Yoshida, J.; Nagaki, A.; Yamada, T. *Chem. Eur. J.* **2008**, *14*, 7450, and references within.
15. Nagaki, A.; Takabayashi, N.; Tomida, Y.; Yoshida, J. *Org. Lett.* **2008**, *10*, 3937.
16. Nagaki, A.; Kim, H.; Yoshida, J. *Angew. Chem. Int. Ed.* **2008**, *47*, 7833.
17. van der Linden, J. M. J.; Hilberink, P. W.; Kronenburg, C. M. P.; Kemperman, G. J. *Org. Process Res. Dev.* **2008**, *12*, 911.
18. Bogdan, A. R.; Sach, N. W. *Adv. Synth Catal*, **2009**, *351*, 849.

19. Ehrfeld, W.; Hessel, V.; Lowe, H. *Microreactors: New Technology for Modern Chemistry*, Wiley-VCH, Weinheim, 2000.
20. Hornung, C. H.; Mackley, M. R.; Baxendale, I. R.; Ley, S. V. *Org. Process Res. Dev.* **2007**, *11*, 399.
21. Acke, D. R. J.; Stevens, C. V. *Org. Process Res. Dev.* **2006**, *10*, 417
22. Sahoo, H. R.; Kralj, J. G.; Jensen, K. F. *Angew. Chem. Int. Ed.* **2007**, *46*, 5704.
23. Baxendale, I. R.; Deeley, J.; Griffiths-Jones, C. M.; Ley, S. V.; Saaby, S.; Tranmer, G. K. *Chem. Commun.* **2006**, 2566.
24. I. R. Baxendale, S. V. Ley, A. C. Mansfield, C. D. Smith, *Angew. Chem. Int. Ed.* **2009**, *48*, 4017.
25. D. Grant, R. Dahl, N. D. P. Cosford, *J. Org. Chem.* **2008**, *73*, 7219.
26. Bogdan, A. R.; Mason, B. P.; Sylvester, K. T.; McQuade, D. T. *Angew. Chem. Int. Ed.* **2007**, *46*, 1698.
27. Bogdan, A. R.; McQuade, D. T. *Beilstein Journal of Organic Chemistry*, **2009**, *5*, 17.
28. Poe, S. L.; Kobašlija, M.; McQuade, D. T. *J. Am. Chem. Soc.* **2006**, *128*, 15586.
29. Poe, S. L.; Kobašlija, M.; McQuade, D. T. *J. Am. Chem. Soc.* **2007**, *129*, 9216.
30. Tamura, Y.; Yakura, T.; Shirouchi, Y.; Haruta, J. *Chem. Pharm. Bull.* **33**, *3*, 1097.
31. Roberts, R. M. G.; Sadri, A. R. *Tetrahedron*, **1983**, *39*, 137.
32. Effenberger, F.; Epple, G. *Angew. Chem. Int. Ed.*, **1972**, *11*, 300.
33. In our flow reactor, the use of PFA tubing and unions was *critical* to withstand the caustic nature of TfOH. For a detailed description of the materials used, see the supporting information.
34. Batch reactions with vigorous mixing at low temperature were also slow, indicating that mixing is not the only variable that impacts reaction rate.
35. This reaction generated ~5% of the 1,2-adduct, as indicated by GC and GC/MS. This by-product was ultimately converted to the 1,2-derivative of

ibuprofen in the continuous flow synthesis, and was removed after recrystallization.

36. Singh, O. V.; Prakash, O.; Garg, C. P.; Kapoor, R. P. *Ind. J. Org. Chem.* **1989**, *28B*, 814.
37. Prakash, O.; Goyal, S.; Moriarty, R. M.; Khosrowshahi, J. S. *Ind. J. Org. Chem.* **1990**, *289B*, 304.
38. Iodobenzene is the byproduct of the 1,2-aryl migration. It can be converted back to  $\text{PhI}(\text{OAc})_2$  by treatment with peracetic acid.
39. It was found to be necessary to cool the tee junction due to significant off-gassing that occurred when held at room temperature. This off-gassing did not occur during the optimization and therefore this tee junction did not need to be cooled.
40. The low yield from the recrystallization most likely stems from recrystallization of ibuprofen on small scale. As larger batches of ibuprofen were recrystallized, higher yields were obtained.
42. Gordon, R. E.; Amin, S. I. U.S. Patent 4,476,248, **1984**.

## CHAPTER 7

### Progress Toward Multi-Step Reaction Sequences using Solid-Supported Catalysis

#### *Abstract*

This chapter highlights progress toward performing multi-step, catalytic reaction sequences in our simplified microreactor. Two new solid-supported catalysts were synthesized to facilitate asymmetric reactions in flow. Preliminary results of one of these catalysts, a supported proline derivative, indicate high enantioselectivity can be obtained in flow, an unprecedented result for organocatalysis. Multi-step reaction sequences are proposed using the catalysts already developed in the group, as are designs for continuous flow syntheses of other important small molecules.

#### *Introduction*

Since the early 2000s, the application of microreactors to organic synthesis has continued to garner a lot of attention.<sup>1-12</sup> Early publications applying this new technology to organic synthesis focused on the ability to perform single reaction steps more efficiently in flow. More recently, however, research groups have been pushing the limits of these systems by performing multiple reactions in sequence with little to no purification.<sup>13-16</sup>

The modularity of microreactors enables multiple reaction steps to be performed in sequence by mixing the outlet stream from one reactor with another reagent stream. This setup thereby minimizes the number of work-up steps for an entire process, offering potentially higher yields, selectivity, purity, and efficiency. Designing a continuous synthesis is a significant challenge, however, as it requires the entire synthesis to be considered as an entity, as opposed to a series of independent

reactions steps. To be successful, excess reagents and byproducts from one reaction must be compatible with downstream reactions.

Multi-step reaction sequences in flow have been reported in the literature, but these syntheses are essentially void of any catalytic steps.<sup>13-16</sup> One could argue that catalysis is one of the most significant innovations in organic chemistry as its use oftentimes increases reaction efficiency and selectivity.<sup>17</sup> The reduced use of raw materials such as solvents and reagents, as well as the ability to introduce chemical complexity into a molecule are just a few of the benefits of catalysis.<sup>18</sup> Few reports describe multi-step catalytic reactions in flow (Figure 7.1), although recent advances using catalysts in flow for single reaction steps<sup>19-22</sup> suggest that coupling these catalysts in series may soon be accomplished.

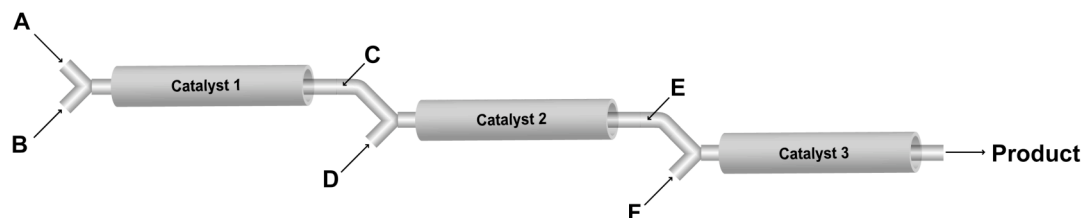


**Figure 7.1.** Multi-step, catalytic reaction sequence in flow.

Perhaps an even more promising avenue is the use of heterogeneous catalysis in these flow.<sup>23-27</sup> Catalysts are typically the most expensive component of a reaction mixture and can be difficult to separate. Immobilizing a catalyst for use in flow is advantageous as the catalyst is essentially performing the reaction and being removed simultaneously.<sup>28</sup> These solid-supported catalysts will be isolated in separate catalyst beds and users need not worry about catalyst compatibility since these species will never interact with one another. As a result, a level of complexity is potentially removed while running a multi-step sequence as catalyst fouling is a non-issue. The

use of flow enables long-term activity as no agitation or stress is exerted on these supported catalysts, which oftentimes shortens the lifetime of these materials. Therefore, a high throughput of product can potentially be achieved as these catalytic systems can be used continuously.<sup>26,27</sup>

In this chapter, the development of new strategies to make small molecules continuously in microreactors will be discussed using our simplified packed-bed microreactor platform. Two new asymmetric catalysts were synthesized for use in multi-step reaction sequences. Furthermore, other potential multi-catalyst flow syntheses for important small molecules will be proposed.

## ***Results and Discussion***

### **The Development of New Solid-Supported Catalysts for Flow Chemistry.**

Catalysis has been studied extensively in flow; however most of these reactions are nonselective.<sup>1-12</sup> Few examples do exist that perform asymmetric transformations, however, that use homogeneous and heterogeneous flow catalysis, the majority of which use chiral ligands and transition metals.<sup>28</sup> We set out to develop new solid-supported catalysts to perform enantioselective transformations in our simplified microreactor with the ultimate goal of running two or more steps relying solely on catalytic reactions.

Over the past few years, the field of organocatalysis has been gaining attention due to the ever-expanding number of selective transformations described in the literature.<sup>29-37</sup> Recently, Seeberger and co-workers developed a system that uses a proline derivative in flow to facilitate the aldol condensation between benzaldehyde and acetone (Figure 7.2).<sup>38</sup> In this example, the reaction was performed at higher temperatures and with shorter reaction times than similar batch reactions. While there

is no significant increase in yield or selectivity compared to traditional methods, this is still the first example using organocatalysis in flow.

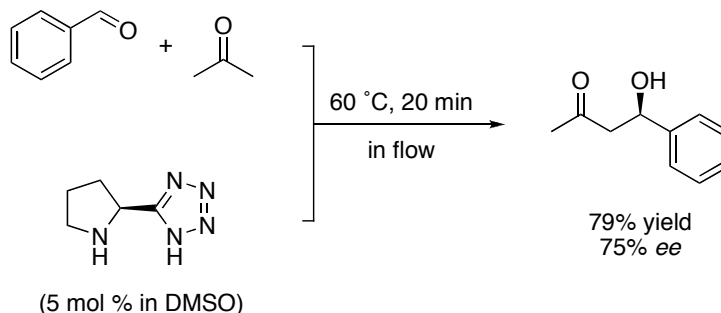


**Figure 7.2.** Seeberger's aldol condensation in flow.

We chose to explore organocatalysis in flow using the simplified packed-bed microreactor platform developed in our group.<sup>26, 27</sup> In doing so, we were determined to demonstrate that an immobilized proline derivative<sup>39</sup> (AO-proline, Figure 7.3) could provide excellent yields and selectivities in flow. Furthermore, as the starting material of this reaction is an aldehyde, it could potentially be coupled to our TEMPO packed-bed microreactor<sup>27</sup> discussed earlier in this dissertation.

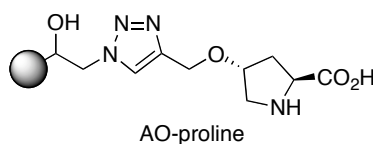
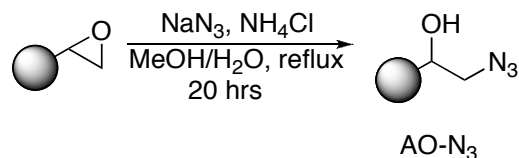
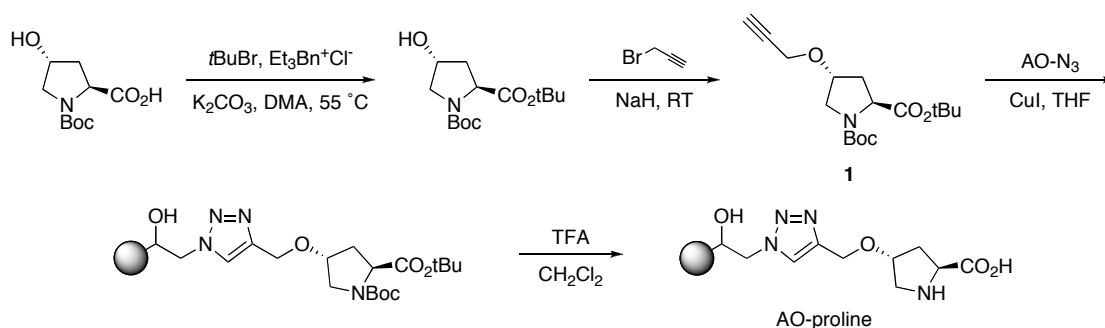


**Figure 7.3.** The structure of AO-proline.

We prepared the AO-proline packed-bed reactor using the azide-functionalized Amberzyme Oxirane resin (AO-N<sub>3</sub>, Scheme 7.1).<sup>26, 27</sup>



**Scheme 7.1.** The preparation of AO-N<sub>3</sub>.



**Scheme 7.2.** The synthesis of AO-proline.

Using AO-N<sub>3</sub>, AO-proline was synthesized using a four-step reaction sequence, starting from *N*-Boc-4-hydroxyproline (Scheme 7.2).<sup>39</sup> After carboxylate protection, NaH and propargyl bromide were used to synthesize proline derivative **1**. Using click chemistry, this protected proline derivative was tethered to AO-N<sub>3</sub> using CuI. Protected AO-proline was subsequently treated with TFA to cleave both protecting groups.

Though proline catalysis is quite versatile, limitations exist, such as slow reaction rates and the need for high catalyst loadings.<sup>40, 41</sup> Furthermore, immobilizing a catalyst on a support frequently decreases the catalyst's activity.<sup>42</sup> Flow chemistry is best utilized when reaction rates are fast, indicating that these issues may have detracted chemists from exploring supported proline catalysis in flow.

Our group has recently developed a bifunctional urea (**2**, Figure 7.4) that significantly increases the rate of proline-catalyzed  $\alpha$ -aminoxylations and Mannich

reactions. This work was performed by Sarah Poe and will not be discussed in great length here.<sup>43</sup>

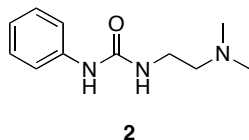


**Figure 7.4.** The bifunctional urea used in AO-proline-catalyzed flow reactions.

It is proposed that urea **2** accelerates the rate of enamine formation, and thus significantly increases reaction rates (Table 7.1, entries 1 and 2). Furthermore, the addition of this urea does not impact the yield or the enantioselectivities of the  $\alpha$ -aminoxylation of aldehydes (Table 7.1, entries 3-9).

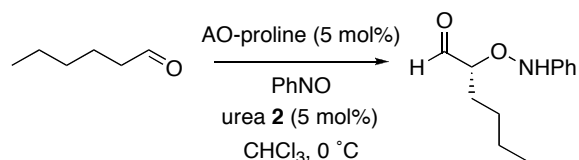
**Table 7.1.** Results of the  $\alpha$ -aminoxylation of aldehydes.



Entry	R	Time (hrs)	Yield (%) <sup>a</sup>	ee (%)
1	nBu	0.67	NR	-
2	nBu	0.67	81	98
3	nBu	2.0	96	99
4	Me	3.0	90	98
5	iPr	3.5	97	99
6	nHex	5.0	84	99
7	CH <sub>2</sub> Ph	3.5	84	>99
8	Ph	2.0	55	99
9	CH <sub>2</sub> CHCH <sub>2</sub>	2.5	75	99

<sup>a</sup> Products were reduced to the corresponding 2-aminoxy alcohols prior to isolation.

The  $\alpha$ -aminoxylation of hexanal was later performed substituting proline with AO-proline (Scheme 7.3). Initially, the reaction was run without the urea additive and reaction rates were slow. The reaction was then run in the presence of urea **2** to determine if the same effect was observed when using a solid-supported proline.



**Scheme 7.3.** The AO-proline-catalyzed  $\alpha$ -aminoxylation of hexanal.

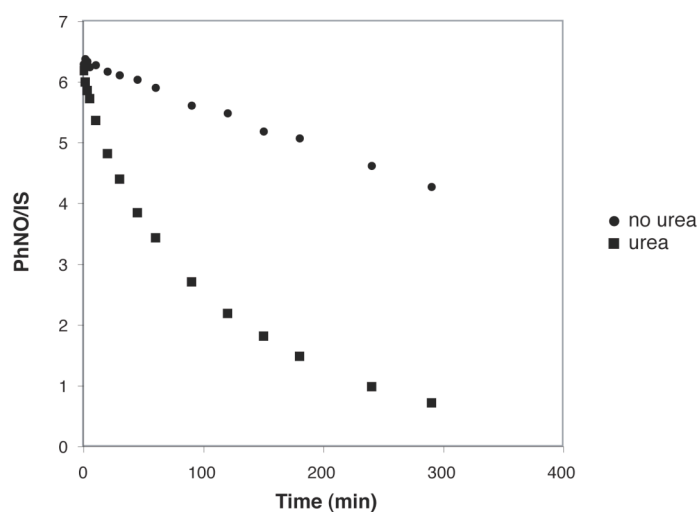


**Figure 7.5.** The AO-proline-catalyzed  $\alpha$ -aminoxylation of hexanal with and without urea additive.

**Figure 7.5** shows data for the  $\alpha$ -aminoxylation of hexanal in batch, with and without urea **2** using AO-proline as the catalyst. As can be seen, a substantial increase in rate occurs when urea **2** is present. It was therefore determined that urea **2** should be added to the flow  $\alpha$ -aminoxylation to help facilitate reaction.

Using the simplified procedure developed within our group,<sup>26,27</sup> flow reactions were performed by packing fluoroelastomeric tubing (60 cm, 1.6 mm i.d.) with the AO-proline resin (~400 mg). For the flow experiments, a solution of PhNO in chloroform was mixed with a solution of urea **2** and hexanal in chloroform at a Y-junction, and the reaction stream was allowed to pass through the AO-proline packed-bed cooled to 0 °C. At the outlet of the reactor was a solution of ethanolic NaBH<sub>4</sub>, used to reduce the product to the 2-aminoxy alcohol. Preliminary results indicated the  $\alpha$ -aminoxylation of hexanal could be successfully performed in flow. While a yield was not obtained for this reaction, an enantioselectivity of 95% was obtained, which is only slightly lower than batch reactions with proline (Figure 7.6).

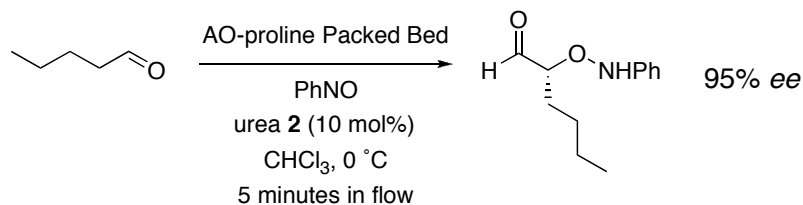


**Figure 7.6.** Results of the flow  $\alpha$ -aminoxylation of hexanal.

Another solid-supported catalyst synthesized was a triphenylethanol derivative (AO-PTPE, Figure 7.7) used to add alkyl zincs to aldehydes (Scheme 7.4).<sup>44-47</sup>

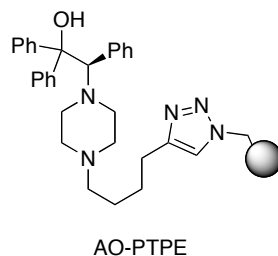
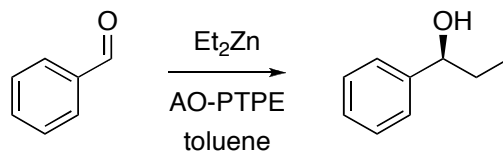
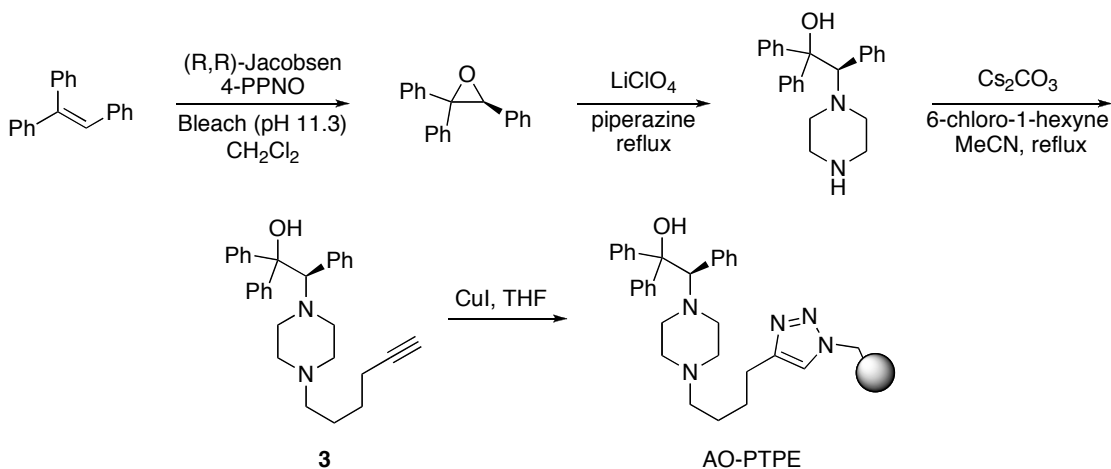


**Figure 7.7.** The structure of AO-PTPE.



**Scheme 7.4.** The asymmetric addition of diethyl zinc to benzaldehyde using AO-PTPE.

AO-PTPE was synthesized using the route shown in Scheme 7.5.<sup>46</sup> The synthesis starts with an asymmetric epoxidation of triphenylethylene, followed by a LiClO<sub>4</sub>-mediated epoxide ring opening with piperazine. This intermediate is subsequently treated with 6-chloro-1-hexyne and base to give the acetylene-modified ligand **3**, which is clicked on to AO-N<sub>3</sub> using CuI.



**Scheme 7.5.** The synthesis of AO-PTPE.

While the enantiomeric purity of the final catalyst was not determined, the *ee* of the epoxide was determined to be >99% after recrystallization. The assumption is being made that AO-PTPE is also of comparable enantiomeric purity.

To date, the activity of AO-PTPE is yet to be tested. However, during the development of this chemistry, similar work by Pericas was carried out to perform asymmetric 1,2-additions in flow.<sup>47</sup> Pericas' system proved to be highly efficient

(very short residence times), demonstrating high conversions and enantioselectivities for a number of aldehydes. We are optimistic that this system will work with AO-PTPE in flow and that we will be able to perform multi-step catalytic reaction sequences using this catalyst.

### ***Future Direction***

**Multi-step Catalytic Reaction Sequences in Flow.** Our group has published a number of papers detailing the creation and characterization of multi-catalyst systems in batch.<sup>48,49</sup> Using the packed-bed microreactor platform that we have developed,<sup>26,27</sup> we hope to achieve a similar goal by performing two or more catalytic reactions continuously in flow.

Using the solid-supported catalysts previously developed in our group, various proof-of-concept multi-step reaction sequences could be tested. All proposed reaction sequences using our technology start with the AO-TEMPO-catalyzed oxidation of an alcohol to an aldehyde, followed by an asymmetric reaction step. This method is advantageous as aldehydes have limited availability compared to alcohols and are susceptible to various forms of degradation, such as over-oxidization, hydrate formation, or polymerization.<sup>14</sup>

By coupling the AO-TEMPO packed-bed microreactor with the AO-proline or AO-PTPE packed-bed microreactors, various two-step reaction sequences could be performed. After the AO-TEMPO flow oxidation, microextractors used by the Jensen group<sup>15</sup> will most likely be a necessity to separate the organic and aqueous phases. As the aqueous stream is diverted to waste, the organic aldehyde stream is relayed into the next reaction. Using this methodology, we propose three multi-step reaction sequences, two using AO-proline packed-beds and one using the AO-PTPE packed-bed (Figure 7.8).

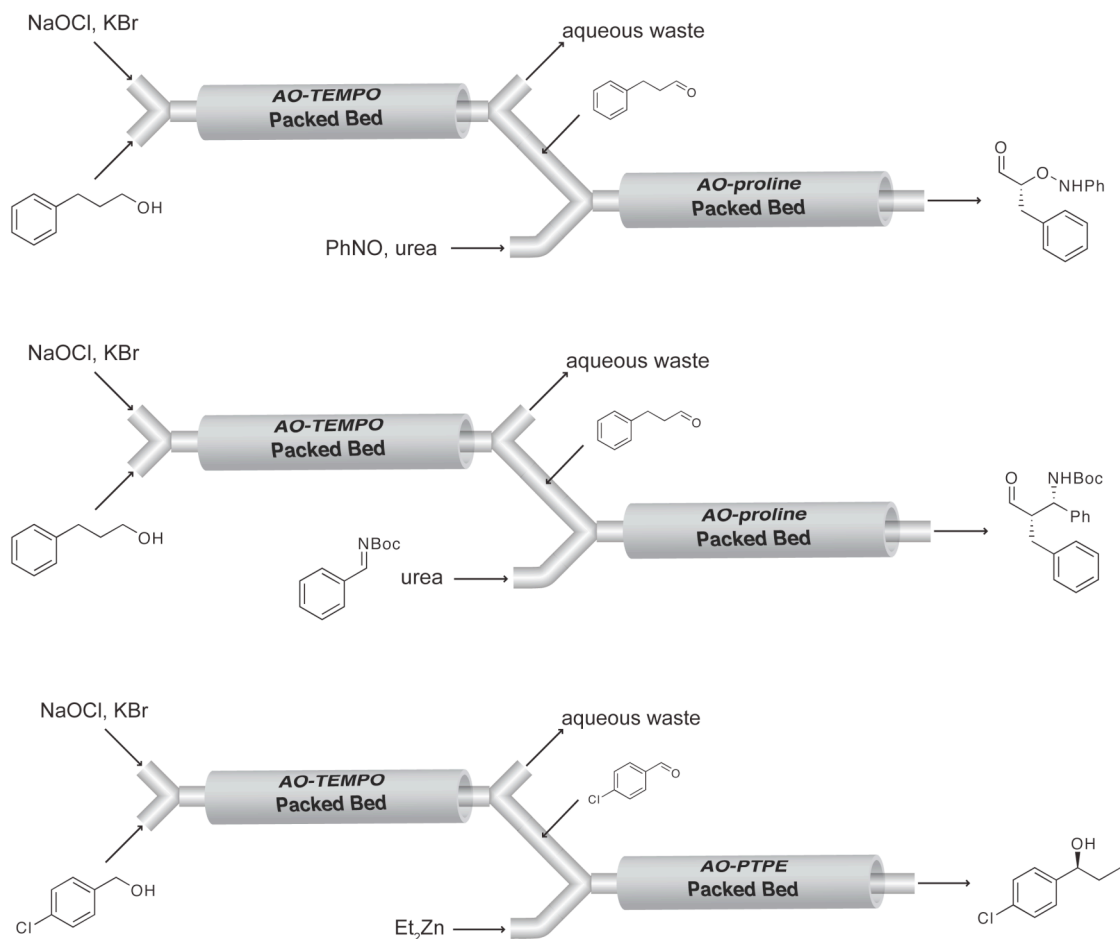


**Figure 7.8.** The proposed two-step, catalytic reaction sequences in flow. AO-TEMPO and AO-proline are coupled together in an oxidation/ $\alpha$ -aminooxylation sequence (top), AO-TEMPO and AO-proline are coupled together in an oxidation/Mannich reaction sequence (middle), or AO-TEMPO and AO-PTPE are coupled together in an oxidation/1,2-addition sequence (bottom).

Following the alcohol oxidation, the first two multi-step sequences rely on an AO-proline-catalyzed  $\alpha$ -aminooxylation or Mannich reaction. It is being assumed that the urea **2** is required in these cases to increase the rate of the AO-proline catalyzed steps. The final two-step reaction sequences would convert the aldehyde from the AO-TEMPO oxidation to the 1-aryl-1-propanol derivative using AO-PTPE. The microextractors developed by Jensen and co-workers are a necessity as they have been

demonstrated to quantitatively remove water from organic streams, indicating that the second, water-sensitive step may take place without great difficulty.

In addition to these two-step sequences being proposed, a three-step purely catalytic synthesis could be achieved as seen in Figure 7.9. The system relies on a similar motif as presented in the cases described above, but the alcohol eluting from the AO-PTPE packed-bed could subsequently be relayed into an AO-DMAP packed-bed to acylate the alcohol.

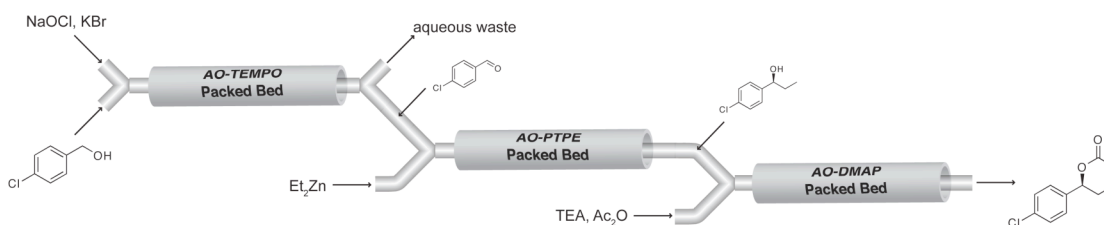


**Figure 7.9.** The proposed three-step, catalytic reaction sequence in flow. AO-TEMPO, AO-PTPE, and AO-DMAP are coupled together in an oxidation/1,2-addition/acylation sequence.

**Multi-Step Catalytic Reaction Sequences for APIs in Flow.** Chemical processing would substantially benefit from the use of solid-supported catalysis in flow. As previously stated, these flow reactions can rely on catalytic packed-beds to constantly perform the reactions and separate catalysts simultaneously. The catalysts presumably have long-term activity as there is no mechanical degradation of the support, indicating that continuous processing is an option.

While we have demonstrated the continuous flow synthesis of the API ibuprofen, the route does have its downfalls. The current route employed uses excess triflic acid to facilitate the Friedel-Crafts acylation. Using large quantities of acid is typically problematic as these materials cannot be regenerated and ultimately end up in aqueous waste streams.<sup>50</sup> Ideally this step would be performed with a solid-

supported catalyst such as a zeolite. In addition, the second step of the ibuprofen synthesis, the  $\text{PhI}(\text{OAc})_2$ -mediated 1,2-aryl migration, would be facilitated by a solid-supported oxidant that could be regenerated in-line. Following hydrolysis, ibuprofen could be obtained in a more efficient manner (Figure 7.10).

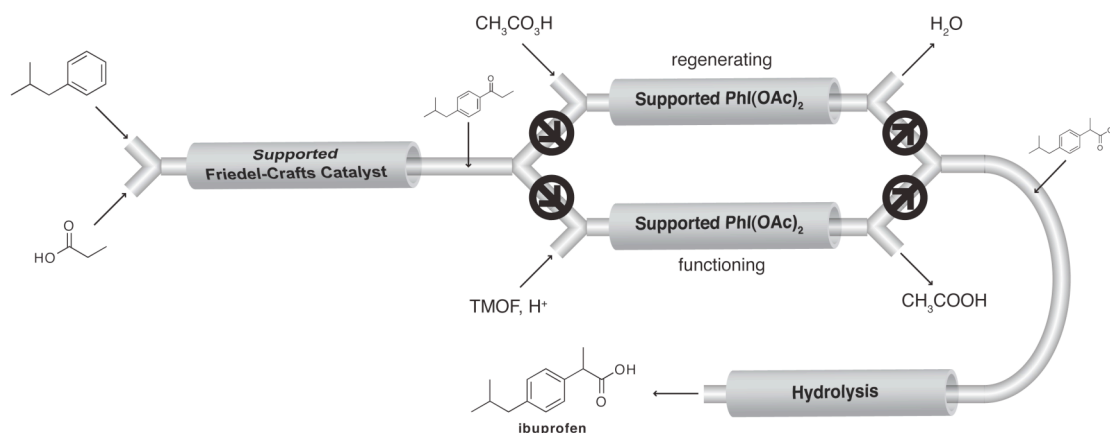


**Figure 7.10.** The proposed continuous flow synthesis of ibuprofen using a supported Friedel-Crafts acylation and a supported oxidant that is regenerated inline.

We also propose a continuous flow synthesis to the anticonvulsant drug pregabalin (Figure 7.11). Our group has reported the synthesis of pregabalin using a

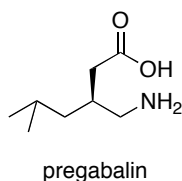
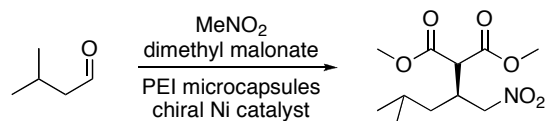


**Figure 7.11.** The structure of pregabalin.

novel one-pot reaction to produce an important nitroester intermediate in the synthesis (Scheme 7.6).<sup>48, 49</sup> Isovaleraldehyde is converted to a nitroester in one-pot, which is reduced and hydrolyzed to give pregabalin in high yield and enantioselectivity.



**Scheme 7.6.** The one-pot reaction used to synthesize the nitroester intermediate.

To synthesize pregabalin in flow, isoamyl alcohol would be converted to isovaleraldehyde using the AO-TEMPO flow oxidation. A major complication with the one-pot synthesis shown in Scheme 7.6 was the instability of isovaleraldehyde. Purification steps were necessary before carrying out the reaction as impure aldehyde gave significantly lower yields. Having the ability to generate the aldehyde *in situ* and relay it into the second reaction step is therefore highly advantageous. The second step of the synthesis would use an immobilized primary amine catalyst to facilitate the nitroalkene formation. In batch, this reaction can also be problematic as increased reaction times lead to an undesired dinitro product. By limiting the reaction times in flow, the desired nitroalkene should be obtained preferentially in high yield. Subsequent catalytic packed-beds would perform the asymmetric addition of dimethyl malonate to the nitroalkene, followed by a nitro group reduction, and hydrolysis to yield pregabalin in a continuous flow process (Figure 7.12).

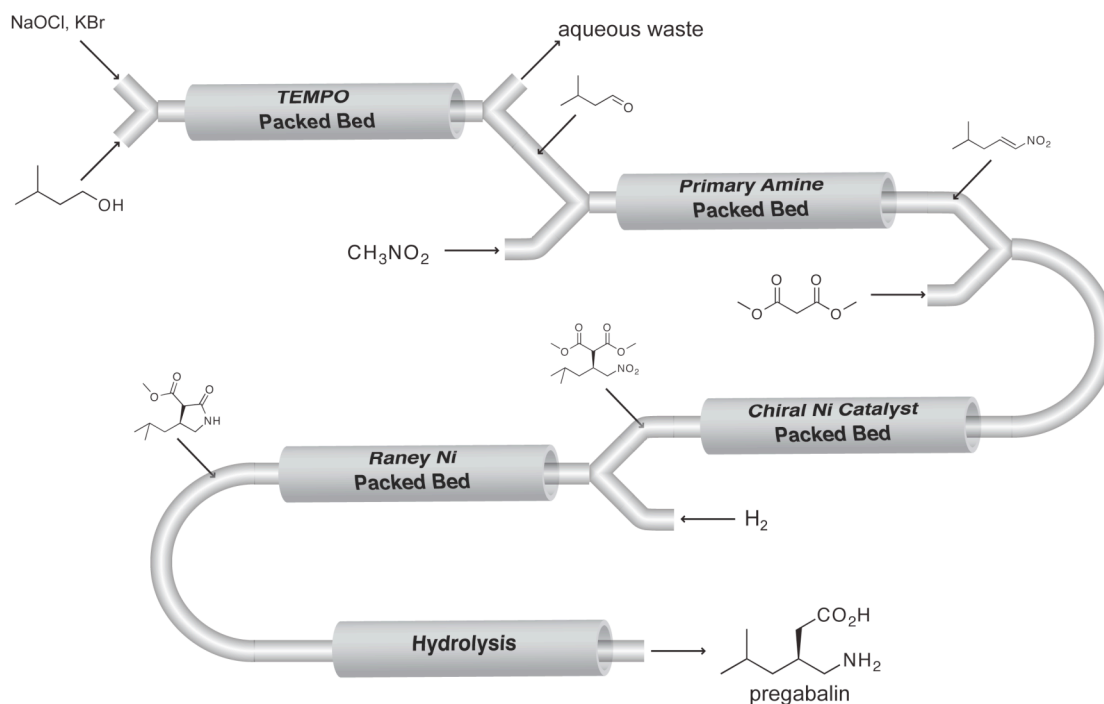


**Figure 7.12.** The proposed continuous flow synthesis of pregabalin.

### Conclusion

Our group has had a long-standing interest in the development of new methodologies that enable the rapid and efficient synthesis of small molecules. New solid-supported catalysts have been developed for use in two- or three-step reaction sequences in flow to generate products with stereocenters. Preliminary results indicate that these supported catalysts are capable of obtaining high enantioselectivity in flow.

Finally, our group has successfully synthesized two drugs, pregabalin and ibuprofen, using multi-step reaction sequences in batch and flow, respectively. Using the chemistry developed in these systems, it is our ultimate goal to perform these syntheses continuously in flow relying heavily on the use of solid-supported catalysts. By developing innovative, new strategies to make drugs continuously in microreactors, there are potential environmental and socioeconomic benefits. These continuous routes will ensure that drugs are produced more efficiently, selectively and

with a higher degree of safety. This increased efficiency would in due course generate less waste and reduce the cost of syntheses, limiting the environmental impact of the synthesis, and potentially lowering the cost of important small molecules.

### ***Experimental Section***

**General Considerations.** Solvents were purified by standard procedures. All other reagents were used as received, unless otherwise noted.  $^1\text{H}$  NMR and  $^{13}\text{C}$  NMR spectra were recorded in  $\text{CDCl}_3$  on Varian Mercury 300 MHz operating at 300.070 MHz and 75.452 MHz, respectively, using the residual solvent peak as reference. ATR-IR was performed on a Nicolet Avatar DTGS 370 infrared spectrometer with Avatar OMNI sampler and OMNIC software. Elemental analysis was performed by Robertson Microlit Laboratories, Inc., in Madison, New Jersey. Gas chromatographic (GC) analyses were performed using an Agilent 7890A GC equipped with an Agilent 7683B autosampler, a flame ionization detector (FID), and a J&W Scientific 19091J-413 column (length = 30 m, inner diameter = 320  $\mu\text{m}$ , and film thickness = 250  $\mu\text{m}$ ). The temperature program for GC analysis held the temperature constant at 80  $^\circ\text{C}$  for 1 minute, heated samples from 80 to 200  $^\circ\text{C}$  at 20  $^\circ\text{C}/\text{min}$  and held at 200  $^\circ\text{C}$  for 1 minute. Inlet and detector temperatures were set constant at 220 and 250  $^\circ\text{C}$ , respectively. High performance liquid chromatography (HPLC) was performed using a chromatograph using a CHIRALPAK IA column (250 mm x 4.6 mm) and CHIRALPAK IA guard column (1 cm x 0.4 cm). Retention times for *R* and *S* isomers were determined by using (DL)-proline instead of (L)-proline in the general procedure. All chromatograms were obtained using a wavelength of 254 nm.

**Azide Modified AMBERZYME® Oxirane (AO-N<sub>3</sub>):** Sodium azide (5.26 g, 81 mmol, 8.1 eq.) and ammonium chloride (2.27 g, 42.4 mmol, 4.2 eq.) were dissolved in

500 mL 90:10 v/v water in methanol. AMBERZYME® Oxirane (10.0 g, 1.0 mmol epoxide/g resin, 10.0 mmol, 1.0 eq.) was suspended in the azide solution and the reaction mixture refluxed overnight with gentle stirring. The resin was filtered using a Buchner funnel, washed with deionized H<sub>2</sub>O (2x 50 mL), MeOH (2x 50 mL), Et<sub>2</sub>O (1x 25 mL), and dried under vacuum. Elemental analysis afforded a loading of 1.0 mmol N<sub>3</sub>/g resin.

***t*-Butyl (2*S*,4*R*)-*N*-Boc-4-hydroxyprolinate.** *N*-Boc-4-hydroxyproline (2.0 g, 8.65 mmol, 1.0 eq), *t*BuBr (40 mL, 0.36 mol, 41.2 eq), Et<sub>3</sub>NBn<sup>+</sup>Cl<sup>-</sup> (2.0 g, 8.8 mmol, 1.0 eq), and K<sub>2</sub>CO<sub>3</sub> (32.0 g, 0.23 mol, 26.8 eq) were added to dimethylacetamide (40 mL), placed under nitrogen and stirred at 55 °C overnight. H<sub>2</sub>O was added to the reaction mixture until it turned white, and the aqueous phase was extracted with ether (3x 50 mL). The organic extracts were dried with MgSO<sub>4</sub>, filtered, concentrated and dried under vacuum to give a viscous oil. The oil was purified by column chromatography (silica gel, 1:1 hexanes/EtOAc) to give the title compound as a viscous oil (80% yield): <sup>1</sup>H NMR (300 MHz, CDCl<sub>3</sub>): δ 4.43 (bs, 1H), 4.24 (m, 1H), 3.55 (m, 2H), 2.24 (m, 1H), 1.43 (d, 18H). <sup>13</sup>C NMR (75 MHz, CDCl<sub>3</sub>): δ 172.4, 154.4, 81.3, 80.4, 69.4, 58.7, 54.8, 39.3, 28.5, 28.2.

***t*-Butyl (2*S*,4*R*)-*N*-Boc-4-propargyloxyprolinate (1).** NaH (247.0 mg, 10.3 mmol, 1.5 eq) was stirred in DMF (20 mL) at 0 °C under nitrogen. *t*-Butyl (2*S*,4*R*)-*N*-Boc-4-hydroxyprolinate (1.97 g, 6.9 mmol, 1.0 eq) in DMF (20 mL) was added by a syringe and stirred for 20 minutes at 0 °C. Propargyl bromide (80% w/w in toluene, 1.1 mL, 10.3 mmol, 1.5 eq) was added dropwise 0 °C and the reaction was allowed to warm up to room temperature overnight. The reaction was quenched with H<sub>2</sub>O (10 mL) and the aqueous phase was extracted with CH<sub>2</sub>Cl<sub>2</sub> (3x 50 mL). The organic extracts were

dried with MgSO<sub>4</sub>, filtered, concentrated and dried under vacuum to give a viscous oil. The oil was purified by column chromatography (silica gel, 4:1 hexanes/EtOAc) to give the title compound as a viscous oil (72% yield): <sup>1</sup>H NMR (300 MHz, CDCl<sub>3</sub>): δ 4.15 (m, 4H), 3.56 (m, 2H), 2.42 (m, 1H), 2.24 (m, 1H), 2.03 (m, 1H) 1.41 (d, 18H). <sup>13</sup>C NMR (75 MHz, CDCl<sub>3</sub>): δ 172.8, 154.0, 100.3, 81.2, 80.1, 79.4, 75.7, 74.9, 58.6, 56.5, 51.1, 36.6, 28.4, 28.1.

**Protected AO-Proline Resin.** *t*-Butyl (2*S*,4*R*)-*N*-Boc-4-propargyloxyprolinate (434 mg, 1.33 mmol, 1.1 eq) and CuI (50 mg, 0.26 mmol, 0.2 eq) were suspended in anhydrous THF (20 mL). AO-N<sub>3</sub> (1.18 g, 1.0 mmol N<sub>3</sub>/g resin, 1.18 mmol, 1.0 eq) was added to the solution and placed under a N<sub>2</sub> atmosphere. The suspension was shaken for 3 days. The resin was washed with CH<sub>2</sub>Cl<sub>2</sub> (3x 10 mL).

**AO-Proline.** Protected AO-proline (taken directly from the previous step) was suspended in CH<sub>2</sub>Cl<sub>2</sub> (20 mL), TFA (3.0 mL) was added, and the reaction was allowed to stir overnight at room temperature. The resin was washed with CH<sub>2</sub>Cl<sub>2</sub> (2x 10 mL), MeOH (2x 10 mL), 10% TEA in THF (2x 10 mL), 1 M HCl (3x 10 mL), 10% TEA in THF (3x 10 mL), MeOH (2x 10 mL), and Et<sub>2</sub>O (2x 10 mL), and dried under vacuum to yield the off-white AO-proline resin (1.30 g, 0.57 mmol proline/g resin). The loading was calculated by mass difference.

**Channel Packing:** A 60 cm section of tubing (Swagelok PFA Tubing, 1/8" outer diameter) was attached to a Swagelok PFA union packed with glass wool. A separate union (not packed with glass wool) was attached to the inlet side of the 60 cm column. Two 10 cm sections of tubing were attached to the channel, serving as the outlet. A

1/16" female Luer was attached to the inlet. Functionalized resin was suspended in CH<sub>2</sub>Cl<sub>2</sub> and the column slurry packed using a syringe.

**1-(2-(dimethylamino)ethyl)-3-phenylurea (2).** Phenyl isocyanate (1.08 mL, 10 mmol, 1 eq) was added dropwise to a solution of *N,N*-dimethylethylenediamine (1.1 mL, 10 mmol, 1 eq) in CHCl<sub>3</sub> (10 mL) at room temperature and the reaction was stirred for 30 min. The solvent was removed *in vacuo* and the product was recrystallized from EtOAc to afford white crystals (1.8 g, 87%). <sup>1</sup>H NMR (300 Hz, CDCl<sub>3</sub>) δ 7.35 (d, 2H), 7.22 (t, 2H), 6.97 (t, 1H), 6.36 (t, 1H), 3.30 (q, 2H), 2.42 (t, 2H), 2.12 (s, 3H); <sup>13</sup>C NMR (75 Hz, CDCl<sub>3</sub>) δ 157.8, 139.9, 129.2, 122.7, 120.0, 60.1, 45.5, 38.7.

**General Procedure for Aminoxylation of Aldehydes.** Nitrosobenzene (214 mg, 2.0 mmol, 1.0 eq), (L)-proline (11.6 mg, 0.1 mmol, 0.05 eq) and 1-(2-(dimethylamino)ethyl)-3-phenylurea (20.8 mg, 0.1 mmol, 0.05 eq) were added to a 7 mL screw cap vial equipped with a stir bar. Ethyl acetate (4 mL) was added to the vial, upon which the reaction mixture turned green. The reaction mixture was submerged in an ice bath and stirred for 15 minutes. The appropriate aldehyde (6.0 mmol, 3.0 eq) was added to the reaction mixture in one portion at 0 °C. The reaction mixture was continuously stirred at 0 °C until the reaction color changed from green to yellow and was complete by GC.

The reaction was transferred to a suspension of sodium borohydride (300 mg, 8.0 mmol, 4.0 eq) in ethanol (10 mL) at 0 °C. An additional 5 mL of ethanol was used to rinse the reaction vessel and added to the sodium borohydride suspension. After 20 minutes, the reaction mixture was poured into a separatory funnel containing 25 mL saturated aqueous NaHCO<sub>3</sub> and the aqueous phase extracted with CH<sub>2</sub>Cl<sub>2</sub> (3 x 20 mL).

The combined organic extracts were dried with MgSO<sub>4</sub>, filtered, concentrated *in vacuo*, and dried under vacuum to remove any residual starting materials. The resulting residue was purified using column chromatography to afford the desired compounds. Enantioselectivities were determined using chiral HPLC analysis.

**(R)-2-(N-Phenyl-aminoxy)-propan-1-ol.** Prepared according to the general procedure using propionaldehyde (437  $\mu$ L, 6.0 mmol, 3.0 eq) for 3 hours to afford the title compound as a yellow oil (300 mg, 90 % yield, 98 % ee) after column chromatography (silica gel, 4:1 hexanes/EtOAc, R<sub>f</sub> = 0.09). The enantiomeric ratio was determined by HPLC using a CHIRALPAK IA and IA guard column (5 % IPA/hexanes, 1 mL/min); (*S*) isomer t<sub>r</sub> = 20.2 min and (*R*) isomer t<sub>r</sub> = 22.0 min. <sup>1</sup>H NMR (300 Hz, CDCl<sub>3</sub>)  $\delta$  7.28 (m, 2H), 7.00 (m, 3H), 4.13 (m, 1H), 3.76 (m, 2H), 1.26 (d, 3H); <sup>13</sup>C NMR (75 Hz, CDCl<sub>3</sub>)  $\delta$  148.8, 131.1, 129.1, 122.1, 80.2, 65.8, 15.5.

**(R)-2-(N-Phenyl-aminoxy)-hexan-1-ol.** Prepared according to the general procedure using hexanal (750  $\mu$ L, 6.0 mmol, 3.0 eq) for 2 hours to afford the title compound as a yellow oil (400 mg, 96 % yield, 99 % ee) after column chromatography (silica gel, 4:1 hexanes/EtOAc, R<sub>f</sub> = 0.18). The enantiomeric ratio was determined by HPLC using a CHIRALPAK IA and IA guard column (5 % IPA/hexanes, 1 mL/min); (*S*) isomer t<sub>r</sub> = 15.0 min and (*R*) isomer t<sub>r</sub> = 17.6 min. <sup>1</sup>H NMR (300 Hz, CDCl<sub>3</sub>)  $\delta$  7.28 (m, 2H), 6.99 (m, 2H), 3.95 (m, 1H), 3.81 (m, 2H), 2.50 (bs, 1H), 1.68 (m, 1H), 1.40 (m, 6H), 0.93 (t, 3H); <sup>13</sup>C NMR (75 Hz, CDCl<sub>3</sub>)  $\delta$  148.7, 129.0, 122.1, 114.6, 84.0, 64.7, 29.7, 28.0, 22.9, 14.0.

**(R)-2-(N-Phenyl-aminoxy)-octan-1-ol.** Prepared according to the general procedure using octanal (940  $\mu$ L, 6.0 mmol, 3.0 eq) for 5 hours to afford the title compound as a

yellow oil (400 mg, 84 % yield, 99 % ee,  $R_f$  = 0.14) after column chromatography (silica gel, 4:1 hexanes/EtOAc). The enantiomeric ratio was determined by HPLC using a CHIRALPAK IA and IA guard column (5 % IPA/hexanes, 1 mL/min); (*S*) isomer  $t_r$  = 13.9 min and (*R*) isomer  $t_r$  = 16.0 min.  $^1\text{H}$  NMR (300 Hz,  $\text{CDCl}_3$ )  $\delta$  7.28 (m, 2H), 7.00 (m, 4H), 3.95 (m, 1H), 3.78 (m, 2H), 2.62 (bs, 1H), 1.48 (m, 10H), 0.91 (t, 3H);  $^{13}\text{C}$  NMR (75 Hz,  $\text{CDCl}_3$ )  $\delta$  148.7, 129.0, 122.2, 114.8, 84.1, 64.8, 31.8, 30.1, 29.3, 25.9, 22.7, 14.2.

**(*R*)-2-(*N*-Phenyl-aminooxy)-pent-4-en-1-ol.** Prepared according to the general procedure using 4-pentenal (621  $\mu\text{L}$ , 6.0 mmol, 3.0 eq) for 2.5 hours to afford the title compound as a yellow oil (290 mg, 75 % yield, 99 % ee) after column chromatography (silica gel, 4:1 hexanes/EtOAc,  $R_f$  = 0.14). The enantiomeric ratio was determined by HPLC using a CHIRALPAK IA and IA guard column (5 % IPA/hexanes, 1 mL/min); (*S*) isomer  $t_r$  = 20.2 min and (*R*) isomer  $t_r$  = 23.1 min.  $^1\text{H}$  NMR (300 Hz,  $\text{CDCl}_3$ )  $\delta$  7.28 (m, 2H), 7.05 (s, 1H), 7.00 (m, 3H), 5.89 (m, 1H), 5.14 (dt, 2H), 4.04 (m, 1H), 3.89 (m, 2H), 2.94 (m, 1H), 2.38 (m, 2H);  $^{13}\text{C}$  NMR (75 Hz,  $\text{CDCl}_3$ )  $\delta$  148.6, 134.2, 129.2, 122.6, 117.9, 114.9, 83.5, 64.6, 34.8.

**(*R*)-3-methyl-2-(*N*-Phenyl-aminooxy)-butan-1-ol.** Prepared according to the general procedure using isovaleraldehyde (650  $\mu\text{L}$ , 6.0 mmol, 3.0 eq) for 3.5 hours to afford the title compound as a yellow oil (380 mg, 97 % yield, 99 % ee,  $R_f$  = 0.18) after column chromatography (silica gel, 4:1 hexanes/EtOAc). The enantiomeric ratio was determined by HPLC using a CHIRALPAK IA and IA guard column (5 % IPA/hexanes, 1 mL/min); (*S*) isomer  $t_r$  = 13.4 min and (*R*) isomer  $t_r$  = 15.4 min.  $^1\text{H}$  NMR (300 Hz,  $\text{CDCl}_3$ )  $\delta$  7.28 (m, 2H), 7.03 (bs, 1H), 7.01 (m, 3H), 3.88 (m, 2H), 3.75 (m, 1H), 2.84 (bs, 1H), 2.04 (m, 1H), 1.04 (dd, 6H);  $^{13}\text{C}$  NMR (75 Hz,  $\text{CDCl}_3$ )  $\delta$

148.6, 129.1, 122.5, 115.1, 88.7, 63.4, 28.8, 18.9, 18.7.

**(R)-3-phenyl-2-(N-Phenyl-aminoxy)-propan-1-ol.** Prepared according to the general procedure using phenylpropionaldehyde (793  $\mu\text{L}$ , 6.0 mmol, 3.0 eq) for 3.5 hours to afford the title compound as a yellow oil (410 mg, 84 % yield, >99 % ee) after column chromatography (silica gel, 4:1 hexanes/EtOAc,  $R_f$  = 0.09). The enantiomeric ratio was determined by HPLC using a CHIRALPAK IA and IA guard column (5 % IPA/hexanes, 1 mL/min); (*S*) isomer  $t_r$  = 25.8 min and (*R*) isomer  $t_r$  = 31.2 min.  $^1\text{H}$  NMR (300 Hz,  $\text{CDCl}_3$ )  $\delta$  7.18 (m, 7H), 6.97 (bs, 1H), 6.86 (t, 1H), 6.78 (d, 2H), 4.08 (m 1H), 3.78 (m, 1H), 3.66 (m, 1H), 3.02 (dd, 1H), 2.80 (dd, 1H), 2.38 (bs, 1H);  $^{13}\text{C}$  NMR (75 Hz,  $\text{CDCl}_3$ )  $\delta$  148.5, 138.0, 129.6, 129.1, 128.6, 126.6, 122.3, 114.7, 85.2, 64.0, 36.6.

**(R)-2-phenyl-2-(N-Phenyl-aminoxy)-ethan-1-ol.** Prepared according to the general procedure using phenylacetaldehyde (766  $\mu\text{L}$ , 6.0 mmol, 3.0 eq) for 2 hours to afford the title compound as a yellow oil (250 mg, 55 % yield, 99 % ee) after column chromatography (silica gel, 4:1 hexanes/EtOAc,  $R_f$  = 0.20). The enantiomeric ratio was determined by HPLC using a CHIRALPAK IA and IA guard column (5 % IPA/hexanes, 1 mL/min); (*S*) isomer  $t_r$  = 25.9 min and (*R*) isomer  $t_r$  = 28.9 min.  $^1\text{H}$  NMR (300 Hz,  $\text{CDCl}_3$ )  $\delta$  7.30 (m, 7H), 7.00 (m, 4H), 5.03 (dd, 1H), 3.98 (m, 1H), 3.86 (m, 1H), 2.58 (bs, 1H);  $^{13}\text{C}$  NMR (75 Hz,  $\text{CDCl}_3$ )  $\delta$  148.1, 138.0, 129.1, 128.7, 128.6, 127.2, 122.5, 115.0, 86.6, 66.1.

**Representative Flow  $\alpha$ -Aminoxylation Experiment.** PhNO (0.2 M) and mesitylene (0.02 M) in chloroform was placed in a syringe and placed on a syringe pump set to 50  $\mu\text{L min}^{-1}$  (10  $\mu\text{mol PhNO min}^{-1}$ , 1.0 eq  $\text{min}^{-1}$ ). Hexanal (0.6 M) and urea **2** (0.02 M)

in chloroform was placed in a syringe and placed on a syringe pump set to  $50 \mu\text{L min}^{-1}$  ( $30 \mu\text{mol hexanal min}^{-1}$ ,  $3.0 \text{ eq min}^{-1}$ ,  $1.0 \mu\text{mol urea } 2 \text{ min}^{-1}$ ,  $0.1 \text{ eq min}^{-1}$ ). The phases combined at a Y-junction and passed through a 60 cm channel packed with AO-proline (~400 mg) submerged in an ice bath. The reaction mixture was collected in a 20 mL screw cap vial submerged in an ice bath containing ethanolic  $\text{NaBH}_4$ . After the reaction collection was complete, the reaction was quenched with sat.  $\text{NaHCO}_3$ , and the aqueous phase extracted with  $\text{CH}_2\text{Cl}_2$  (2x 10 mL). Organic extracts were dried over  $\text{MgSO}_4$ , concentrated and analyzed by HPLC. The enantiomeric ratio was determined by HPLC using a CHIRALPAK IA and IA guard column (5 % IPA/hexanes, 1 mL/min); (*S*) isomer  $t_r = 15.0 \text{ min}$  and (*R*) isomer  $t_r = 17.6 \text{ min}$ .

**(*S*)-2,2,3-triphenyloxirane.** Triphenylethylene (1.02 g, 4.0 mmol, 1.0 eq), (*R,R*)-Jacobsen catalyst (130.1 mg, 0.2 mmol, 0.05 eq), and 4-PPNO (150 mg, 0.88 mmol, 0.22 eq) were stirred in  $\text{CH}_2\text{Cl}_2$  (20 mL) at room temperature.  $\text{NaOCl}$  (11 mL, 8.14 mmol, 2.04 eq, adjusted to pH 11.3 using  $\text{NaHCO}_3$ ) was added dropwise and the reaction was stirred overnight. The reaction was filtered through Celite and the layers were separated. The organic phase was washed with  $\text{H}_2\text{O}$  (2x 25 mL), dried over  $\text{MgSO}_4$ , filtered and concentrated. The residue was purified by column chromatography (silica gel, 9:1 hexanes/EtOAc) to give the title compound as a white solid (84% yield, 88% ee). Recrystallization with hexanes improved the ee to >99%. Enantiomeric excess determined using NMR with  $\text{Eh}(\text{hfc})_3$  as a chiral shift reagent.  $^1\text{H}$  NMR (300 MHz,  $\text{CDCl}_3$ ) 7.05-7.36 (m, 15H), 4.33 (s, 1H).  $^{13}\text{C}$  NMR (75 Hz,  $\text{CDCl}_3$ )  $\delta$  141.3, 135.82, 135.79, 129.6, 128.8, 128.23, 128.18, 128.09, 128.03, 127.95, 127.13, 126.7, 69.0, 68.4

**(R)-2-(1-piperazinyl)-1,1,2-triphenylethanol.** (*S*)-2,2,3-triphenyloxirane (206.4 mg, 0.76 mmol, 1.0 eq), piperazine (2.0 g, 23.2 mmol, 30.6 eq) and LiClO<sub>4</sub> (220.5 mg, 2.1 mmol, 2.7 eq) were heated to 140 °C for 5 hours. The reaction was cooled to room temperature and H<sub>2</sub>O (15 mL) and CH<sub>2</sub>Cl<sub>2</sub> (15 mL) were added to dissolve the residue. The phases were separated and the organic phase was washed repeatedly with H<sub>2</sub>O (8x 10 mL). The organic phase was extracted with 1 M HCl (30 mL), and the aqueous phase was with CH<sub>2</sub>Cl<sub>2</sub> (2x 20 mL) to remove an unknown impurity. The aqueous phase was the basified with 10 M NaOH and the aqueous layer extracted with CH<sub>2</sub>Cl<sub>2</sub> (5x 10 mL). The organic extracts were washed with water (10 mL), dried over MgSO<sub>4</sub>, filtered, concentrated, and dried under vacuum to yield a the title compound as a white solid (92% yield): <sup>1</sup>H NMR (300 MHz, CDCl<sub>3</sub>) 7.70 (d, 2H), 6.98-7.31 (m, 13H), 5.58 (bs, 1H), 4.56 (s, 1H), 2.71 (m, 4H), 2.39 (m, 2H), 2.06 (m, 2H).

**(R)-2-(4-(hex-5-yn-1-yl)-piperazin-1-yl)-1,1,2-triphenylethanol (3).** (*R*)-2-(1-piperazinyl)-1,1,2-triphenylethanol (503 mg, 1.4 mmol, 1.0 eq), 6-chloro-1-hexyne (200 μL, 1.65 mmol, 1.2 eq) and cesium carbonate (1.4 g, 4.3 mmol, 3.1 eq) were stirred in acetonitrile (40 mL) at 70 °C for 3 days. The reaction was concentrated and the residue was dissolved in equal volumes of H<sub>2</sub>O and CH<sub>2</sub>Cl<sub>2</sub>. The aqueous phase was extracted with CH<sub>2</sub>Cl<sub>2</sub> (2x 20 mL), and the organic extracts were dried over MgSO<sub>4</sub>, filtered concentrated, and dried under vacuum. The residue was purified by column chromatography (silica gel, 1:1 hexanes/EtOAc) to give the title compound as a white solid (44% yield). <sup>1</sup>H NMR (300 MHz, CDCl<sub>3</sub>) 7.68 (d, 2H), 6.98-7.31 (m, 13H), 6.2 (bs, 1H), 4.58 (s, 1H), 2.14-2.45 (m, 12H), 1.90 (t, 1H), 1.47 (m, 4H).

**AO-PTPE.** (*R*)-2-(4-(hex-5-yn-1-yl)-piperazin-1-yl)-1,1,2-triphenylethanol (104.4 mg, 0.24 mmol, 1.2 eq) and CuI (5.0 mg, 0.026 mmol, 0.13 eq) were suspended in

anhydrous THF (20 mL). AO-N<sub>3</sub> (200.6 mg, 1.0 mmol N<sub>3</sub>/g resin, 0.20 mmol, 1.0 eq) was added to the solution and placed under a N<sub>2</sub> atmosphere. The suspension was shaken for 3 days. The resin was washed with THF (3x 10 mL), H<sub>2</sub>O (2x 10 mL), 1 M HCl (3x 10 mL), H<sub>2</sub>O (1x 10 mL), sat. NaHCO<sub>3</sub> (3x 10 mL), H<sub>2</sub>O (2x 10 mL), MeOH (2x 10 mL), Et<sub>2</sub>O (2x 10 mL), and dried under vacuum to yield the white AO-PTPE resin (225.9 mg, 0.26 mmol PTPE/g resin). The loading was calculated by mass difference.

## REFERENCE

1. Mason, B. P.; Price, K. E.; Steinbacher, J. L.; Bogdan, A. R.; McQuade, D. T. *Chem. Rev.* **2007**, *107*, 2300.
2. Hessel, V.; Lob, P.; Lowe, H. *Curr. Org. Chem.* **2005**, *9*, 765.
3. Hessel, V.; Lowe, H. *Chem. Eng. Technol.* **2005**, *28*, 267.
4. Hodge, P. *Curr. Opin. Chem. Biol.* **2003**, *7*, 362.
5. Jas, G.; Kirschning, A. *Chem. Eur. J.* **2003**, *9*, 5708.
6. Kirschning, A.; Monenschein, H.; Wittenberg, R. *Angew. Chem. Int. Ed.* **2001**, *40*, 650.
7. Pennemann, H.; Watts, P.; Haswell, S. J.; Hessel, V.; Lowe, H. *Org. Process Res. Dev.* **2004**, *8*, 422.
8. Haswell, S. J.; Watts, P. *Green Chem.* **2003**, *5*, 240.
9. *Microreactors in Organic Synthesis and Catalysis*: Wirth, T., Ed. Wiley-VCH: Weinheim, 2008.
10. Yoshida, J.; Nagaki, A.; Yamada, T. *Chem. Eur. J.* **2008**, *14*, 7450.
11. Watts, P.; Wiles, C. *Org. Biomol. Chem.* **2007**, *5*, 727.
12. Ahmed-Omer, B.; Brandt, J. C.; Wirth, T. *Org. Biomol. Chem.* **2007**, *5*, 733.
13. Baxendale, I. R.; Deeley, J.; Griffiths-Jones, C. M.; Ley, S. V.; Saaby, S.; Tranmer, G. K. *Chem. Commun.* **2006**, 2566.
14. Baxendale, I. R.; Ley, S. V.; Mansfield, A. C.; Smith, C. D. *Angew. Chem. Int. Ed.* **2009**, *48*, 4017.
15. Sahoo, H. G.; Kralj, J. G.; Jensen, K. F. *Angew. Chem. Int. Ed.* **2007**, *46*, 5704.
16. Grant, D.; Dahl, R.; Cosford, N. D. P. *J. Org. Chem.* **2008**, *73*, 7219.
17. Denmark, S. E.; Jacobsen, E. N. *Acc. Chem. Res.* **2000**, *33*, 324.
18. Federsel, H. J. *Drug Discovery Today* **2006**, *11*, 966.

19. Rahman, M. T.; Fukuyama, T.; Kamata, N.; Sato, M.; Ryu, I. *Chem. Commun.* **2006**, 2236.
20. Murphy, E. R.; Martinelli, J. R.; Zaborenko, N.; Buchwald, S. L.; Jensen, K. F. *Angew. Chem. Int. Ed.* **2007**, *46*, 1734.
21. Leeke, G. A.; Santos, R. C. D.; Al-Duri, B.; Seville, J. P. K.; Smith, C. J.; Lee, C. K. Y.; Holmes, A. B.; McConvery, I. F. *Org. Process Res. Dev.* **2007**, *11*, 144.
22. Comer, E.; Organ, M. G. *J. Am. Chem. Soc.* **2005**, *127*, 8160.
23. Kobayashi, J.; Mori, Y.; Kobayashi, S. *Adv. Synth. Catal.* **2005**, *347*, 1889.
24. Kobayashi, J.; Mori, Y.; Kobayashi, S. *Chem. Commun.* **2005**, 2567.
25. Kobayashi, J.; Mori, Y.; Okamoto, K.; Akiyama, R.; Ueno, M.; Kitamori, T.; Kobayashi, S. *Science* **2004**, *304*, 1305.
26. Bogdan, A. R.; Mason, B. P.; Sylvester, K. T.; McQuade, D. T. *Angew. Chem. Int. Ed.* **2007**, *46*, 1698.
27. Bogdan, A. R.; McQuade, D. T. *Beilstein Journal of Organic Chemistry*, **2009**, *5*, 17.
28. Mak, X. Y.; Laurino, P.; Seeberger, P. H. *Beilstein Journal of Organic Chemistry*, **2009**, *5*, 19.
29. Pellissier, H. *Tetrahedron* **2007**, *63*, 9267.
30. Guillena, G.; Na'jera, C.; Ramo'n, D. J. *Tetrahedron: Asymmetry* **2007**, *18*, 2249.
31. List, B. *Acc. Chem. Res.* **2004**, *37*, 548.
32. List, B. *Tetrahedron* **2002**, *58*, 5573.
33. Bertelsen, S.; Nielsen, M.; Jørgensen, K. A. *Angew. Chem., Int. Ed.* **2007**, *46*, 7356.
34. Ting, A.; Schaus, S. E. *Eur. J. Org. Chem.* **2007**, 5797.
35. List, B.; Lerner, R. A.; Barbas, C. F. *J. Am. Chem. Soc.* **2000**, *122*, 2395.
36. Wang, W.; Wang, J.; Li, H.; Liao, L. *Tetrahedron Lett.* **2004**, *45*, 7235.

37. Notz, W.; Tanaka, F.; Barbas, C. F. *Acc. Chem. Res.* **2004**, *37*, 580.
38. Odedra, A.; Seeberger, P. H. *Angew. Chem. Int. Ed.* **2009**, *48*, 2699.
39. Font, D.; Jimeno, C.; Pericas, M. A. *Org. Lett.* **2006**, *8*, 4653.
40. Hayashi, Y.; Yamaguchi, J.; Sumiya, T.; Hibino, K.; Shoji, M. *J. Org. Chem.* **2004**, *69*, 5966
41. Hayashi, Y.; Yamaguchi, J.; Hibino, K.; Sumiya, T.; Urushima, T.; Shoji, M.; Hashizume, D.; Koshino, H. *Adv. Synth. Catal.* **2004**, *346*, 1435.
42. Price, K. E.; Mason, B. P.; Bogdan, A. R.; Broadwater, S. J.; Steinbacher, J. L.; McQuade, D. T. *J. Am. Chem. Soc.* **2006**, *128*, 10376.
43. Poe, S. L.; Bogdan, A. R.; Mason, B. P.; Steinbacher, J. L.; Opalka, S. M.; McQuade, D. T. *J. Org. Chem.* **2009**, *74*, 1574.
44. Pericas, M. A.; Castellnou, D.; Rodriguez, I.; Riera, A.; Sola, L. *Adv. Synth. Catal.* **2003**, *345*, 1305.
45. Castellnou, D.; Sola, L.; Jimeno, C.; Fraile, J. M.; Mayoral, J. A.; Riera, A.; Pericas, M. A. *J. Org. Chem.* **2005**, *70*, 433.
46. Bastero, A.; Font, D.; Pericas, M. A. *J. Org. Chem.* **2007**, *72*, 2460.
47. Pericas, M. A.; Herrerias, C. I.; Sola, L. *Adv. Synth. Catal.* **2008**, *350*, 927.
48. Poe, S.L.; Kobašlija, M.; McQuade, D. T. *J. Am. Chem. Soc.* **2006**, *128*, 15586.
49. Poe, S.L.; Kobašlija, M.; McQuade, D. T. *J. Am. Chem. Soc.* **2007**, *129*, 9216.
50. Sheldon, R. A.; Arends, I.; Hanefeld, U. *Green Chemistry and Catalysis*. Wiley-VCH: Weinheim, 2007.

## APPENDIX 1

### Supporting Information for Chapter 2

**Residence Time Determination.** Three columns (10 cm, 30 cm, and 60 cm) were packed with AO resin. A dye solution was prepared by dissolving 15 mg of Disperse Red 1 in 20 mL  $\text{CH}_2\text{Cl}_2$ . A 5 mL syringe was filled with the dye and passed through the channel. Using a flow rate of 2.0 mL/min, the residence time was determined for all three packed columns. The residence time was measured from initial appearance of the dye on the column to the appearance of a pink hue at the outlet of the channel. This was repeated in triplicate for all three column lengths and residence time increased linearly with channel length. Between trials, the channel was rinsed with 3 mL of methylene chloride.

**Table A1.1.** Residence time as a function of column length.

Column Length (cm)	Average Residence Time (sec)	St. Dev.
60	13.82	0.33
30	5.90	0.35
10	1.75	0.13

A second set of experiments was conducted to determine the relationship between the flow rate and residence time. A 30 cm column was packed with 137 mg of AO. The residence times were measured using the above procedure.

**Table A1.2.** Residence time as a function of flow rate.

<b>Flow Rate (mL/min)</b>	<b>Average Residence Time (sec)</b>	<b>St. Dev.</b>
3.90	2.60	0.05
2.00	5.05	0.45
1.00	11.20	0.68
0.40	30.56	0.99
0.20	68.20	1.73
0.10	141.70	2.83

The data from Table A1.2 was used to devise an equation relating residence times to column length and flow rate (Equation A1.1).

$$\text{Residence Time} = \frac{\text{Column length}}{30} \times 22811x^{-1.1} \quad (\text{Equation A1.1})$$

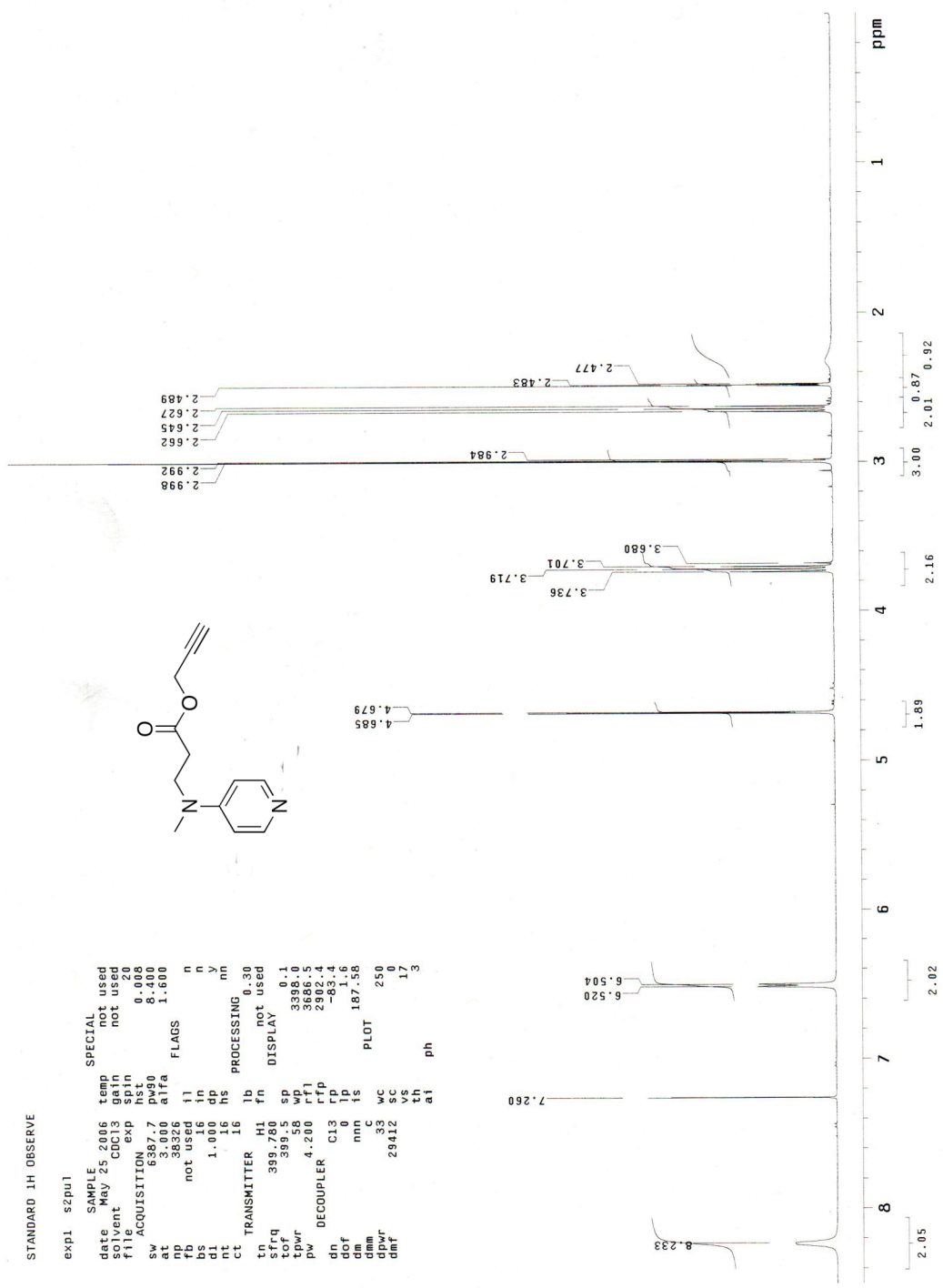
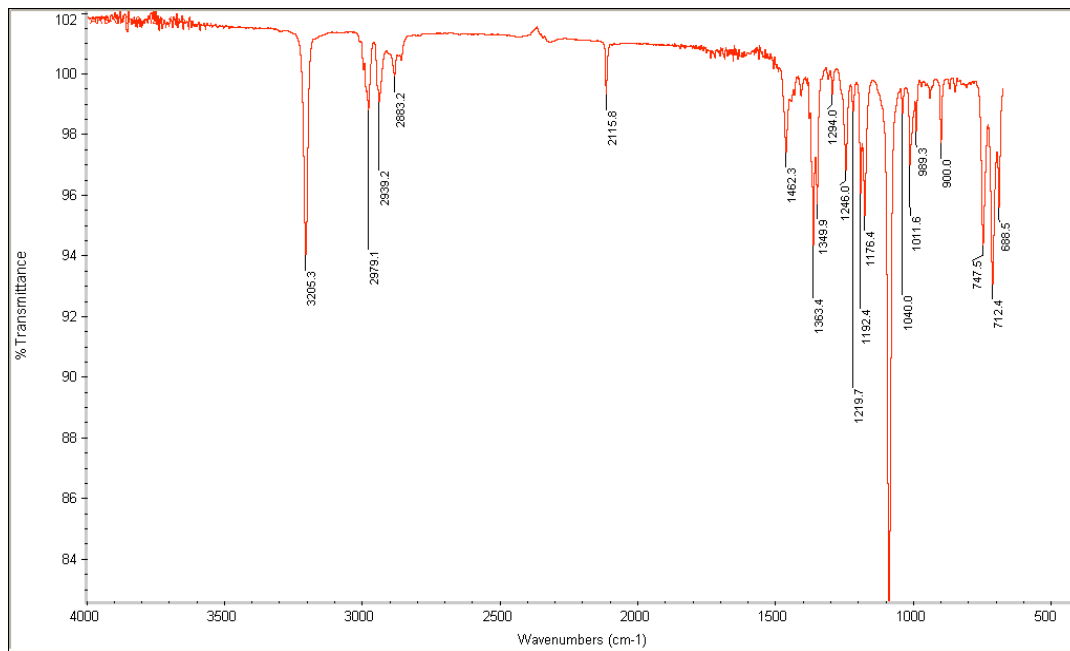


Figure A1.1. <sup>1</sup>H NMR spectrum of acetylene-modified DMAP.

## APPENDIX 2

### Supporting Information for Chapter 3

For data relating to residence time determination, see Appendix 1 and Equation A1.1.



**Figure A2.1.** AT-IR spectrum of acetylene-modified TEMPO.

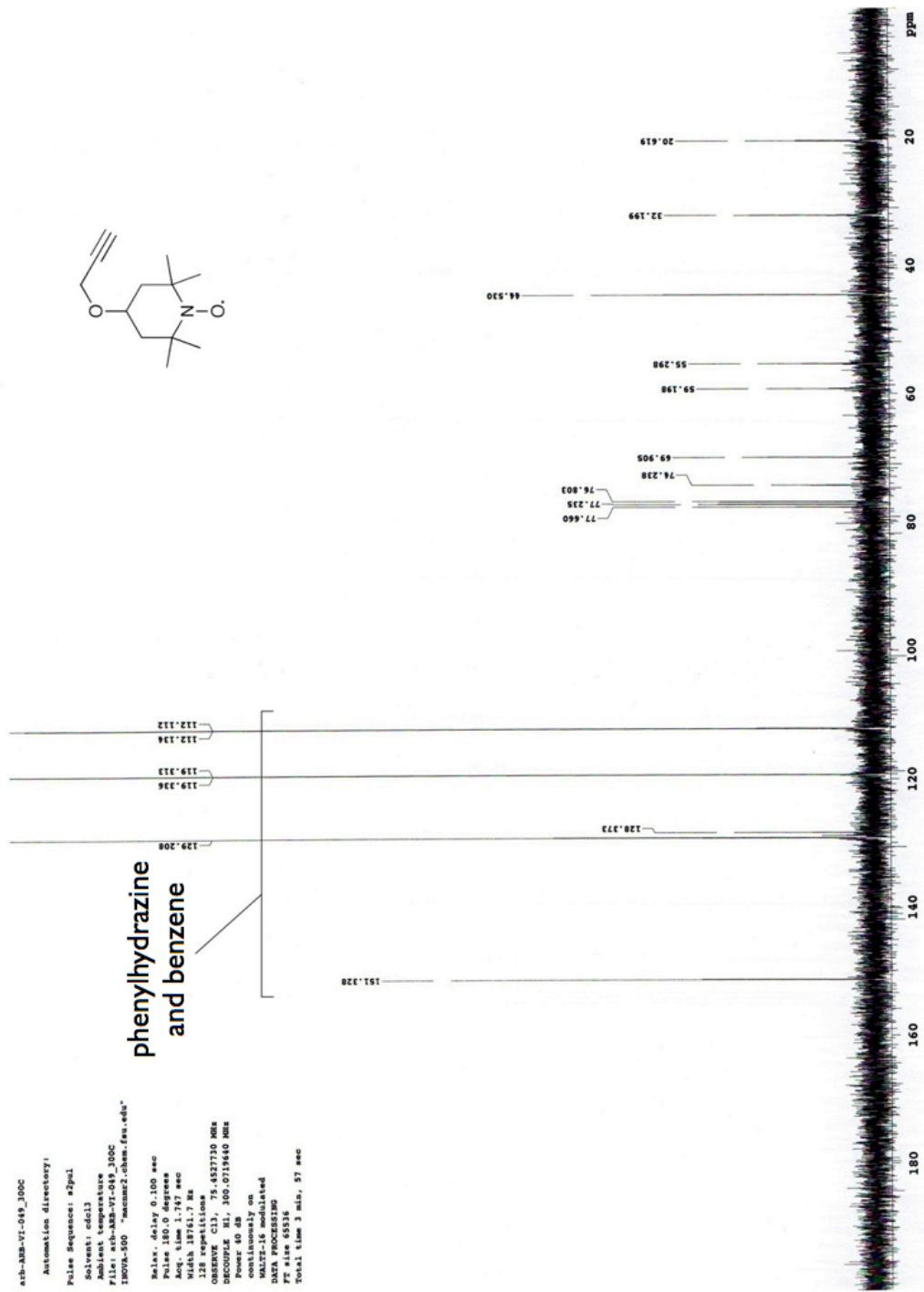
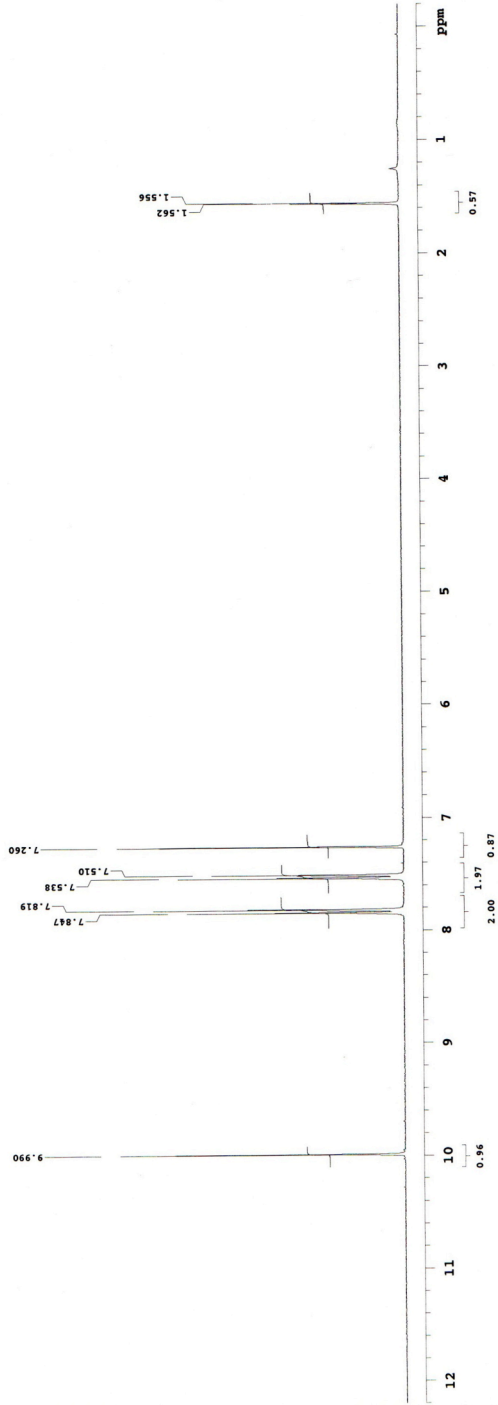
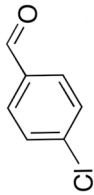


Figure A2.2. <sup>13</sup>C NMR spectrum of acetylene-modified TEMPO.

ANS-VZ-212\_100H  
 Automation directory:  
 Pulse Sequence: #2pul  
 Solvent: cdcl3  
 Ambient temperature: 300K  
 Acquisition time: 0.00000000  
 INOVA-500 "macms2.chem.fsu.edu"  
 Relax. delay: 1.000 sec  
 Pulse: 22.5 degrees  
 Acq. time: 1.666 sec  
 Width: 6909.2 Hz  
 Spectrometer: spect  
 CHANNELS: 1  
 CHANNEL F1: 300.0704275 MHz  
 DATA PROCESSING  
 FT size: 16384  
 Total time: 0 min, 42 sec

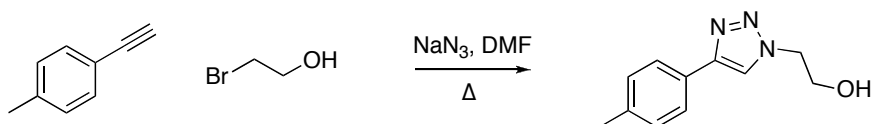


**Figure A2.3.**  $^1\text{H}$  NMR spectrum of 4-chlorobenzaldehyde from AO-TEMPO flow oxidation of 4-chlorobenzyl alcohol.

## APPENDIX 3

### Supporting Information for Chapter 4

#### Design of Experiments (DOE) Data.



**Scheme A3.1.** Model reaction for DOE.

**Table A3.1.** Conditions screened in DOE.

Variable	Low	High
Temperature	100 °C	175 °C
Residence Time	5 minutes	15 minutes
Equivalents 4-ethynyltoluene	0.5	1.0

\*four center points

**Table A3.2.** Results of DOE.

<b>Equivalents 4-ethynyltoluene</b>	<b>Residence Time (min)</b>	<b>Temp (°C)</b>	<b>HPLC Area Percent Product</b>
0.75	5	100	4.8
0.5	5	137.5	32.6
1.0	5	137.5	9.2
0.75	5	175	65.6
0.5	10	100	9.8
1.0	10	100	4.1
0.75	10	137.5	44.7
0.75	10	137.5	58.4
0.75	10	137.5	40.3
0.75	10	137.5	40.3
0.5	10	175	86.2
1	10	175	72.5
0.75	15	100	15.4
0.5	15	137.5	40.1
1	15	137.5	-
0.75	15	175	-

## APPENDIX 4

### Supporting Information for Chapter 6



Friedel-Crafts  
150 °C, 5 min

1,2-migration  
50 °C, 2 min

Saponification  
65 °C, 3 min

**Figure A4.1.** The three-step flow reaction setup.

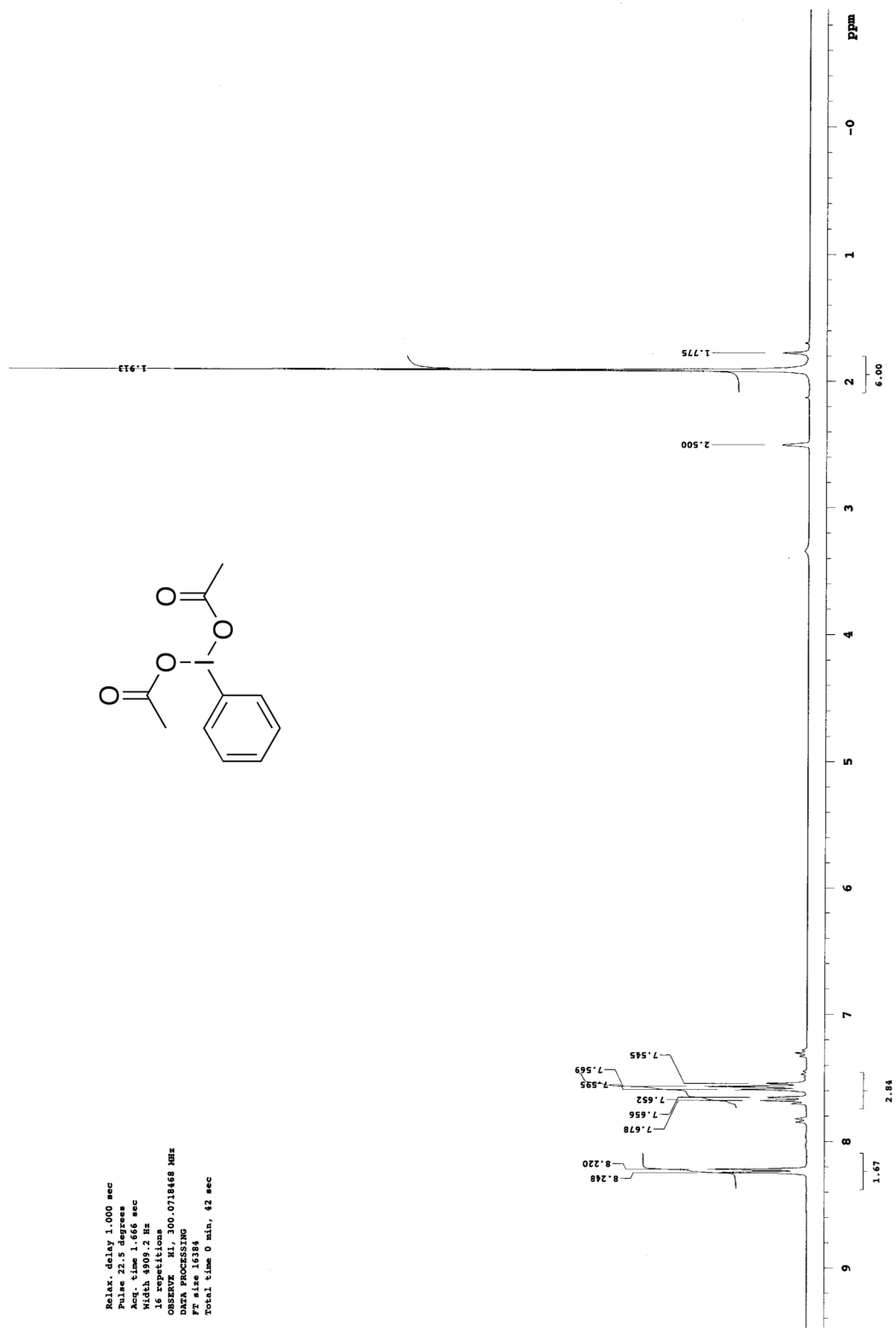


Figure A4.2. <sup>1</sup>H NMR spectrum of PhI(OAc)<sub>2</sub>.

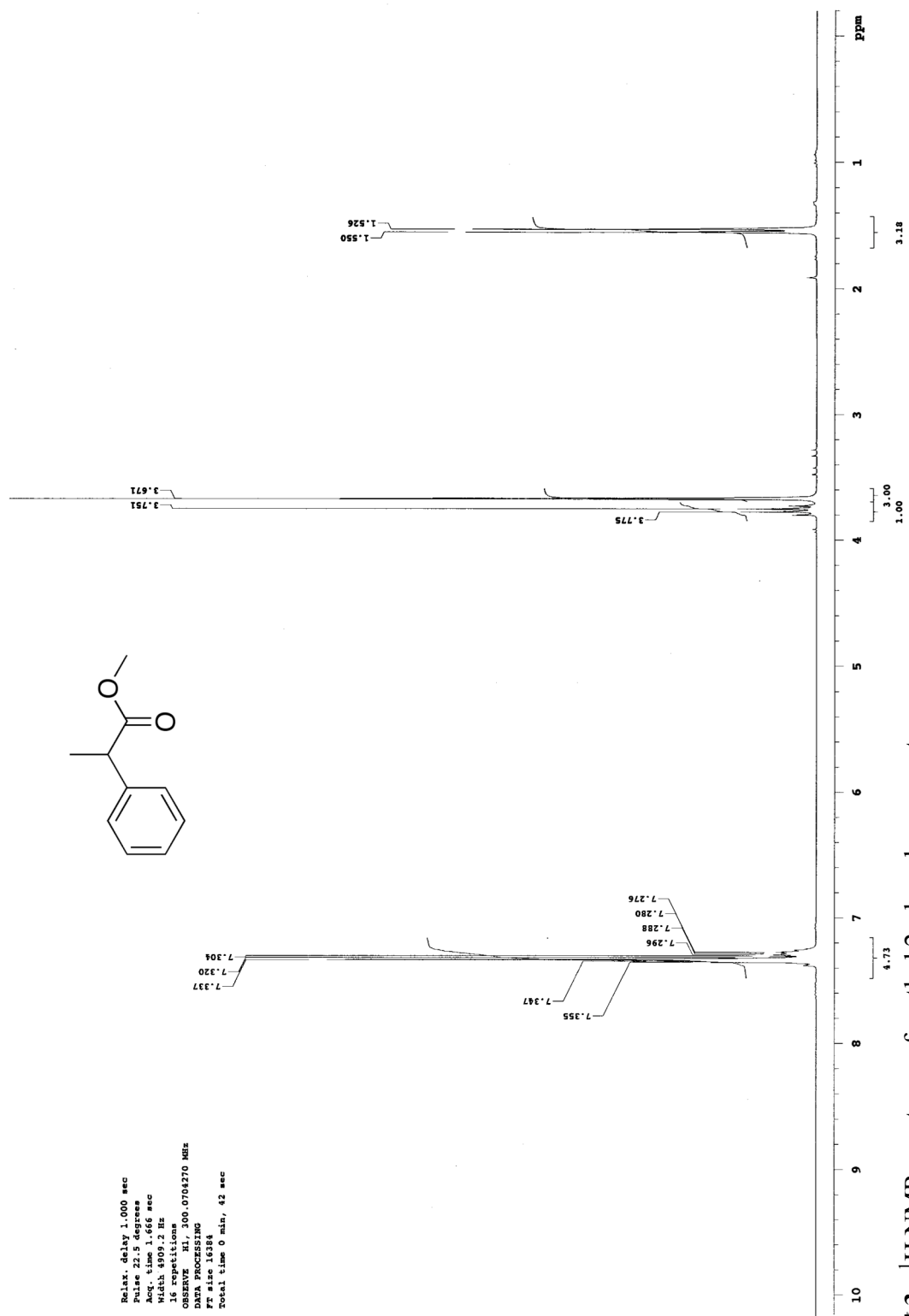


Figure A4.3. <sup>1</sup>H NMR spectrum of methyl 2-phenylpropanoate.

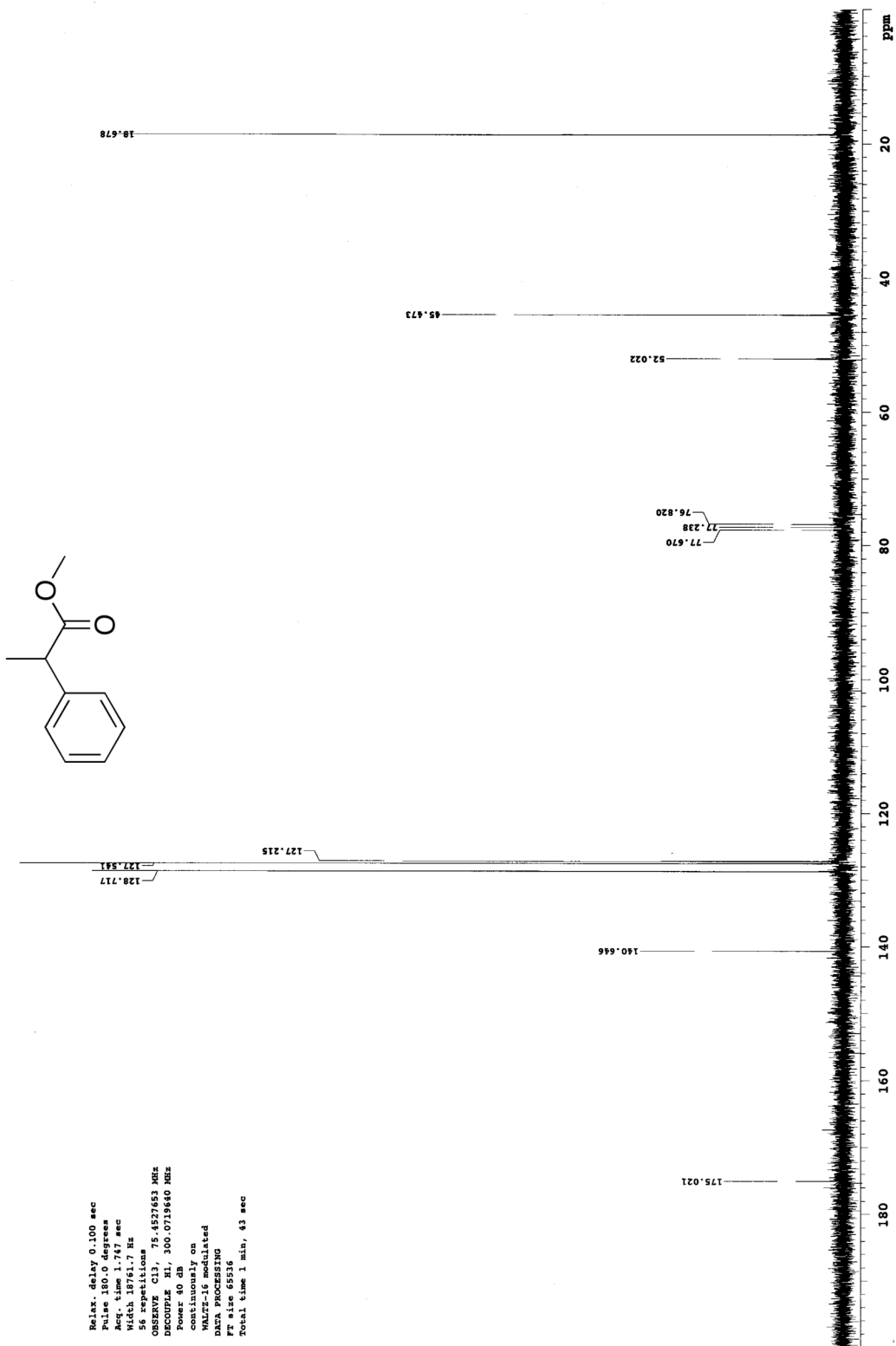
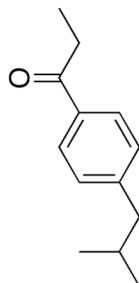


Figure A4.4. <sup>13</sup>C NMR spectrum of methyl 2-phenylpropanoate.



Relax. delay 1.000 sec  
 Pulse 22.5 degrees  
 Width 4.00 sec  
 Mith 4905.2 Hz  
 16 repetitions  
 OBSERVE H1, 300.07042715 MHz  
 DATA PROCESSING  
 FT size 16384  
 Total time 0 min, 42 sec



Figure A4.5. <sup>1</sup>H NMR spectrum of 4-isobutylpropiophenone.

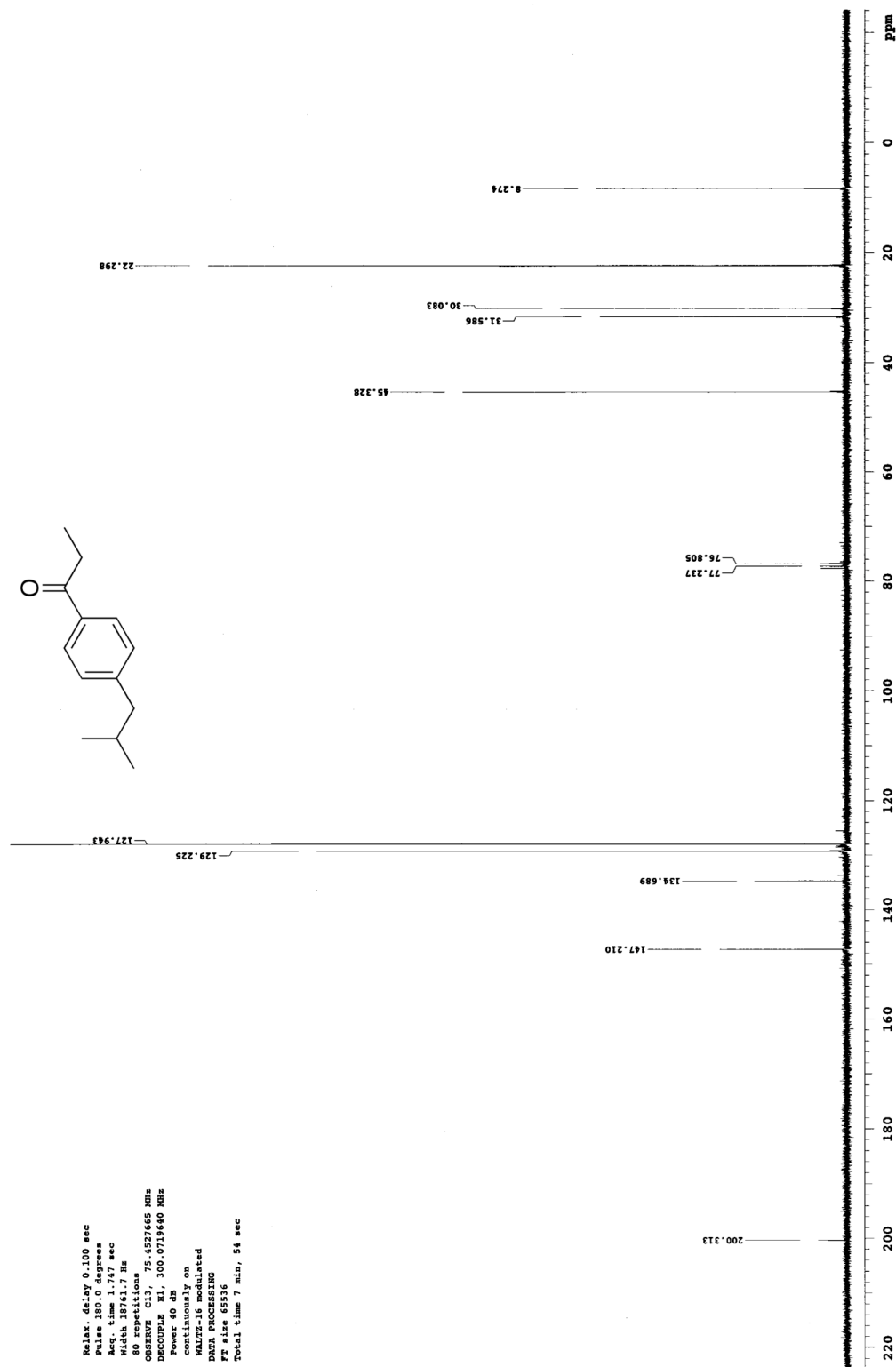


Figure A4.6. <sup>13</sup>C NMR spectrum of 4-isobutylpropiophenone.



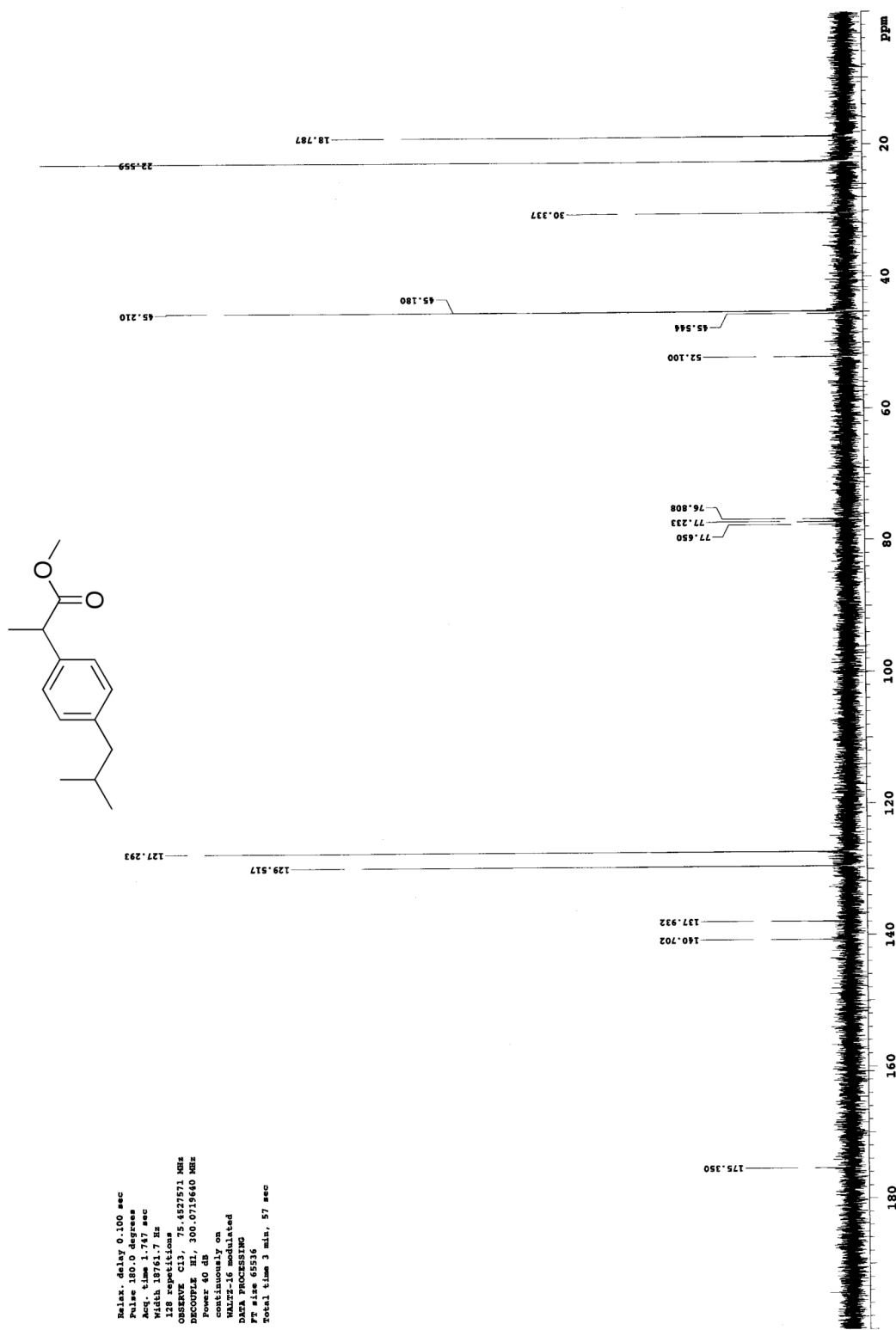


Figure A4.8. <sup>13</sup>C NMR spectrum of methyl 2-(4-isobutylphenyl)propanoate.

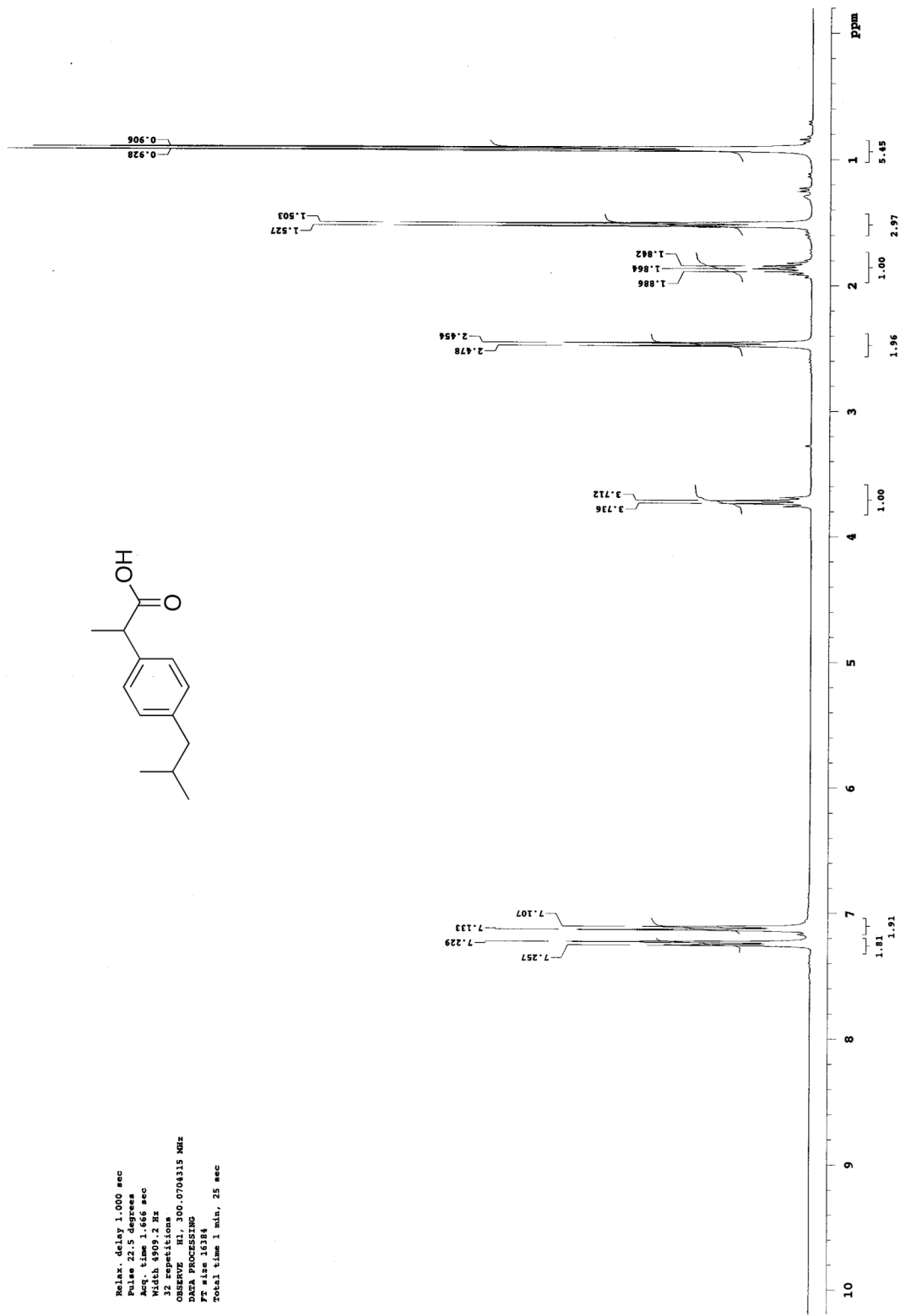


Figure A4.9. <sup>1</sup>H NMR spectrum of ibuprofen.

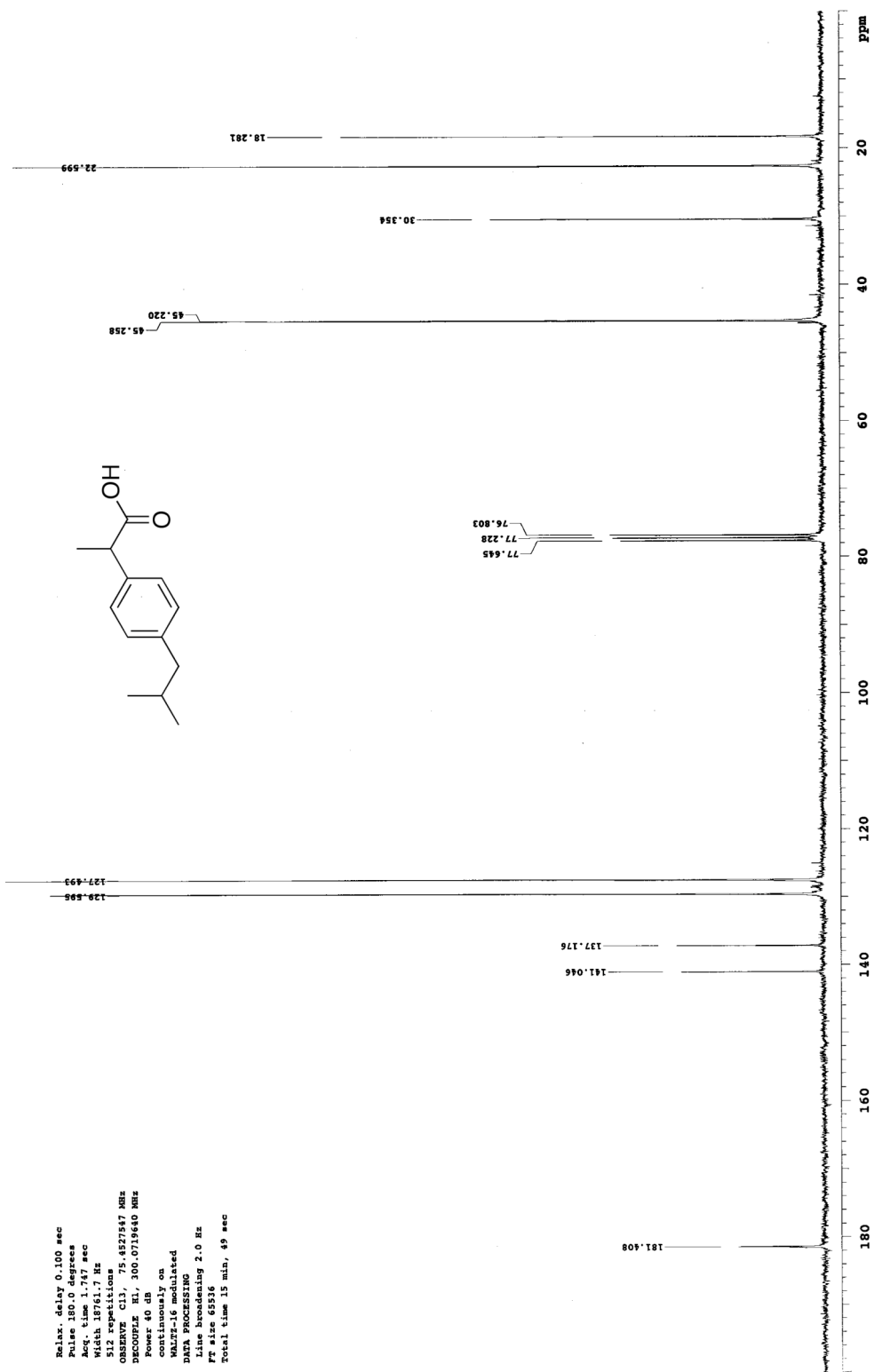


Figure A4.10. <sup>13</sup>C NMR spectrum of ibuprofen.

File : C:\HPCHEM\1\DATA\ARB7142R.D  
Operator : Bogdan  
Acquired : 2 Jun 2009 8:57 am using AcqMethod MCQ\_20M  
Instrument : GC/MS Ins  
Sample Name: ARB-VII-142 recrystallized  
Misc Info :  
Vial Number: 1

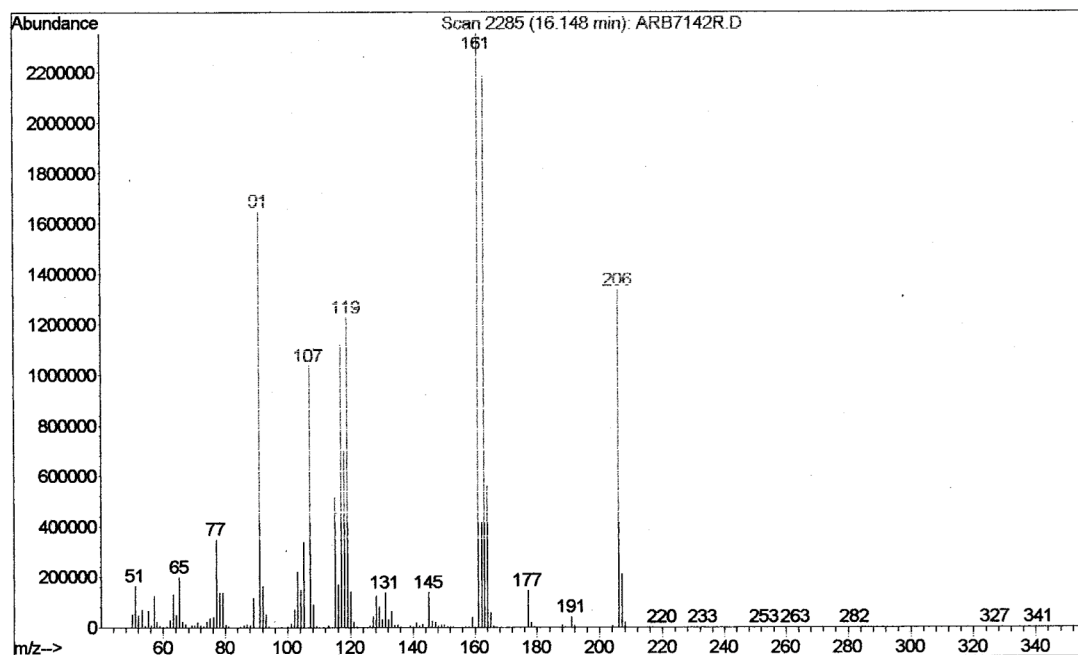
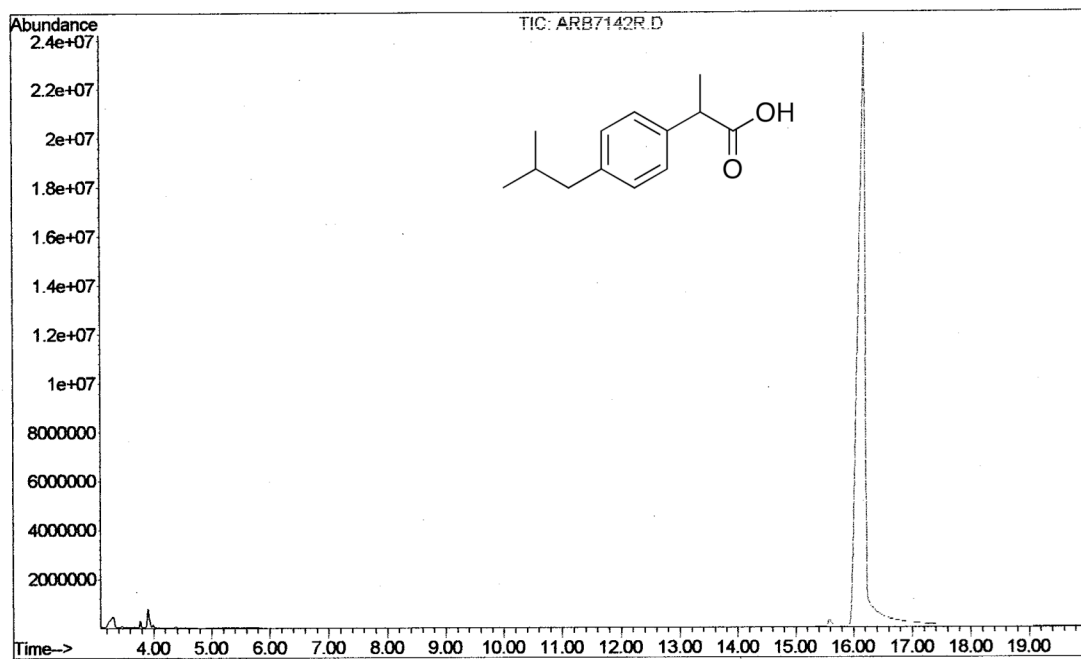
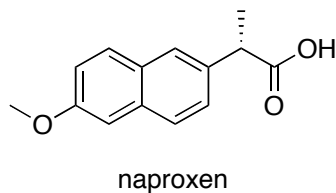


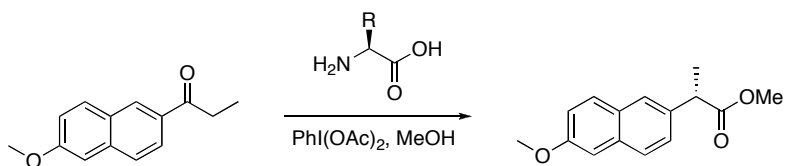
Figure A4.11. GC/MS trace of recrystallized ibuprofen.

**Development of a Stereoselective 1,2-Aryl Migration.** Naproxen is an NSAID similar to ibuprofen with a 2-arylpropanoate core (Figure A4.12). Unlike ibuprofen,

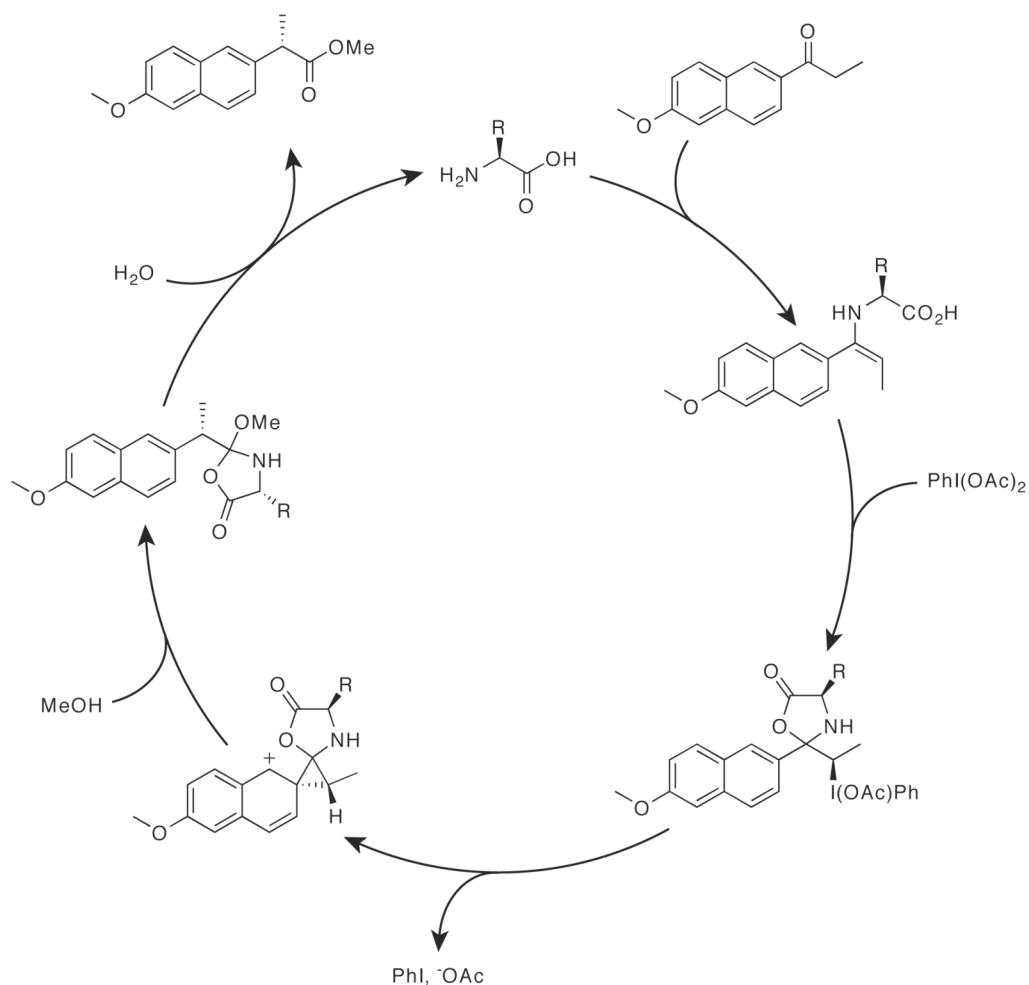


**Figure A4.12.** The structure of naproxen.

however, the stereocenter is essential in order to achieve any biological activity. Syntheses often result in the racemic form of naproxen and use a resolution step to obtain the *S*-isomer. Resolution steps like this ultimately lead to half of the product being discarded. For this reason, we looked at performing the  $\text{PhI}(\text{OAc})_2$ -mediated 1,2-aryl migration stereoselectively using a chiral amine (Scheme A4.1). We propose this reaction will proceed as illustrated in Figure A4.13.



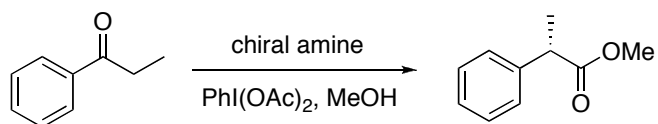
**Scheme A4.1.** The stereoselective  $\text{PhI}(\text{OAc})_2$ -mediated 1,2-aryl migration.



**Figure A4.13.** The proposed catalytic cycle of the stereoselective  $\text{PhI}(\text{OAc})_2$ -mediated 1,2-aryl migration

Preliminary experiments have been unsuccessful thus far, but we are confident that with more work this transformation could be achieved. Catalysts and reaction conditions attempted to date are shown in Table A4.1 using propiophenone as the starting material.

**Table A4.1.** Results of the stereoselective 1,2-aryl migration.



Entry	Catalyst	Result
1	 (10 mol%)	N.R.
2	 (20 mol%)	N.R.
3	 (10 mol%)	N.R.
4	 (20 mol%)	N.R.
5	 (10 mol%)	N.R.
6	 (20 mol%)	N.R.
7	 (10 mol%)	N.R.
8	 (20 mol%)	N.R.
9	 (10 mol%)	N.R.